UNIVERSITÉ LAVAL

Optimized Modeling of Membrane Gas Phase Separation Processes

Thèse

Sina Gilassi

Doctorat en génie chimique
Philosophiæ doctor (Ph. D.)

Québec, Canada

Optimized Modeling of Membrane Gas Phase Separation Processes

Thèse

Sina Gilassi

Sous la direction de :

Seyed Mohammad Taghavi, directeur de recherche
Denis Rodrigue, codirecteur de recherche
Serge Kaliaguine, codirecteur de recherche

Résumé

Le schéma traditionnel d'utilisation de l'énergie est désormais considéré comme un problème sérieux en raison de sa relation directe avec le changement climatique. Actuellement, notre dépendance vis-à-vis des combustibles fossiles augmente de façon spectaculaire, ce qui peut être attribué à la croissance de la population mondiale et à la forte demande d'énergie pour le développement économique. Ce modèle semble être préférable uniquement pour une économie florissante, mais ses perspectives pour les générations futures seront sans aucun doute décevantes. Dans ce scénario, un volume gigantesque de CO_2 produit par la combustion des combustibles fossiles dans les industries chimiques, les cimenteries et les centrales électriques, est rejeté de manière irresponsable dans l'atmosphère. Il ne fait aucun doute qu'une telle exploitation des combustibles fossiles nous conduit à des catastrophes environnementales sans précédent en ce qui concerne l'émission de CO_2, qui est le principal contributeur aux gaz à effet de serre (GES). L'une des solutions disponibles pour faire face à cette situation critique est de moderniser les centrales existantes qui émettent du CO_2 avec des technologies de capture et de stockage du carbone (CSC) afin de lutter systématiquement contre le changement climatique. Toutefois, les technologies actuelles de CSC présentent encore des problèmes techniques et des limites opérationnelles qui entraînent un surcoût pour les dépenses d'une usine et une augmentation de sa consommation d'énergie.

La technologie membranaire est actuellement considérée comme une méthode de séparation prometteuse pour la séparation des gaz en raison de la simplicité de son procédé et de son mécanisme écologique. Par rapport aux autres méthodes de séparation, cette technologie est encore en cours de développement. Actuellement, la recherche se concentre sur l'amélioration des caractéristiques des membranes afin de faire face à un compromis bien connu entre la perméabilité et la sélectivité décrit par les graphiques de Robeson. Cette approche pourrait viser à commercialiser cette technologie plus efficacement dans le domaine de la séparation des gaz, tandis qu'une technologie d'absorption à base d'amines sera encore utilisée de manière dominante à cette fin pendant plusieurs années. Malgré cela, il est également nécessaire d'évaluer la performance des membranes fabriquées pour la séparation de différents mélanges de gaz avant de les utiliser pour des projets industriels réalistes. Pour ce faire, un outil de simulation est nécessaire pour prédire la composition des composants gazeux dans les flux de produits du rétentat et du perméat dans différentes conditions de fonctionnement. Ainsi, au chapitre 1, un modèle fiable est développé pour la simulation de la séparation des gaz à l'aide de modules de membranes à fibres creuses. Ensuite, ce modèle permet d'identifier les propriétés requises de la

membrane, ce qui permet d'obtenir des performances intéressantes pour le module. Un procédé membranaire à plusieurs étapes est nécessaire pour atteindre les spécifications du produit qui sont une pureté et une récupération élevées du CO_2 dans le cas de projets de capture du CO_2. Dans ce cas, au chapitre 2, un modèle d'optimisation est proposé pour déterminer les valeurs optimales des paramètres de fonctionnement pour chaque étape et surtout pour déterminer une disposition optimisée à différents taux de récupération tout en minimisant le coût de la capture du CO_2. Dans le chapitre 3, nous comparons les performances de séparation de la technologie membranaire et du procédé d'absorption enzymatique en effectuant plusieurs analyses technico-économiques. Cette approche vise à démontrer la viabilité technique et l'efficacité économique de ces méthodes pour la modernisation d'une centrale électrique de 600 MWe par rapport aux procédés traditionnels d'absorption à base d'amines. Enfin, au chapitre 4, un système hybride est présenté en combinant les procédés d'absorption membranaire et enzymatique pour capturer le CO_2 des gaz de combustion d'une centrale électrique de 600 MWe. Ce système hybride est ensuite évalué pour révéler la faisabilité du procédé et pour étudier les performances de séparation en partageant la capture partielle du CO_2 entre ces deux unités de séparation. Dans l'ensemble, cette thèse de doctorat contribue à tirer parti de la fusion de la technologie membranaire avec d'autres méthodes de séparation conventionnelles telles que le procédé d'absorption enzymatique pour faciliter plus rapidement son intégration industrielle et sa commercialisation sur le marché de la séparation des gaz.

Abstract

The traditional pattern of energy use is now regarded as a serious problem due to its direct relationship to the climate change. Currently, our dependency on fossil fuels is dramatically increasing which can be attributed to the world population growth and heavy energy demand for economic development. This model appears to be preferable only for flourishing economy but undoubtedly its outlook for the future generations will be disappointing. Under this scenario, a gigantic volume of CO_2 produced by burning the fossil fuels in chemical industries, cement manufactures, and power plants, is recklessly released in the atmosphere. Undoubtedly, such exploitation of the fossil fuels is bringing us further to unprecedented environmental disasters pertaining to the emission of CO_2 which is the major contributor to the greenhouse gases (GHGs). One of the available solutions to deal with this critical situation is to retrofit existing CO_2 emitter plants with carbon capture and storage (CCS) technologies in order to systematically combat with the climate change. However, the current CCS technologies still have technical issues and operational limitations resulting in incurring extra cost to a plant's expenditures and increasing its energy consumption.

Membrane technology is currently regarded as a promising separation method for gas separation due to its process simplicity and eco-friendly mechanism. In comparison to other separation methods, this technology is still under progress. Currently, the research focus is on the enhancement of membrane characteristics in order to deal with a well-known trade-off between permeability and selectivity described by Robeson plots. This approach might aim at commercializing this technology more efficiently in the gas separation area while an amine-based absorption technology will still be dominantly utilized for this purpose for several years. Despite this, it is also needed to evaluate the performance of fabricated membranes for the separation of different gas mixtures prior to utilizing for realistic industrial projects. To do so, a simulation tool is required to predict the composition of gas components in retentate and permeate product streams under different operating conditions. Thus, in Chapter 1, a reliable model is developed for the simulation of gas separation using hollow fiber membrane modules. Later, this model allows identifying the required membrane properties hence, resulting in module performances of interest. A multi-stage membrane process is required to hit product specifications which are high CO_2 purity and recovery in the case of CO_2 capture projects. In this case, an optimization model is proposed in Chapter 2 to determine the optimal values of operating parameters for each stage and more importantly to determine an optimized layout at different recovery rates while CO_2 capture cost is minimized. In Chapter 3, we compare the separation performance of

membrane technology and the enzymatic-absorption process through performing several techno-economic analyses. This approach aims at demonstrating the technical viability and economic efficiency of these methods for retrofitting to a 600 MWe power plant compared to traditional amine-based absorption processes. Finally, a hybrid system is introduced in Chapter 4 by combining membrane and enzymatic-absorption processes to capture CO_2 from flue-gas of a 600 MWe power plant. This hybrid system is then assessed to reveal the process feasibility and to investigate separation performance through sharing partial CO_2 capture between these two separation units. Overall, this PhD thesis contributes to leverage the merge of membrane technology with other conventional separation methods such as the enzymatic-absorption process to more rapidly facilitate its industrial integration and commercialization in the gas separation market.

Table of contents

Résumé ii
Abstract iv
Table of contents vi
List of Tables ix
List of Figures x
Acknowledgements xiv
Foreword xv
Introduction 1
I.1 Gas separation 1
I.1.1 Conventional separation methods 2
I.1.2 Membrane technology 2
I.1.3 Hybrid process 4
I.2 Objectives and research contributions 5
I.3 Structure of this thesis 5
Simulation of Gas Separation Using Partial Element Stage Cut Modeling of Hollow Fiber Membrane Modules 8
1.1 Résumé 8
1.2 Abstract 8
1.3 Introduction 9
1.4 Modeling Background 10
1.5 Model development 13
1.5.1 Model assumption 13
1.5.2 Modeling algorithm 14
1.5.3 Co-current flow (shell side feed) configuration 14
1.5.4 Model validation 19
1.6 Case study: oxygen enrichment 24
1.7 Case study: natural gas processing 28
1.8 Use of the model in guiding experimental membrane development 32
1.9 Conclusion 35
Optimizing Membrane Module for Biogas Separation 38
2.1 Résumé 38
2.2 Abstract 38
2.3 Introduction 39
2.4 Problem statement and optimization approach 43

2.4.1 Superstructure membrane network 44
2.4.2 Model Formulation 45
2.5 Case study: biogas upgrading process 52
2.5.1 Optimized biogas process 53
2.5.2 Effects of CO_2 content and CH_4 recovery on upgrading cost 59
2.5.3 Effect of CO_2/CH_4 selectivity on upgrading cost 61
2.5.4 Effect of membrane cost on upgrading cost 63
2.6 Conclusion 67
Techno-Economic Evaluation of Membrane and Enzymatic-Absorption Processes for CO_2 Capture from Flue-Gas 72
3.1 Résumé 72
3.2 Abstract 72
3.3 Introduction 73
3.3.1 With or without the MEA solution: that is the question! 78
3.3.2 Enzymatic reaction system 83
3.3.3 Objective of this study 84
3.4 Modeling and optimization of the membrane process 84
3.5 Modeling of enzymatic-absorption process 86
3.5.1 Process description 86
3.5.2 Modeling approach 87
3.6 Optimization outline to minimize CO_2 capture cost 88
3.6.1 Enzymatic-absorption process 88
3.6.2 Cost model 89
3.7 Results and discussion 90
3.7.1 Process description 90
3.7.2 Optimized membrane process 90
3.7.3 Optimized enzymatic-absorption process 98
3.8 Conclusion 106
Techno-Economic Analysis of a Hybrid System for Flue-Gas Separation: Combining Membrane and Enzymatic-Absorption Processes 108
4.1 Résumé 108
4.2 Abstract 108
4.3 Introduction 109
4.3.1 Performance, limits, and potentials of conventional separation methods 110
4.3.2 Hybrid systems for flue-gas separation 114
4.3.3 Membrane-Absorption (MA) hybrid system 116
4.3.4 Objectives of the present study 118

4.4 Modeling and optimization of hybrid system 119
4.4.1 Membrane permeation model 119
4.4.2 Enzymatic-absorption model 119
4.4.3 Optimization method 120
4.5 Results and discussion 121
4.5.1 Process description 121
4.5.2 Required solvent for CO_2 capture in the hybrid process 122
4.5.3 Hybrid process energy analysis 125
4.5.4 Separation efficiency of the hybrid process 129
4.5.5 Cost analysis of CO_2 capture 134
4.6 Conclusion 136
Conclusion 140
Annexe A Chapter 1 supplementary materials 145
A.1 Cross-flow configuration 145
A.2 Counter-current flow configuration 147
A.3 Heat Transfer Analysis 149
Annexe B Biogas Upgrading and Optimization 153
B.1 Abstract 153
B.2 Introduction 153
B.3 Biogas production and uses 155
B.4 Biogas upgrading methods 159
B.4.1 Absorption 159
B.4.2 Adsorption 163
B.4.3 Cryogenic distillation 165
B.4.4 Membrane technology 166
B.4.5 Hybrid systems 168
B.5 Case study: biogas membrane separation 174
B.6 Conclusions and perspectives 178
Bibliography 180

List of Tables

Table 1.1 The properties of the experimental hollow fiber modules and feed conditions. 20
Table 1.2 Parameters used for the modeling of the O_2 production unit. 25
Table 1.3 Summary of the modeling results of a two-stage membrane separation unit for O_2 production. 28

Table 2.1 Techno-economic parameters and assumptions applied to the optimization case. 52
Table 2.2 Operating and feed conditions used for the optimization cases. 53
Table 2.3 Summary of the techno-economic analysis of optimized membrane separation processes. 67

Table 3.1 Flue-gas properties used for the optimization problem. 87
Table 3.2 Techno-economic analysis of CO_2 capture from a 600 MW_e power plant using a two-stage membrane process. 94
Table 3.3 Comparison of separation performance of the optimized process with different membrane processes. 97
Table 3.4 Input data used for optimization of the enzymatic-absorption process. 98
Table 3.5 Summary of techno-economic analysis of CO_2 capture using the enzymatic-absorption process. 105

Table 4.1 Flue-gas properties used for the optimization problem. 122
Table 4.2 Summary of techno-economic analysis of CO_2 capture using the hybrid process (ICC 30%, 0.3 bar). 135
Table 4.3 Techno-economic results of hybrid, standalone membrane and enzymatic-absorption processes (CAP 90%). 136

Table B.1 Typical biogas composition [23]. 156
Table B.2 Environmental requirements for AD systems [73]. 157
Table B.3 Characteristics of different fuel gases [235]. 158
Table B.4 Pipeline specifications when supplying upgraded biogas to the natural gas grid [23]. 159
Table B.5 Membrane characteristics, feed properties, and cost analysis parameters. 175

List of Figures

Figure 1.1 Schematic diagram of a co-current flow membrane separation module, and the feed and permeate flows in the first and two successive elements..... 15
Figure 1.2 Comparison of modeling results with the experimental data of: (a) Sidhoum, Sengupta, and Sirkar [62], (b) Pan [36]..... 21
Figure 1.3 Comparison of modeling results with the experimental data of Tranchino et al. [61], (a) at two different feed temperatures (25 and 65°C), (b) at two different feed pressures (200 and 600 kPa). 22
Figure 1.4 Comparison between modeling results and the experimental data of: (a) Sada et al. [65], (b) Feng et al. [63]. 23
Figure 1.5 Comparison between case VI modeling results and the experimental data of Pan [36]. 24
Figure 1.6 Separation performance in terms of stage cut and O_2 mole fraction as a function of module feed flow rate: (a) Pf = 600 kPa, Pp = 100 kPa, number of fibers = $3x10^5$, (b) Pf = 600 kPa, Pp = 100 kPa, number of fibers = $6x10^5$. 26
Figure 1.7 Separation performance in terms of stage cut and O_2 mole fraction as a function of module feed flow rate (Pf = 600 kPa, Pp = 100 kPa, number of fibers = $6x10^5$). 27
Figure 1.8 Effect of different CO_2/CH_4 selectivities on the CH_4 retentate mole fraction and total membrane area, (a) CO_2 content in feed = 10 mol.%, (b) CO_2 content in feed = 25 mol.%. 30
Figure 1.9 Effect of different CO_2/CH_4 selectivities on the CH_4 retentate mole fraction and total membrane area: (a) CO_2 content in feed = 50 mol.%, (b) CO_2 content in feed = 75 mol.%. 31
Figure 1.10 Process flow diagram of the natural gas purification using two membrane units. 32
Figure 1.11 Effect of O_2/N_2 selectivity on the O_2 permeate mole fraction and O_2 recovery in a single membrane unit, (N_2 permeance = 1.8 GPU, O_2 permeance variable). 33
Figure 1.12 Effect of O_2/N_2 selectivity on the O_2 permeate mole fraction and O_2 recovery in a single membrane unit, (O_2 permeance = 9.3 GPU, N_2 permeance variable). 34
Figure 1.13 Effect of O_2/N_2 selectivity on the O_2 permeate mole fraction and O_2 recovery in a single membrane unit, (N_2 permeance = 3.6 GPU, O_2 permeance variable). 34

Figure 2.1 Schematic diagram of the optimization of a three-stage separation process. 45
Figure 2.2 Schematic flow diagram of an optimized two-stage separation process at 10% biogas CO_2 content. 54
Figure 2.3a Relation between the FA index and results of the optimization problem (*UMn*, φ) outlined in Table 2.2 (Ultem 1000 membrane, Q_{CO2} = 86.3 GPU, Q_{CH4} = 2.60 GPU). 57
Figure 2.3b Relation between FA index and separation unit volume with module lengths of 50 and 100 cm. 57
Figure 2.4 Relation between the inlet gas flowrate and unit modules number when the module diameter is set to 12.7 cm (5 inches). 58
Figure 2.5 Effects of module diameter (5 and 12 in) on the required *UMn* over a range of unit feed flowrate..... 59
Figure 2.6 Effects of CO_2 feed content changes on the biogas separation cost. 60
Figure 2.7 Effect of CH_4 recovery improvement on the gas separation cost when the CO_2 feed content is 40%. 61
Figure 2.8 Effects of change in CO_2/CH_4 selectivities on the biogas separation cost for the following membrane CO_2/CH_4 selectivity and CO_2 permeance: a) 33.2, 86.3; b) 66.4, 86.3; c) 66.4, 172.6..... 63

Figure 2.9 Effects of membrane cost (25 and 50 $/m^2) on the optimized separation cost, membrane area and feed pressure (CO_2/CH_4 selectivity of 33.2 with a CO_2 permeance of 86.3 GPU and a feed composition of 40% CO_2). 65
Figure 2.10 Effect of the membrane cost (25 and 50 $/m^2) on the optimized separation cost, membrane area and feed pressure (CO_2/CH_4 selectivity of 66.4 with a CO_2 permeance of 172.6 GPU, and a feed composition of 40% CO_2). 66

Figure 3.1 Process flow diagram of a multi-structure membrane process used in the process optimization. 86
Figure 3.2 Process flow diagram of an enzymatic-absorption process for flue-gas treatment. 87
Figure 3.3 Optimized membrane layout for 90% CO_2 capture from flue-gas. 91
Figure 3.4 Effects of CO_2 capture on the purchase cost of the equipment in the optimized two-stage membrane process. 92
Figure 3.5 Effects of CO_2 capture on the membrane process costs. 95
Figure 3.6 Effects of CO_2 capture on the energy consumption of equipment in the membrane process. 96
Figure 3.7 a) Effects of solvent flowrate on the CO_2 capture in the enzymatic-absorption process (example of a 600 MW_e power plant), b) Effects of the lean CTB index on the heat of CO_2 regeneration (90% CO_2 capture). 100
Figure 3.8 Heat analysis of the desorption process at different lean CTB level (90% CO_2 capture). 101
Figure 3.9 Relation between the lean CTB and performance of vacuum system. 103
Figure 3.10 Effects of the lean CTB level on the electricity loss of plant. 104

Figure 4.1 Process flow diagram of a hybrid process including pre-treatment, membrane, and enzymatic-absorption units. 121
Figure 4.2 Relation between the L/G ratio in the absorber and total CO_2 capture rate in the hybrid process. 124
Figure 4.3 Variation of the lean and rich CTB indexes at different L/G ratio in the single and hybrid enzymatic-absorption processes. 125
Figure 4.4 Effects of lean CTB index and ICC in the hybrid process on the heat of CO_2 recovery in the stripper column. 126
Figure 4.5 Effects of vacuum pressure in the stripper and ICC in the hybrid process on electricity loss for a 600 MW_e power plant. 127
Figure 4.6 Electricity loss by the vacuum systems at different pressure setpoints in the enzymatic-absorption process. 128
Figure 4.7 Comparison between the circulation rate of solvent between absorption and desorption in the standalone enzymatic-absorption and hybrid processes. 129
Figure 4.8 Relation between the extent of CO_2 capture and electricity loss for a standalone two-stage membrane unit integrated into a 600 MW_e power plant (Calculated from results in [218]). 131
Figure 4.9 Overall electricity loss of the hybrid process at different operating and design conditions. 133

Figure A.1 Schematic diagram of a cross-flow membrane separation module. 145
Figure A.2 Schematic diagram of the first element in contact with the feed gas for the cross-flow configuration. 146
Figure A.3 Schematic diagram of two successive elements in the cross-flow configuration. 147
Figure A.4 Schematic diagram of a counter-current flow membrane separation module. 147
Figure A.5 Schematic diagram of the last element in the counter-current flow configuration. 148

Figure A.6 Schematic diagram of two successive elements in the counter-current flow configuration. 148
Figure A.7 Schematic diagram of heat transfer in a fiber [47]..... 151

Figure B.1 Schematic diagram of the conversion of organic matter to CH_4, CO_2 and other biogas components. 156
Figure B.2 The process flow diagram of acid gas removal using amine scrubbing. 160
Figure B.3 The flow diagram of a water scrubbing process using scrubber and regeneration units. 161
Figure B.4 The flow diagram of an organic solvent scrubbing process. 163
Figure B.5 The process flow diagram of a pressure swing adsorption unit for biogas upgrading..... 164
Figure B.6 The flow diagram of a cryogenic distillation process used for biogas upgrading. 165
Figure B.7 The schematic flow diagram of various single stage membrane units. 167
Figure B.8 Two stage membrane configuration. 168
Figure B.9 Three stage membrane configuration. 168
Figure B.10 The schematic flow diagram of a hybrid process including membrane and chemical absorption units. 169
Figure B.11 The schematic flow diagram of hybrid systems including membrane and a, b) pressurized water scrubbing processes, c, d) amine absorption processes, e) cryogenic distillation..... 171
Figure B.12 Annual cost of biogas upgrading processes for a gas flow rate of 1000 m3 (STP)/h. 172
Figure B.13 The flow diagram of another hybrid process including TSA and membrane units for the separation of CO_2 from biogas..... 173
Figure B.14 The schematic flow diagram of the hybrid separation process. 173
Figure B.15 Relations between the CH_4 mole fraction, membrane separation area and total cost at different pressures. 176
Figure B.16 Relations between the CH_4 mole fraction, membrane separation area and CH_4 loss at different pressures. 176
Figure B.17 Relations between CH_4 mole fraction, total membrane area and total cost for three different pressures (3, 4.5 and 6 bars). 177
Figure B.18 Relations between the CH_4 mole fraction and CH_4 loss for two membrane units. 178

To my parents for their wonderful encouragement, to my wife for her endless love.

Acknowledgements

I would like to express my deep gratitude and appreciation to Prof. Serge Kaliaguine, for the patient guidance, encouragement and advice he has provided throughout my time as his student. I would also like to thank Prof. Seyed Mohammad Taghavi and Prof. Denis Rodrigue for their academic guidance, support and encouragement throughout my doctoral program at Laval University.

I would like to thank the Chemical Engineering department staffs for all the technical and administrative assistance that I received during the entire period of my study. Finally, I would like to thank the Natural Sciences and Engineering Research Council (NSERC) of Canada and the Mathematics of Information Technology and Complex Systems (MITACS) programme for their financial support.

Foreword

This thesis consists of four chapters presented as articles in the insertion form. The three chapters of the thesis are published, and Chapter 4 is now submitted and currently under review. The introduction and conclusion sections are original, and they have never been published before. The articles are listed below:

> Chapter 1: **Gilassi, S.**, Taghavi, S.M., Rodrigue, D., and Kaliaguine, S. *Simulation of gas separation using partial element stage cut modeling of hollow fiber membrane modules.* AIChE Journal, 2018. **64**(5): p. 1766-1777.
>
> Chapter 2: **Gilassi, S**., Taghavi, S.M., Rodrigue, D., and Kaliaguine, S. *Optimizing membrane module for biogas separation.* International Journal of Greenhouse Gas Control, 2019. **83**: p. 195-207.
>
> Chapter 3: **Gilassi, S.**, Taghavi, S.M., Rodrigue, D., and Kaliaguine, S. *Techno-Economic Evaluation of Membrane and Enzymatic-Absorption Processes for CO_2 Capture from Flue-Gas* Separation and Purification Technology, 2020: p. 116941.
>
> Chapter 4: **Gilassi, S.**, Taghavi, S.M., Rodrigue, D., and Kaliaguine, S. *Techno-Economic Analysis of a Hybrid System for Flue-Gas Separation: Combining Membrane and Enzymatic-Absorption Processes.* Chemical Engineering and Processing: Process Intensification, 2020: p. Under review.

Furthermore, a review of the current gas separation methods available for biogas treatment process was written as a book chapter and published by Nova Science (ISBN: 978-1-53612-787-4).

> **Gilassi, S.**, Taghavi, S.M., Kaliaguine, S., and Rodrigue, D., "*Biogas Upgrading and Optimization"* In Biogas: Production, Applications and Global Developments, A. Vico, et al., Editors. 2017, Nova Science: USA.

In all cases, I performed the literature review, the numerical calculations and the data analysis, as well as writing the first draft of the complete manuscript. Prof. Kaliaguine, Taghavi and Rodrigue helped with the data analysis and discussion of the results, as well as making the necessary corrections in the documents.

Introduction

I.1 Gas separation

Gas processing is commonly regarded as a critical step in most chemical plants and industrial manufactures in order to separate impurities and undesired materials, to ultimately reach a target product as per standard quality requests. Statistics demonstrate a rising trend in the global energy demand due to rapid growth of population, modernization, and economy. This scenario might be translated to a serious challenge of choosing an energy source which has lower impacts on the environment. At present, natural gas as a clean energy-future source is dominating the global market compared to other fossil fuels. Thus, great attentions have been made to facilitate the transition of this strategic energy source in the world while the effects of fossil fuels (oil, gas, and coal) combustion on climate change is undeniable. Raw natural gas which contains carbon dioxide (CO_2) usually ranging from 10 to 60% depending on the depth and location of a well head, needs to be treated prior to injecting into natural gas grids or using for other applications. In recent years, numerous attempts have also been made to decrease the level of dependency on the fossil fuels through using sustainable and renewable energy sources. Accordingly, biogas production has come into effects as a solution in many countries to cope with the coming energy crisis. In this way, a large number of fermentation plants have been constructed especially in Europe and Asia Pacific to produce biogas by anaerobic digestion (AD) of biodegradable organic materials, enriched in methane (CH_4). The treatment process is also necessary as the biogas product might contain a trace of contaminating substances (halogen, organic silicon, and aromatic compounds) and acid gases (CO_2 and H_2S) depending on materials fed to anaerobic digesters or bioreactors. Likewise, hydrogen (H_2) is considered as a promising energy source, which can be produced by steam reforming of natural gas in a reformer at high temperature and pressure in presence of a catalyst (usually nickel). Then, the final product, the so-called syngas, which also comprises undesired components including CO and CO_2, needs to be treated before use for other applications. Despite all initiatives and strategies to take advantage of cleaner energies such as solar, wind, and nuclear, natural gas still remains a major energy source in the world. Power plants are currently the main consumers of natural gas for generating electricity. Following combustion in reboilers, an exhaust gaseous mixture including nitrogen (N_2) and CO_2, known as flue-gas, requires treatment before releasing in the atmosphere. Similarly, cements plants are known as CO_2 emitters owing to the use of fossil fuels for the production of clinker inside rotary kilns. In all the above-mentioned cases, gas separation process is compulsory to capture CO_2, not only to avoid technical issues but also to comply with environmental rules and regulations. This scenario, which is described in the United Nations Framework Convention on Climate Change (UNFCCC), is then considered as

one of the promising paths to deal with climate change. As such, CO_2 capture and storage (CCS) is a technically feasible strategy to reduce the emission of CO_2 as the dominant contributor to the greenhouse gases (GHGs), form large emitting sources. The CCS strategy consists of one of three main approaches. In the pre-combustion process, the fossil fuels are initially converted into a clean-burning gas enriched in H_2, and then removing the remaining CO_2, whereas the post-combustion process aims at removing the CO_2 from flue-gas after the combustion of the fossil fuels. In the oxy-fuel combustion process, burning the fossil fuels in the presence of pure oxygen (O_2) is performed and then the CO_2 generated is finally captured at lower cost since it is not diluted in atmospheric nitrogen [1, 2]. Overall, the post-combustion process appears to be the most successful approach as resulting in a better retrofitting to the existing industrial sectors including raw natural gas and biogas treatment units, as well as cement manufacturers and power plants [3].

I.1.1 Conventional separation methods

The conventional post-combustion process may consist of absorption, adsorption, and cryogenic distillation technologies but so far none of them has offered satisfactory outcome for CO_2 capture prospects. The absorption process is preferable to be used for treating a gas mixture containing low CO_2 concentration. The capture cost is then estimated at a range of 40-100 \$/ton CO_2 for CO_2 recovery higher than 90% [4]. This process seems to be less economically and environmentally attractive due to its high energy requirement for CO_2 recovery and traditional dependency on amine solutions [5]. In comparison, the adsorption process is eco-friendlier as removing CO_2 by binding it temporarily on the surface of a solid adsorbent. Cryogenic distillation allows capturing CO_2 based on the thermodynamic properties of a gas mixture and being moreover independent of the type of absorbent or adsorbent. Thus, numerous researches have been performed not only to enhance the current performance of the above-mentioned processes but also to exploit other promising separation methods.

I.1.2 Membrane technology

This technology is not developed enough compared to the above-mentioned separation methods to be deployed for industrial-scale CO_2 capture [6]. However, it has comparatively a more straightforward separation mechanism in that gas components in a mixture pass through a thin membrane layer depending on their permeation abilities. Thus, this mechanism can be easily extended to separate different gas mixtures such as CO_2/CH_4, CO_2/N_2, CO_2/H_2, and O_2/N_2. This separation method initially appears to have no technical barrier for process scale-up and operation for a typical CO_2 removal project. As a result, numerous experimental works have been conducted in order to fabricate membranes with excellent separation characteristics. This might simply increase membrane

permselectivity and reinforce its chemical and physical stabilities under different operating conditions. In fact, this path would conceptualize a well-known trade-off between selectivity and permeability described by Robeson plots [7]. A few commercial membranes are currently available on the market and thus, this situation has resulted in some commercialization of the membrane technology for CO_2 capture. Under this scenario, using a single-stage membrane process for efficient capture of CO_2 is certainly not sufficient. Undoubtedly, a large separation area would also be required for industrial separation projects to reach high CO_2 purity and recovery while using current commercial and even advanced membranes. It is therefore needed to take advantage of multiple membrane-based separation modules in parallel and/or in series. For simulation of such a process, a robust model needs to be used to predict the performance of each unit under different operating conditions. The desired model may be developed on the basis of the solution-diffusion theory, to consider the effects of parameters such as gas permeability and separation area for various membrane module types. Obviously, the result of modeling allows portraying a realistic outlook on the separation performance of fabricated membranes for different gas mixtures. This approach also allows preparing a practical guideline for experimentalists in order to modify individual gas permeances for desired membrane types and see their effects on separation process efficiency. This approach certainly narrows the gap between experimental works and industrial-scale CO_2 capture projects by developing an optimization model to find the optimal values of decision variables.

Numerous studies on the optimization of multi-stage membrane separation systems were carried out to evaluate the effect of using different membrane types on CO_2 removal performance [8-10]. In most cases, the main objective was to minimize the cost of CO_2 separation through manipulating decision variables in pre-design process layouts. This approach certainly fails to find a global optimum as a limited number of process layouts is considered for optimization search. It is therefore necessary to deploy a more robust optimization approach to deal with a superstructure membrane-based separation system. Thus, this new approach will allow determining the optimal process by considering all possible layouts in a multi-stage superstructure membrane network while the CO_2 separation cost is minimized. The optimization model is then used to specify the footprint of each separation stage including required number and size of hollow fiber membrane modules in a realistic industrial case. Under this scenario, a techno-economic analysis can be performed to more accurately present the current state of membrane technology compared to other CO_2 capture methods. It is then expected that this approach is precisely designed to resolve technical limitations and remove economic barriers in the face of better commercialization of membrane technology.

I.1.3 Hybrid process

A membrane separation process appears to be more attractive due to its simplicity compared to an amine absorption process which is currently dominating the CO_2 separation market. This superiority might be taking advantage of an interesting idea to incorporate the membrane technology into a hybrid separation system, combining it with other separation methods. In turn, the hybrid system would benefit from advantages of the incorporated processes in order to either reduce CO_2 capture cost or to solve existing technical issues of individual processes. Few studies have been conducted to precisely design and evaluate such a hybrid system in CO_2 separation projects. For example, Belaissaoui et al. [11] proposed a hybrid membrane-cryogenic process to remove CO_2 from flue-gas of a power plant. In this case, the heat requirement for CO_2 recovery was then estimated at 1.4-3.7 GJ/ton CO_2 captured, while CO_2 mole fraction was varied in the permeate product. In another case, Kundu et al. [12] also suggested a hybrid process through combining membrane and absorption systems to remove CO_2 from a flue-gas stream. Overall, the required energy of this hybrid system was found to be 1.83-3.70 GJ/ton CO_2 which was lower than that in the standalone absorption process (3.5 GJ/ton CO_2).

As stated in the previous section, the absorption method is highly used as a technology for CO_2 capture projects. However, even the most advanced process, the so-called Econamine FG Plus^{SM} (EFG+), which is a fluor proprietary amine-based technology, has some critical limitations. It is therefore needed to keep focusing on the development of non-amine solvents which would have lower technical and environmental impacts. One of these types of solvents is carbonate solutions such as potassium carbonate (PC) which has a lower heat of CO_2 desorption and is eco-friendlier compared to amine solvents [13]. However, the intrinsic PC rate of reaction is slower than in amine solvents resulting in a lower mass transfer of CO_2 into the liquid phase. This probably increases the circulation rate of PC solvent in the absorption process for the same rate of CO_2 capture. This critical issue might be resolved by adding active components such as organic, inorganic, and enzymatic promoters to accelerate the rate of CO_2 absorption. In this case, CO_2 Solutions Inc. (CSI) recently tested a proprietary PC solution catalyzed with carbonic anhydrase (CA) enzyme for the removal of CO_2 from flue-gas stream [14]. The heat requirement for CO_2 recovery was estimated to be 3.6 GJ/ton CO_2 for a CO_2 capture of 80% CO_2. The total CO_2 capture cost was then found to be at 28$/ton which was more economical than those reported for the amine-based absorption process (40-100$/ton CO_2) [4]. The higher the CO_2 recovery, the higher the energy demanded to strip off CO_2 from the rich solvent and probably the higher circulation flowrate between absorption and desorption units needs to be. Currently, the enzymatic-absorption process might be regarded as a proper alternative to displace the

amine-based absorption processes provided alleviating its technical and economic bottlenecks. The current gap might be filled through utilizing a hybrid system in which a membrane separation unit initially captures part of CO_2 in the feed gas and thereafter the complete CO_2 removal is carried out in an enzymatic-absorption unit. In turn, the hybrid process would benefit from most of the technical and economic aspects of the above-mentioned separation methods.

I.2 Objectives and research contributions

Most current research studies focus on the development of membranes with better separation characteristics and test them in lab-scale projects. However, the full incorporation of the membrane in realistic industrial separation projects needs further consideration. In all cases, a multi-stage layout is required to meet product specifications which is high recovery and purity predicted for CO_2 capture projects. Thus, a techno-economic analysis is necessary to realistically specify the outlook of the implementation of membrane technology in global gas separation markets. This thesis aims at optimizing membrane-based separation processes by performing techno-economic analysis in order to determine technical and economic barriers towards the commercialization of membrane technology. Under this scenario, this comprehensive approach also allows revealing the pros and cons of this technology compared to the current industrial separation methods. Later, a hybrid system including membrane and enzymatic-absorption units is investigated to reveal the effects of partial CO_2 removal on technical and economic aspects of the individual processes. In detail, the objectives are also specified as follows:

- Developing a reliable model to investigate the effects of membrane characteristics including permeabilities and selectivities on the layout of commercial scale membrane module systems.
- Optimizing standalone membrane-based gas separation and enzymatic-absorption processes to minimize energy penalty and CO_2 capture cost.
- Performing a techno-economic analysis for the hybrid system to reveal potentials of a preliminary membrane CO_2 separation step, on the overall separation performance of the hybrid process.

I.3 Structure of this thesis

This thesis is composed of the following chapters.

Introduction

This section presented a brief introduction about the use of membrane technology in the gas separation area and listed the existing technical issues and economic barriers towards the commercialization of this technology. As such, the contribution of this PhD thesis is to address this gap through simultaneous incorporation of experimental data as well as simulation and optimization of typical CO_2 separation processes.

Chapter 1 Simulation of gas separation using partial element stage cut modeling of hollow fiber membrane modules

This chapter is dedicated to an original modeling for the simulation of membrane-based separation processes. A reliable model is developed to simulate gas separation using hollow fiber membrane modules. It is then validated by comparing the modeling results with experimental data taken from the literature. Later, this model is used as a robust simulation tool to identify the required membrane properties resulting in module performance of interest.

This chapter is published in AIChE Journal 64.5 (2018): 1766-1777, DOI: 10.1002/aic.16044.

Chapter 2 Optimizing membrane module for biogas separation

In this chapter, an optimization model is developed to determine the optimal values of operating parameters and the optimized layout while CO_2 capture cost is minimized. This model is then used to specify the optimal values of module packing fraction and dimensions by minimizing the required module number for a typical membrane-based separation process. Finally, a novel modeling approach is proposed to select membrane characteristics by which the effects of CO_2 permeance and CO_2/CH_4 selectivity on optimal process layouts for purification of biomethane are investigated.

This chapter is published in International Journal of Greenhouse Gas Control. 2019, DOI: 10.1016/j.ijggc.2019.02.010.

Chapter 3 Techno-Economic Evaluation of Membrane and Enzymatic-Absorption Processes for CO_2 Capture from Flue-Gas

This chapter presents a thoughtful comparison between membrane technology and enzymatic-absorption process through conducting individual techno-economic analysis. This approach allows demonstrating the technical viability and economic profitability of these two methods for retrofitting to a 600 MW_e power plant compared to traditional amine-based absorption processes. To do so, two distinctive optimization methods are exploited to find the optimized process with the lowest energy

penalty. Above all, this study aims at recognizing bottlenecks in each process and then proposing initiatives to improve the capture efficiency.

This chapter is now accepted in the journal Separation and Purification Technology, 2020.

Chapter 4 Techno-Economic Analysis of a Hybrid System for Flue-Gas Separation: Combining Membrane and Enzymatic-Absorption Processes

This chapter introduces a hybrid system by combining membrane and enzymatic-absorption processes to remove CO_2 in the flue-gas emitted from a 600 MW_e power plant. This hybrid system is then assessed to reveal the process feasibility and to investigate separation performance through sharing partial CO_2 capture between two separation units. In this case, an optimization approach is also suggested to minimize the total energy penalty required for gas compression and evacuation units in the membrane process as well as heat of CO_2 recovery in the stripper of the enzymatic-absorption process.

This chapter is submitted to the journal of Chemical Engineering and Processing: Process Intensification.

Conclusions

This section summarizes the highlights and findings from this research work and proposes some recommendations for a more appropriate incorporation of membrane technology in CO_2 capture projects.

Appendix A Chapter 1 supplementary material

More details about the stage cut modeling of cross-flow and counter-current hollow fiber membrane contactors are discussed.

Appendix B Biogas Upgrading and Optimization

This work which contains a comprehensive review of current gas separation methods available for biogas treatment process is a book chapter in Biogas: Production, Applications and Global Developments published by Nova Science (ISBN: 978-1-53612-787-4).

Chapitre 1

Simulation of Gas Separation Using Partial Element Stage Cut Modeling of Hollow Fiber Membrane Modules

1.1 Résumé

Un modèle mathématique est développé pour simuler le procédé de séparation des gaz par un module membranaire de fibres creuses. En particulier, une nouvelle technique numérique est introduite sur la base du calcul flash. Une telle analyse permet d'identifier les propriétés requises de la membrane nécessaires pour atteindre la performance souhaitée du module. Ce modèle a été validé pour six exemples de séparation de gaz différents obtenus de la littérature. Puis, le modèle validé a été utilisé pour investiguer l'effet des perméances du O_2 et N_2 sur la récupération et la fraction molaire de O_2 dans un courant de perméat. Un procédé réaliste d'enrichissement de l'air en deux étapes est aussi proposé pour la production de O_2 en utilisant un module industriel avec différents nombres de fibres. Cependant, ce modèle a été utilisé pour simuler un procédé de purification du gaz naturel en utilisant une seule unité pour déterminer la surface requise de séparation de membrane et la perte de CH_4. Finalement, un procédé en deux étapes a été proposé pour améliorer simultanément la fraction molaire de CH_4 du rétentat et réduire la perte du CH_4.

1.2 Abstract

A mathematical model is developed to simulate a gas separation process using a hollow fiber membrane module. In particular, a new numerical technique is introduced based on flash calculation. Such analysis allows identifying the required membrane properties needed to reach module performances of interest. This model was validated for six different gas separation cases taken from literature. Then, the validated model is used to investigate the effect of O_2 and N_2 permeances on O_2 recovery and O_2 mole fraction in the permeate stream. A realistic two-stage air enrichment process is also proposed for O_2 production using an industrial module with different fibers numbers. Moreover,

this model is used to simulate a natural gas purification process using a single unit to determine the required membrane separation area and CH_4 loss. Finally, a two-stage process is proposed to equally enhance CH_4 retentate mole fraction and decreasing CH_4 loss.

1.3 Introduction

Based on current data, a substantial growth in global energy consumption is predicted for the coming years [15]. The world population was about 7.5 billion in 2017, and this number is expected to increase to around 9.2 billion by 2050 [16]. This population growth inevitably poses serious challenges to the global energy needs. At present, a large amount of energy is supplied from fossil sources which unwillingly forces the governments to deal with controversial challenges such as greenhouse gas (GHG) emission. The reduction of GHG emissions demands strong and global collaboration. Kyoto protocol (1992) and Paris agreement (2016) based on United Nations Framework Convention on Climate Change (UNFCCC) hopefully determined essential plans to mitigate and control these GHG emissions. The Canadian government has also undertaken CO_2 mitigation plans to honor the Canadian's conditional commitment. In this way, the GHG emissions' intensity will decline to 17% below the 2005 levels by 2020 that is equivalent to 622 Mt of CO_2 [17].

Gas separation is one of the main processes in chemical and industrial plants. For example, in the field of natural gas transportation and treatment, gas composition needs to meet some criteria to avoid instability in operational conditions and decline in process performance. In terms of pipeline system, the content of acidic gases needs to be carefully controlled because at high concentration they can corrode the network. Flue gas separation (CO_2/N_2), air enrichment (O_2/N_2), hydrogen separation (CO_2/H_2) and bio-methane separation from syngas are other examples of industrial gas treatment processes. The current methods for gas separation are: absorption, adsorption and cryogenic distillation [18, 19]. Over the last 30 years, numerous attempts have been made to replace these conventional methods suffering from operation instability, high energy consumption, as well as high capital and maintenance costs. Today, the main option is membrane technology [20-24].

Gas separation using membrane processes requires a large membrane surface area for high gas capacity. Presently, three types of membrane contactors including hollow fiber, spiral wound, and envelope are commonly used. The hollow fiber and spiral wound membranes provide larger surface area than the envelope. Efficient gas separation processes require however an active area from hundreds to thousands of square meters. Hollow fiber membrane modules (HFMM) are more economical as they have the highest effective surface area per unit volume of the membrane module. HFMM consists of large numbers of thin tubular fibers bundled and sealed together on each end with

epoxy in a housing [25]. HFMM operating at low-pressure, are commonly used for gas separation compared to other module types. In the gas separation process, the gas mixture is fed to the HFMM, the penetrants pass through the polymer membrane depending on their permselectivity and desorb on the permeate side whereas non-penetrants remain on the residue side and finally leave the module. The gas mixture can enter tube-side or shell-side of the module depending on the separation objectives. In terms of flow configuration, three HFMM including counter-current, co-current, and cross-flow can also be used for gas separation. Other parameters, such as number of fibers, membrane material, module size, as well as feed pressure, temperature, and flow rate can directly affect the separation efficiency.

The modeling of membrane gas separation systems is of importance in engineering and design thereby both process efficiency and cost analysis can accurately be estimated. A robust model developed on the basis of heat and mass transfer can be used as a reliable tool to initiate a feasibility study of a separation project. In this work, a new approach based on flash equilibrium calculation, which is used to calculate liquid-vapor concentration in a distillation system, is modified to find a solution for heat and mass transfer equations inside a hollow fiber membrane system. A mathematical model is proposed to determine the flow rate and composition of both permeate and retentate streams for different module configurations (counter-current, co-current, and cross-flow). Furthermore, a highly efficient new numerical technique is introduced for the membrane gas separation systems. The modeling results are validated with various experimental data obtained from literature and to determine the model's performance. The model is also allowing to be useful in establishing target performance in the development of new membrane materials. Finally, the validated model is used to simulate air enrichment (O_2/N_2 separation) and natural gas purification (CO_2/CH_4) processes using an asymmetric polymer membrane in single and two stage units.

1.4 Modeling Background

Numerous models with various limitations were proposed for HFMM simulation under different operating conditions [26-31]. For instance, Bansal et al. [32] introduced a numerical method for the separation of multi-component gas mixtures in a single membrane unit. The model equations for a co-current system constituted an initial boundary problem solved by a Runge-Kutta method. The flow rates and mole fractions of the permeate and retentate streams were also calculated by an iteration method. The results showed that this numerical algorithm was slow for multi-component gas systems. More theoretical studies of the performance of single-stage permeation showing the effects of pressure, membrane area, and flow patterns are also available in reference [33, 34]. Shindo et al. [35] developed a model based on Fick's law for the single stage permeation of a multi-component gas

mixture with different flow patterns. In their study, they did not consider the effect of temperature on gas components' permeability and pressure variation in the feed and permeate sides. Later, Pan [36] developed a model of multi-component permeation systems for high-flux hollow fiber membranes in which the pressure variation along the fiber was also taken into consideration. The solution method consists in the calculation of local mole fractions of the permeate stream by an iteration method. The bulk mole fraction was calculated from the mass balance using the compositions and flow rates of the feed and residue streams. The pressure drop inside the fibers was calculated using the Hagen-Poiseuille equation with a trial-and-error shooting method. In terms of pressure variation, Lim et al. [37] developed a model to accurately estimate the pressure drop inside the fibers. The advantage of their improved Hagen-Poiseuille model was computation simplicity when the fiber permeability and gas compressibility changed. Murad Chowdhury et al. [38] presented a new numerical method for the model developed by Pan [36], which could be incorporated in process simulators such as Aspen Plus. They reported that the equations were solved faster by their numerical technique without initial guess on the pressure, flow rate, and mole fraction inside the fiber. In terms of the numerical solution, a system of non-linear algebraic equations for the permeate stream was solved with a Powell hybrid algorithm and finite-difference approximation for the derivatives. The bulk mole fraction and flow rate of the permeate and retentate streams were later calculated from the known permeate local mole fraction and this procedure was repeated until the end of the module. Khalilpour et al. [39] also presented a new solution technique for the model developed by Pan [36]. They converted all mass balance equations (Ordinary Differential Equation, ODE, system) for co-current and counter-current flows to derive algebraic equations using backward finite differential equations over all elements and then solved them by Gauss-Seidel algorithms. This method had a major difficulty in setting initial values for the residue flow rate and permeate pressure. The iteration method was slow because this numerical algorithm had an extra loop for pressure calculations. More details are also available in reference [40]. Kundu et al. [41] introduced a new solution technique to solve the balance equations. They transformed the model equations to ODE systems as an initial-value problem in two successive steps using Gear's BDF method. This technique required minimum computational time and effort, and presented better solution stability for a multi-component gas membrane separation system.

Thundyil and Koros [42] presented and analyzed a new modeling approach to solve the mass transfer equations in the HFMM. The numerical algorithm was improved by the succession of states method (SSM) to separate the module into small size elements. This model was suitable for gas separation under isothermal conditions. The results revealed that the cross-flow pattern was more effective than the other patterns due to a better feed distribution inside the module whereas the counter-current

pattern was more suitable for the module with larger bundle size. Later, Ahmad et al. [43] modified the model developed by Thundyil and Koros [42] to show the effect of temperature and pressure on membrane permeation. The results showed that increasing the feed CO_2 concentration for CO_2/CH_4 separation, increased the temperature difference between the feed and residue end, but they did not report any data about permeate temperature. Under non-isothermal conditions, the temperature of the feed and permeate streams noticeably change because of the Joule-Thomson (JT) effect and membrane conductivity. The JT effect is also attributed to the high ratio of transmembrane pressure between the permeate and retentate sides. More details about the numerical procedure to calculate the JT coefficient are available elsewhere [44, 45].

Coker et al. [46] presented a new model of multi-component gas separation using a hollow fiber membrane for the various types of flow pattern. The model was compatible with any change in pressure sweep, permeability, and pressure gradient on both sides of the membrane. The module was divided into a number of segments and the mass balance was applied to each one. The solution method to solve a system of the algebraic equation was however complicated as initial guesses needed to be made for the flow rate and pressure on each segment. Later, Coker et al. [47] modified the previous model to exhibit the effect of gas expansion on heating or cooling inside the membrane permeator. The results showed that increasing either CO_2 concentration in the feed gas or stage cut, increased the temperature difference between the feed and residue sides. They reported that the numerical solution based on nested successive substitution method could also be instable due to the limited radius of convergence. Lock et al. [48] developed a new solution technique for the model developed by Thundyil and Koros [42]. The calculation method started with an initial guess for the more permeable gas component to calculate an initial stage cut. The flow rate and composition of the permeate and retentate streams were later calculated for this initial stage cut. The proposed method was slow because an iteration method was needed to numerically calculate the permeate local mole fraction at each node. Moreover, this method was only suitable for isothermal conditions.

Scholz et al. [49] studied the effect of concentration polarization, Joule-Thomson effect, pressure losses, and real gas behavior for the simulation of membrane separation systems. They coded the modeling algorithm in Aspen Custom Modeler (ACM) and reported acceptable performance and high potential of their model for gas separation. Later, Hosseini et al. [50] modified the model presented by Kundu et al. [41]. They also presented a comprehensive model for non-ideal conditions in which real gas behavior, temperature, pressure, and concentration polarization effects were taken into account.

The HFMM can also be used for another type of gas separation system when an absorbent flows inside the fiber. In this case, the membrane is seen as a physical barrier between the liquid and gas phases and prevents liquid penetration to the shell side. In the case of CO_2, penetrants which pass through the membrane react with an absorbent such as an alkanolamine solution. Later, the permeate stream rich in CO_2 is sent to a regeneration unit and then recirculated to the membrane separation unit. A mathematical model can also be developed based on continuity, mass, and momentum equations for the shell, membrane, and fiber sides and a numerical software such as COMSOL is allowing to find accurate solutions for this system. More details about the equations and model development are also available in references [51-60].

1.5 Model development

A new numerical technique is introduced here for the modeling of HFMM for gas separation to calculate the flow rate and mole fraction in permeate and retentate streams. In this modeling approach, a system of ODE for a binary feed gas contains six dependent equations to be solved simultaneously using ODE solution methods like Runge-Kutta or finite difference method (FDM). Increasing the number of feed gas components not only increases the computation time but also decreases the efficiency of the numerical technique for a multi-stage separation system. The new numerical technique presented in this work introduces the concept of partial element stage cut which has similarity with K-value used in flash calculation of distillation column. This approach greatly reduces the computation time and improves the modeling result efficiency.

1.5.1 Model assumption

The assumptions for the model development are as follows:

1. The HFMM operates at steady state under isothermal or non-isothermal conditions.
2. The permeability is independent of pressure and gas composition.
3. The fibers do not deform during operation at high pressure.
4. Polarization at the membrane surface is negligible.
5. Pressure drop inside the fibers is calculated using the Hagen-Poiseuille equation.
6. The gas flow is laminar and ideal gas behavior is considered.

1.5.2 Modeling algorithm

The numerical solution is based on the 'succession of states' method. The module is discretized into a large number of independent finite elements in which the mass transfer driving force is constant. For the first element, the computation starts from the inlet with initial feed conditions (flow rate, mole fraction, pressure, and temperature) to the outlet (residue end). The outlet conditions of the first element are selected as the known inlet variables for the next element to compute the mass and energy balances, and pressure variation along the module. The same solution procedure is repeated until the residue end. The packing fraction (φ), defined as the ratio of the fibers cross-sectional area to the cross-sectional area of the fiber module, is defined as:

$$\varphi = 1 - \varepsilon = n_f \frac{d_o^{\,2}}{d_m^{\,2}} \tag{1.1}$$

where ε and n_f are the void fraction and fiber number in the module, respectively. d_o and d_m are the outer fiber diameter and inner module diameter. A multi-component feed gas with a flow rate of V_f and mole fraction of x_f is fed to the HFMM. Based on the numerical method used, the permeate and retentate flow rates (V_p, V_s) and mole fractions (y_p, x_s) are calculated with the known variables of each element. The driving force is the pressure difference between the shell (P_s) and fiber (P_t) sides.

1.5.3 Co-current flow (shell side feed) configuration

In the co-current flow pattern, the feed gas flows in the axial direction and parallel to the fiber bundle while the penetrant gases diffuse through the membrane and finally leave the module. Figure 1.1 shows a schematic diagram of a co-current flow membrane separation module and, the feed and permeate flows in the first and two successive elements.

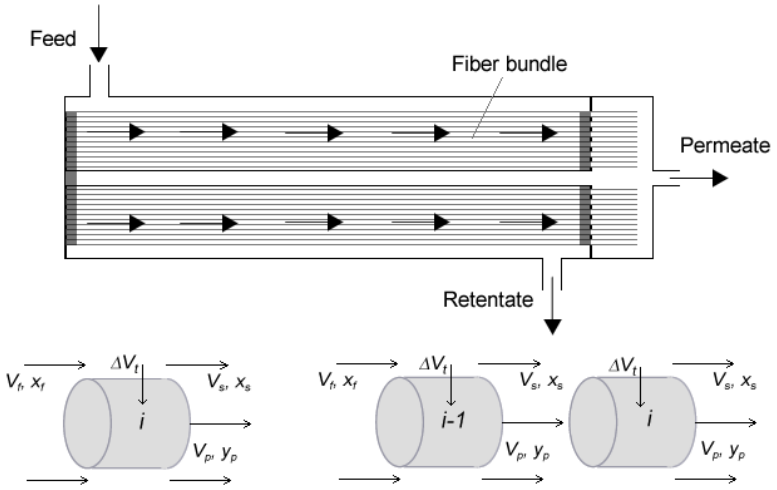

Figure 1.1 Schematic diagram of a co-current flow membrane separation module, and the feed and permeate flows in the first and two successive elements.

The volume and surface area for each element are calculated as:

$$\Delta v = \pi r_m^2 \Delta L \tag{1.2}$$

$$\Delta A_f = \frac{4\pi r_m{}^2 (1-\varepsilon)\Delta L}{d_o} \tag{1.3}$$

where r_m and ΔL stand for the module inner radius and element length, respectively. Based on the solution method, the mass balance equations for this element can be given by:

$$\Delta V_t(i) = \sum_{c=1}^{m} \Delta V_c(i) \tag{1.4}$$

$$\begin{aligned} &\Delta V_c(i) = \Delta A_f Q_c [P_s x_{s,c}(i-1) - P_t y_{p,c}(i)] \\ &c = 1, 2, ..., m \\ &i = 1, 2, ..., n \end{aligned} \tag{1.5}$$

where m and n are the numbers of components and elements, respectively.

$$V_s(i) = V_s(i-1) - \Delta V_t(i) \tag{1.6}$$

$$V_p(i) = V_p(i-1) + \Delta V_t(i) \tag{1.7}$$

where ΔV_t and ΔV_c represent the total and individual local permeate molar flow rates through the *i* element, respectively. The exact number of elements is determined after the mesh size analysis. For the first element, index (*i-1*) represents the feed conditions (V_f, x_f) whereas the permeate flow rate, $V_p(i-1)$, is zero. The stage cut, which is the ratio of permeate to feed flow rate in a single membrane module, is defined as:

$$\theta = \frac{V_p}{V_f} \tag{1.8}$$

Analogous to the vapor-liquid separation in a distillation column, a new parameter called the partial element stage cut, which determines the permeation efficiency of an individual gas component in each element, is introduced in a manner similar to a separation equilibrium constant similar to a K-value as:

$$\psi(i,c) = \frac{y_{p,c}(i)V_p(i)}{V_s(i-1)} \tag{1.9}$$

where $V_p(i)$ stands for the net flow rate of permeate stream in the fiber leaving element *i*. The sum of partial element stage cuts for all components in each element is equivalent to a local element stage cut (ψ_t) and defined for element *i* as:

$$\psi_t(i) = \psi(i,1) + \psi(i,2) + ... + \psi(i,m) \tag{1.10}$$

$$\psi_t(i) = \frac{y_{p,1}V_p(i)}{V_s(i-1)} + \frac{y_{p,2}V_p(i)}{V_s(i-1)} + ... + \frac{y_{p,m}V_p(i)}{V_s(i-1)} \tag{1.11}$$

$$\psi_t(i) = (y_{p,1} + y_{p,2} + ... + y_{p,m})\frac{V_p(i)}{V_s(i-1)} \tag{1.12}$$

$$y_{p,t}(i) = y_{p,1}(i) + y_{p,2}(i) + ... + y_{p,m}(i) = 1 \tag{1.13}$$

$$\psi_t(i) = \frac{V_p(i)}{V_s(i-1)} \tag{1.14}$$

The partial element stage cut in Eq. (1.9) is then substituted into Eq. (1.5) yielding a new equation for the *c* components of the first element as:

$$\psi(1,c)V_s(0) = \Delta A_f Q_c (P_s x_{f,c}(0) - P_t y_{p,c}(1)) \tag{1.15}$$

$$\psi(1,c) = \frac{P_s x_{f,c}(0)}{V_s(0)(\frac{1}{Q_c \Delta A_f} + \frac{P_t(1)}{V_p(1)})} \tag{1.16}$$

Similarly, Eq. (1.16) can be written for all components and later substituted into Eq. (1.14) to give:

$$\frac{P_s x_{f,1}(0)}{(\frac{1}{Q_1 \Delta A_f} + \frac{P_t(1)}{V_p(1)})} + \frac{P_s x_{f,2}(0)}{(\frac{1}{Q_2 \Delta A_f} + \frac{P_t(1)}{V_p(1)})} + \ldots + \frac{P_s x_{f,m}(0)}{(\frac{1}{Q_m \Delta A_f} + \frac{P_t(1)}{V_p(1)})} = V_p(1) \tag{1.17}$$

Eq. (1.17) is called the Membrane Flash Equilibrium Equation (MFEE) which can be written as:

$$\psi_t(1) = f(x_{f,c}(0), P_s(1), P_t(1)_t, Q_c, \Delta A_f, V_p(1)) \tag{1.18}$$

In terms of the numerical solution, Eq. (1.17) can be solved by iteration via Bisection, Newton-Raphson, and Brent's methods. Consequently, the stage cut, permeate composition, and retentate flow rate of the first element can be calculated by the numerical algorithm. The retentate composition is then obtained from a mass balance calculation over the element via:

$$x_{f,c}(0)V_f(0) = x_{s,c}(1)V_s(1) - \Delta V_t(1) \tag{1.19}$$

For the element beside the first element, the permeate composition and flow rate are also dependent on the permeate flow rate of the previous element. Similarly, a new equation can be derived for the other elements as:

$$\psi(i,c)V_s(i-1) - y_{p,c}(i-1)V_p(i-1) = Q_c \Delta A_f (P_s x_{s,c}(i-1) - P_t y_{p,c}(i)) \tag{1.20}$$

$$\psi(i,c)=\frac{P_s x_{s,c}(i-1)+\dfrac{y_{p,c}(i-1)V_p(i-1)}{Q_c\Delta A_f}}{V_s(i-1)\left(\dfrac{1}{Q_c\Delta A_f}+\dfrac{P_t(i)}{V_p(i)}\right)} \tag{1.21}$$

Thus, Eq. (1.21) can be written for all components and then substituted into Eq. (1.14) to give:

$$\begin{aligned}&\frac{P_s x_{s,1}(i-1)+\dfrac{y_{p,1}(i-1)V_p(i-1)}{Q_1\Delta A_f}}{\left(\dfrac{1}{Q_1\Delta A_f}+\dfrac{P_t(i)}{V_p(i)}\right)}+\frac{P_s x_{s,2}(i-1)+\dfrac{y_{p,2}(i-1)V_p(i-1)}{Q_2\Delta A_f}}{\left(\dfrac{1}{Q_2\Delta A_f}+\dfrac{P_t(i)}{V_p(i)}\right)}+\ldots\\&+\frac{P_s x_{s,m}(i-1)+\dfrac{y_{p,m}(i-1)V_p(i-1)}{Q_m\Delta A_f}}{\left(\dfrac{1}{Q_m\Delta A_f}+\dfrac{P_t(i)}{V_p(i)}\right)}=V_p(i)\end{aligned} \tag{1.22}$$

This new MFEE equation is also a function of the previous element conditions and simply written as:

$$\psi_t(i)=f\left(x_{x,c}(i-1),P_s(i),P_t(i),Q_c,\Delta A_f,V_p(i),y_{p,c}(i-1),V_{p,c}(i-1)\right) \tag{1.23}$$

The same numerical approach is used to solve Eq. (1.22), to calculate $V_p(i)$ and other unknown variables.

The pressure variation in the shell and fiber is calculated using the Hagen-Poiseuille equation as:

$$\frac{d(P_t^2)}{dL}=\frac{25.6R_gT\eta_{mix}}{\pi d_i^4}\left(\frac{V_p}{n_f}\right) \tag{1.24}$$

$$\frac{dP_s}{dL}=-\lambda\frac{\rho}{2d_{hyd}}\gamma \tag{1.25}$$

where P_t, R, T, and η_{mix} are the fiber pressure, universal gas constant, gas temperature, and mixture viscosity, respectively. P_s, d_{hyd}, λ, ρ, and γ represent the shell pressure, hydraulic diameter, friction factor, density, and gas velocity, respectively. Since a laminar flow is assumed in both shell and fiber sides, the friction factor is inversely proportional to the Reynolds number and expressed as:

$$\mathrm{Re} = \frac{2G_s d_o}{\eta_{mix}} \tag{1.26}$$

$$\lambda = \frac{64}{\mathrm{Re}} \tag{1.27}$$

where G_s is the mass flow rate per unit cross-sectional area of the module. According to the process design data, the gas velocity is set between 1.5 and 1.7 m/s on the shell side and between 0.01 and 0.38 m/s on the fiber side [49]. The fiber pressure in the first element is unknown and an iteration method is needed to calculate the pressure profile along the module length. Wike's equation is also chosen to calculate the gas-mixture viscosity with an average error of 2% [42].

$$\eta_{mix} = \sum_{\alpha=1}^{m} \frac{x_\alpha \eta_\alpha}{x_\alpha + \sum_\beta x_\beta \sigma_{\alpha\beta}} \tag{1.28}$$

$$\sigma_{\alpha\beta} = \frac{1}{\sqrt{8}}\left(1+\frac{M_\alpha}{M_\beta}\right)^{-0.5}\left[1+\left(\frac{\eta_\alpha}{\eta_\beta}\right)^{0.5}\left(\frac{M_\beta}{M_\alpha}\right)^{0.25}\right]^2 \tag{1.29}$$

where α and β are the gas component indices. η and M are Wike's coefficient and molecular weight, respectively.

The mass balance equations for cross-flow and counter-current flow configurations are also available in the supplementary materials.

1.5.4 Model validation

The model combined with the proposed numerical procedure was used to predict the separation performance of six different gas mixtures under different operating conditions and the results are compared with experimental data reported in the literature [36, 61-64]. Table 1. presents the module characteristics and feed conditions for the modeling cases.

Table 1.1 The properties of the experimental hollow fiber modules and feed conditions.

Parameters	**Unit**	**Case I**	**Case II**	**Case III**	**Case IV**	**Case V**	**Case VI**
Fiber outer diameter (d_o)	μm	230	200	735	156	160	200
Fiber inner diameter (d_i)	μm	84	80	389	63	80	80
Active length (L)	cm	63.8	15	15	26	25	15
Number of elements	-	128	30	30	52	50	30
Module inner diameter	cm	0.48	2.1	1	0.5	0.95	0.21
Packing fraction (φ)	-	0.16	0.18	0.54	0.26	0.10	0.18
Temperature (T)	K	298	298	301	303	301	298
Feed pressure (P_s)	kPa	404	6964	405.3	1570	690	3520
Permeate pressure (P_t)	kPa	101	1123	101.3	101.3	100	92.80
Feed composition (x_f)	%	CO_2 40	H_2 51.78	CO_2 60	CO_2 50	O_2 20.5	CO_2 48.5
		N_2 60	N_2 24.69	CH_4 40	O_2 10.5	N_2 79.5	CH_4 27.9
			CH_4 19.57		N_2 39.5		C_2H_6 16.26
			Ar 3.96				C_3H_8 7.34
Permeance (Q_n)	GPU	CO_2 63.6	H_2 284	CO_2 31.6	CO_2 204.20	O_2 9.30	CO_2 40.04

An asymmetric cellulose acetate (CA) membrane was used in case I to separate a binary gas mixture of CO_2 and N_2. Figure 1.2a shows a comparison between the modeling results and experimental data [62]. As shown, the highest value of CO_2 mole fraction in the permeate (0.85%) is observed for the lowest value of stage cut (0.1). As a general rule, increasing the stage cut results in a reduction of the CO_2 mole fraction in the permeate stream. In terms of modeling, the stage cut value can be increased by two different scenarios: a) increasing fiber's length and b) reducing in feed flow rate.

Pan [36] conducted an experiment to separate a gas mixture (H_2, N_2, CH_4, and Ar) by using a high-flux asymmetric cellulose acetate membrane. Figure 1.2b shows a comparison between the modeling results of case II with the experimental data. The high value of H_2 permeance (284 GPU) compared to the other gases makes this membrane very selective for the separation of H_2. As seen, increasing the stage cut up to 40% does not have a very significant effect on H_2 mole fraction in the permeate stream. A moderate stage cut of 50% still provides high H_2 mole fraction (~0.92%) which is appropriate for a single stage separation unit.

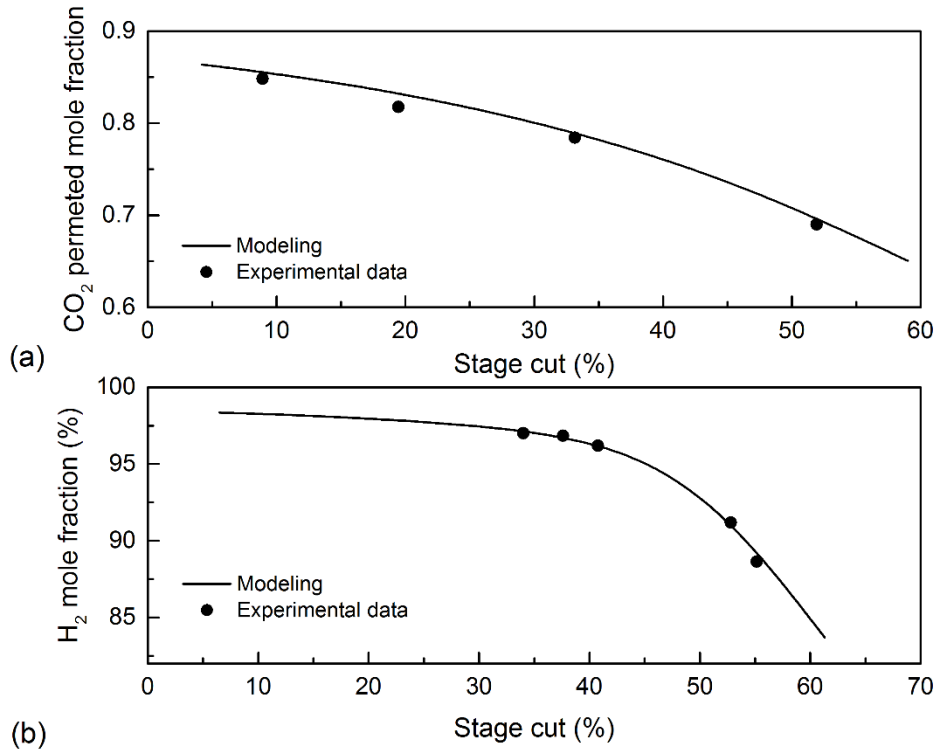

Figure 1.2 Comparison of modeling results with the experimental data of: (a) Sidhoum, Sengupta, and Sirkar [62], (b) Pan [36].

Tranchino et al. [61] used a composite membrane with a support polymer (polysulfone) and an aliphatic copolymer coating to separate CO_2 and CH_4 under different operating conditions. Figure 1.3a shows a comparison between the modeling of case III with experimental data at two different temperatures. As shown, a higher feed temperature produces lower CO_2 mole fraction in the permeate stream while the selectivity of CO_2/CH_4 decreases with increasing temperature. The non-isothermal option of the model is used to calculate the permeability of CO_2 and CH_4 along the fiber. In this case, a good agreement is also seen between the modeling result and experimental data at 65°C. However, a deviation of 5% between both curves can be considered negligible when the CO_2 mole fraction and stage cut values are high and moderate, respectively. The model's performance is also investigated for the cases in which the transmembrane pressure changes moderately. Figure 1.3b shows the effect of pressure change from 200 to 600 kPa on CO_2 mole fraction. The modeling results show that CO_2 mole fraction increases with increasing feed pressure due to the higher separation driving force.

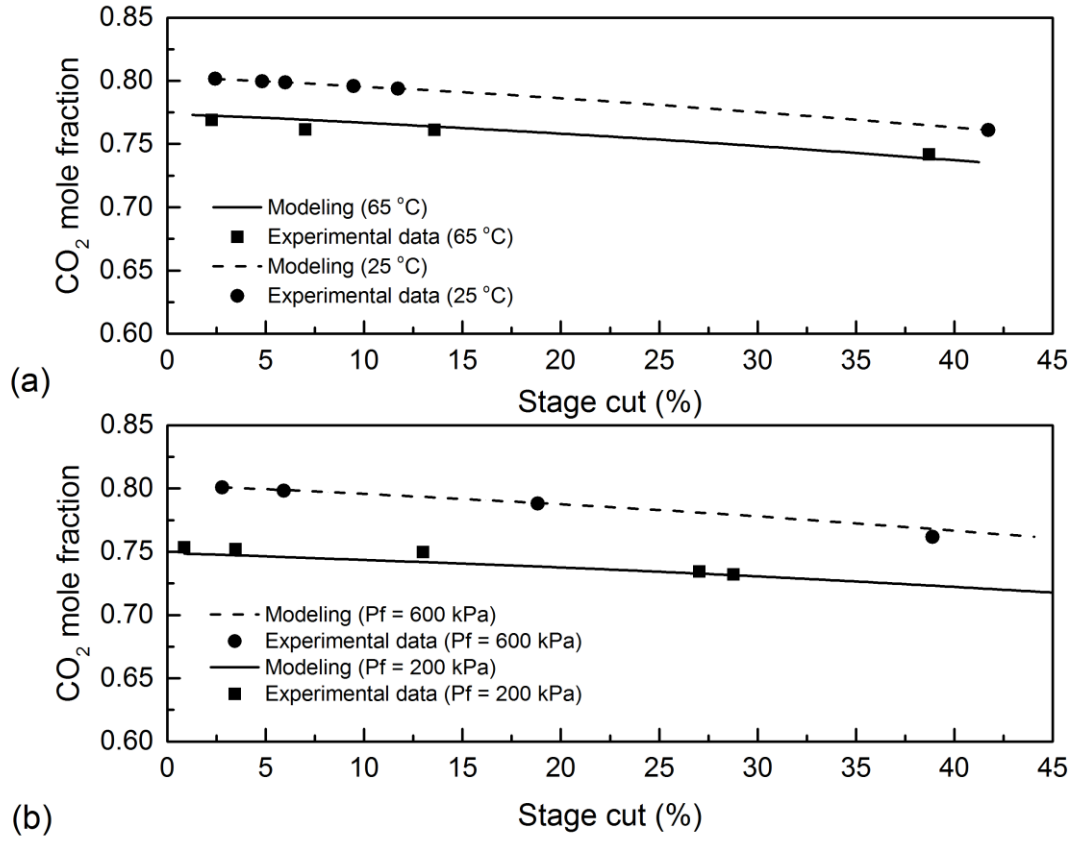

Figure 1.3 Comparison of modeling results with the experimental data of Tranchino et al. [61], (a) at two different feed temperatures (25 and 65°C), (b) at two different feed pressures (200 and 600 kPa).

Sada et al. [65] also investigated the performance of an asymmetric cellulose triacetate membrane for the separation of CO_2-air mixtures at 30°C by using a hollow fiber membrane module. Figure 1.4a shows a comparison between the case IV modeling results and experimental data. The CO_2 mole fraction on the permeate side slowly decreases from 0.85 to 0.70 up to a stage cut as high as 0.7 for a single stage separation unit. This indicates the high potential use of the selected membrane in a multi-stage separation system.

Feng et al. [63] conducted an experiment to separate O_2/N_2 mixtures with asymmetric hollow fiber membranes. Figure 1.4b shows the case V modeling results which fitted the experimental data for both co-current and counter-current configurations. The N_2 mole fraction in the retentate side shows no significant difference between the two modes over the lowest range of stage cut values. When the stage cut increases however from 0.4 to 0.9, the conditions become more interesting for production

of nitrogen at low oxygen content. Similarly, the modeling results show that the separation performance for the counter-current configuration is better than the one of the co-current configuration, especially when the separation process is designed for high stage cut ranges.

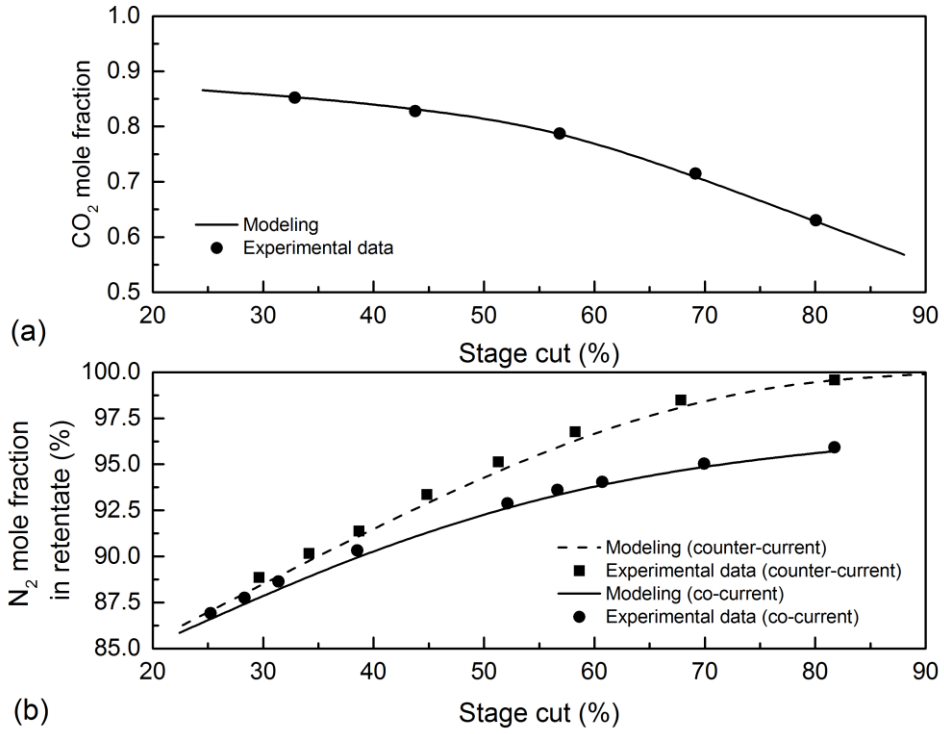

Figure 1.4 Comparison between modeling results and the experimental data of: (a) Sada et al. [65], (b) Feng et al. [63].

Pan [36] also carried out another experiment to illustrate the good potential of asymmetric cellulose acetate membranes for CO_2 separation from a hydrocarbon mixture. Figure 1.5 shows a comparison between the case VI modeling results and experimental data. High CO_2 mole fraction (>90%) can be achieved in the permeate side for stage cut values of 30-50%. The modeling results also show that increasing the stage cut value results in a reduction of the quality of the permeated stream. More interestingly, CH_4 mole fraction lost in the permeate side is in an acceptable range (2-6%) when the stage cut value is around 40-50%. According to these results, CA membranes have good potential for natural gas separation.

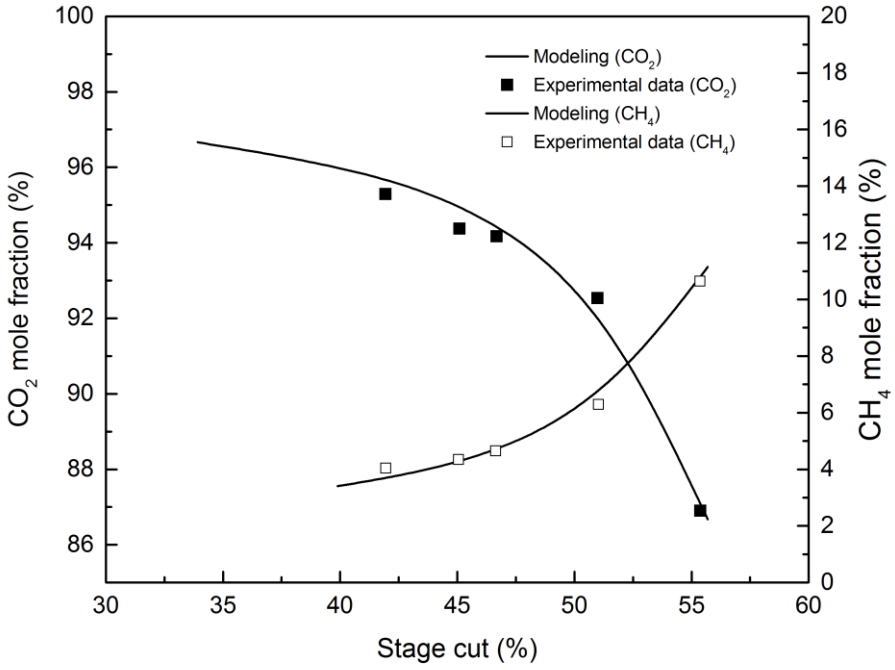

Figure 1.5 Comparison between case VI modeling results and the experimental data of Pan [36].

As shown above, the new modeling approach was used to predict the separation performance of six different experimental systems. In all cases, the modeling results were in good agreement with the experimental data. It is expected that the model proposed combined with the new numerical technique is robust and reliable for the modeling and simulation of gas separation modules and two typical examples are presented next.

1.6 Case study: oxygen enrichment

Air separation can be carried out by several processes such as cryogenic distillation, pressure swing adsorption, and membrane separation in which the main target is to enrich air in either nitrogen or oxygen [66-69]. Oxygen Enriched Air (OEA) production with different purities is used in various chemical applications such as combustion enhancement of natural gas and coal gasification. A membrane separation system may be used to produce oxygen with lower energy consumption compared to conventional methods. Membranes with O_2/N_2 selectivities above 2 are sufficient to produce 99% pure N_2, but N_2 recovery is low which consequently, would impose an extra cost for gas compression [70]. On the contrary, O_2 production strongly depends on the membrane O_2/N_2 selectivity. This separation is more difficult as the feed gas (air) only contains 21% O_2 and a large

amount of N_2 must be removed. Therefore, the number of membrane modules needed is high to produce a high volume of oxygen with a desired purity in the permeate stream. Future improvement in membrane selectivity may result in a solution for this problem.

Here, the proposed model is used to design single and multi-stage separation processes to predict the required number of commercial modules for a given oxygen production. The model and numerical technique are used to simulate a membrane gas separation system for the production of 16387 cm^3/s (50000 ft^3/day) O_2 with a purity of 60% as the permeate which can be consumed in other industrial units. Referring to the above validation section (case V), Feng et al. [63] used an asymmetric hollow-fiber membrane with a selectivity of 5.7 and conducted experimental work to separate a O_2/N_2 gas mixture. The aim is to compare the separation performance and show the potential of these membranes for O_2 production using a membrane gas separation unit. It is important to define a real case unit to compare with experimental results. Hence, the same feed composition, permeability and fiber size as in case V are chosen as input. The gas mixture (O_2/N_2) is firstly fed to a single stage unit and then distributed into a number of parallel membrane modules to produce O_2 with the desired quality. Then, the exact number of required modules is calculated based on the membrane O_2/N_2 selectivity as reported by Feng et al. [63] and on typical ranges of gas velocity in the retentate and permeate sides which are 1.5-1.7 m/s and 0.01-0.38 m/s, respectively [49]. Table 1.2 presents the parameters used for the modeling of the O_2 production unit.

Table 1.2 Parameters used for the modeling of the O_2 production unit.

Parameters	Unit	Value
Feed pressure	kPa	600
Feed temperature	K	296
Fiber length	cm	183
Shell diameter	cm	20.5
Fiber outer diameter	µm	160
Fiber inner diameter	µm	90
Fibers number	-	$3x10^5$, $6x10^5$
Packing density	%	48
Packing fraction	-	0.19

In all modeling cases, the element refinement approach is taken to determine the most accurate modeling results under different operating conditions. Hence, the number of elements along the module active length used in the calculation may be varied to find the optimal value above which no changes in stage cut and product concentration of both permeate and retentate streams are observed.

For the modeling, the feed and permeate pressures are chosen to be 600 and 100 kPa, respectively. Figure 1.6 presents the separation performance of the membrane used for O_2 production using a single stage system, while the number of fibers per module is set to $3x10^5$ and $6x10^5$, respectively. Referring to the above-mentioned ranges of gas velocity, the feed flow rates needed for the O_2 production of 50,000 ft^3/day are different for both cases so that an intrinsic stage cut can be defined for a primary analysis of separation performance. The modeling results show that an increase in the number of fibers results in a reduction in O_2 mole fraction in the permeate side and an increase in the stage cut. A comparison between Figure 1.6 shows that the average permeated flow rates are 2600 and 5000 cm^3/s for $3x10^5$ and 6 $x10^5$ fibers, respectively.

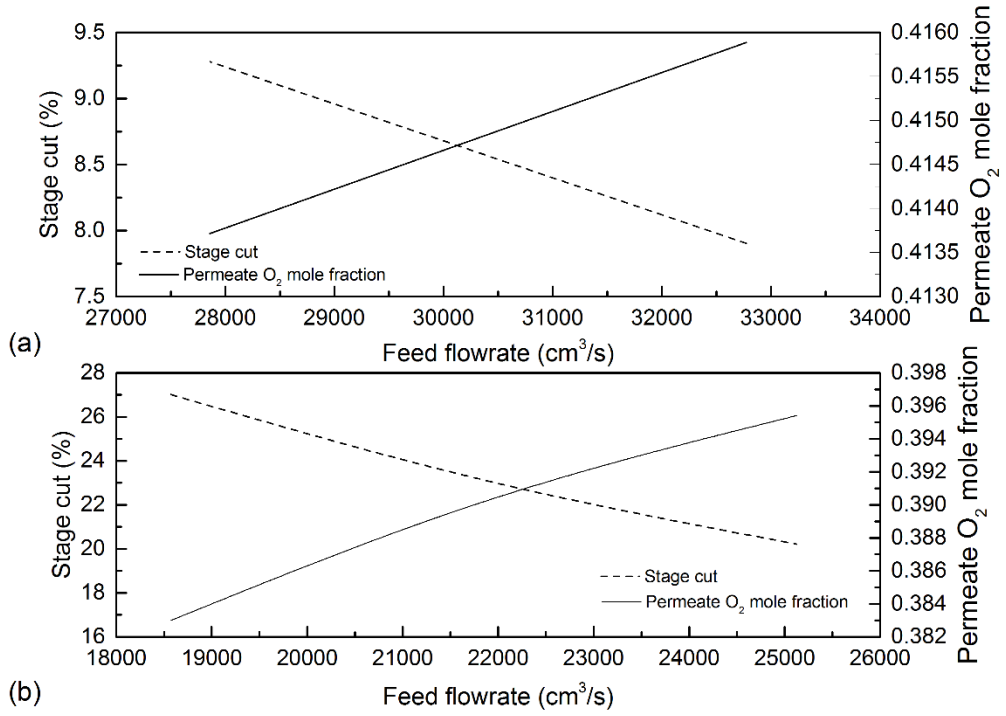

Figure 1.6 Separation performance in terms of stage cut and O_2 mole fraction as a function of module feed flow rate: (a) Pf = 600 kPa, Pp = 100 kPa, number of fibers = $3x10^5$, (b) Pf = 600 kPa, Pp = 100 kPa, number of fibers = $6x10^5$.

The modeling results show that the average O_2 mole fraction on the permeate side is about 40% for both cases under the same operating conditions that is below the separation target (60%). As an alternative, an extra membrane gas separation unit can be added to improve O_2 purity. In this case, the same membrane modules with $3x10^5$ and $6x10^5$ fibers are used in the second unit. In the case of designing a two stage gas separation system, the inlet flow rate of the module is calculated based on the gas velocity inside the module, number of fibers, and number of modules in each unit. In the case

of N_2 production, as air already has 79% N_2, the residue stream usually contains N_2 in higher purity. Thus, the production of pure N_2 using a single stage separation unit is easier. On the contrary, the design of an O_2 production unit is more difficult as N_2 can also permeate along with O_2, limiting O_2 purity in the permeate stream. Referring to the selected membrane properties, high O_2/N_2 selectivity results in an increase in the permeate flow rate. In the techno-economic analysis, it is expected that the number of modules in the first separation unit increases to supply the required inlet flow for the second unit. Referring to the single stage separation results, the permeate flow (40% O_2 purity) is relatively low to feed the second unit. Thus, the number of modules must be increased in the first separation unit. In this case, 25 (for $3x10^5$ fibers) or 13 (for $6x10^5$ fibers) modules are needed to supply enough flow for the second unit.

Based on the estimated number of modules, the permeate flow leaving the first separation unit is compressed and thereafter fed to the second separation unit. Figure 1.7 shows the separation performance of the second unit while the number of fibers is set to $6x10^5$. In these conditions, the mole fraction of O_2 in the permeate reaches 62% at a flow rate of 22000 cm^3/s.

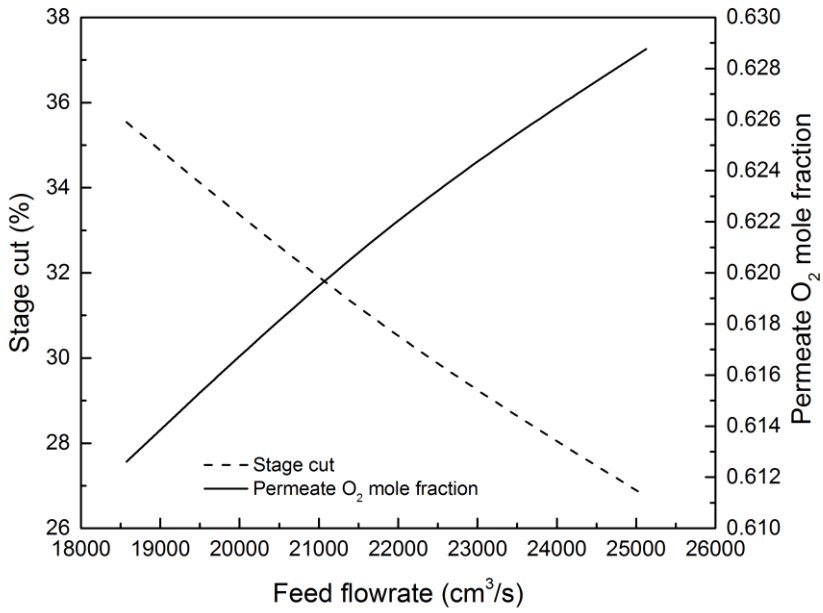

Figure 1.7 Separation performance in terms of stage cut and O_2 mole fraction as a function of module feed flow rate (Pf = 600 kPa, Pp = 100 kPa, number of fibers = $6x10^5$).

Table 1.3 presents a summary of the current case study of O_2 production using a two stage separation unit. With respect to the modeling results, 13 and 3 membrane modules are required for the first and second separation stages to produce 16387 cm^3/s (50000 ft^3/day) O_2 with a purity higher than 60%. The permeate product could also be fed to a third separation unit to further enhance O_2 purity. This configuration would, however, require more equipment and pipelines to recompress the permeate flow of the second unit resulting in a higher energy consumption. The optimization of the membrane separation system for O_2 production is beyond the scope of this study but the further analysis can also be carried out to optimize the operational costs by finding the optimum values of required separation area, transmembrane pressures, and efficient ranges of O_2/N_2 selectivities.

Table 1.3 Summary of the modeling results of a two-stage membrane separation unit for O_2 production.

Unit	O_2 mole fraction		Number of modules	Number of fiber/module	Total separation area (m^2)
	permeate	retentate			
First	0.390	0.149	13	$6x10^5$	7135
Second	0.622	0.295	3	$6x10^5$	1646

1.7 Case study: natural gas processing

Raw natural gas collected at a wellhead as a gaseous mixture contains a wide range of compounds in addition to methane, for example, heavier alkanes and aromatics, water, hydrogen sulphide, mercury and silicon-containing compounds, carbon dioxide, nitrogen, and helium. The composition highly depends on the geological area and the underground deposit type, depth, and location of reservoirs. Some of these components might cause serious operational problems and therefore need to be removed through a series of separation processes. In terms of acid gases, H_2S can be removed by a desulphurization process and its product can then be utilized for other applications such as Sulphur Recovery Unit (SRU). The CO_2 content in raw natural gas varies from 2 to 80%. As CO_2 reduces the natural gas heating value and is highly corrosive, it needs to be removed and thereafter sent to the CO_2 Sequestration Unit or used for Enhanced Oil Recovery (EOR) projects. The current conventional separation methods including absorption, adsorption, and cryogenic distillation can be employed to capture CO_2. Despite the CO_2 content, these methods are even capable of removing 99% of CO_2 from the feed stream. Referring to the gas pipeline standards, the product enriched to methane >97% which has a CO_2 content as low as 2-3%, can be injected into the natural gas grid. Moreover, the current

natural gas sweetening market is dominated by amine absorption process. However, this process is highly energy-intensive and suffers from serious operational problems. In this case, membrane technology can be regarded as an alternative method for the natural gas purification due to its simplicity, ease of installation, and low operation cost.

The model and new numerical technique were used to simulate a natural gas purification process using incorporation of Aspen Plus (version 8.8) and MATLAB (2015b) software. As there is no unit component in Aspen Plus toolbox for hollow fiber membrane, Excel software is deployed to link Aspen Plus to MATLAB software. In this case, Aspen Plus indirectly calls the model's function through Excel interface to use for its internal calculation. In the first part, raw natural gas with different CO_2 contents (10, 25, 50, and 75%) was chosen as feed to a single membrane unit. The gas flow rate is set to 10 mol/s and the feed and permeate pressures are kept at 35 and 1 bar, respectively. The initial CO_2 and CH_4 permeance are also experimental data [71] of 17.7 and 0.73 GPU, respectively. The aim of this simulation is to find the proper CO_2/CH_4 selectivity while a single membrane unit is used for the natural gas purification. Figure 8a shows the relation amongst stage cut, retentate CH_4 mole fraction, and membrane area when the feed gas contains CO_2 10%. As shown, increasing the CO_2/CH_4 selectivity results in increasing the retentate CH_4 mole fraction. Using CO_2/CH_4 selectivity of 48 and 72 is appropriate to reach CH_4 mole fraction of 97% for the stage cut of 10%. The required membrane area is 500 m^2 which is much lower than in the other cases reported in Figure 1.8a. This also ensures a lower CH_4 loss in the permeate stream. The simulation findings reveal that no significant difference in the retentate CH_4 mole fraction is seen between CO_2/CH_4 selectivities of 48 and 72. The retentate CH_4 mole fraction reaches 97% by using CO_2/CH_4 selectivities of 12 and 24 only as the required membrane area is set to 2500 m^2. In this case, stage cut increases approximately to 20% resulting in a higher CH_4 loss in the permeate stream. Figure 1.8b and Figure 1.9 show the effect of CO_2/CH_4 selectivities on the retentate CH_4 mole fraction and membrane area for the different CO_2 (25, 50, and 75%) content in the feed gas. As expected, using low CO_2/CH_4 selectivities results in a dramatic increase in the required membrane area particularly when the selectivities are 12 and 24. This causes an increase in CH_4 loss even if some amount of permeate gas is recycled. The higher the retentate CH_4 mole fraction, the higher the membrane area is required which results in an uneconomical and unrealistic process.

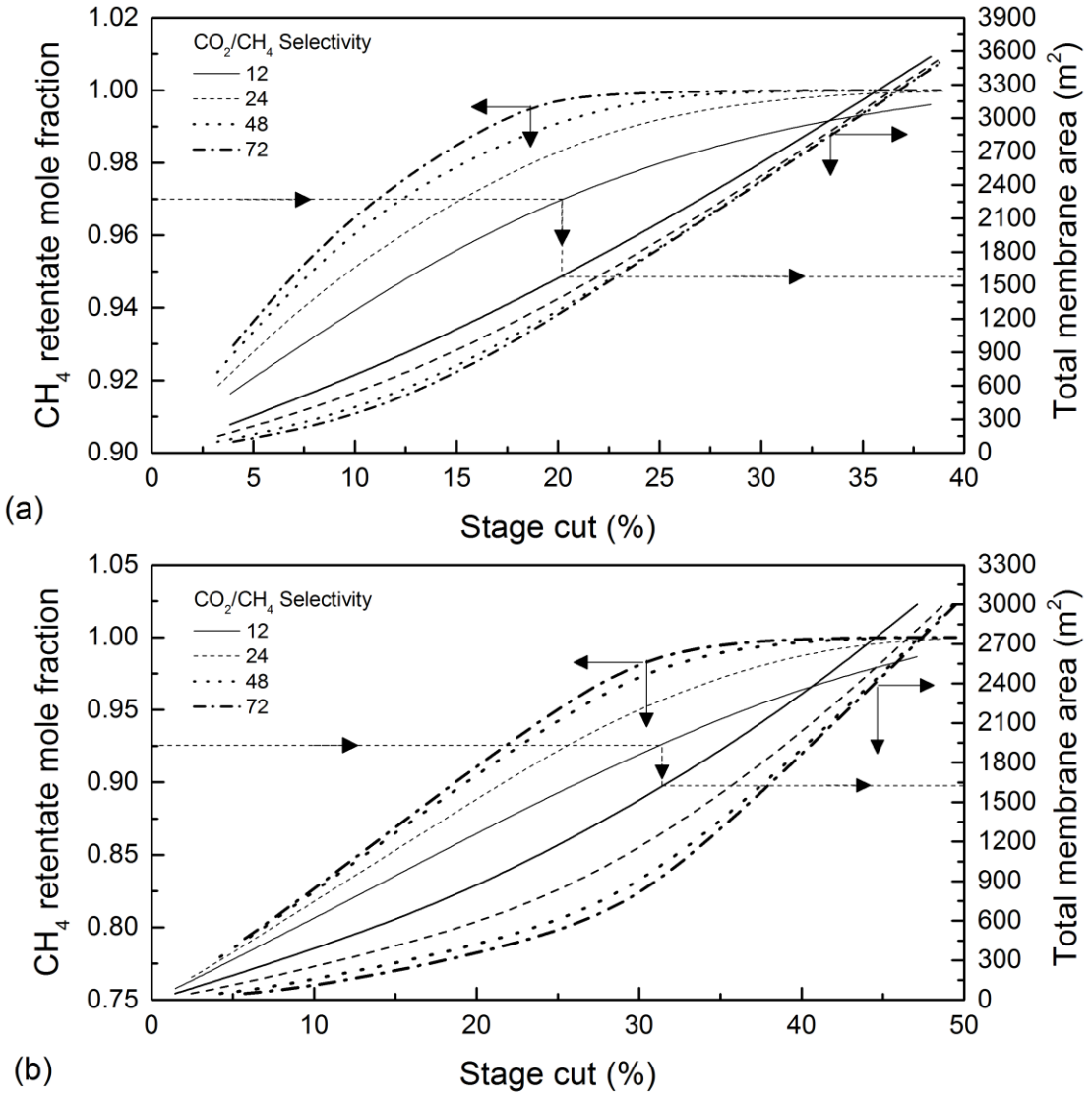

Figure 1.8 Effect of different CO_2/CH_4 selectivities on the CH_4 retentate mole fraction and total membrane area, (a) CO_2 content in feed = 10 mol.%, (b) CO_2 content in feed = 25 mol.%.

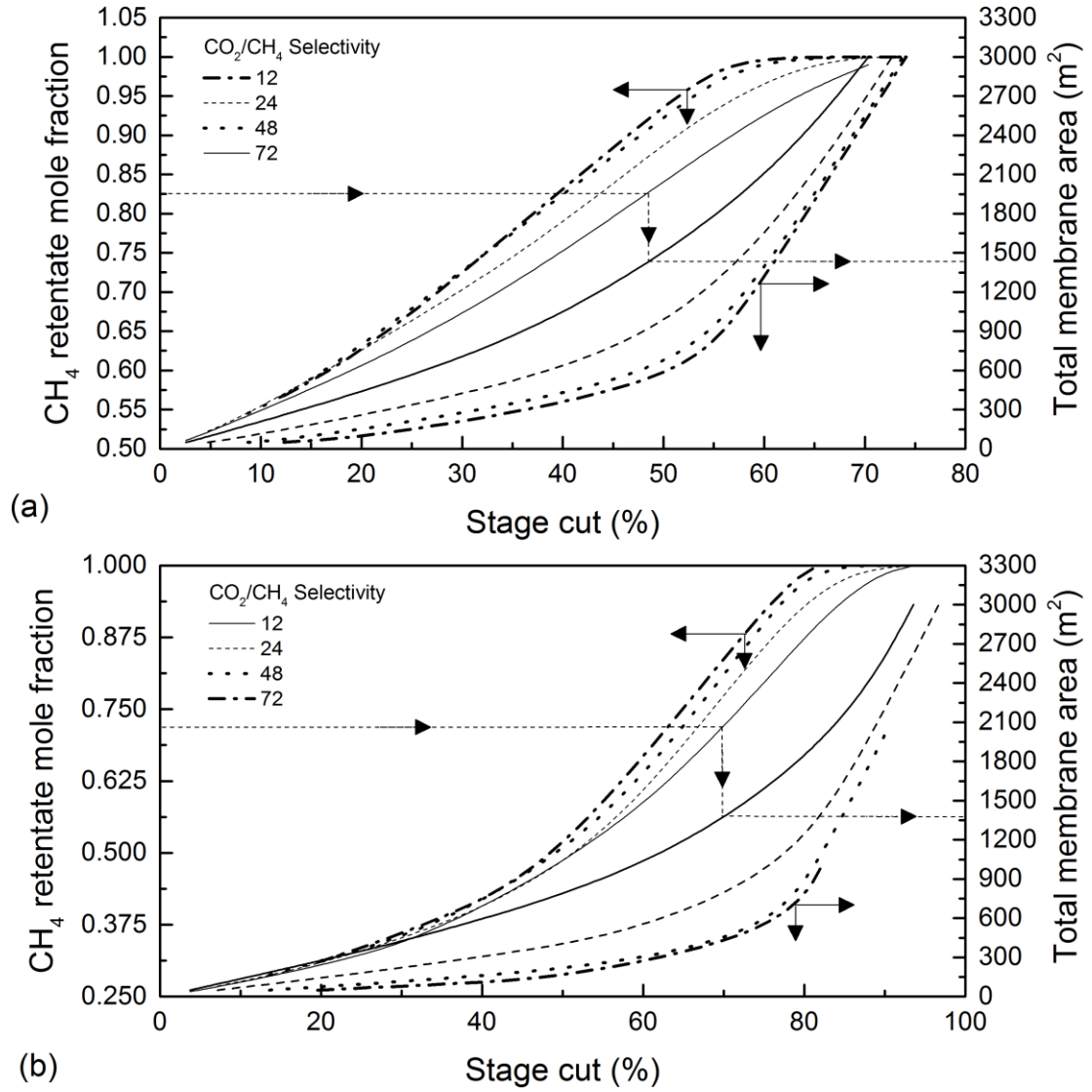

Figure 1.9 Effect of different CO_2/CH_4 selectivities on the CH_4 retentate mole fraction and total membrane area: (a) CO_2 content in feed = 50 mol.%, (b) CO_2 content in feed = 75 mol.%.

In the second part, a two-stage separation unit was designed to simultaneously reduce the CH_4 loss in the permeate stream and the total required membrane area. Figure 1.10 shows the process flow diagram of the natural gas purification process using two membrane units. The feed (CO_2 50%) has a flow rate of 10 mol/s and a membrane with a CO_2/CH_4 selectivity of 72 was chosen for this simulation case. As shown, the raw natural gas is initially fed to the first membrane unit and the retentate product is then sent to the second one. The permeate product of the second unit is recompressed and recirculated to the mixer. The simulation result shows that the retentate and

permeate CH_4 mole fraction can reach 97 and 2% while the required membrane areas of the first and second units are 200 and 300 m^2, respectively. The CH_4 loss in the permeate stream also decreases by 2.6%. The current simulation result also unveils the high potential of membrane technology for natural gas separation area.

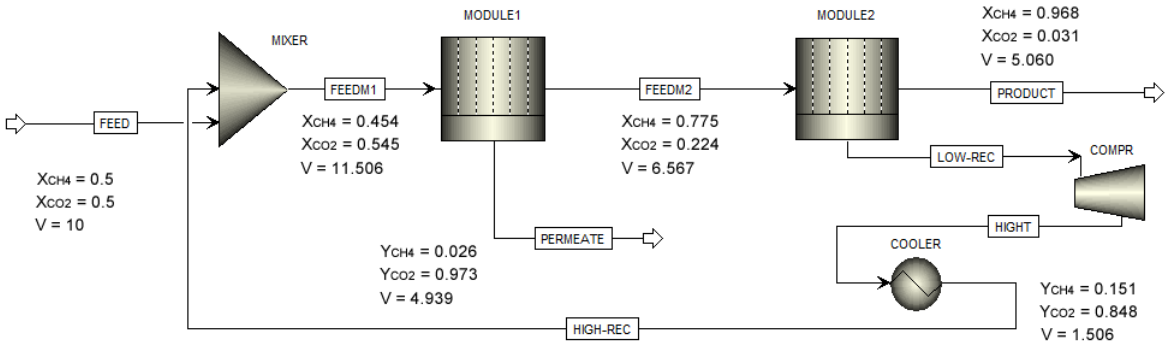

Figure 1.10 Process flow diagram of the natural gas purification using two membrane units.

1.8 Use of the model in guiding experimental membrane development

The new modeling approach which results in significant reduction in computation time allows a rapid estimation of the effects of membrane properties on large scale separation performance. The problem is made especially significant by recent developments of new membrane materials with exceptional properties, either extremely large selectivities or extremely large permeabilities [72].

How will such developments affect the dimensions of commercial hollow fiber modules? Figures 1.11-13 show the effect of O_2/N_2 selectivity (α) changes on O_2 permeate mole fraction and O_2 recovery in a single stage process. In these simulation cases, the total membrane separation area was varied from 500 to 9000 m^2 which can be fitted in approximately from 3 to 15 typical industrial modules with a module length of 180 cm. The initial O_2 and N_2 permeances were experimental data [63] of 9.3 and 1.8 GPU, respectively. In addition, the feed gas (air) with a flowrate of 10 mol/s is initially compressed up to 6 bar and the permeate side is kept at ambient pressure. As shown, in the case of varied O_2 permeance and constant N_2 permeance (Figure 1.11), increasing the O_2/N_2 selectivity from 5 to 40 increases the O_2 mole fraction in the permeate stream from 0.42 to 0.65 for a single unit having 500 m^2 membrane area. This figure also indicates that the enhancement of O_2 mole fraction in the permeate stream for a given membrane selectivity entails the reduction of the O_2 recovery.

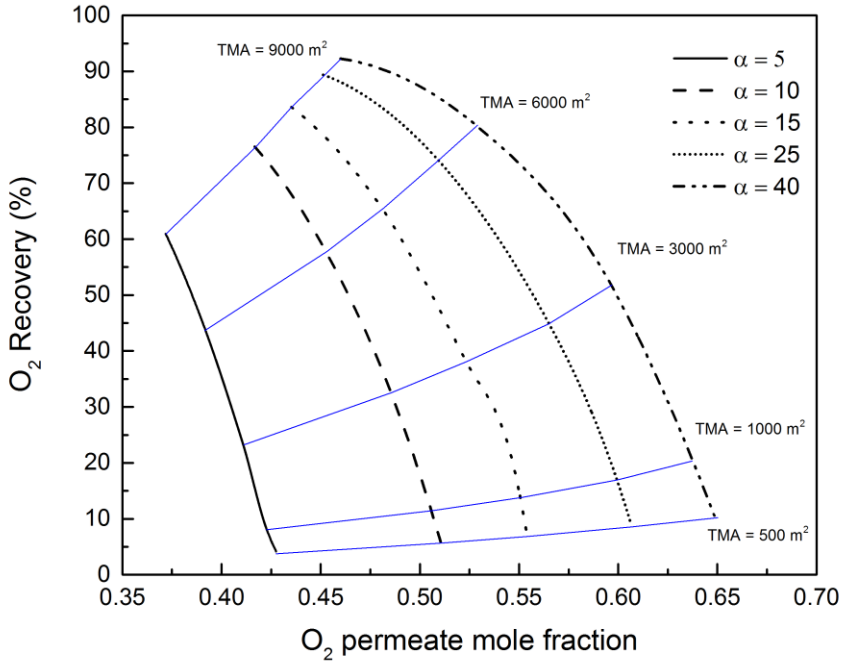

Figure 1.11 Effect of O_2/N_2 selectivity on the O_2 permeate mole fraction and O_2 recovery in a single membrane unit, (N_2 permeance = 1.8 GPU, O_2 permeance variable).

Similarly, at a constant O_2 permeance (Figure 1.12), increasing the O_2/N_2 selectivities from 5 to 40 by decreasing N_2 permeance improves the O_2 mole fraction in the permeate stream. The major difference between the two simulation cases is associated with the O_2 recovery. The simulation results show that a lower O_2 permeance leads to an increase in the required membrane area in order to compensate for the O_2 loss in the retentate stream. Figure 1.13 also shows the effect of O_2/N_2 selectivities on the O_2 permeate mole fraction and O_2 recovery using a single stage process. In this case, N_2 permeance is doubled reported in Figure 1.11 whereas O_2 permeance increases to make O_2/N_2 selectivities from 5 to 40. This change in membrane permselectivities results in a reduction in O_2 permeate mole fraction and an increase in O_2 recovery compared to the simulation case of Figure 1.11. It is obvious that a membrane with lower N_2 permeance and higher O_2 permeance is more effective for a realistic air enrichment process. Most importantly, the simulation results show that using high selectivities cannot allow enriching to 99% O_2 through a single stage process and it is therefore essential to use a multi stage process to separate O_2 using a moderate O_2/N_2 selectivity. The calculations reported in Figures 1.11-13 indicate how the model would allow setting realistic membrane performance targets in the development of new membrane materials.

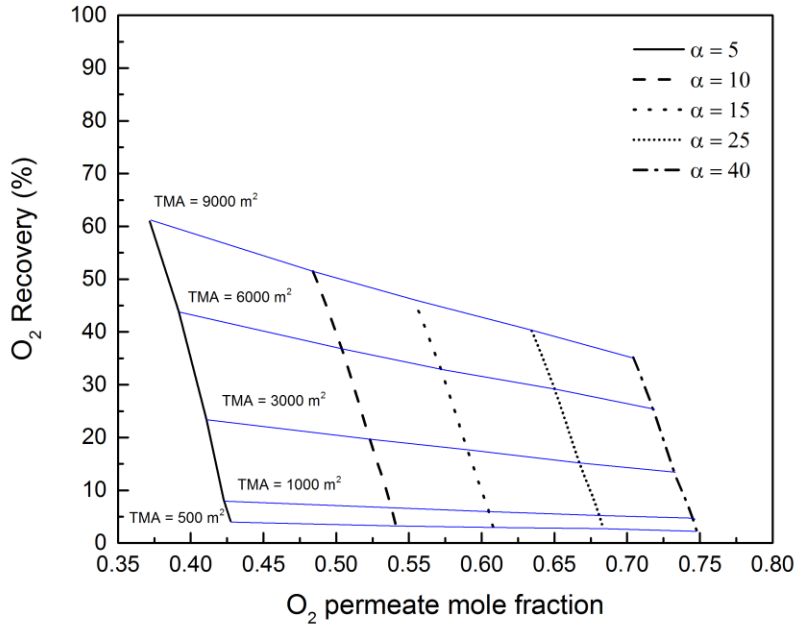

Figure 1.12 Effect of O_2/N_2 selectivity on the O_2 permeate mole fraction and O_2 recovery in a single membrane unit, (O_2 permeance = 9.3 GPU, N_2 permeance variable).

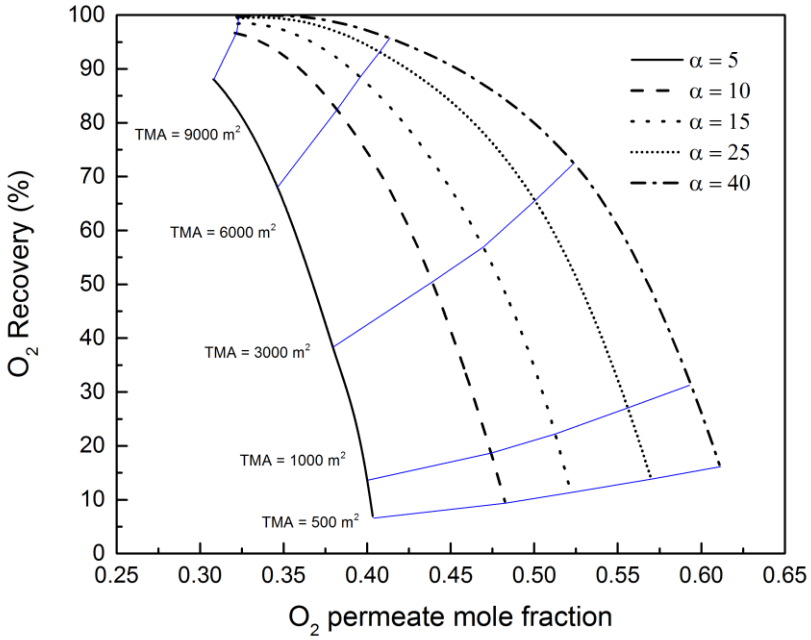

Figure 1.13 Effect of O_2/N_2 selectivity on the O_2 permeate mole fraction and O_2 recovery in a single membrane unit, (N_2 permeance = 3.6 GPU, O_2 permeance variable).

1.9 Conclusion

In this study, the simulation of a gas separation process was carried out by developing a model for hollow-fiber membrane modules. A new numerical technique was introduced on the basis of the flash calculation method. In order to validate the model, the results for co-current and counter-current gas separation processes were compared with experimental data taken from literature and good agreements were observed for six different cases. The results showed that the current model, using the new numerical technique, was also useful for the simulation of separation units using multi-component gas mixtures under different operating conditions. In this numerical technique, the membrane flash equilibrium equation (MFEE) was introduced to calculate the mole fractions and gas flow rates on the permeate and retentate sides. After validation, the model was also used to simulate a real case air-enrichment process using an asymmetric hollow-fiber membrane in single and two stage separation units. The results showed that low O_2 mole fraction (~40%) could be achieved in the permeate side using a single stage unit with two different numbers of fibers ($3x10^5$ and $6x10^5$). Then, a two stage membrane unit was selected to reach the target O_2 purity (60%) and flow rate (16387 cm^3/s). The results also showed that 13 and 3 modules with a total number of fibers of $6x10^5$ for the first and second membrane separation units are required to meet these targets. Either improvement of O_2/N_2 selectivity or adding more membrane separation units is required to get higher purity (above 60%). For oxygen production, different economic parameters such as membrane fabrication cost, membrane life, and transmembrane pressure ranges should be considered to confirm the feasibility of these membrane separation processes. Furthermore, the model with the numerical technique was used to simulate the natural gas purification process using the incorporation of Aspen Plus and MATLAB software. Four different CO_2/CH_4 selectivities (12, 24, 48, and 72) were chosen to show the separation performance of a single membrane unit. The simulation result showed that CO_2/CH_4 selectivities of 48 and 72 were more effective to reach 97% CH_4 and the required membrane area significantly decreased. Lower CO_2/CH_4 selectivity resulted in an increase in the required membrane area and CH_4 loss in the permeate stream dramatically went up. A two stage separation unit was suggested to decrease both the required membrane area and the CH_4 loss in the permeate stream. The simulation finding revealed that the feed gas (CO_2 50%) was enriched to 97% CH_4 in the retentate stream while the CH_4 loss was also declined by 2.6%. Finally, the model was used to estimate the effect of membrane properties on the separation performance. The model was capable of showing the effect of intrinsic and modified O_2 and N_2 permeances on O_2 recovery and O_2 mole fraction in the permeate stream using a single membrane unit. The results showed that increasing O_2/N_2 selectivity calculated based on constant and varied O_2 permeances was more in favor of increasing the product quality. The lower O_2 permeance, however, led to increase the membrane separation area in order to compensate

for the O_2 loss in the retentate stream. By doubling N_2 permeance and increasing O_2 permeance, the consequent change in the membrane permselectivities also resulted in a reduction in O_2 permeate mole fraction and an increase in O_2 recovery. Hence, using the membrane with the lower N_2 permeance and the higher O_2 permeance was the proper modification target resulting in the more economical air enrichment process. Thus, using this model, it is now possible to assess how improvements in membrane properties will affect the size and configuration of membrane modules for a given set of production conditions (design parameters). It is therefore shown that the model is an especially useful tool in setting membrane properties' targets for experimentalists when developing advanced new membrane materials. Referring to the model performances and simulation results, it can be concluded that the proposed methodology based on the flash calculation method can be utilized to design single and multi stage gas separation processes using polymeric hollow fiber membranes under different operating conditions. In future works, a techno-economic analysis based on these simulations will be made to optimize a membrane separation process for O_2 production and natural gas purification processes.

Nomenclature

ΔA_f	membrane separation area
A	cross-section area
C_p	specific heat capacity at constant pressure
d	diameter
E	activation energy
F	molar flow rate
G	mass flow rate
H	enthalpy
h	heat transfer coefficient
k	gas thermal conductivity
L	fiber active length
M	molecular weight
n_f	number of fibers
P	pressure
p	permeability
Q	permeance
q	heat
r	module inner radius
R_g	universal gas constant
Re	Reynolds number
T	temperature
TMA	total membrane area
U	overall heat transfer coefficient

$\Delta\upsilon$	element volume
V	molar flow rate
ΔV_t	permeate flow rate
x	shell side mole fraction
y	fiber side mole fraction
z	element thickness

Greek symbols

α	component index
β	component index
γ	gas velocity
ε	void fraction
η	viscosity
θ	stage cut
λ	friction factor
μ	Joule-Thomson coefficient
ρ	density
ϑ	molar volume
η	Wike's coefficient
τ	stress tensor
χ	volume fraction
φ	packing fraction
ψ	element stage cut

Subscripts

c	gas component index
cond	conduction
f	feed side
g	gas
hyd	hydraulic
i	element number
in	inner
JT	Joule-Thomson
m	membrane
mix	mixture
o	outer
P	permeate
p	permeate
pe	permeate
po	polymer
R	retentate
r	retentate
ref	reference
s	shell side
t	fiber side

Chapitre 2

Optimizing Membrane Module for Biogas Separation

2.1 Résumé

Le biogaz comme source d'énergie durable produite par différentes technologies de fermentation nécessite d'être amélioré avant d'être utilisé comme carburant ou pour la production de chaleur et d'électricité. Aujourd'hui, la technologie de séparation par membrane est devenue de plus en plus acceptée pour concourir avec les autres méthodes conventionnelles de séparation du biogaz. Nous avons développé un modèle d'optimisation de membrane afin de trouver les valeurs optimales des paramètres opérationnels et la configuration la plus efficace tout en minimisant les coûts annuels de séparation. Pour concevoir un module de membrane à fibres creuses, ce modèle est aussi utilisé pour spécifier les valeurs optimales de la fraction de remplissage et les dimensions du module tout en minimisant les nombre de modules requis pour un procédé de séparation. Nous proposons aussi une nouvelle approche de modélisation pour sélectionner les caractéristiques de membrane par lesquelles les effets de perméance de CO_2 et la sélectivité de CO_2/CH_4 sur les configurations optimales d'un procédé sont investiguées. Cette approche fournit un guide pratique pour les expérimentateurs afin de vérifier rapidement les effets de la technique de modification sur les membranes avant les utilisations dans un procédé réaliste. Les résultats démontrent que le coût de la séparation est moins sensible qu'a la récupération du CH_4 (<95%). Pour la même sélectivité de CO_2/CH_4, non seulement le coût de la séparation est réduit par l'augmentation de la perméance de CO_2 par un facteur de 2, mais cela produit aussi une réduction de 40% dans la superficie totale de membrane. L'analyse technico-économique révèle finalement que la technologie de séparation par membrane a un potentiel élevé à la fois pour déplacer les méthodes conventionnelles ou pour être utilisée dans un procédé hybride.

2.2 Abstract

Biogas as a sustainable energy source produced via different fermentation technologies needs upgrading prior to use as fuel or for heat and electricity productions. Today, membrane gas separation technology is becoming more and more accepted to compete with other conventional biogas separation methods. Herein, we develop a membrane optimization model to find optimal values of operating parameters and the most effective layout while minimizing annual separation cost. To design a hollow fiber module, this model is also used to specify the optimal values of module packing

fraction and dimensions while minimizing the required module number for a separation process. We also propose a new modeling approach to select membrane characteristics by which effects of CO_2 permeance and CO_2/CH_4 selectivity on optimal process layouts are investigated. This approach provides a practical guideline for experimentalists to quickly verify the effect of modifications on membranes prior to using them in a realistic process. The results show that the separation cost is less sensitive to the CH_4 recovery (<95%). For the same CO_2/CH_4 selectivity, not only the separation cost is reduced by increasing the CO_2 permeance by a factor of 2 but this also results in a 40% reduction in the total membrane area. The techno-economic analysis finally reveals that the membrane technology has a high potential either to displace the conventional methods or to be used in a hybrid process.

2.3 Introduction

The lack of sufficient energy resources for future generations is one of the controversial topics in both political and scientific communities. Today, the economic growth rate of oil and gas supplier countries is reliant on the global markets which are highly vulnerable to sudden changes due to political decisions and events. In general, the global dependency to the energy resources is also increasing at a frantic pace due to the world modernization and growing population. Undoubtedly, the depletion of fossil fuel resources will bring about uncertainties in many countries. On the other hand, the current indiscriminate use of fossil fuels is damaging the environment and raising a serious concern about global warming due to greenhouse gases (GHG) emissions. This environmental legacy also needs to be fixed through international commitments and collaborations to avoid global catastrophes. Hence, a large group of researchers and scientists focuses on the field of sustainable and clean energy sources. For instance, biogas is one of the valuable and renewable energy sources produced by the anaerobic digestion (AD) of biodegradable organic materials [73, 74]. The biological waste, landfills, dairy waste, and water treatment plants can be converted to biogas through the fermentation technology [75]. Depending on the process conditions and environment, biogas might consist of methane (CH_4) 40-70%, carbon dioxide (CO_2) 15-60% and traces of contaminants such as ammonia (NH_3), water vapor (H_2O), hydrogen sulfide (H_2S), methyl siloxanes, nitrogen (N_2), oxygen (O_2), carbon monoxide (CO) and hydrocarbons [76].

Biogas cleaning and upgrading are later necessary to improve the CH_4 quality and remove CO_2 before using as a vehicle fuel or for electricity production, or injecting into the natural gas grid [76]. Conventional separation methods including absorption, adsorption and cryogenic distillation can be used for biogas purification [76-80]. Depending on the biogas composition, a pre-treatment process might be needed to remove trace compounds such as siloxanes, aromatics, volatile organic

compounds (VOC), ammonia, and water [81]. The separation mechanism of the above-mentioned processes is industrially mature and adequate to produce products enriched either in CH_4 or CO_2 (>99%) [78, 82]. The CO_2-rich stream might be then easily delivered to the enhanced oil recovery (EOR) and carbon capture and storage (CCS) units or used for other industrial applications such as in the food industry. Despite the high separation efficiency, these processes generally suffer from operational instabilities and have adverse effects on the environment [83]. For instance, the regeneration unit (stripper column) in the amine absorption process requires a high amount of energy to recover the laden absorbent and to release CO_2 at high temperature (100-120^{o}C). The water scrubbing process has also inferior removal performance as some gas components (O_2 and N_2) cannot be removed by the absorbent and therefore remain in the CH_4-rich stream [84]. They also have other disadvantages such as high investment costs, high energy consumption, absorbent corrosion, absorbent degradation, salts precipitation, and foaming. Similarly, adsorption and cryogenic distillation processes have high investment costs, high operation costs and complex process control, making them less attractive than absorption processes [23, 83, 85, 86]. Despite all economical and environmental issues, absorption is currently regarded as the dominant technology in the gas separation industry.

Membrane technology is still seen as an alternative for gas separation since its introduction into the gas processing industries in the 1980s [87]. This separation method exhibits a high potential to displace the above-mentioned conventional methods for gas upgrading due to its process simplicity, environment-friendly separation, low energy consumption, simple design and scale-up, ease of installation, and, low operation and maintenance costs. More interestingly, the membrane-based systems are of high interest to be used for the off-shore separation projects due to the smaller footprint and lower weight compared to absorption processes. For instance, a membrane-based separation plant was installed in the Gulf of Thailand to upgrade an untreated gas from 37% to 15% CO_2 and then delivered it to the buyer's pipelines [88]. Thus far, there are still some limitations such as material selection and membrane fabrication as well as process design and optimization which dramatically postpone the complete commercialization of this gas separation technology [83]. Hence, most researchers focus on experimental works to improve membrane characteristics, resulting in better fitting into the membrane separation market. Different modeling works have also reported the effects of operating parameters, flow configurations, and membrane permselectivity on separation performance and hydrocarbon loss [26, 31, 34, 35, 40, 42, 89-93]. In the case of CO_2/CH_4 separation, the modeling results have truly shown that the use of a single stage membrane unit is not economical due to the high required membrane area and high CH_4 loss in the permeate stream [90]. Therefore, it

is necessary to design the optimized multi-stage membrane system to meet both economic and removal targets of CO_2/CH_4 separation process. Using an optimization approach to process design will probably make the membrane technology more competitive than conventional separation methods due to more economical separation and fewer environmental issues.

Several studies on the optimization of multi-stage gas membrane systems have been carried out. All these works aimed at minimizing the gas separation cost while specifying the optimum values of decision variables (i.e. transmembrane pressure, required separation area, and membrane permselectivity). No specific optimized process layout is available for a typical gas mixture as the operating and economical parameters are required to be taken into consideration to determine the number of separation stages. Hence, fixed and multi-structure optimization approaches are used to simultaneously find the process layout and to minimize the gas separation costs. In the first method, a number of process layouts are arbitrarily chosen and thereafter optimized by manipulating the decision variables. For instance, Bhide and Stern [8] proposed seven different layouts to assess the economics of membrane-based CO_2/CH_4 separation process while the CO_2 mole fraction changed from 5 to 40%. The target was to obtain the retentate stream to meet the specification of pipeline-quality gas (CO_2<2 mol% or less). Then, assigning the "case study" method to the optimization technique, a multi-dimensional grid was created to cover the entire range of all values of decision variables. The result showed that the three-stage system including a single-stage unit in series with a two-stage cascade process had the lowest separation cost when the feed CO_2 mole fraction exceeded 15%. Ahmad et al. [9] made a sensitivity analysis to optimize the separation cost for single and multi-stage membrane processes by changing the feed pressure and CO_2/CH_4 selectivities. The results showed that increasing the CO_2 feed content resulted in CH_4 recovery reduction while increasing the feed pressure enhanced the CH_4 recovery due to the higher separation driving force. They also reported that a two-stage process with a permeate recycle was the optimum configuration in terms of the annual separation cost. The CH_4 recoveries over the whole range of the feed CO_2 content were also below 95% even upon increasing the CO_2/CH_4 selectivity from 5 to 80. Deng and Hägg [10] evaluated a biogas membrane-based upgrading system using a highly efficient CO_2-selective membrane in different predefined process layouts. A parametric optimization technique was then proposed to show the effects of operating pressure, feed flowrate and composition on the final product (CH_4 purity and recovery). They concluded that the two-stage cascade layout was the most efficient configuration for the biogas upgrading. They pointed out that a membrane area of 1440 m^2 and a compressor duty of 234 kW were required to reach the CH_4 purity and recovery of 98%. Kundu et al. [12] also proposed different membrane configurations to upgrade a gas mixture of CO_2 and CH_4 using

the fixed-site-carrier (FSC) membranes. These two stage cascade systems related to the permeate-low and retentate-high feed CO_2 concentration of 10 and 50% operated at 20-40 bar. Both systems were able to enrich CH_4 in the retentate stream to 96% whereas the CH_4 losses of the first and second systems reached 2 and 7%, respectively. It was also reported that the reduction of CH_4 loss led to increase the processing cost (~30%) and membrane footprint (~25%). The main drawbacks of this optimization technique are how to determine the membrane stages number and to define the effective layout for a typical gas separation system. This brings up a problem of great complexity about the selection of operating parameters and of the connections between gas streams and membrane units. In all the above-mentioned cases, the optimization results were achieved based on heuristic design experience. This approach allows to find the optimum separation system but is in no way viable to assure whether the separation cost value is a global optimum.

It is expected that the multi-structure optimization approach can allow optimizing the decision variables and find the optimal process layout simultaneously. This concept is based on a network superstructure by which a large number of potential membrane-based separation layouts can be defined by progressively deleting elements of the structure. This approach allows examining even novel layouts which have not been proposed to date through the previous optimization works. Qi and Henson [94] introduced this approach for the first time to optimize a multi-stage spiral-wound gas permeator system. They made a superstructure model by using the material balance formulation between the membrane units and auxiliary equipment. This problem later required a Mixed Integer Non-Linear Programming (MINLP) solution strategy to optimize the total annual process cost. Scholz et al. [95] also used this approach to determine the most profitable layout for the biogas cleaning process. They used different strategies (i.e. feed compression, permeate vacuum, and sweep gas injection) to generate the driving force. The results showed that the use of a three-stage layout with a single compressor resulted in a high CH_4 purity (96 mol%) and recovery (~99.6%) when using membranes with CO_2/CH_4 selectivities of 60 and 20 with CO_2 permeances of 60 GPU. This technique can also be used to optimize the separation cost for other membrane-based systems (natural gas, flue gas, and air enrichment processes). For instance, Uppaluri et al. [96] found an optimal design layout for an air enrichment process. They reported that a two-stage process using a membrane with a O_2/N_2 selectivity of 2.1 enriched O_2 to 30%. The results also revealed that both the required membrane area and network cost were reduced compared to the case reported by Bhide and Stern [97]. Arias et al. [98] also used this approach to design a membrane-based process for CO_2 removal from flue gas. For a membrane with a CO_2/N_2 selectivity of 50, it was seen that the optimal stage number varied according to the CO_2 purity in the permeate stream. Thus, a two-stage process with one recycle stream

was proposed for a range of CO_2 purities from 90 to 93% whereas a three-stage process with two recycle streams was the optimal layout for a range of CO_2 purities from 94 to 96%. A CO_2 purity up to 98% was obtained using a four-stage process with two recycle streams. The other membrane-based multi-structure optimization problems can be found in references [99-102]. For all cases, the superstructure optimization model needs to be solved using optimization solvers such as Branch-And-Reduce Optimization Navigator (BARON) and COUENNE (Convex Over and Under ENvelopes for Nonlinear Estimation) which guarantee to find the global optimum.

The optimal value of the required membrane area allows anticipating the footprint of typical membrane-based separation systems. But for a realistic separation process, more investigation is needed to determine the required modules number in each separation stage. To our knowledge, there is no published articles addressing an optimization model to simultaneously determine the optimum values of operating conditions, stages number as well as modules number and size for a hollow fiber membrane-based separation system. In the present study, a multi-structure optimization technique is used to find the optimum biogas layout as well as the optimal fibers number and length for all separation stages. Thus, a new optimization framework is proposed to formulate a general form of module separation model (MSM) while using hollow fiber membranes. The fluid dynamic constraints are embedded into the MSM to develop a laminar flow and to set realistic values for the inlet gas flowrate and packing density of a single module. This approach allows determining the optimum module number while minimizing the membrane separation plant footprint. In the case of the optimization of biogas separation, three polymer membranes previously produced in our laboratory [71] were chosen to show the effects of changes in the CO_2 permeance and CO_2/CH_4 selectivity on the biogas separation cost, process layout, and modules number.

2.4 Problem statement and optimization approach

The membrane-based gas separation systems are developing at high-speed. However, some bottlenecks still prevent them from taking the market share away from the consolidated competitors. The use of super-structure optimization technique is suitable to estimate the gas separation cost under specific operating conditions. In the next step, the optimization results are required to be further analyzed technically prior to deploy in realistic membrane-based gas separation projects. In the currently published optimization cases, the optimum value of membrane separation area can be regarded as a rough estimate of the membrane plant's footprints [9, 10, 95]. The approach used does not allow determining the required number of hollow fiber modules for the optimized process. The main concern is then how to adjust module dimensions and packing fraction as to fulfill the separation

targets in line with the optimization results. Thus, the problem statement for a multi-stage membrane-based system can be outlined as:

- Given the feed gas flow rate, composition, and permeances, stage pressures, and economic data, an optimum separation layout which emerged from a larger membrane network configuration, should achieve the desired product specifications while minimizing the separation cost and in a successive step module number.

For a membrane-based separation process, the optimum separation cost includes the capital cost (CAPEX) associated to the membrane modules, heat exchangers, compressors, and in some cases turbine, as well as the operational cost (OPEX) for the energy consumption and, membrane replacement and maintenance. The latter optimum cost gives a valuable outlook on the use of a proposed membrane with specific CO_2/CH_4 selectivity and CO_2 permeance in the biogas upgrading process. Hence, a robust super-structure optimization technique including two modeling steps is proposed. Firstly, the optimum total fiber number and length for all separation stages at the minimum gas separation cost are determined according to [94]. Then, a second modeling step, based on the first step optimum results, specifies the optimal gas inlet flowrate and fiber number (packing fraction) of each module while conforming to the gas velocity range of standard commercial processes in the hollow fiber modules [49, 90].

2.4.1 Superstructure membrane network

Following the pre-treatment and water removal processes, the dried gas which is now essentially a mixture of CH_4 and CO_2, needs to be further purified prior to injection into the natural gas grid (CO_2<2% in retentate) or prior to its use for other applications such as EOR projects (CH_4<5% in permeate). In our previous work [90], the use of a single stage membrane process was shown to result in important CH_4 loss over a range of CO_2/CH_4 selectivities from 20 to 70. It was also reported that a two-stage membrane process was able to simultaneously yield higher CH_4 purity and recovery. However, this configuration led to extra costs due to the non-optimized values of the membrane separation area and compressor power. In the current study, the super-structure optimization approach, which *a priori* would provide a large number of process configurations, is therefore proposed to find the optimum multi-stage layout at the minimum gas separation cost. The number of required membrane units can be determined depending on the product specification and process cost limitations in the optimization framework. Scholz et al. [95] reported that it was unsuitable to use more than three membrane stages for biogas upgrading process due to the potential risks of process complexity and instability. Hence, the optimization of a three-stage separation process illustrated in

Figure 2.1 is used in this study as the first step superstructure modeling. It is assumed that every membrane stage consists of chambers, on the low and high-pressure sides, separated by a diffusional interface through which the mass transfer occurs based on the solution-diffusion model. Figure 2.1 also features the ancillary equipment such as piping streams, mixers and splitters, compressors, heat exchangers, and water coolers. The superstructure optimization model can later be mathematically formulated to satisfy the mass and energy balances. Depending on the model's constraints, different process configurations might be extracted from this superstructure, using this optimization technique. In other words, this approach allows to remove systematically the unnecessary process components and to disrupt the predefined connections to reach a smaller optimum layout while minimizing the separation cost.

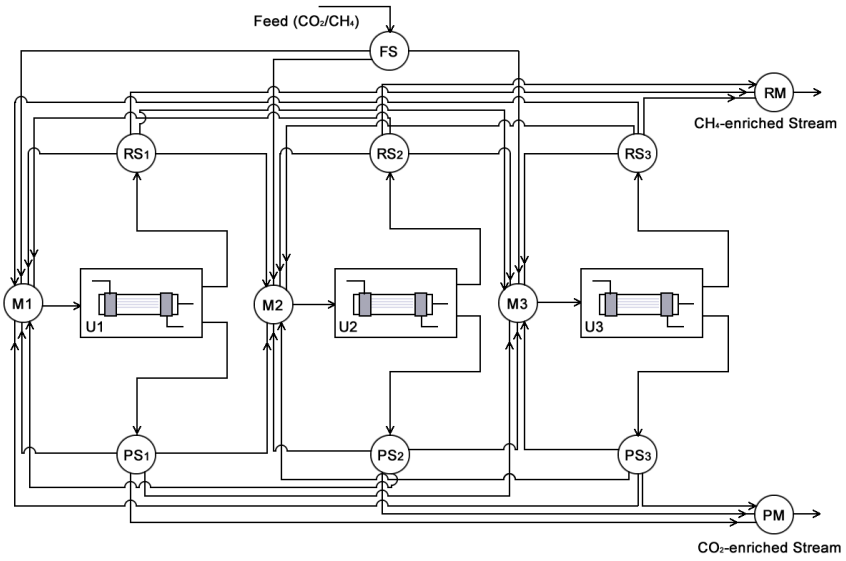

Figure 2.1 Schematic diagram of the optimization of a three-stage separation process.

2.4.2 Model Formulation

2.4.2.1 Permeator

In our previous study [90], a gas permeance model was developed and solved using the partial stage cut modeling approach to predict the separation performance of a hollow fiber membrane module. The model was also validated by comparing its results with different experimental data and good agreements were observed. Here, this model is used with the following assumptions: a) isothermal condition, b) ideal gas behavior, c) no pressure drop in shell and fiber sides, d) no concentration polarization at the membrane surface, e) fibers have no deformation at high pressure, f) constant

permeances over the range of gas phase composition. Thus, the mass balance equations for a counter-current hollow fiber module can be given as:

$$\begin{aligned} &\Delta F_c(i) = \Delta A Q_c [P_r x_{r,c}(i-1) - P_p y_{p,c}(i)] \\ &\Delta A = N_f d_o l_e \\ &c = 1,2,...,m,\ \ i = 1,2,...,n \end{aligned} \tag{2.1}$$

$$F_r(i) = F_r(i-1) - \sum_{N=1}^{C} \Delta F_N(i) \tag{2.2}$$

$$F_p(i) = F_p(i-1) + \sum_{N=1}^{C} \Delta F_N(i) \tag{2.3}$$

where ΔF_c, ΔA, P, and Q represent the permeate molar flow rates (*mol/s*), membrane separation area (m^2), pressure (*Pa*), and gas permeance (mol/sm^2Pa), respectively. N_f is the fiber number, d_o the fiber outer diameter in *cm*, l_e length of an element in *cm*. *c* and *i* stand for the numbers of gas components and hollow fiber elements, respectively. F_r and F_p are also the molar flow rates (*mol/s*) on the retentate and permeate sides, respectively. The mole fractions at the retentate and permeate sides are given by:

$$x_{r,c}(i) = F_{r,c}(i) / \sum_{N=1}^{C} F_{r,c}(i) \tag{2.4}$$

$$y_{p,c}(i) = F_{p,c}(i) / \sum_{N=1}^{C} F_{p,c}(i) \tag{2.5}$$

In case of cost analysis, the membrane skid cost, CC_{MES}, and membrane equipment installation cost, CC_{MEI}, are estimated as:

$$CC_{MES} = \sum_{i=1}^{N_p} N_{f,i} \pi d_o L_{m,i} C_{MEA} \tag{2.6}$$

$$CC_{MEI} = f_{ic} CC_{MES} \tag{2.7}$$

where L_m and C_{MEA} represent the module fiber length in *cm* and the membrane cost per unit area in $\$/m^2$.

2.4.2.2 Compressor and turbine

The feed and recycled permeate gas flows need to be compressed using adiabatic (isentropic) compressors to provide the adequate separation driving force. Thus, the required compressor power (*kW*) allowing to choose the right size and type of compressor, and then to estimate its cost, is given by [103]:

$$W_{CO} = 2.78\times10^{-4} N_{st} V p_1 \left(\frac{k}{k-1}\right)\left[\left(\frac{p_2}{p_1}\right)^{\alpha} - 1\right] / \eta$$
$$\alpha = \frac{k-1}{k N_{st}} \tag{2.8}$$

where N_{st} is the number of compression stages, V the volumetric flow rate at the compressor inlet in m^3/h, k the isentropic expansion factor, and η the isentropic compression efficiency. The isentropic temperature of discharge flow, T_2, in K, is also obtained from:

$$T_2 = T_1\left(1 + \frac{1}{\eta}\left((p_2 / p_1)^{\alpha} - 1\right)\right) \tag{2.9}$$

where T_1 is the inlet temperature in K, as well as p_2 and p_1 represent the charge and discharge pressures of the compressor in *kPa*, respectively. As expected, the retentate outlet stream enriched in CH_4 is collected at the same pressure as the feed gas whereas the permeate outlet stream enriched in CO_2 may require to be compressed before transportation. Thus, the required compression power (*kW*) including the pressurization stages for the feed, permeate recycle and product flows, is given as:

$$W_{RP} = W_F + \sum_{i=1}^{N_p} W_R + W_{CO_2} \tag{2.10}$$

Moreover, a turbine might be embedded in the process network to recover the compression energy from the outlet stream of retentate product. Thus, the turbine power, W_{TU}, in *kW* is given by:

$$W_{TU} = m R_g T_1 \left(\frac{k}{k-1}\right)\left[1 - \left(\frac{p_2}{p_1}\right)^{\beta}\right] / \eta$$
$$\beta = \frac{k-1}{k} \tag{2.11}$$

where m and R_g represent the mass flow rate in *kg/s* and universal gas constant in *J/kgK*, respectively. In the optimization model, the overall required power for the optimal layout in *kW* might be calculated with or without turbine as:

$$W_{OV} = W_{RP} - W_{TU} \tag{2.12}$$

Moreover, the total operation cost (CC_{OV}) is estimated based on the electricity consumption cost (C_{EP}) per hour in *kWh* for the expected operation time (one year). The capital costs of compressors (CC_{CO}) and turbine (CC_{TU}) can also be estimated using the module costing technique at reference year as [104]:

$$OC_{OV} = W_{OV} C_{EP} H_{AO} \tag{2.13}$$

$$\log_{10} CC_{CO} = 2.2897 + 1.3604 \log_{10}(W_r) - 0.1027 \left[\log_{10}(W_r)\right]^2 \tag{2.14}$$

$$\log_{10} OC_{TU} = 2.7051 + 1.4398 \log_{10}(W_{TU}) - 0.1776 \left[\log_{10}(W_{TU})\right]^2 \tag{2.15}$$

where W_r and W_{TU} are the compressor power capacity in *kW*.

2.4.2.3 Heat exchanger

For an adiabatic multi-stage compression, it is assumed that the equivalent compression work is shared among the compressors to avoid a drastic increase in the discharge temperature (T_2). In this state, the outlet gas is cooled after each stage so as to return to the original inlet temperature (T_1). The required heat, Q_{EH}, *in kW* which is exchanged between the hot gas and cooling water stream, is also given as [105]:

$$Q_{EH} = F_{gas} C_{p,gas} (T_2 - T_1) \tag{2.16}$$

$$Q_{EH} = U A_{he} \Delta T_{lm} \tag{2.17}$$

where F is the inlet gas flowrate in *mol/s*, C_p the specific heat capacity in *kJ/molK*, U the overall heat transfer coefficient in *kW/m^{2}K*, A_{he} the required heat transfer area *m^2*, and ΔT_{lm} the logarithmic mean temperature difference *K*. The capital and operation costs of the required heat exchangers in the process layout can also be estimated as [45]:

$$CC_{HE} = \sum_{i=1}^{N_p} A_{he,i} C_{HEA} \tag{2.18}$$

$$OC_{HE} = \sum_{i=1}^{N_p} Q_{EH} C_{RP} H_{AO} \tag{2.19}$$

In this study the module costing technique is used to estimate the investment cost of a membrane-based biogas separation plant [104]. In brief, the purchase cost of equipment is initially evaluated for base conditions and then modified using deviation factors including specific equipment type, system pressure, and materials of construction. The effect of time on the purchased equipment costs is finally projected using cost index method [104].

2.4.2.4 Mixer and splitter

The superstructure configuration examines all the possible options to connect the permeators using mixers and splitters. It is then expected that an optimal layout is screened through removing the dummy variables by using the optimization technique. Thus, the mass balance relations for the mixers and splitters can be defined as:

$$F_F = F_1 + F_2 + C_{bi} F_3 \tag{2.20}$$

$$R_1 + R_2 + C_{bi} R_3 = 1 \tag{2.21}$$

$$F_{RM,i} = \sum_{i=1}^{N_p - 1} (F_{R,i} + F_{P,i}) + C_{bi} (F_{R,N_p} + F_{P,N_p}) + R_i F_F \tag{2.22}$$

$$F_{RS,i} = \sum_{i=1}^{N_p - 1} \sum_{j=1}^{N_p - 1} R_{R,i} F_{R,i} + C_{bi} R_{R,i} F_{R,i} + R_{R,o} F_{R,i} \tag{2.23}$$

$$F_{PS,i} = \sum_{i=1}^{N_p - 1} R_{P,i} F_{P,i} + C_{bi} R_{P,i} F_{P,i} + R_{P,o} F_{P,i} \tag{2.24}$$

where F and R denote the molar flowrate (*mol/s*) and recycle ratio for each equipment, respectively. C_{bi} is a binary variable in the membrane network and can be set to 0 and 1.

2.4.2.5 Module constraints

The first step of the optimization model (objective function OF1, Eq. 31) allows to specify the most economic process layout in which the gas flow rates and total membrane area (fibers number and length) in each separation stage are optimum. Then, these optimum values are assigned for the decision variables and bound to initiate the second step of the optimization model. The model incorporation scenario leads to find the optimum module packing fraction and inlet gas flowrate as

well as the required module number within each separation stage. It is expected that the inlet gas flowrate of each module is optimized by defining integer variables in the second step of the optimization model with respect to the required module number within each separation stage. It is also essential to set the module packing fraction when the gas velocity, υ, remains below the recommended limits (<1.5-1.7 *m/s*) under laminar flow condition (*Re* < 2300) [49, 90]. In this case, the module constraints for each separation stage can be given as:

$$F_U - UM_N F_M = 0 \tag{2.25}$$

$$N_f \frac{d_o^2}{D_M^2} - \varphi = 0 \tag{2.26}$$

$$UM_N N_f \pi d_o L_m - A_{mT} = 0 \tag{2.27}$$

$$F_M - \left[(1-\varphi)(\pi \frac{D_M^2}{4}) \right] \upsilon_{\max} \frac{\rho}{Mw} \leq 0 \tag{2.28}$$

$$F_M - \left[(1-\varphi)(\pi \frac{D_M^2}{4}) \right] \upsilon_{\min} \frac{\rho}{Mw} \geq 0 \tag{2.29}$$

$$\frac{F_M Mw}{\frac{\pi}{4} N_f d_0 \mu} \leq \mathrm{Re}_{\max} \tag{2.30}$$

F_U and F_M denote the inlet molar flowrate (*mol/s*) of a separation unit and a hollow fiber module, respectively. UM_N which is an integer variable stands for the required module number in each separation stage. A_{mT} is the value of required membrane area (m^2) in a separation stage and is optimized with respect to the first objective function (OF1). *Mw* and μ are the average molecular weight (*g/mol*) and viscosity (*Pa.s*) of the retentate gas mixture, respectively.

2.4.2.6 Objective functions

The proposed optimization model correlating the gas permeators and ancillary equipment number and size with their capital and operation costs finally constitutes a Mixed Integer Non-Linear Programming (MINLP) case introducing two objective functions:

$$OF1 = \frac{C_{AS}}{F_{RP}} \tag{2.31}$$

$$OF2 = UM_N V_M \tag{2.32}$$

where C_{AS} is the annual separation cost in *$/year* and F_{RP} the CH_4 retentate production in *tons*. Equations (2.1-30) represent a system of equality and inequality constraints for this optimization problem. Table 2.1 also shows the details of the techno-economic parameters and assumptions applied here for the optimization of a membrane-based separation process. All equations of the proposed optimization model need to be coded using algebraic modeling language such as A Mathematical Programming Language (AMPL), which can accurately solve a large number of complex optimization problems. In terms of a solver selection, as the model includes binary and integer variables defined for the permeators and connections, as well as the linear and nonlinear Equations (2.1-30), this problem forms a non-convex MINLP, which has a number of local optima. This problem might be solved on the Network-Enable Optimization System (NEOS) servers, which provide an access to different global optimization solvers such as BARON and COUENNE. Different approaches such as initializing decision variables at different points and setting reasonable bounds on variables might also be implemented to guarantee the optimum solution. The ranges for the variables used in these calculations are reported in Table 2.2.

Table 2.1 Techno-economic parameters and assumptions applied to the optimization case.

Parameter	Description
Total capital cost (TCC):	
Membrane module cost (CC_{MM})	$CC_{MM} = CC_{MES}+CC_{MEI}$
Compressor cost (CC_{CO})	*Eq. 2.14*
Turbine cost (CC_{TU})	*Eq. 2.15*
Heat exchanger cost (CC_{HE})	*Eq. 2.18*
Fixed cost (FC)	$FC = CC_{MM}+CC_{CO}+CC_{TU}+CC_{HE}$
Base plant cost (BPC)	$BPC = 1.12\times FC$
Project contingency (PC)	$PC = 0.20\times BPC$
Total facility investment (TFI)	$TFI = BPC + PC$
Start-up cost (SC)	$SC = 0.10\times VOM$
	$TCC = TFI + SC$
Variable operating and maintenance cost (VOM)	
Contract and material maintenance cost (CMC)	$CMC = 0.05\times TFI$
Membrane replacement cost (MRC)	$\$50/m^2$
Heat transfer area cost (HTAC)	$\$300/m^2$
Utility cost (UC)	$UC = (OC_{OV} + OC_{HE})\times OSF\times AO$
	$VOM = CMC+MRC+UC$
Annual capital related cost (CRC)	$CRC = 0.2\times TFI$ *(5-year payout period)*
Gas separation cost (GSC)	$GSC = \dfrac{CRC+VOM}{365\times OSF\times F_F\times(1-SCE)\times 1000}$
Other assumptions	
Membrane life (ML)	*5 years*
Electricity price (EP)	*$0.04/kWh*
Refrigeration price (RP)	*$4.43/GJ*
On-stream factor (OSF)	*0.96*
Compressor and turbine efficiency	*80%*
Membrane installation factor (f_{ic})	*1.6*
Annual operation (AO)	*12 months*
Equivalent operation hours	*8760*
Chemical index factor 2016	*541.7*

2.5 Case study: biogas upgrading process

The case study involves the design of a biogas upgrading process by which CO_2 and CH_4 are separated using hollow fiber polymer membranes (i.e. Ultem 1000) with CO_2/CH_4 selectivities of 33.2 and 66.4 [71]. In this case, the raw biogas as the product of an anaerobic digestion process is at first transferred to a separation plant and thereafter pre-treated to remove undesirable components. Thus, the biogas is here regarded as a binary mixture (CO_2 and CH_4). Table 2.2 reports on the operating conditions, feed and product specifications used for all optimization cases. A superstructure separation system including three gas permeators is proposed for the biogas upgrading in which the number of the required stages is determined by the optimization model. The optimization approach is then used to

minimize the biogas separation cost (OF1) and to derive the optimal HFM layout. In principle, this also aims at optimizing the HFM number (OF2) of each stage by simultaneously optimizing the packing fraction, module length, and inlet gas flow rate.

Table 2.2 Operating and feed conditions used for the optimization cases.

Parameter	Unit	Value		
Feed specification				
Pressure (P_R)	*bar*	Between 10 and 18		
Temperature (T_R)	*°C*	30		
Flowrate (F_F)	Nm^3/h	1000 (12.4 mol/s)		
Composition (x_R)				
CO_2		0.10~0.40		
CH_4		Balance		
Permeate pressure (P_P)	*bar*	1		
Product specification				
CH_4 Recovery (R_{CH4})	*%*	>99		
CO_2 fraction (y_{CO2})		>0.98		
Selectivity (α)		33.2	66.4	66.4
CO_2 permeance	*GPU*	86.30	86.30	172.6
CH_4 permeance	*GPU*	2.60	1.30	2.60
Fiber inner diameter (d_i)	μm	220		
Fiber outer diameter (d_o)	μm	400		
Isentropic expansion factor (k)		1.29		
Heat capacity (C_P)	*J/molK*	36.59		
Inlet cooling water (T_{CI})	*°C*	5		
Outlet cooling water (T_{CO})	*°C*	15		
Overall heat transfer coefficient (U)	W/m^2K	580		

2.5.1 Optimized biogas process

From the superstructure model optimization emerges the optimum process layout over a range of CO_2 feed contents while minimizing the annual biogas upgrading costs (OF1) and unit module number (*UMn*). Figure 2.2 illustrates a schematic flow diagram of this optimized two-stage separation process at 10% biogas CO_2 content. Optimizing the objective functions reveals that the use of two membrane units is enough to enrich CH_4 up to 98% in the retentate stream as well as to reach a CH_4 recovery of 99%. As shown, the first separation stage is related to CH_4 enrichment in which 98% of the total separation area is used. In agreement with the product specifications, the high-pressure (15.8 bar)

retentate product might directly be sent to other units for different applications such as injection into the natural gas grid and/or electricity production. The low-pressure (1 bar) permeate product after compression using a multi-stage compressor is fed to the second separation stage. In turn, the CH_4-enriched product is completely recirculated and injected into the mixer (M1). Similarly, the permeate product enriched in CO_2 can then be used for other applications such as EOR projects or be transported for sequestration.

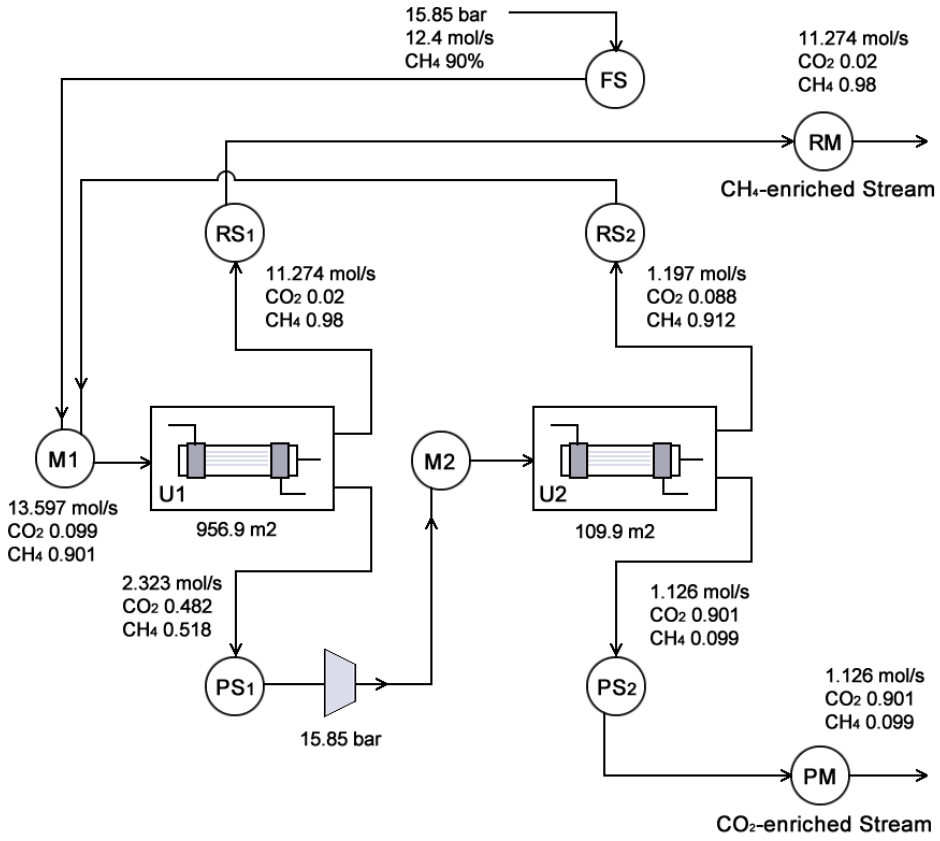

Figure 2.2 Schematic flow diagram of an optimized two-stage separation process at 10% biogas CO_2 content.

In the present case, the first membrane (Ultem 1000) with a CO_2 permeance of 86.3 and a CO_2/CH_4 selectivity of 33.2 was chosen for both separation stages. It is also observed that the stage-cuts of the first and second membrane units reach 17 and 48%, respectively. The optimization model reconciles the capital and operation costs mostly associated with the required feed pressure and total membrane area to find the optimum for each separation stage. As a result, according to the separation targets and membrane characteristics, the feed pressure optimum value is set to the rather low value of 15.8 bar. The membrane area needs to compensate for the pressure reduction and hence is found to 956.9 m^2

to meet the separation targets and maximizing CH_4 enrichment. Referring to the stage-cut of the first stage (17%), the proposed membrane is suitable to meet the separation target (CH_4>98%) while only a small amount of CH_4 is lost in the permeate stream. In this stage, the low permeate flowrate of ~2.32 mol/s results in reductions in the required second compressor power and capital cost. In the second separation stage (CO_2 enrichment unit), the optimum membrane area reaches 109.9 m^2 at a reasonable feed pressure (15.8 bar) to enrich CO_2 to 90% in the permeate stream.

As discussed above, the distinctive advantages of the membrane technology in gas separation are the process simplicity and ease of installation compared to the other conventional methods. Referring to the optimization result, a two-stage process is able of upgrading biogas to meet the separation targets. This optimized process involves two compression units to adjust the inlet gas pressure as well as two membrane units to constitute the base structure of hollow fiber modules. In case of realistic industrial projects, it is of high interest to determine the exact number of hollow fiber modules installed in each unit for a typical membrane-based biogas separation process. The optimum membrane area allows to calculate the required number of fibers in relation with the fiber diameters and the module length. The first criterion might be to specify the membrane physical and chemical resistance as well as the limit of feed pressure to use the membrane in a realistic gas separation process. The latter needs a precise consideration as it directly impacts the membrane skid cost. It is therefore essential to find the optimum values of these criteria to decrease both the membrane module fabrication and biogas upgrading costs. The membrane manufacturers must comply with some industrial standards to design a typical hollow fiber module package. For instance, Cynara (NATCO Group, Inc.) produces hollow fiber modules with diameters of 5, 12, 16, and 30 inches. In addition to finding the optimal values of operational parameters, the other target here is to minimize the module number used for a biogas upgrading process. In principle, this probably leads to reduce the material required for the skid fabrication and separation package including housing, pipes, flanges, and valves. Furthermore, this approach might be considered to design a more compact membrane-based unit not only for biogas upgrading plants but also for off-shore gas sweetening projects when reductions of plant structure and equipment size are challenging.

In general, the design of most gas separation plants requires a heuristic consideration in both engineering concepts and feasible plant performance. In turn, this approach particularly allows designing a realistic scheme for a separation process properly matching the desired product specifications. In the case of a membrane-based separation system, the appropriate selection of a hollow fiber module size needs to be precisely made with respect to the inlet gas flowrate and pressure as well as the packing density. In the following optimization cases, the selection of module diameter

satisfies the existing standards in the membrane equipment and accessories markets [87]. Hence, the module diameter is set to be 5 in (12.7 cm) while the module length varies between 50 and 200 cm. This module is then used for biogas upgrading with the feed properties and membrane characteristics listed in Table 2.2.

To design an optimum module, the *FA* index (*mol/sm*^{2}) (calculated using Eqs. (25-30) as FA = F_u/A_{mT}), which is the ratio of the inlet gas flow rate to total membrane area, can be conceptualized in each separation unit since the *FA* index corresponds to the realistic unit separation capacity at a given driving force provided by the combination of the optimal values of pressure ratio, membrane area, and inlet gas flow rate. Thus, the optimization model is initialized with different *FA* indices to determine the integer value of modules number as well as the optimal values of module inlet gas flowrate, packing fraction (fibers number in the module), and module length using a global optimum solver.

To initiate the numerical optimization procedure, preliminary estimations of the unit module number (UMn) and packing fraction (φ) within one module were made by arbitrarily assuming a total stage membrane area (A_{mT}) of 1000 m^2. Moreover, as mentioned above, the module diameter (Dm) value of 5 in (12.7 cm) was therefore considered in these calculations. In the calculations only the second step of the optimization procedure for the objective function OF2 (Eq. 32) was implemented. Preliminary minimization of $UMnV_m$ is intended to provide realistic values for number and length of modules which control the plant footprint. The results are plotted in Figure 2.3a-b as functions of the FA index which was varied over the realistic range of 0.01 to 0.1 mol/sm^2. These calculations were performed for two different values of the module length, namely 50 and 100 cm. The data plotted in Figure 2.3 allows establishing that a 50 cm length module is preferable to a 100 cm one. Indeed, the values of packing fraction (φ) are in the range of 50 to 90%. In the case of a 100 cm long module, this would be met for the FA index between 0.01 and 0.03. Figure 2.3b also shows the relation between the same FA index and objective function 2 (OF2, Eq. 32). According to Figure 2.3a-b, by increasing the FA index from 0.03 to 0.10, the separation unit volume drastically decreases and then levels off for higher FA. Under these conditions, the module packing fraction would be set between 50 to 15% which is considered unrealistically low. As mentioned above, the use of hollow fiber module with a length of 50 cm and a diameter of 12.7 cm in the separation unit favours reducing the separation unit over different ranges of the FA index while the optimal values of packing density are set between 50 and 90%.

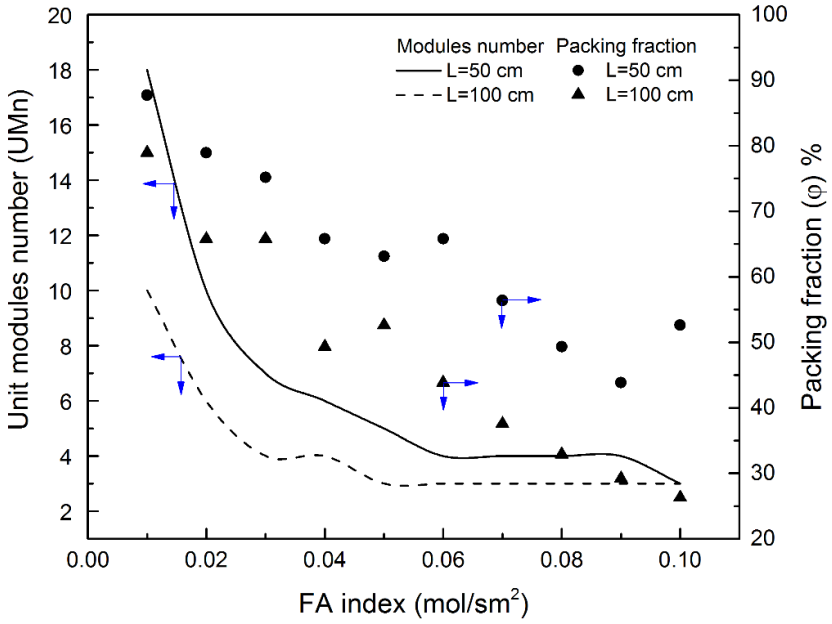

Figure 2.3a Relation between the FA index and results of the optimization problem (*UMn*, φ) outlined in Table 2.2 (Ultem 1000 membrane, Q_{CO2} = 86.3 GPU, Q_{CH4} = 2.60 GPU).

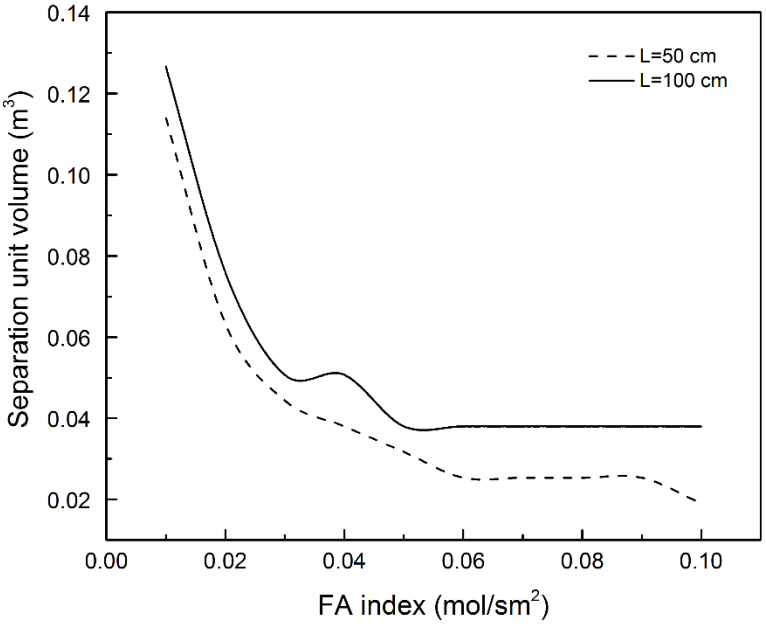

Figure 2.4b Relation between FA index and separation unit volume with module lengths of 50 and 100 cm.

Figure 2.4 presents the relation between the inlet gas flowrate and unit modules number when the module diameter is set to 12.7 cm (5 inches). The inlet gas flow rate was varied from 2 to 100 mol/s to encompass a large range of membrane unit capacity, while the *FA* index was varied from 0.01 to 0.08 mol/sm^2. In this case, the module length, which is expected to vary between 50 to 200 cm, was introduced as a decision variable in the optimization model. In most cases, the optimal module length is equal to 50 cm or below 70 cm over different ranges of the inlet gas flowrate and *FA* index. As discussed before, increasing the *FA* index results in lower *UMn*. The overall conclusion is that Figure 2.4 can be seen as a general guideline to determine the required *UMn* for a realistic CO_2/CH_4 separation process based on primary experimental results. Similarly, this optimization approach can be implemented to analyze the effect of larger module diameters by plotting the optimum *UMn* as a function of the inlet gas flow rate. Figure 2.5 shows the effects of module diameter (5 and 12 in) on the required *UMn* over a range of unit feed flowrate.

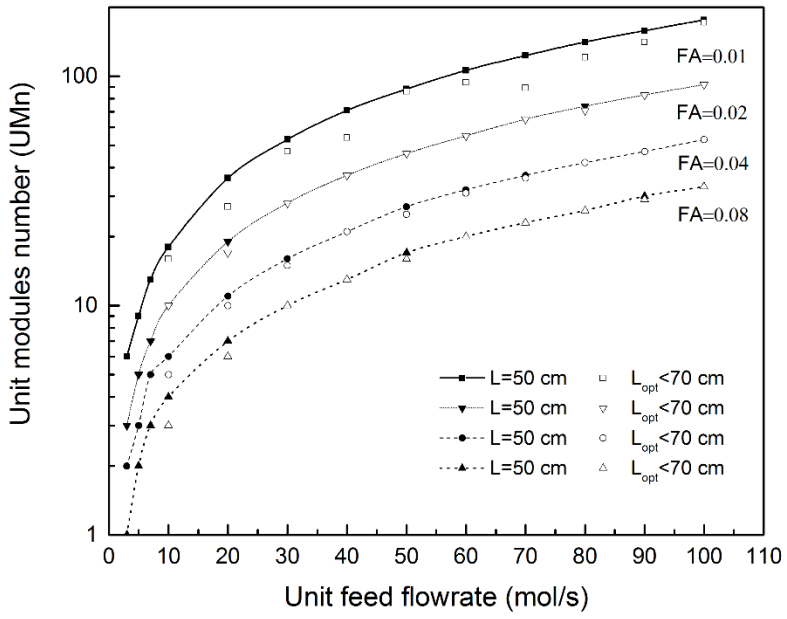

Figure 2.5 Relation between the inlet gas flowrate and unit modules number when the module diameter is set to 12.7 cm (5 inches).

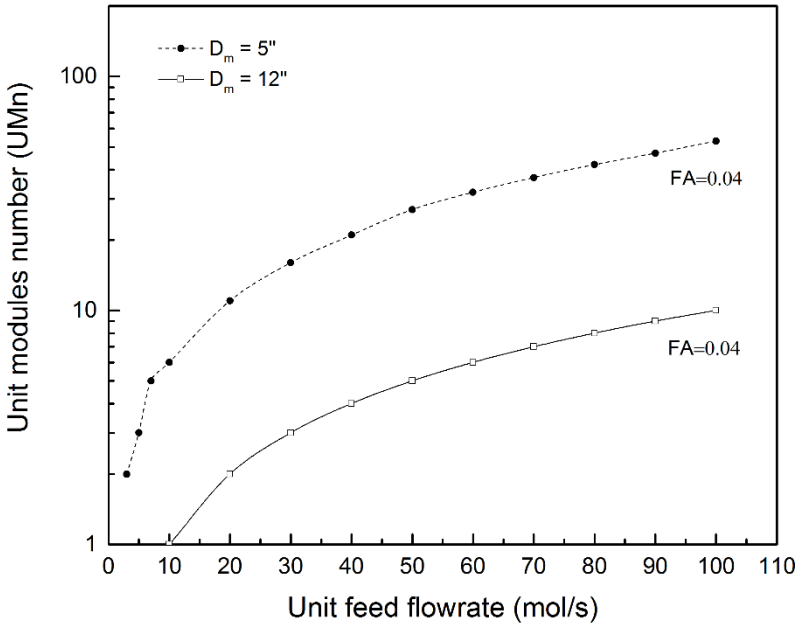

Figure 2.6 Effects of module diameter (5 and 12 in) on the required *UMn* over a range of unit feed flowrate.

2.5.2 Effects of CO_2 content and CH_4 recovery on upgrading cost

It is of great interest to design a viable membrane separation process to not only reduce separation costs but also to easily deal with a sudden change in feed composition. Such a flexibility can be found in most conventional separation processes in which any unexpected change is compensated through quick responses signaled from a process control room. In such a situation, we also studied the effect of CO_2 feed content on the separation cost, required equipment, and process layout using the optimization model. This aims to retrofit this process to efficiently upgrade a biogas with different compositions via minor changes of decision variables leading to adjust the feed pressure and membrane separation area. The optimization results reveal that a change in the CO_2 feed content (from 10 to 40%) has no specific impact on the optimum process layout. However, the feed pressure and total membrane area must increase to meet the same separation targets (CH_4>98% and R_{CH4}>99%). In these cases, the biogas needs to be compressed up to 18 bar and thereafter mixed with the recycle stream from the second stage. Figure 2.6 shows the change in the biogas separation cost for different CO_2 contents in the feed. It is seen that increasing the CO_2 content from 10 to 40% results in higher gas separation cost due to increasing total membrane area and total compressor power. The

optimum feed pressure approaches the higher bound (18 bar) defined in the optimization model whereas the total membrane area slightly increases from 1066 to 1221 m^2 when the CO_2 content is increased. In terms of process analysis, this indicates that at 40% CO_2 in the feed, the CO_2/CH_4 selectivity of 33 is not adequate which is not the case at 10% CO_2 feed mole fraction. Thus, a higher compressor power is needed to provide the necessary driving force for such a high CO_2 content to minimize the gas separation cost.

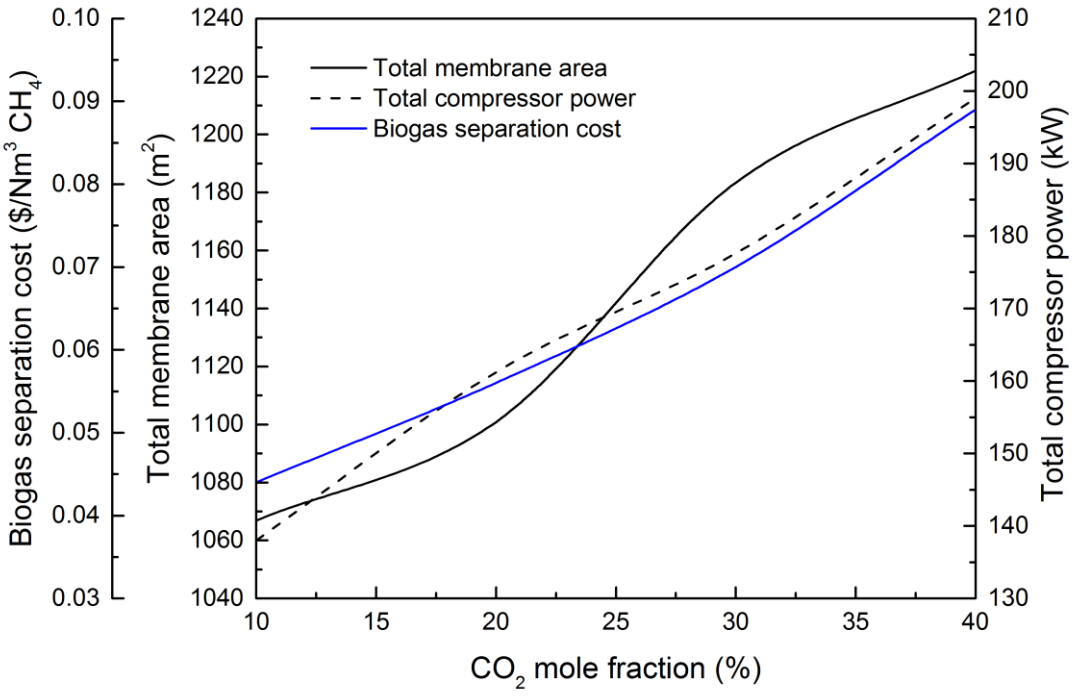

Figure 2.7 Effects of CO_2 feed content changes on the biogas separation cost.

Figure 2.7 shows the effect of CH_4 recovery on the gas separation cost when the CO_2 feed content is 40%. In the first part, the gas separation cost has no change upon enhancing the CH_4 recovery from 90 to 95% and can be estimated at 0.073 $/Nm^3 CH_4. For a 90% CH_4 recovery, the total membrane area and feed pressure are set to 1302.8 m^2 and 14.71 bar, respectively. It is expected that the gas separation cost is more controlled by the membrane area. To further improve the CH_4 recovery, the compressor power must slightly increase whereas the total membrane area sharply decreases to get a 95% CH_4 recovery. This indicates that the CO_2/CH_4 selectivity of 33 can be ta realistic benchmark for a range of CH_4 recoveries between 90 and 95%. On the contrary, the feed pressure and therefore compressor power are the dominant factors when high CH_4 recoveries ranging from 95 to 99% are

required. For a 99% CH_4, the optimum total membrane area and feed pressure needed are 1202.6 m^2 and 18 bar, respectively. It is also observed that the total membrane area and compressor power simultaneously increase for further CH_4 recovery. This results in a substantial increase in the gas separation cost. Overall, the optimization model determined three different scenarios to minimize the annual biogas separation cost when a high CH_4 recovery is needed. For the range of CO_2/CH_4 selectivity studied, this result shows that the feed compression scenario is still the first choice in the process and has an adverse effect on the separation cost. This issue might be less important as the membrane separation characteristics are improved.

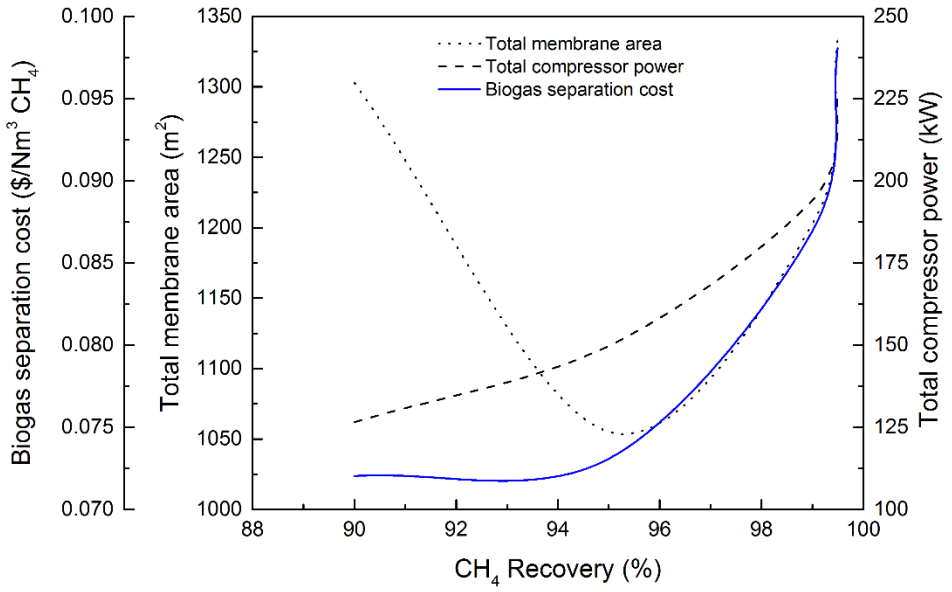

Figure 2.8 Effect of CH_4 recovery improvement on the gas separation cost when the CO_2 feed content is 40%.

2.5.3 Effect of CO_2/CH_4 selectivity on upgrading cost

Many efforts have been made to fabricate novel membranes with enhanced separation characteristics. Unfortunately, few of these membranes are used for industrial separation projects probably due to commercial and/or technical issues. This gap brings up an ambiguous situation regarding the sensible effect of the membrane modification approach on the reduction of gas separation cost instead of the removal performance. It is therefore of high necessity to reconsider all the possible operational parameters in view of the experimental and practical expectations. From the point of view of designing a membrane-based separation plant, the membrane characteristics including permeability

and selectivity would have a great effect on both the removal performance and cost. The well-known trade-off between permeability and selectivity limits the choice of membrane type for an efficient separation. In case of biogas upgrading, using high CO_2/CH_4 selectivity membranes results in a dramatic reduction in the unit permeance. A high membrane area is required to offset the unit deficiency and hence the capital and maintenance costs inevitably increase. The use of low CO_2/CH_4 selective membranes also results in increasing the compression duty to enhance the separation driving force. Hence, the priority of the current experimental works is to modify the fabricated membranes to improve their permeability and selectivity not necessarily considering implementation in a realistic separation plant. To our knowledge, no published optimization work has shown the effects of enhancing CH_4 and CO_2 permeances on biogas separation cost. In the present work, the CO_2/CH_4 selectivity of the original membrane (Ultem 1000) was increased to 66.4 according to specific permeance enhancement scenarios (Table 2.2).

Figure 2.8 shows the effects of CO_2/CH_4 selectivity on the biogas separation cost. As expected, the higher the CO_2/CH_4 selectivity is, the lower the achievable biogas separation cost will be. The optimization result shows that in case b (α=66.4), the feed pressure still needs to be kept at 18 bar to provide the adequate driving force in the CH_4 enrichment unit similar to the initial case a. Referring to the optimum process layout, in the first unit, the CH_4 content is enriched to 98% in the retentate product whereas the permeate product requires to be sent to the second enrichment unit. For higher CO_2/CH_4 selective membrane with a CH_4 permeance of 1.30 GPU, a lower gas circulation in the whole process is required. This leads to partly reduce the total power consumption in the mixer (M1) and splitter (PS1) according to Eq. (8). However, this change is also followed by a slight increase in the total membrane area (1279 m^2) compared to case a (1202.6 m^2) to meet the separation target. Taken together, the optimal solution in case b results in a 5% reduction in the biogas separation cost (Fig. 2.8).

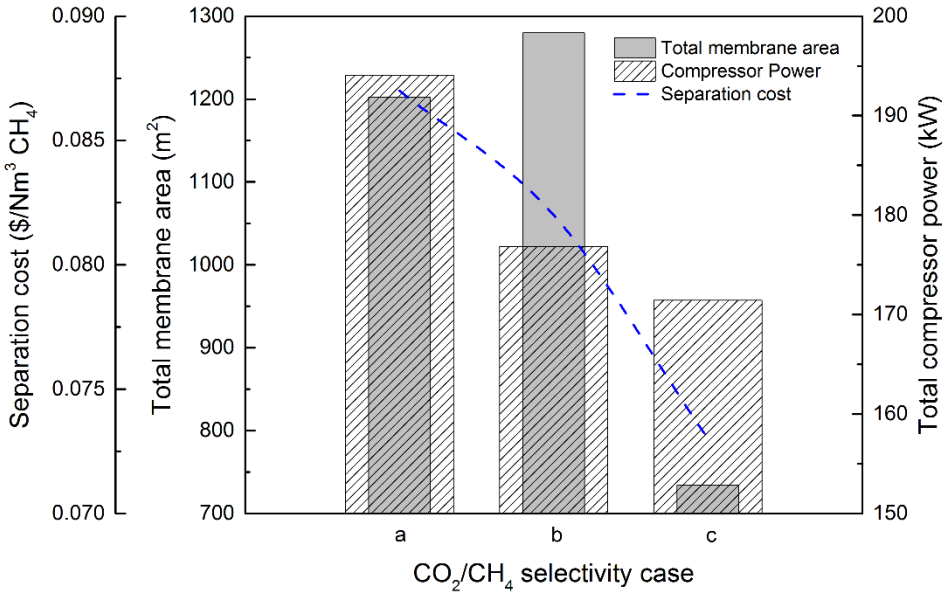

Figure 2.9 Effects of change in CO_2/CH_4 selectivities on the biogas separation cost for the following membrane CO_2/CH_4 selectivity and CO_2 permeance:
a) 33.2, 86.3; b) 66.4, 86.3; c) 66.4, 172.6.

Similarly, in case c (α=66.4), the total membrane area remarkably decreases from 1202.63 (case a) to 734.07 m^2 due to the enhancement in the CO_2 permeance (172.60 GPU). This results in 37 and 46% reduction in the required membrane area in the first and second enrichments units, respectively. More precisely, the optimum feed pressure also decreases to 16.48 bar. Thus, these changes in the membrane characteristics have a strong effect on the separation process. In turn, the biogas separation cost decreases to 15% compared to that of the case a. Referring to the optimization results, the membrane modification techniques, aiming to increase CO_2/CH_4 selectivity, should be favored to improve the CO_2 permeance instead of decreasing the CH_4 permeance. A further decrease in the biogas separation cost might be achievable by increasing the CO_2/CH_4 selectivity. However, it should be taken into account that this scenario might induce severe operational issues as the membranes with high permselectivity might be highly susceptible to deterioration with time on stream.

2.5.4 Effect of membrane cost on upgrading cost

As discussed above, most experimental works focus on membrane modification techniques so as to deal with the current separation trade-off and plasticization issues. In this case, different works have even announced the development of novel generations of membrane materials with excellent

permselectivity [72, 106, 107]. It is also reported that these materials are highly resistant to the side effects of high CO_2 concentration in the feed on the polymer structure at even high pressure. Despite the promising results, the most important concern undoubtedly pertains to the outlook of commercialization cost compared to the current commercial membranes. In the market of membrane gas separation technology, it is of high interest to estimate how much these developments will affect equally the removal performance and upgrading cost in a realistic commercial separation process compared to other techniques.

The membrane costs reported in previous works are estimated at \$20-100 per unit area (m^2) depending on the membrane types [87, 108, 109]. Referring to the previous sections, the annual biogas separation cost which consists of the capital and operation costs is calculated with the average purchased cost of \$50/m^2 area for all the modules. In this section a comparison was made assuming the membrane cost decreases to \$25/m^2 area for the two different CO_2/CH_4 selectivities of 33.2 and 66.4. This allows to disclose the effect of a possible change in membrane module cost on the required feed pressure and total membrane area, as well as the process layout while minimizing the annual biogas separation cost. Figure 2.9 shows the results for membrane cost of 50 and 25 \$/m^2 area in the optimization model for the CO_2/CH_4 selectivity of 33.2 with the CO_2 permeance of 86.30 GPU. For the membrane cost of 50 \$/m^2 area, the optimal values of feed pressure and total membrane area are set to 18 bar and 1202.6 m^2, respectively. In this case, the required driving force to upgrade a biogas feed with 40% CO_2 is achieved when the feed pressure is increased up to the maximum value of 18 bar. The annual biogas separation cost is reduced by 10% from 0.087 to 0.078 \$/Nm^3 of the upgraded CH_4 product.

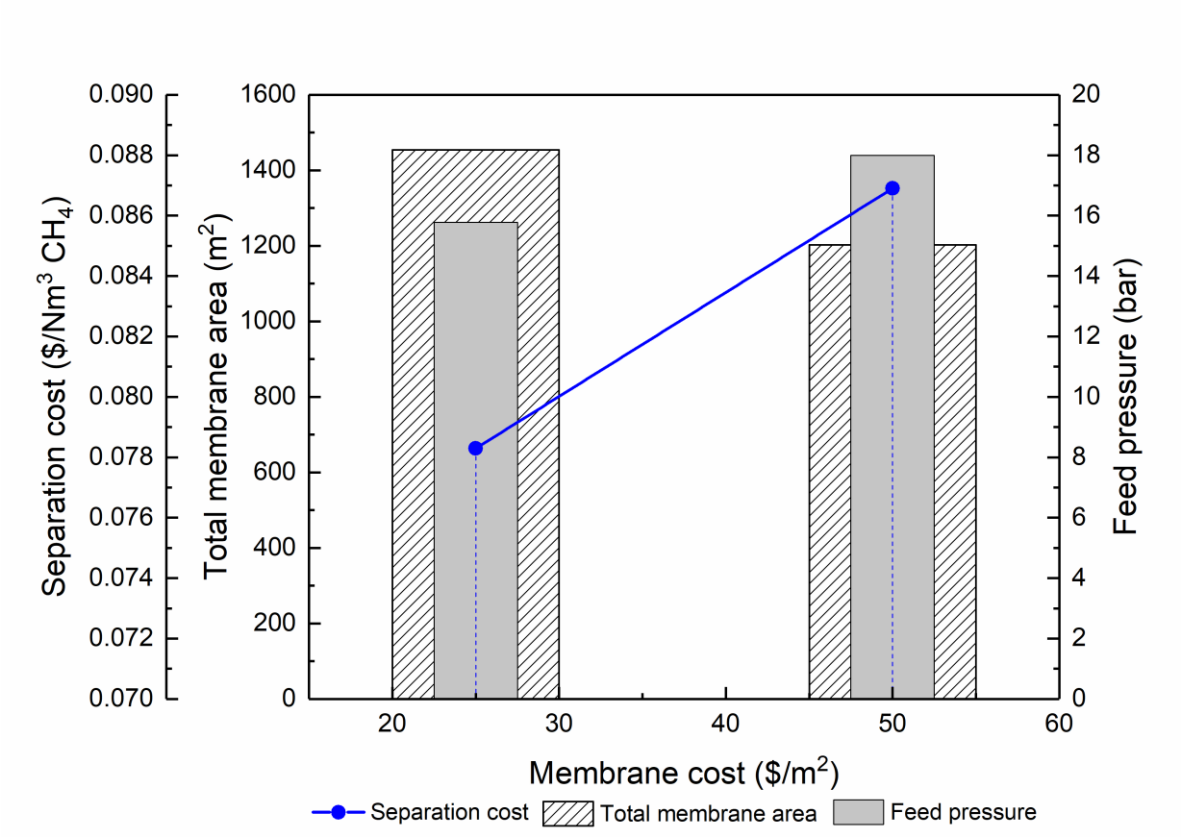

Figure 2.10 Effects of membrane cost (25 and 50 $/m^2) on the optimized separation cost, membrane area and feed pressure (CO_2/CH_4 selectivity of 33.2 with a CO_2 permeance of 86.3 GPU and a feed composition of 40% CO_2).

Figure 2.10 shows the effect of the actual change in the membrane cost from 50 to 25 $/m^2 on the biogas optimized separation cost after modifying the membrane by increasing the CO_2 permeance to 172.6 GPU and by keeping constant the CH_4 permeance to 2.6 GPU. The optimization procedure allowed finding the optimal values of the feed pressure (16.7 bar) and total membrane area (717.7 m^2) to minimize the separation cost to 0.044 $/Nm^3 upgraded CH_4. As shown, a 50% reduction of membrane purchase cost results in a 30% reduction in the feed pressure but an increase of 80% in the total membrane area. The membrane area takes the dominant role in the separation process cost and hence determines a reduction of 10% in the biogas separation cost from 0.044 to 0.039 $/Nm^3 of the upgraded CH_4. Comparing both cases in Figures 2.9 and 2.10, the reductions of 10% and 40% in the capital cost of membrane modules are observed (Table 2.3) upon 50% reduction of membrane cost for CO_2/CH_4 selectivities of 33.2 and 66.4, respectively. Actually, negligible change is seen in the biogas separation cost even by reducing the membrane purchase cost by half. Overall, this indicates

that the main parameters for a membrane-based separation process is the pressure ratio between the feed and permeate sides rather than the membrane separation characteristics. However, the recycle flow (RS2 in Fig. 2) in the separation system decreases upon increasing CO_2 permeance and lower compression power is required. But it is still necessary to compress the inlet feed gas (FS in Fig. 2.2) before injecting into the enrichment units resulting in higher inlet pressure. The estimation of separation cost is here performed by using a two-stage membrane process, as a single stage would never meet the process separation targets (CO_2/CH_4 recovery>99%). As indicated by our calculations, the results suggest the use of economical membranes with moderate permselectivity and long operation life, instead of focusing on improving selectivity.

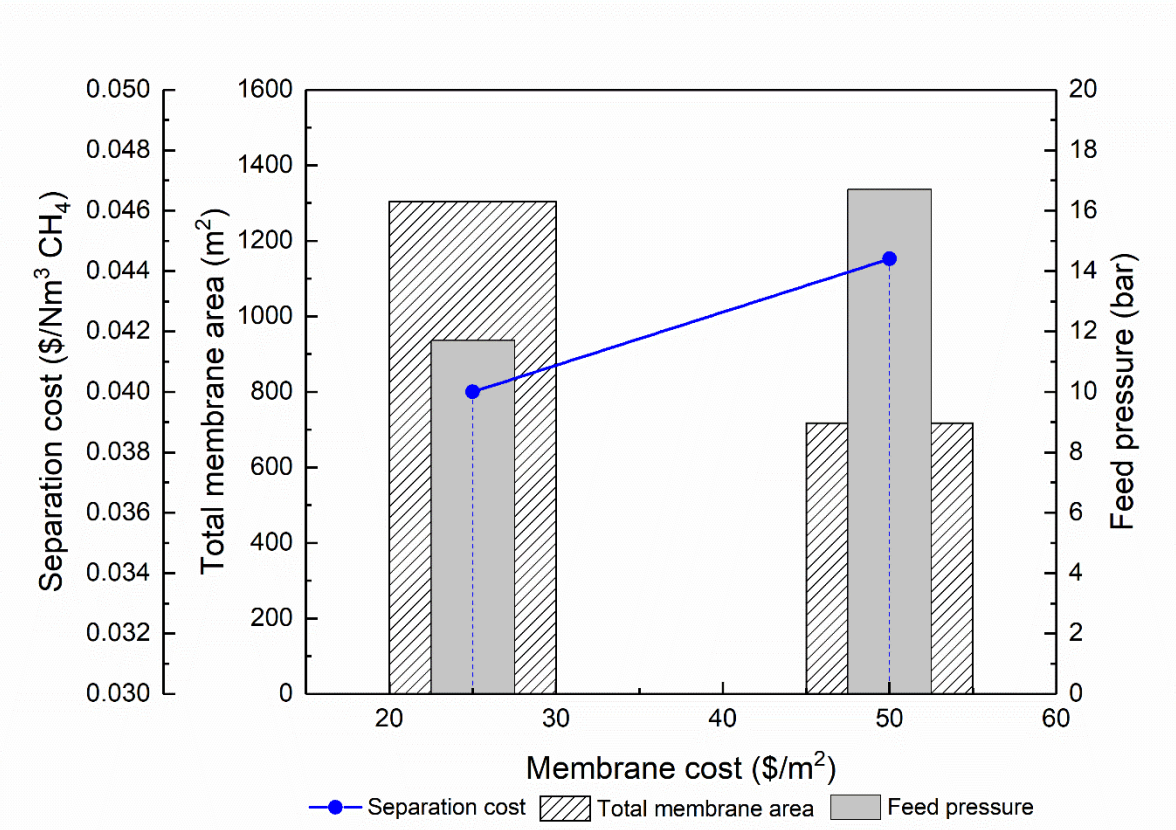

Figure 2.11 Effect of the membrane cost (25 and 50 $/m^2) on the optimized separation cost, membrane area and feed pressure (CO_2/CH_4 selectivity of 66.4 with a CO_2 permeance of 172.6 GPU, and a feed composition of 40% CO_2).

Table 2.3 Summary of the techno-economic analysis of optimized membrane separation processes.

Parameters		Symbol	Value				Unit
CO_2 content in feed		-	40				%
Permeance	CO_2	-	86.3		172.6		GPU
	CH_4	-	2.6		2.6		
Selectivity		-	33.2		66.4		-
Membrane cost		*MC*	50.00	25.00	50.00	25.00	$/m^2$
Total capital cost		*TCC*	809,175	709,045	666,815	605,751	$
Total membrane module cost		CC_{MM}	156,342	94,494	93,303	84,740	$
Installed compressor cost		CC_{CO}	372,155	360,881	334,943	301,092	$
Total power		-	194.08	186.97	172.30	151.54	kW
Installed heat exchanger cost		CC_{HE}	61,203	60,769	57,232	55,373	$
Total heat transfer area		-	9.44	9.31	8.61	8.11	m^2
Total compression unit cost		CC_{TC}	433,358	421,650	392,175	356,465	$
Fixed cost		*FC*	589,700	516,145	485,478	441,205	$
Base plant cost		*BPC*	660,464	578,083	543,736	494,150	$
Project contingency		*PC*	132,092	115,616	108,747	98,830	$
Total facilities investment		*TFI*	792,557	693,699	652,483	592,980	$
Start-up cost		*SC*	16,617	15,345	14,331	12,770	$
Annual variable operating and		*VOM*	166,178	153,457	143,319	127,705	$/y
Contract and material maintenance cost		*CMC*	39,627	34,684	32,624	29,649	$/y
Local taxes and insurance		*LTI*	11,888	10,405	9,787	8,894	$/y
Membrane replacement cost		*MRC*	6,013	3,634	3,588	3,259	$/y
Equipment maintenance		*EMA*	15,600	15,179	14,118	12,832	$/y
Utility cost		*UC*	93,048	89,552	83,200	73,070	$/y
Annual capital related cost		*CRC*	161,835	141,809	133,363	121,150	$/y
Gas separation cost		*GSC*	0.0869	0.0783	0.0444	0.0390	$/Nm^3$

2.6 Conclusion

This work presented a new process optimization approach for a fairly complete gas separation setup, in particular for CH_4/CO_2 biogas upgrading. This optimization technique, which considers initially a large number of possible combinations of gas permeators in a superstructure network, aims at finding the most efficient layout at minimum annual gas separation cost. The model equations constitute a Mixed Integer Nonlinear Programming (MINLP) problem as such; it is coded using A Mathematical Programming Language (AMPL) as an algebraic modeling language to determine the global optimum separation cost. For a CO_2/CH_4 selectivity of 33.2 and a CO_2 permeance of 86.3 GPU, the optimization results showed that a two-stage process is the most profitable layout to upgrade biogas for different CO_2 contents ranging from 10 to 40% in feed. The optimal layout enriches CH_4 and CO_2 in the first and second membrane units, respectively. An increase in the feed CO_2 content from 10 to 40% results in increasing both the feed pressure and membrane area without changing the layout.

Using the Branch-And-Reduce Optimization Navigator (BARON) solver enabled the model to reconcile the gas flowrate and pressure, and membrane area in each unit and thereby find the global optimum while minimizing the gas separation cost. It was observed that the gas separation cost is highly dependent on the CH_4 recovery. The membrane area, as decision variable, has a determinant role in the optimization model when a low CH_4 recovery of 90% is required. On the contrary, the feed pressure needs to be maximized to provide sufficient driving force for a CH_4 recovery higher than 95%. This model was then used to minimize the required module number in a typical membrane-based separation process. The FA index related to unit separation capacity at a given driving force was introduced in the model to specify the exact module number for a given capacity. The results at first showed that the use of smaller modules was more realistic as the packing fraction was highly decreased by increasing the module length (<50%). It was also shown that the use of current modules with high packing fraction (>90%) led to drastically increased weight and footprint of a separation package. Furthermore, this approach aimed at considering a general guideline showing correlations between required module number in a realistic separation process and unit *FA* index based on primary experimental results. The model also highlighted the effect of better membrane characteristics on the annual gas separation cost. For two membranes with an identical CO_2/CH_4 selectivity of 66.4, membrane modification techniques should favor an increase in CO_2 permeance rather than a decrease in CH_4 permeance resulting in a reduction of 15% in the gas separation cost. Decreasing membrane purchase cost from 50 to 25 $\$/m^2$ would result in decreasing the optimized feed pressure for both CO_2/CH_4 selectivities of 33.2 and 66.4. The gas separation costs thereby decreased from 0.087 to 0.078 $\$/Nm^3$ and from 0.044 to 0.039 $\$/Nm^3$ of the upgraded CH_4, respectively, when the CO_2 feed content was 40%. Then, lower membrane purchase cost had moderate impact on the gas separation cost, but the optimized feed pressure significantly decreased. In terms of techno-economic evaluation, the gas separation cost of the optimized two-stage process allowed to be competitive with conventional separation processes. It is worth noting that the optimized process becomes more profitable at low CH_4 recovery. Hence, the membrane technology might efficiently be used in hybrid systems in which lower CH_4 recovery and purity would be required from the membrane part of the process. Such strategy would undoubtedly result in significant reductions in both the required feed pressure and membrane area. Finally, the results obtained certainly have a direct effect on the future of this technology as experimentalists should realize that the main effect of the fabrication techniques on reducing separation cost compared to increased membrane permselectivity.

Nomenclature

A_{he}	Heat transfer area
A_{mT}	Unit membrane area
ΔA	Membrane separation area
AMPL	A Mathematical Programming Language
AO	Annual operation
BPC	Base plant cost
C_{AS}	Annual separation cost
C_{bi}	Binary variable
C_{EP}	Electricity consumption cost
C_{HEA}	Heat transfer area cost per unit area
C_p	Specific heat capacity in constant pressure
C_{RP}	Refrigeration cost
CMC	Contract and material maintenance cost
CRC	Annual capital related cost
CC_{CO}	Capital cost of compressors
CC_{HE}	Capital cost of heat exchanger
CC_{MES}	Membrane skid cost
CC_{MEA}	Membrane purchased cost per unit area
CC_{MEI}	Membrane installation cost
CC_{MM}	Membrane module cost
CC_{TC}	Total compression unit cost
d_o	Fiber outer diameter
D_M	Module diameter
EP	Electricity price
EMA	Equipment maintenance
f_{ic}	Installation factor
ΔF_c	Permeate molar flowrate
F_M	Module molar flowrate
F_p	Permeate molar flowrate
F_r	Retentate molar flowrate
F_{RP}	CH_4 retentate production
F_U	Unit molar flowrate
FA	Ratio of the inlet gas flow rate to total membrane area
FC	Fixed cost
FS	Feed splitter
GSC	Gas separation cost
H_{AO}	Annual operation time
HTAC	Heat transfer area cost
HFM	Hollow fiber membrane
k	Isentropic expansion factor
LTI	Local tax and insurance
l_e	Fiber length

L_m	Module length
M	Mixer
MC	Membrane cost
MINLP	Mixed-integer non-linear programming
ML	Membrane life
MRC	Membrane replacement cost
Mw	Molecular weight
N_f	Fibers number
N_p	Number of stages
N_{st}	Compression stages
OC_{HE}	Operation cost of heat exchanger
OC_{OV}	Total operation cost of compressors
OC_{TU}	Operation cost of turbine
OSF	On-stream factor
P_p	Permeate pressure
P_r	Retentate pressure
PC	Project contingency
PM	Permeate mixer
PS	Permeate splitter
Q_c	Membrane permeance
Q_{EH}	Heat exchanged between gas and water
R	Recycle ratio
R_g	Gas universal constant
Re	Reynolds number
RM	Retentate mixer
RP	Refrigeration price
RS	Retentate splitter
SC	Start-up cost
T	Temperature
ΔT_{lm}	Logarithmic mean temperature
TFI	Total facility investment
U	Overall heat transfer coefficient
UC	Utility cost
UM_N	Modules number
V	Compressor inlet volumetric flowrate
V_m	Module volume
VOM	Variable operating and maintenance cost
W_{co}	Compressor power
W_{CO2}	Permeate compressor power
W_F	Feed compressor power
W_{OC}	Net compressor power
W_R	Recycle compressor power
W_{RP}	Required compressor power
W_{TU}	Turbine compressor power
x_r	Retentate Mole fraction

y_p	Permeate mole fraction

Greek symbols

η	Isentropic compression efficiency
μ	viscosity
ρ	density
υ	Gas velocity
φ	Module packing fraction

Chapitre 3

Techno-Economic Evaluation of Membrane and Enzymatic-Absorption Processes for CO_2 Capture from Flue-Gas

3.1 Résumé

Une large part de l'énergie globale est fournie par des centrales électriques à combustion fossile qui libèrent une quantité élevée de CO_2 dans l'atmosphère. Aussi longtemps que ce modèle d'énergie prévaudra dans le monde, les inquiétudes à propos du changement climatique associé à la hausse soudaine de la quantité de gaz à effet de serre ne pourront être allégées que par l'équipement des centrales électriques à combustion fossile avec des unités de captures de CO_2. Les méthodes de la séparation de gaz telles que l'absorption à base d'amine pourraient être suggérées pour atteindre cet objectif mais elles pourraient résulter en un procédé coûteux et hautement intensif. Cette étude analyse l'intégration d'une centrale électrique de 600 MWe avec deux méthodes prometteuses, incluant la technologie de séparation par membrane et le procédé d'absorption enzymatique. Une analyse technico-économique a été réalisée pour démontrer la viabilité technique et l'efficacité économique de ces deux méthodes aux procédés traditionnels de séparation. Il a été trouvé que les pertes d'électricité sont respectivement estimées à 95 et 89 MW, pour capturer 90% du CO_2 qui serait aussi peu que 15% de la puissance de sortie. Cette étude présente aussi les résultats de l'optimisation de coût, incluant les dépenses d'investissement et les dépenses d'entretien, pour chaque méthode. En comparaison, l'absorption à base d'enzyme est plus attractive économiquement et implique un moindre coût de capture de CO_2. En général, cette étude permet de reconnaitre les obstacles dans chaque procédé puis propose des initiatives pour améliorer l'efficacité de capture.

3.2 Abstract

A large part of the global energy is supplied through fossil-fuel power plants which release a high amount of CO_2 into the atmosphere. As long as this energy pattern prevails in the world, concerns about climate change due to sudden rise in the content of green-house gasses (GHGs) might be alleviated only through retrofitting the power plants with CO_2 capture units. Gas separation methods such as amine-based absorption could be suggested to hit this target but they could result in a costly and highly intensive process. This study analyzes the integration of a 600 MW_e power plant with two

promising methods, including membrane separation technology and enzymatic-absorption process. A techno-economic analysis is then carried out to demonstrate the technical viability and economic efficiency of these two methods compared to traditional separation processes. It is found that the electricity losses are estimated at 95 and 89 MW respectively, to capture 90% of the CO_2 which is as low as 15% of the output power. This study also presents cost optimization results including capital and operation expenditures for each method. In comparison, enzyme-based absorption is more economically attractive and results in a lower CO_2 capture cost. Overall, this study allows to recognize bottlenecks in each process and then proposes initiatives to improve the capture efficiency.

3.3 Introduction

The rise of carbon dioxide (CO_2) level in the atmosphere is unanimously considered as a global concern. Despite a stable growth in the CO_2 emission between 2014 and 2016, a dramatic increase by 1.4% was again observed in 2017, indicating a historic high of 32.5 gigatons in global energy-related CO_2 emissions [6]. The fact remains that most of CO_2, which is the major contributor to greenhouse gases (GHGs), is released through human activities such as burning fossil fuels (coal, oil, and gas). Knowing that excessive amount of CO_2 in the atmosphere is regarded as the primary reason of dramatic climate changes in recent years, inconsiderate use of fossil fuels to increase economic output is unacceptable. Therefore, it is a must to avoid unabated CO_2 accumulation in the atmosphere through integration of current potential emitters into the CO_2 mitigation policies and laws. According to the Paris Agreement (PA), the CO_2 emissions should be reduced to keep the global temperature rise below 2^{o}C compared to pre-industrial levels, trying to hold the temperature increase even further to 1.5^{o}C [1]. In doing so, Carbon Capture and Storage (CCS) is a promising option to pragmatically deal with the mitigation of CO_2 emission through retrofitting existing industrial sectors [2]. The CO_2 capture which is more energy-intensive than transportation and storage steps accounts for 80% of the entire CSS chain cost. Despite CCS still being called “pre-commercial”, it is the only mitigation technology to effectively curtail CO_2 emissions from power plants and cement manufacturers [110].

Currently, the use of power plants as a prototype case to generate electricity represents our high dependency on fossil fuels. Referring to energy trends in 2017, fossil fuels including coal, oil, and gas contributed, respectively, 38, 23, and 4% to generate the global electrical energy of 25,570 TWh [6]. Following the energy conversion, the CO_2 content in the flue-gas accounts for 7-8% and 10-15% in gas- and coal-fired power plants, respectively. As a 500 MW coal-fired power plant with a thermal efficiency of 40% would emit approximately 426-455 tons of CO_2 per hour (~ 850-910 kg CO_2/MWh) [111], neglecting such a gigantic emission would fail meeting the PA capture scenarios. It is therefore compulsory to treat the flue-gas before releasing in the atmosphere to avoid such a tremendous CO_2

emission. The statistics show that Canada's GHG emissions were 704 megatons of CO_2 equivalent in 2016 which was a net reduction of 28 Mt or 3.8% from 2005 emissions [112]. In 2016, the electricity generation was estimated at 648.4 terawatt-hour (TWh) using different sources such as hydro (59%), nuclear (15%), oil and gas (10%), coal (9%), and non-hydro renewable (7%) [112]. Thus, 19% of the Canadian electrical energy industry still hinges on fossil fuels and hence deployment of CCS technology should be considered to impede the inconsiderate CO_2 emission. In cement plants, the atmospheric stack gas is also composed of 15-30% CO_2 which is formed during the burning process due to carbonate decomposition into CO_2 and combustion of fossil fuel to provide heat [113]. Thus, the cement plants also contribute to GHGs emissions and they are particularly regarded as the third largest energy consumer and the second industrial CO_2 emitter, with about 7% of global emissions [112]. In Canada, the cement and concrete product manufacturing accounts for 13% of total CO_2 emissions in the industry sector which was estimated at 77 Mt CO_2 in 2016 [112]. Canada, as a committed member of the United Nations Framework Convention on Climate Change (UNFCCC) which ratified the PA, is developing CO_2 mitigation plans to reduce GHG emissions in line with estimated annual baselines. As a solution, the CCS approach can be implemented to viably capture low content CO_2 from the flue-gas produced in either power plants or cement manufactures. Unfortunately, this solution also faces some limitations which pose serious questions about the loyalty of nations to the UNFCCC treaties.

The post-combustion carbon capture (PCC), which consists of absorption, adsorption, cryogenic distillation, and membrane technology, might be complementing the existing processes [6]. Owing to the low partial pressure of CO_2 and high flowrate of flue-gas stream, the selection of a separation method needs careful technical and economic considerations. The full energy for CO_2 capture is supplied by the power plant and mainly consumed through heat exchanger units and compression equipment such as blowers and compressors. Thus, the thermal efficiency of a thermo-electrical power plant and its output of electricity are highly susceptible to be decreased upon the implementation of a high-performance CO_2 removal process [114]. The absorption process is the most mature and reliable choice, as is was successfully incorporated into the CO_2 separation from various industrial gas mixtures for decades. This process relies on a solvent's chemical affinity with CO_2 to dissolve it in the liquid phase while the other gas components (mainly N_2 and O_2) remain in the gas phase. Accordingly, in most cases, CO_2 is of high purity in the final product, indicating high-selective capacity of the absorption process. The solvent might be chosen from a variety of reactive solvents such as amines, hot potassium carbonate, chilled ammonia, and ionic liquids [115]. Thus far, amines such as monoethanolamine (MEA) are the most developed and effective solvents used for the

post-combustion CO_2 capture regardless of being less eco-friendly and more corrosive to equipment [5]. A solvent's CO_2 selectivity over N_2 and O_2 can also be improved through blending with other solvents. For instance, the absorption efficiency increases to 92.2% by adding triethanolamine (TEA) to an aqueous solution of MEA (20%) [116]. The main concern about the absorption process is the high energy requirements to recover a rich solvent in the regeneration unit. To reduce this, the mix of MEA and methyldiethanolamine (MDEA), which requires lower regeneration energy and low reaction rate, could be regarded as an alternative [117]. Numerous studies on the techno-economic analysis of CO_2 capture in absorption processes are available in the literature [82, 118-120]. In addition, the thermal energy requirement for MEA absorption process to capture CO_2 from power plants or cement manufactures is estimated to be 3-4 GJ/ton CO_2 [12, 121]. Such energy required for solvent regeneration accounts for 70-80% of total operating cost of capture plants. Three scenarios including optimization of operating parameters, modification of the process layout, and improvements of solvent reactivity need to be taken into account to reduce the energy consumption of CO_2 capture [122].

Currently, the other separation methods might still be less competitive compared to the solvent absorption process. The main barrier concerns the separation driving force which is strongly dependent on feed gas pressure. Hence, a large energy penalty should be paid through pressurization steps to liquify/compress the flue-gas whatever the main separation process. In the adsorption process, the separation involves allowing a target gas through a solid adsorptive bed to temporarily trap CO_2 on its surface. The bed is composed of either non-reactive or reactive sorbents such as molecular sieves, carbonaceous materials, zeolites, metal organic frameworks, and amine-based porous structures [123, 124]. The amine-based sorbent dissolves CO_2 via the same reaction which occurs in the amine absorber column and theoretically demands less energy for the regeneration [125]. In the case of a Temperature Swing Adsorption (TSA) process, CO_2 recovery is highly restricted by the regeneration temperature. The cycle times for heating and cooling steps are also another limitation especially for large-scale CO_2 capture. For instance, for a CO_2 purity higher than 91%, CO_2 recoveries of 55, 76.2, and 83.6 at specific energy consumptions of 3.4, 3.8, and 4.5 MJ/kg CO_2 can be achieved when the regeneration temperature increases from 150 to 200, and 250^{o}C, respectively [126]. Despite the rapid cycling (in minutes), the size of adsorbent bed decreases in a Pressure Swing Adsorption (PSA) process compared to a TSA process, resulting in an increase of the process footprint due to the increased number of PSA subunits to treat the same flow of gas. To process high flowrate flue-gas (66.2 kg/s), a large number of PSA trains (~72) is required only for the first-stage that seems not to be feasible compared to the baseline absorption process [127]. On the contrary, a Vacuum Swing

Adsorption (VSA) process might be more prospective for CO_2 capture from flue-gas as the energy requirement is estimated at 3.3 MJ/kg CO_2 [128]. In brief, the VSA is of high interest to compete with the MEA absorption process. It is therefore essential to ensure high CO_2 recovery for large-scale capture and to enhance the efficiency of vacuum equipment [129]. The target might be achieved by developing new adsorbents with higher equilibrium capacity, CO_2 selectivity, stability to water and impurities, and low cost [124].

Cryogenic condensation is considered as another alternative for CO_2 capture from a flue-gas stream. The separation relies on phase change due to the difference in boiling and freezing points of CO_2 and other gas components [6]. The flue-gas undergoes multistage compression and cooling steps and thereafter expansion of the high-pressure gas to largely drop its temperature [130]. Through this process, CO_2 in the flue-gas turns to liquid or solid phases, and is sequentially separated from the other gas components. In this case, higher CO_2 purity and recovery (99.99%) can be obtained compared to the other separation methods. More interestingly, CO_2 product which is a high-pressure liquid is ready to be transported via pipeline for sequestration. This scenario seems to be unrealistic when a large flowrate gas released at atmospheric pressure needs to be compressed until CO_2 phase changes. As a result, this process looks energy-intensive without any chance to compete with other separation methods. Considering studies on process developments, the current cryogenic CO_2 capture can be categorized in the following technologies: Packed bed [131], Anti-sublimation [132], Cryocell® [133], Distillation [5], and Stirling coolers [134]. The main barrier to integration into power plants stems from the unavailability of cold energy sources. Thus, substantial energy should be granted to cool the system resulting in high energy penalties. In the presence of an energy source, its capital and operation costs might be lower than the solvent absorption process [135]. However, pre-treatment is always recommended to remove H_2O and impurities (SO_x, NO_x, and mercury) to avoid clogging and corrosion in cooling equipment. This compulsory step affects the capital cost of the cryogenic process. Moreover, process modification might lead to promising results however not avoiding the pre-treatment step. For instance, the state-of-the-art of cryogenic method is to remove CO_2 from flue-gas at atmospheric pressure through three consecutive steps: a cooling, capture, and recovery step [136]. The flue-gas is cooled down to temperature below the sublimation temperature of CO_2 to avoid operational issues due to CO_2 crystal formation. To reach a CO_2 recovery higher than 99%, the required cold duty is estimated at 1.8 MJ/kg CO_2 when the flue-gas contains 10 and 1 vol.% CO_2 and H_2O, respectively. The CO_2 removal efficiency is strongly reliant on the availability of cold sources such as the evaporation of LNG at a regasification terminal. Otherwise, the electricity

generated by the power plant is offset by the energy consumed with the refrigerators to supply cooling capacity [131].

As discussed above, the high energy penalty for solvent regeneration, low CO_2 selectivity, stability of adsorbents, and lack of cold energy sources are the main limitations for the large-scale implementation of PCC methods. Despite researches to resolve these technical issues, membrane technology might also be considered as a promising choice for CO_2 removal from flue-gas. In comparison, the separation mechanism is simple but effective as well. A polymeric membrane, dense or porous with a thin selective layer, acts as physical barrier through which gas components have different permeation rates [6]. For 30 years, applications of gas permeators to remove acid gases have shown the high potential of this technology to displace the conventional separation methods. In 1995-2008, Honeywell UOP established and later developed the world's largest membrane CO_2/natural gas separation plant (265-600 MMSCFD) to reduce CO_2 mole fraction from 5.7 to 2% using cellulose acetate membranes [137]. Schlumberger also introduced state-of-the-art membrane systems called CYNARA and Apura to efficiently polish gases which have a variety of compositions from 5 to 95% CO_2 [138]. Such industrial cases show a very positive outlook for commercialization of membrane technology for CO_2 separation in the near future. Similarly, a great effort has been made to use membrane technology for CO_2 capture from power plant flue-gas. From 2007 to 2009, Membrane Technology and Research Inc. (MTR) launched researches on the development of CO_2 capture plants using a new non-facilitated polymeric membrane (Polaris™). As reported, the CO_2 permeance was tenfold higher than commercial CO_2-selective membrane used in natural gas treatment at that time and has high CO_2/N_2 selectivity ranging from 50 to 200. The Polaris™ membrane was later used to capture 90% of CO_2 from a 600 MW_e coal-fired power plant. About 15% of the power plant's outputs or 90 MW_e was spent to supply the required energy for the membrane process. The high-pressure liquid product enriched in CO_2 was also ready for sequestration and the CO_2 capture cost was estimated at 20-30$/ton CO_2 [139]. Despite the promising progress in the case of flue-gas separation, the US Department of Energy (DOE) defines a baseline to retrofit CO_2 separation and capture technologies into existing coal-fired power plants. Since then, the target is set to capture 90% CO_2 with a purity of 95% at a cost of electricity (COE) 30% less than the baseline CO_2 capture approaches. Thus, membranes which are of high CO_2 permeance, low cost, high thermal and physical stability, and resistant to flue-gas contaminates need to be developed to meet the DOE criteria. Facing this challenge, it is recommended that the membrane properties should reach a CO_2 permeance of 3000 GPU, a CO_2/N_2 selectivity of 140, and a feed pressure close to 1 bar [140]. Such hypothetical membranes appear to be very far from the existing flat and hollow fiber membranes in which CO_2

permeance and CO_2/N_2 selectivities are in the range of 10-300 GPU and 20-50, respectively [141]. Overall, the membrane technology is now maturing, and somehow contingent upon high progress in membrane characteristics to compete with the baseline MEA absorption process. Hence, it is worth noting that this process might be suitable for bulk removal of acid gases. Either permeate or retentate stream may then be redirected to the conventional separation methods such as cryogenic [11], absorption [12], or PSA [142] processes for further treatment.

3.3.1 With or without the MEA solution: that is the question!

As discussed above, MEA is the most widely used solvent for CO_2 absorption, thanks to its high loading capacity. Such reputation of the benchmark amine-based solution is mostly attributed to the relatively high reaction rate with CO_2, high mass transfer rate, high solubility in water and low viscosity, low degradation and volatility, and availability at economical cost. Hence, the MEA absorption process seems to be the most dominant PCC technology for flue-gas separation to achieve high CO_2 recovery and purity. In this case, the typical capture cost is estimated to be in the range of \$40-100/ton CO_2 [143]. Nevertheless, the amine-based process also faces some drawbacks such as high regeneration energy, high corrosiveness to equipment, poor thermal stability, and non-ecofriendly nature [144]. Furthermore, many efforts have been made to potentially overcome these issues in virtue of different scenarios such as deployment of process modification and optimization, integration with industrial plants, and introduction of new solvents.

Pellegrini et al. [145] compared two process configurations to reduce the energy penalty of MEA regeneration in the stripping section designated as double-column [146] and multi-pressure column [147]. In comparison to the baseline MEA absorption process, the use of the second stripper column and vapor compression along the stripper column led to 45 and 54% reductions in the reboiler heat duty, respectively. Moullec and Kanniche [148] also investigated the effects of CO_2 capture unit flowsheet modification of MEA absorption process on the energy consumption compared to a reference of 3.7 GJ/ton CO_2 at 1 atm. The reduction of efficiency penalty by 4-8% was achievable through individual flowsheet modifications, for example, a stripper operating with moderate void pressure (around 0.75 bar); the staged feed of the stripper; the lean solvent vapor compression; the overhead stripper compression; the internal stripper compression. Other scenarios such as intercooler modification, economizer improvement, boiler condensate vapor compression had only 2% reduction of efficiency penalty. In comparison to the other cases, the advance split-flow [118] and direct steam stripping [149] approaches contributed by 30 and 27% to saving on the efficiency penalty, respectively. The authors also provided a very comprehensive review of 80 patents and 26 publications on the modification of MEA absorption process to classify all potential changes into

three main groups including absorption enhancement, heat integration, and heat pumps [150]. They reached the conclusion that a parasitic energy reduction by 45% was achievable at the expense of increasing the process complexity and cost, and of decreasing process operability. Despite this, Cousins et al. [151] also reported that the process improvements with flowsheet modification would induce an increase in the number of unit operations and hence higher capital cost. Later, Oh et al. [152] proposed a systematic optimization approach embedding all possible structural modifications classified by [150] for the MEA absorption process to minimize energy penalty. In comparison to the base case (4.23 MJ/kg CO_2), individual modifications, namely, multiple solvents, flue-gas split, pump-around, semi-lean solvent, all process modifications resulted in the reboiler specific duty of 4.17, 3.99, 4.17, 4.22, 3.93 MJ/kg CO_2, respectively. In turn, the annual energy cost was only 7.8% lower than that of the base absorption case that was 19.92 M$/y. Abu-Zahra et al. [121] optimized a MEA absorption process designed to capture CO_2 from flue-gas of a 600 MW coal-fired power plant. In doing so, the parameters including lean solvent loading, MEA concentration, and stripper operating pressure had the highest impacts on the reduction of the solvent regeneration energy. In the optimal process, these parameters were respectively set to 0.3, 40 wt.%, and 210 kPa resulting in a thermal energy requirement of 3.0 GJ/ton CO_2. This indicated a decrease of 23% compared to that of 3.9 GJ/ton CO_2 in the baseline process (MEA 30 wt.%) to capture 90% of CO_2. To realistically implement the optimization outputs, an MEA solution of 30 wt.% was also considered for which the optimal value of regeneration energy was found to be 3.3 GJ/ton CO_2. Li et al. [153] made a techno-economic analysis of a MEA absorption process used to capture CO_2 from flue-gas of a 650 MW coal-fired power plant. This process was initially improved through optimizing operation parameters such as MEA concentration, lean solvent loading and temperature, and stripper pressure, followed by modifying the flowsheet to effectively reduce energy penalty and capture cost. The optimization framework contributed to reduce the regeneration energy from 4 to 3.6 MJ/kg CO_2 and additionally the CO_2 capture cost was reduced from US$86.4 to US$81.2/ton CO_2 (USD 2013). Then, the optimized process was modified through incorporation of additional processes such as absorber inter-cooling (energy saving and column modification), rich-split process (traditional and modified), stripper inter-heating process, and advanced process for further improvements. These scenarios also led to reduce the reboiler duty from the optimal value of 3.6 to 3.55, 3.60, 3.30, 3.24, 3.36, and 3.08 MJ/kg CO_2, respectively. The advanced process outperformed the other alternatives wherein CO_2 avoided cost also decreased by 13.1% from US$86.4 to US$75.1/ton CO_2.

Numerous scenarios have been suggested to integrate the absorption process into fossil-fuel power plants [154-156]. In comparison, this approach might be more realistic as the required energies for

solvent regeneration, CO_2 compression unit, and other equipment may be supplied by the power plant itself. In this case, part of steam is redirected to the stripper unit and thereafter injected into a reboiler. The steam extraction then results in a reduction of thermal efficiency by 10-15% [157]. The priority is to maintain thermal efficiency which is linearly correlated with the efficiency penalty through finding a proper location to supply the required steam [158]. Duan et al. [159] focused on two scenarios: extraction of regeneration steam to feed a low-pressure turbine and replacement of new system to feed water heater to integrate a 600 MW coal-fired power plant with the MEA absorption unit. They reported that the gross power output was 71.14 MW and 39.7 MW less than that of the baseline process (without capture unit) and the efficiency penalty induced by integration were 8.49 and 6.59% points, respectively. Without integration to capture 85% CO_2, the required energy for the MEA regeneration was estimated at 2.83 MJ/kg CO_2 whereas the integrated unit aimed at reducing it to 2.14 MJ/kg CO_2. Farajollahi and Hossainpour [160] investigated the effect of using Organic Rankine Cycles (ORCs) on the net thermal efficiency of a 350 MW natural gas-fired power plant. For the absorption process, low-grade heat sources identified as CO_2 compression intercoolers, steam cooler before the reboiler, and flue-gas cooler before feeding to the capture unit were recuperated through ORCs to generate 17.38 MW_e net extra power. This approach, followed by process integration using an auxiliary turbine to decompress steam, aimed at reducing the efficiency penalty of power plant to 5.1%.

The improvement scenario either optimizing a process or integrating it into a power plant makes positive impacts on a reduction of total energy requirement and process intensification. Despite considering feasibility studies on the above-mentioned initiatives, the energy requirement for the MEA absorption process is estimated to be in a range of 2.83-3.9 MJ/kg CO_2. Currently, commercial solvents such as Econamine FG+ and KS-1 are extensively used for CO_2 capture from flue-gas, whereby regeneration energies of 3.12 and 3.08 GJ/ton CO_2 with efficiency penalties of 9.2 and 8.4% can be realized, respectively [158]. Hence, further energy reduction might be contingent on contributions of novel solvents by which not only removal efficiency improves but also the stripper boiler requires a lower amount of energy for CO_2 desorption and heating up a rich solvent. Selection of secondary or tertiary amines such as diethanolamine (DEA), triethanolamine (TEA), and methyldiethanolamine (MDEA) is not adopted as it results in reducing not only the rate of reaction but also the energy of regeneration [161]. Hence, the blend of amines might be regarded as a promising solution to enhance both removal and energy efficiency. This plan mainly concerns the fact that no single solvent has demonstrated all excellent features for CO_2 capture. Nwaoha et al. [162] made a comprehensive review on the progress and prospect of blended amine solvents for CO_2

capture. The amine-bi solvent blends as a mixture of a high CO_2 absorption capacity solvent and a highly reactive amine solvent, exhibited considerable performance both in laboratory scale and pilot-plant scale. In turn, lower circulation rate, better absorption rate, and reduction in regeneration energy up to 50% were observed. For instance, the reaction of MDEA is accelerated by adding rate promoters such as piperazine (PZ) and the mixture offers higher CO_2 reaction rate than both MEA and DEA solutions [163]. Fernandez et al. [164] also investigated the performance of MEA and innovative solvent as part of a EU project [165], called CESAR-1 (a blend of aqueous solution of 23% w/w AMP (2-Amino-2-Methyl-Propanol) and 12% w/w PZ) for capturing CO_2 from flue-gas of an advanced supercritical (ASC) pulverized coal-fired power plant. CESAR-1 outperformed the traditional MEA solvent resulting in a reduction in the regeneration energy from 3.7 to 2.7 GJ/ton CO_2. Furthermore, CESAR-1 had better performance than of CESAR-2 (0.32 g/g 1,2-ethanediamine 0.68 g/g H_2O) which was a primary amine with two amine groups [166]. For CESAR-3 (a mixture of the sterically hindered AMP and the primary diamine 1,2-ethanediamine (EDA)), the reboiler heat duty was also found to be 3.7 GJ/ton CO_2 at a L/G ratio of 1.4 kg/kg and hence offered better performance compared to 4.1 GJ/ton CO_2 for MEA at a L/G ratio of 2.5 kg/kg [167]. Despite the promising results, the temperature of the solvent circulated in the reboiler has to be maintained in the range of 100 to 120ºC to realize 90% CO_2 capture. Amines degrade at high temperatures, but blended amines also offer a lower rate of degradation compared to MEA solution. As AMP degradation is limited at 100 and 120ºC [168], and PZ degrades even slower, the blend of AMP/PZ (CESAR-1) might have identical degradation to single AMP and PZ systems [169]. The breakdown of energy consumption of the stripping system for a blend solvent of 18 wt% AMP + 17.5 wt% PZ also shows that the heat of desorption to break the CO_2 bound, sensible heat needed to raise the rich solvent temperature to the regeneration temperature, and latent heat of H_2O vaporization to generate the stripping stream are estimated to 45.89, 15.49, and 38.16% of the total reboiler heat duty, respectively [170]. In summary, the amine-based blending scenario properly contributes to energy requirement for solvent regeneration and consequently to total CO_2 capture cost. However, higher attention is also needed to control the concentration of each constituent of the blended solvent through make-up operation.

The use of carbonate salt solutions, such as potassium carbonate (PC), might be regarded as another alternative for the CO_2 absorption process. As a solvent, it also offers some noticeable advantages in terms of non-volatility, high thermal and chemical stabilities, low corrosiveness, ease of regeneration, and low cost [13]. However, this solvent has a slower CO_2 absorption kinetic than its amine counterparts resulting in poor mass transfer. In brief, using this solvent has potential to compete with well-known, precommercial absorption processes provided its weaknesses are addressed. In doing so,

a large number of promoters which can be divided into organic such as amines, inorganics such as boric acid, and enzymes such as carbonic anhydrase might be added to a PC solvent to improve its absorption efficiency [171]. Mumford et al. [172] simulated a PC-based absorption process (30% K_2CO_3) to remove CO_2 from flue-gas of a 1600 MW coal-fired power plant resulting in only 20-25% CO_2 being captured. Thee et al. [173] later promoted the 30 wt.% K_2CO_3 solvent through adding small quantities of MEA solution, 1.1 M (5 wt.%) and 2.2 M (10 wt.%). The overall rate of CO_2 absorption increased by a factor of 16 and 45 respectively, under realistic process conditions. Also, the addition of 1.0 M glycine, sarcosine, and proline allowed accelerating the overall rate of CO_2 absorption in a 30 wt% K_2CO_3 solvent by a factor of 22, 45, and 14, respectively [174]. Ye and Lu [175] also investigated the removal performance of a mixture of 20 wt.% PC and carbonic anhydrase (CA) by measuring the reaction rate using a stirrer cell reactor. In presence of only 300 mg/L of CA, the CO_2 reaction rate was promoted by two to six times at 40-60^oC. Zhang and Lu [176] via simulating a pack-bed absorption process showed that the CO_2 absorption rate into 20 wt.% PC + 300 mg/L CA could become 2.2 times higher than into a 5M MEA solvent. Undoubtedly, the real application of such PC promoters strictly depends upon being adopted through a long-period operation in pilot plants. Recently, CO_2 Solutions Inc. (CSI) of Québec, Canada has introduced a proprietary absorption technology using a PC+CA solvent for capturing CO_2 from flue-gas [14]. In 2014, the semi-industrial unit was launched to capture around 0.5 tons CO_2 per day from a simulated flue-gas. To fully transit this breakthrough technology to the industrial CO_2 absorption market, a larger-scale of the enzymatic-absorption process was designed and then integrated into a natural gas-fired boiler located in Salaberry-de-Valleyfield, Canada in 2015. This plant operated successfully more than 2,500 hours removing 10 tons CO_2 per day and overall demonstrated stable performance in terms of the enzyme catalyst, solvent degradation, as well as removal efficiency. To achieve ~85% CO_2 capture, the reboiler heat duty was found to be 3.6 GJ/ton CO_2; the CO_2 capture cost was also estimated at 28$/ton CO_2. The reduction of CO_2 capture cost is probably attributed to the positive effects of CA enzyme on the overall rate of CO_2 absorption. This allows reducing both capital and operation costs and hence compensating for the required energy of solvent regeneration. Another key factor is the state-of-the-art stripper system which polishes the rich solvent at low temperature 60-70^oC whereas the PC-based systems desorb CO_2 at temperature above 110^oC [172]. All things considered; the enzymatic-absorption process has higher potential to displace the traditional amine-based counterparts. It is worth noting that the total energy requirement can also be further reduced via a sensitivity study to optimize the solvent circulation rate, lean CO_2 loading, reboiler heat duty, and column size.

3.3.2 Enzymatic reaction system

The CO_2 absorption into the unpromoted PC solution in which carbonate to bicarbonate conversion can be expressed as the following overall reaction [177]:

$$CO_{2(g)} + K_2CO_{3(aq)} + H_2O_{(l)} \rightleftharpoons 2\ KHCO_{3(aq)} \quad (3.R1)$$

And more realistically, as both K_2CO_3 and $KHCO_3$ are strong electrolytes, the above reaction might be represented in the ionic form as:

$$CO_2 + CO_3^{2-} + H_2O \rightleftharpoons 2\ HCO_3^- \quad (3.R2)$$

The exothermic reaction (3.R1) consists of a number of elementary steps depending on the pH value of the solution. In the first mechanism (pH>8), the reaction of dissolved CO_2 with OH^- is the rate-controlling step (3.R3), followed by an instantaneous reaction (3.R4) as:

$$CO_{2(aq)} + OH^-_{(aq)} \rightleftharpoons HCO^-_{3(aq)} \quad (3.R3)$$

$$CO^{2-}_{3(aq)} + H_2O_{(l)} \rightleftharpoons HCO^-_{3(aq)} + OH^-_{(aq)} \quad (3.R4)$$

whereas in the second mechanism (pH<8), the CO_2 hydration is the rate-controlling step (3.R5) and similarly accompanied by an instantaneous reaction (3.R6) as:

$$CO_{2(aq)} + 2H_2O_{(l)} \rightleftharpoons HCO^-_{3(aq)} + H_3O^+_{(aq)} \quad (3.R5)$$

$$CO^{2-}_{3(aq)} + H_3O^+_{(aq)} \rightleftharpoons HCO^-_{3(aq)} + H_2O_{(l)} \quad (3.R6)$$

For both mechanisms, the reaction of dissociation of water is defined as:

$$2H_2O_{(l)} \rightleftharpoons H_3O^+_{(aq)} + OH^-_{(aq)} \quad (3.R7)$$

As a pH value higher than 8 is preferable for industrial processes [178], reaction (3.R3) is fast whereas reaction (3.R5) becomes slow. Thus, the net rate of reaction is expressed as [179]:

$$r_{OH} = k_{OH-}[OH^-]([CO_2] - [CO_2]^{eq}) \quad (3.R8)$$

where OH^- and CO_2 are the concentration (mol/m^3) of hydroxyl ion and carbon dioxide, respectively. Also, k_{OH^-} stands for reaction rate constant ($m^3/mols$). The reaction sequence 3.R5, R6, and R7, known as the acidic mechanism, has a negligible contribution to the overall rate of CO_2 absorption when the pH value is higher than 8 in the non-catalyzed system. On the contrary, in presence of CA enzyme, the reversible reaction (3.R5) is catalyzed and becomes the rate-controlling step [176, 180]. Thus, the rate of promoted reaction can be expressed as [181]:

$$r_{CA} = \frac{k_C}{K_M}[CA]([CO_2] - [CO_2]^{eq}) \quad (3.R9)$$

where CA, K_M, and k_C represent the enzyme concentration (mol/m^3), Michaelis constant (mol/m^3), and turnover number of the enzyme (s^{-1}), respectively. By considering all the reactions, the overall rate of CO_2 absorption into PC solution promoted by CA enzyme (r_{OV}), can be expressed as:

$$r_{OV} = (\frac{k_C}{K_M}[CA] + k_{OH-}[OH^-])([CO_2] - [CO_2]^{eq}) \quad (3.R10)$$

3.3.3 Objective of this study

At first, we investigate individually the simulation of a CO_2 capture unit integrated with a 600 MW_e power plant, by membrane technology and absorption process using a PC+CA solvent. This allows to precisely compare the separation performance of these two methods under the same operating conditions. In the case of an enzymatic-absorption process, this study reveals the potential of using the catalyzed solvent for flue-gas treatment and also shows economic and technical aspects of this method compared to the benchmark MEA-based absorption process. In doing so, a sensitivity analysis is made to find the optimal values of operating variables such as L/G ratio, lean CTB level, and reboiler heat duty. In the case of the membrane technology, a techno-economic analysis is also made to assess the separation performance while the rate of CO_2 capture is varied from 10 to 95%. Finally, a cost model consisting of capital cost (CAPEX) and operation cost (OPEX) is defined to determine the total annual separation cost for each optimized process. It is expected that the findings of this study contribute to rapidly deploy these promising methods for PCC available technologies.

3.4 Modeling and optimization of the membrane process

The optimization of a multi-stage membrane gas permeator requires a robust and efficient model to determine the optimal process parameters. Herein, the model of gas permeation introduced by Gilassi

et al. [90] is adopted due to its excellent performance observed through simulations of various gas separations under different operating conditions. As a simple rule of thumb, CO_2 removal performance in a typical single-stage membrane process highly depends upon separation characteristics of the selected membrane, pressure ratio between retentate and permeate sides, and membrane separation area. For high CO_2 recovery and purity, that is likely required for flue-gas separation case, more than one membrane unit is needed so that the flue-gas treatment is performed by recycling the permeate stream from one module to another unit with higher capacity in CO_2 purification. It is therefore essential to somehow develop a rigorous optimization model to embed not only the process variables, but also all possible process layouts. By doing so, a membrane network superstructure can be defined and thereafter screened by an optimization technique while objective functions and constraints are converged in the given process. Figure 3.1 shows the suggested optimized process layout for the flue-gas separation in this study. Herein, the optimization model is also adapted from our previous work in which the optimized process layout, as well as optimal process variables, were simultaneously found while minimizing gas separation costs [182]. This model involves a large number of equalities such as mass and energy balance equations, inequalities defined to set certain product specifications, as well as an objective function. A new decision variable regarding vacuum pressure is then added to the optimization model to minimize the membrane separation area for the flue-gas separation case. Either the annual CO_2 capture cost or the entire energy requirement for a typical membrane-based separation process could be subjected to minimization. Above all, such formulation for the optimization model leads to a Mixed Integer Nonlinear Programming (MINLP) problem which needs to be solved using an appropriate approach [183].

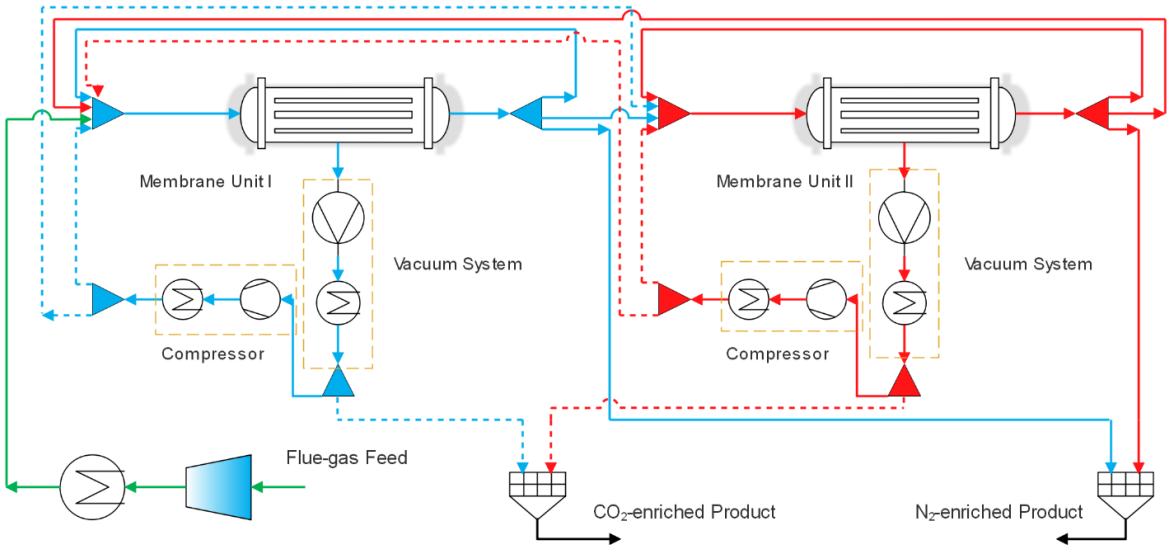

Figure 3.1 Process flow diagram of a multi-structure membrane process used in the process optimization.

3.5 Modeling of enzymatic-absorption process

3.5.1 Process description

A typical 600 MW_e power plant is chosen to be integrated with a CO_2 capture unit introduced by Akermin Inc. Table 3.1 presents the flue-gas properties and characteristics used for this study taken from Ref. [121]. In this process, the flue-gas at 1.01 bar and 47 ºC contains ~13 vol.% CO_2 to be treated using the proprietary PC solvent catalyzed by the CA enzyme. Figure 3.2 also shows a simplified process flow diagram of the CO_2 absorption process. For the sake of clarity, the operation of this CO_2 capture unit is elucidated as: the flue-gas is initially sent to a pre-treatment unit to remove undesirable components; the gas then passes through a blower whereby the pressure is raised to 1.10 bar; it is later injected at the bottom of the pack-bed absorption column while the lean-solvent is sprayed into the top; the gas-liquid interaction occurring in the column allows transferring CO_2 into the liquid phase; the treated gas (CO_2 below 2 mol.%) leaves from the top of the column whereas the enriched CO_2 solvent is conducted to the regeneration unit; the rich-solvent is then pumped through a plate heat exchanger to raise the temperature as per vacuum pressure in the stripper column; the lean-solvent accumulated at the bottom of the stripper column is recirculated *via* a pump to the reboiler to generate the stripping stream; the lean-solvent leaving the reboiler heats up the rich solvent and then is cooled prior to its use in the absorption column; in the stripper column, the vapor stream is enriched to CO_2 upwards by transferring the water to the downward liquid phase; after leaving the

stripper column, the vapor stream, including CO_2 and water, is fed to a condenser where most of the water vapor is condensed; the gas-liquid mixture passes through a flash column to fully separate CO_2 from water; the water is then routed to the make-up tank whereas the CO_2 enriched to +95% is sent to a multi-stage compression unit for final transportation.

Table 3.1 Flue-gas properties used for the optimization problem.

Parameters	Value
Mass flow (*kg/s*)	616.0
Pressure (*kPa*)	101.6
Temperature (˚*C*)	47
Composition	Wet gas (*vol.%*)
N_2 + Ar	71.62
CO_2	13.30
H_2O	11.25
O_2	3.81
SO_2	0.005
NO_x	0.0097

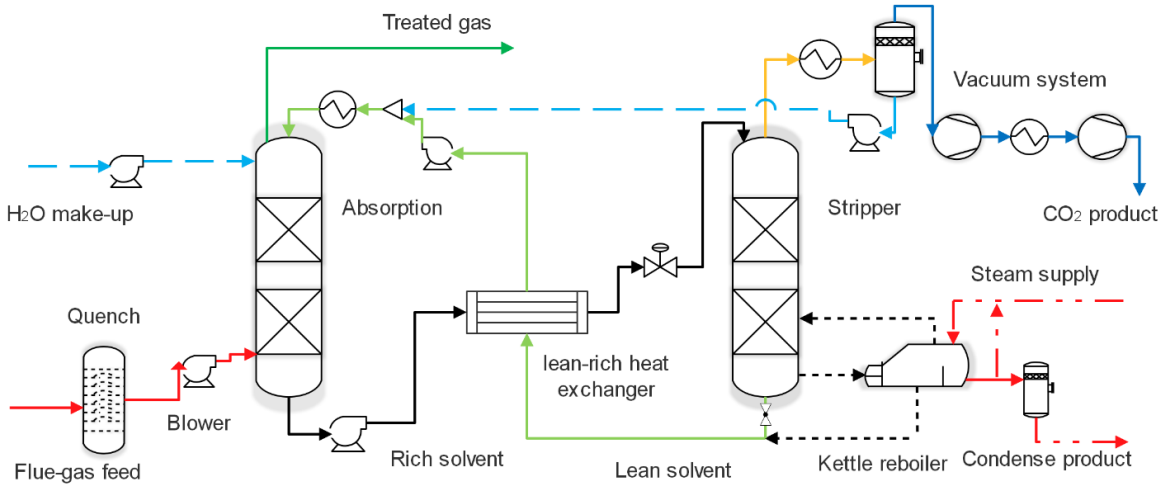

Figure 3.2 Process flow diagram of an enzymatic-absorption process for flue-gas treatment.

3.5.2 Modeling approach

Aspen plus® (version 10.1) is used to simulate the CO_2 absorption/desorption process using a non-equilibrium rate-based model. The model designated as RadFrac is appropriate to effectively describe the simultaneous diffusion and reaction between CO_2 and PC+CA solvent in the framework of the

double film theory. It is considered that CO_2 dissolves into the liquid film, diffuses to the bulk of the liquid phase where CO_2 and the other ionic components all together reach chemical equilibrium. In this simulation, the CO_2 mass transfer is significantly accelerated in the presence of CA enzyme owing to the high turnover frequency of this enzyme. As thermodynamic models, the Redlich-Kwong equation of state and the Electrolyte Non-Random Two-Liquid model (ENRTL) are used to express the non-idealities of the gas and liquid phases, respectively. Henry's coefficients and equilibrium constants for the reactions (R3-7) which take place in the H_2O-K_2CO_3-CO_2 system are calculated based on the experimental results reported in Ref. [184]. Other property data including density and viscosity, diffusivity of CO_2 in PC solvent, PC surface tension, thermal conductivity, and specific heat capacity for both gas and liquid phases are also taken from Aspen data library and NIST database or predicted by the data regression system (DRS) of Aspen Plus®. Above all, the non-equilibrium RadFrac model is built based on the equations of mass and energy balance, equilibrium relations, transfer rates, chemical reactions, phase equilibria, and hydraulics [13]. The flow model of gas and liquid phases in each height increment is set to mixed type and film discretization option is implemented to consider the effect of chemical reaction in the liquid film. Due to the nonlinearity of the reaction rate R10, the overall rate of CO_2 absorption into PC+CA solvent is introduced to Aspen Plus® through adjusting the activation energies for the direct reaction of CO_2 and hydroxide. These data for both forward and backward reactions are taken from Ref. [185]. According to the simulation results provided by Akermin Inc., we adopted the validated model in this study for the simulation and optimization of flue-gas separation.

3.6 Optimization outline to minimize CO_2 capture cost

3.6.1 Enzymatic-absorption process

The optimization is necessary to develop further potentials of the CO_2 absorption process using the promoted PC solvent. This approach aims at systematically setting a large number of decision variables with respect to process objectives. It is of high interest to explore how designs of absorption/desorption column, and packing materials, installation of ancillary equipment (blower, pump, compressor, and vacuum systems), selection of solvents (kinetic, capacity, and degradation), as well as setting of operating parameters would affect process efficiency and CO_2 capture cost. Thus, a comprehensive techno-economic analysis needs to be made to precisely manipulate these variables to reduce energy loss as far as possible. In a typical absorption process, the required energy for solvent regeneration accounts for more than 60% of the entire energy consumption. This type of analysis is more justified since the cost repartition for CO_2 absorption using the benchmark solvent (MEA 30%)

shows contributions of 72 and 28% of OPEX and CAPEX, respectively [186]. It is therefore essential to choose a proper strategy to optimize such an important PCC process for which the OPEX is truly indicative of the CO_2 capture cost. As such, the lower specific energy in MJ/kg CO_2, the lower operation cost could be realized, resulting in minimizing the CO_2 capture cost. On the contrary, the optimization approach implemented for the membrane system aims at simultaneously minimizing the OPEX and CAPEX while determining the most efficient process layout. To do so, feed and vacuum pressures as well as membrane area in each membrane module are regarded as the decision variables whereas desorption pressure and temperature are the main operating parameters in the enzymatic-absorption system to minimize separation cost. In this study, the use of the PC+CA solvent might be regarded as a promising alternative to not only improve the existing cost framework, but also introduce a more profitable process. Hence, a sensitivity study was carried out to find optimal values of the energy of CO_2 regeneration by considering all operational conditions. As part of this methodology, key operating variables such as solvent/gas flowrate (L/G) ratio and CO_2 loading in the lean solvent, as well as stripping pressure and temperature can be considered in the simulation of the CO_2 absorption process.

3.6.2 Cost model

A reliable cost model for the economic analysis is also needed for the enzymatic-absorption process to determine the CO_2 capture cost based on OPEX and CAPEX estimations. As stated in the previous section, the OPEX here consists of the operation costs associated with reboiler duty, CO_2 compression, blower, pumps, as well as enzyme and solvent make-up. The CAPEX corresponds to the purchase costs (direct and indirect) of compressor, absorber, desorber, heat exchanger, pumps, blower, solvent, and miscellaneous. To optimize this process, the minimization of the heat of CO_2 regeneration is defined as the objective function. The OPEX is then optimized through minimizing the reboiler heat duty and thereby the CAPEX also becomes optimum. The module costing technique is used to estimate the purchased cost of the equipment (CAPEX) involved in the process, based on capacity, pressure, and material [104, 187]. Due to time variations of purchase costs, a cost index was also used to convert the cost estimates at a certain date into present costs. Overall, the cost optimization approach used for this work not only provides a means to analyze process expenditures, but it also allows to identify strengths and weaknesses of the process.

3.7 Results and discussion

3.7.1 Process description

The selection of a CO_2 capture technology for flue-gas separation is highly depending on both its technical viability and economic efficiency. Flue-gas emitted from stacks of a power plant has an approximate volumetric flowrate of 500 m^3/s and typically contains 13 vol.% of CO_2. It is therefore needed to conduct the low-pressure gas (~1 bar) to a CO_2 capture plant before releasing into the atmosphere. The feed gas is then dispersed to four parallel trains in which the target is to optimize annual separation cost through optimizing decision variables available in the process. Herein, the separation performances of standalone membrane-based and enzymatic-absorption processes will be compared while retrofitting to a typical 600 MW_e power plant. The flue-gas properties and characteristics used for the optimization problem are given in Table 3.1.

3.7.2 Optimized membrane process

Figure 3.3 shows the optimized process layout to remove 90% of CO_2 in the flue-gas while the CO_2 purity in the permeate stream is kept constant at 98%. As stated in the previous sections, the optimization model allows finding the optimum value of the annual separation cost by screening the multi-structure layout and adjusting the transmembrane pressure as well as the required membrane separation area for each separation stage. As shown, the first membrane stage serves as a bulk capture unit (BCU) where 90% of CO_2 in the feed gas is completely removed. Then, the retentate product stream depleted of CO_2 ($X_{CO_2} \sim 0.02$) is directly sent to the N_2 storage unit where a turbo expander might be installed downstream to recover the energy spent for the feed gas compression. The permeate product stream containing 67 mol.% CO_2 is routed to the second membrane stage which acts as a CO_2 purifier unit (CPU). In comparison, over 90% of the total membrane separation area (~3.78×10^5 m^2) is used in the first stage to attain a threshold level of the separation driving force. Furthermore, the ratio of transmembrane pressure (P_r/P_p) is then maximized to ~14 and 8 in the first and second stages. This optimization strategy allows accomplishing the bulk removal of CO_2 (~1200 mol/s) through the first membrane stage. Merkel et al. [139] reported that required membrane area needs to be increased up to 6×10^5 m^2 without using a vacuum system to capture 90% of CO_2 with a purity of 0.28 mol.% in the permeate side. It was also stated that the use of vacuum pump allowed to reduce the required energy consumption up to 50% but the required membrane area was to be increased 5-fold. As shown in Figure 3.3, similarly, both membrane separation area and vacuum pressure are set to the optimal values of ~1.8×10^4 m^2 and ~0.34 bar respectively, to enrich CO_2 to 98 mol.% in the second stage. Overall, the proposed optimization method allows to sequentially maximize the separation driving

force in the membrane units. This approach results in minimizing CAPEX and OPEX simultaneously and hence total annual cost for different fractions of the CO_2 capture is optimized.

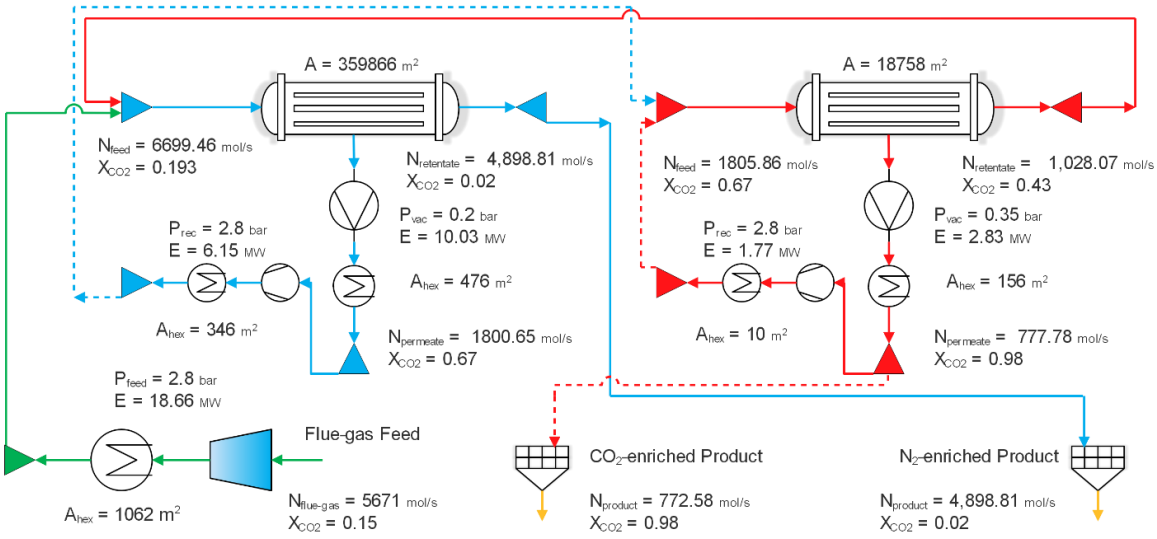

Figure 3.3 Optimized membrane layout for 90% CO_2 capture from flue-gas.

3.7.2.1 Cost analysis

Separation performance seems to be critically dependent on the coexistence of compressors and vacuum pumps in a process layout. This raises many concerns about economic viability of membrane-based processes used for flue-gas separation compared to other technologies. Thus, cost analysis is needed to precisely investigate economic and technical aspects for all optimized processes. Figure 3.4 shows the relation between the rate of CO_2 capture and purchase cost of equipment including compressors, vacuum pumps, and required membrane separation area. As shown, the fixed capital cost (FCC) rises reasonably from 46 to 67 M$ when the CO_2 capture is varied from 10 to 50%, respectively. At higher CO_2 capture, higher energy is demanded resulting in a sharp increase on the individual purchased cost of equipment. The FCC for 90% CO_2 capture increases dramatically to 165 M$ per train that is almost 1.5 times greater than that of for the 50% CO_2 capture. In this case, 54 and 17% of the FCC need to be allotted to the purchase of compressors and vacuum pumps, respectively. Moreover, approximately 30% of the FCC is attributed to the membrane cost when the rate of CO_2 capture changes from 10 to 90%. The FCC tends to steeply increase to 205 M$ for 95% CO_2 capture which is 27% more expensive compared to the 90% CO_2 capture. In this case, the FCC cost is divided equally between compressor and membrane costs to meet the separation targets. The optimization results show that the membrane technology might be economically inefficient for the high rates of

CO_2 capture. However, other criteria such as availability, simplicity, as well as footprint and site location altogether are required to be carefully considered for process design when compared to other separation methods.

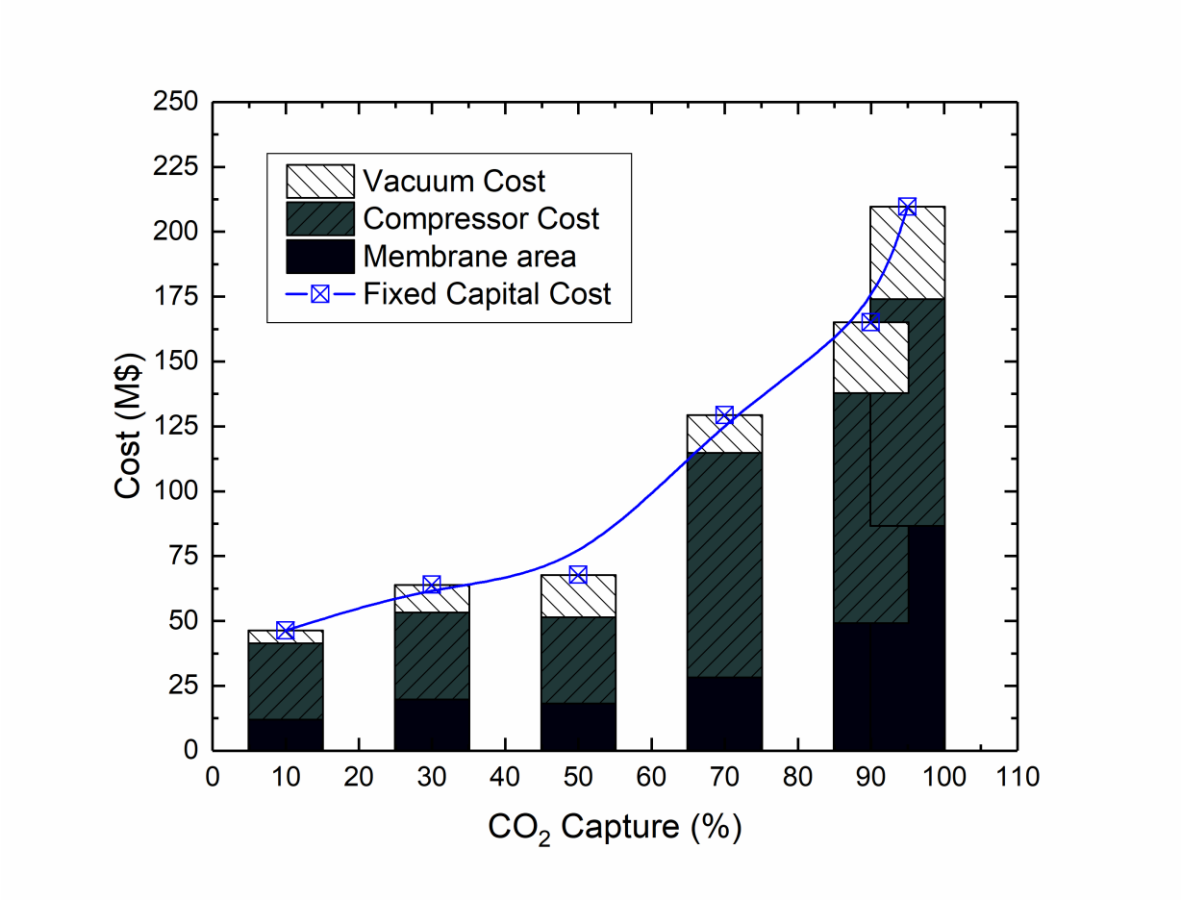

Figure 3.4 Effects of CO_2 capture on the purchase cost of the equipment in the optimized two-stage membrane process.

A summary of the optimization results for the flue-gas separation from a 600 MW_e power plant at different ranges of CO_2 capture (10 to 95%) is given in Table 3.2. The Polaris™ as a commercial advanced membrane is, however, employed for all the optimization cases. The use of feed compressors and permeate vacuum pumps are necessary to leverage the separation driving force and avoid soaring the purchasing cost associated with membrane area. For 90% CO_2 capture, the optimal value of membrane separation area is found to be $15x10^5$ m^2 for the four chains which is 27% lower than that of an optimized four-stage membrane process without permeate vacuum systems [98]. Furthermore, this outperforms a two-stage membrane process requiring $3x10^6$ m^2 membrane area

using two vacuum pumps and one compressor. It might be more competitive than a two-stage countercurrent sweep membrane process requiring $1.3x10^6$ m^2 in which air is fed to the second membrane stage in the permeate side instead of using a vacuum pump [139]. Figure 3.5 presents the effects of CO_2 capture rate on the related process costs including CAPEX, OPEX, as well as CO_2 capture cost. As discussed before, the FCC is more dominated by the compression/vacuum units than the membrane separation modules specifically for the ranges of 10 to 90% CO_2 capture. The optimization results show that high investment cost is probably required for flue-gas separation using membrane technology. It is also seen that a larger part of the annual separation cost is not only related to the direct and indirect costs, but also to the operation. As shown in Figure 3.5 and Table 3.2, the CAPEX is 20% higher than the OPEX which is probably attributed to the higher purchase costs of compressors and vacuum pumps. The cost analysis demonstrates an immature side of the membrane technology which might be solely profitable for small-size separation projects. Improvements in membrane permselectivity like increasing CO_2 permeance could be regarded as an alternative to decrease the dependency of using compressor and/or vacuum systems [182]. Overall, the minimum value of CO_2 capture cost is found to be 35 \$/ton CO_2 when 50% of CO_2 in the flue-gas is removed. For other ratios, the capture costs are also estimated close to 50\$/ton CO_2 on average which is competitive to other separation methods.

Table 3.2 Techno-economic analysis of CO_2 capture from a 600 MW_e power plant using a two-stage membrane process.

Parameter	Value						Unit
CO_2 Capture	10	30	50	70	90	95	*%*
MEMBRANE							
Total membrane cost	4.62	7.61	6.98	10.84	18.93	33.32	*M$*
Unit membrane area	92370.85	152099.7	363153.4	216836.5	378624.6	666452	m^2
COMPRESSORS							
Pressure	150000	156224	150000	267122	279515	248277	*Pa*
Installed compressor cost	29.06	33.14	32.90	85.96	88.00	86.74	*M$*
Unit power	7.06	8.10	7.86	23.36	24.84	24.14	*MW*
Installed heat exchanger cost	0.31	0.34	0.35	0.66	0.62	0.64	*M$*
Total heat transfer area	508.37	573.03	565.67	1344.57	1408.49	1422.30	m^2
VACUUM							
Installed vacuum cost	4.82	10.44	15.99	14.28	26.86	35.19	*M$*
Unit power	1.75	4.08	7.80	6.31	12.87	17.86	*MW*
Installed heat exchanger cost	0.11	0.20	0.36	0.25	0.38	0.46	*M$*
Total heat transfer area	85.89	193.15	539.12	317.78	631.55	864.89	m^2
TURBOEXPANDER							
Installed turbine cost	5.18	5.64	4.86	12.44	12.53	11.00	*M$*
Unit Recover power	5.75	6.27	5.39	13.82	13.92	12.22	*MW*
CAPITAL COST							
Fixed cost	46.30	63.89	67.74	129.33	165.09	209.65	*M$*
CAPEX	7.16	9.89	10.48	20.01	25.55	32.45	*M$*
VOM							
Membrane capital cost	12.01	19.77	18.16	28.19	49.22	86.64	*M$*
Membrane operation cost	0.12	0.20	0.18	0.28	0.49	0.87	*M$*
Equipment capital cost	34.30	44.13	49.59	101.14	115.87	123.02	*M$*
Equipment operation cost	1.23	1.59	1.79	3.64	4.17	4.43	*M$*
UTILITY COST							
Total utility cost	4.035	5.602	7.220	13.518	17.538	19.480	*M$*
OPERATION COST							
OPEX	5.39	7.39	9.19	17.44	22.20	24.78	*M$*
TOTAL ANNUAL COST							
Unit TAC	12.56	17.28	19.67	37.46	47.75	57.23	*M$/year*
Total TAC	50.23	69.11	78.69	149.83	191.02	228.90	*M$/year*
CO_2 PRODUCTION COST							
CO_2 permeate flowrate	85.07	255.21	426.58	578.65	757.13	808.17	*mol/s*
TAC per CO_2 capture	110.79	50.81	34.61	48.59	47.34	53.15	*$/ton CO_2*
Net power per chains	8.81	12.18	15.66	29.67	37.71	42.00	*MW*
Number of chains	4	4	4	4	4	4	-
Total net power	35.23	48.72	62.65	118.70	150.83	168.00	*MW*
Total net power using expander	12.22	23.64	41.07	63.40	95.14	119.12	*MW*
Fraction of energy used	5.87	8.12	10.44	19.78	25.14	28.00	*MW*
Total fixed capital cost	185.23	255.60	270.99	517.32	660.36	838.64	*M$*

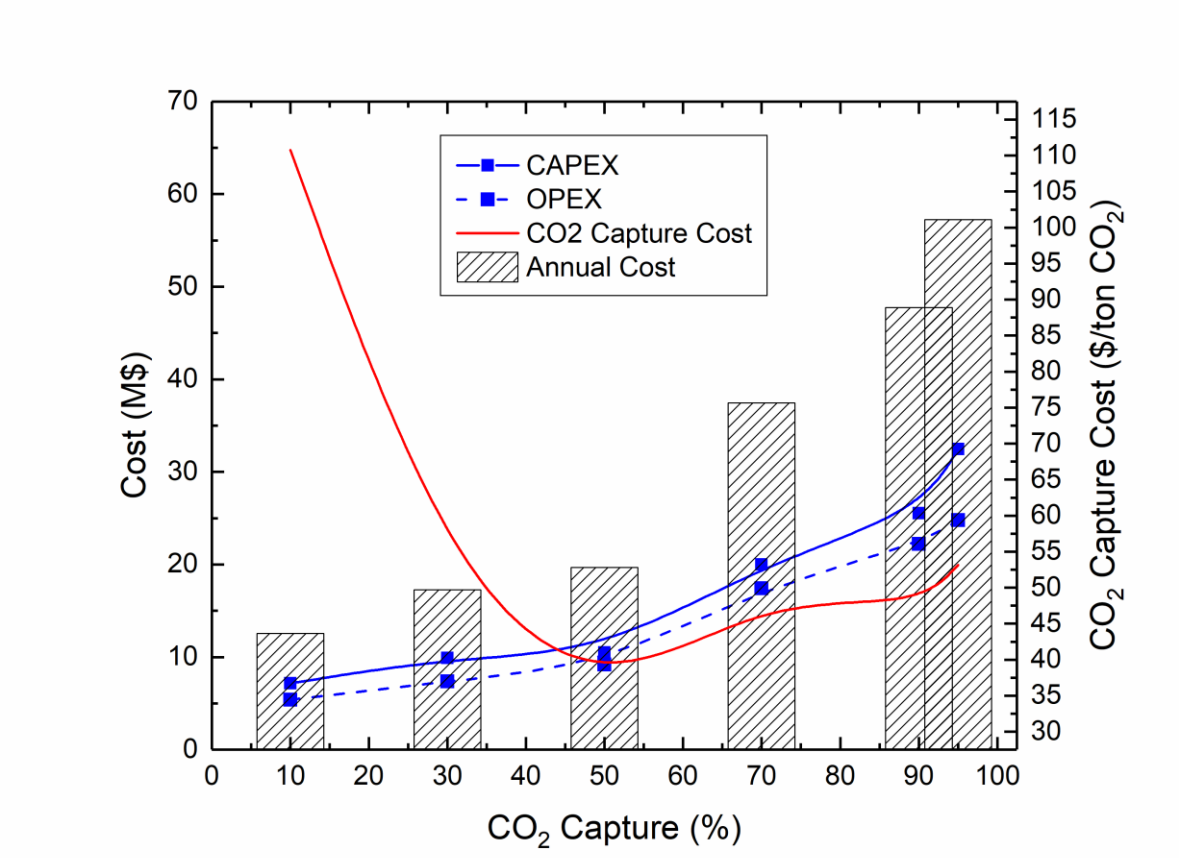

Figure 3.5 Effects of CO_2 capture on the membrane process costs.

3.7.2.2 Energy consumption analysis

A large amount of energy is required for feed compression and permeate evacuation systems in a membrane separation process. This might be attributed more to poor separation efficiency of available membrane materials which necessitate operating at high pressure. Herein, the objective function of the optimization model, which represents the estimated total annual cost (TAC), is minimized while the required feed/vacuum pressure and membrane area are set to the optimal values. This approach then guarantees to provide adequate separation driving force regarding membrane characteristics. Figure 3.6 shows the relation between different ratios of CO_2 capture and power required for equipment in the two-stage membrane process. As reported in Table 3.2, the optimal value of the feed pressure in the main compression unit is found to be ~1.5 bar when a low range of CO_2 capture (<50%) is required. In this case, the pressure ratio is set to 1.48 (flue-gas pressure 1.01 bar) which allows minimizing the electricity loss to 8 MW per chain for the feed transportation to the CO_2 capture unit. It is assumed that the separation mechanism is similar to the 90% CO_2 capture case so that the

main CO_2 capture and CO_2 purifier units are connected in a cascade mode. Then, the membrane separation area varies from $9.3x10^4$ to $3.65x10^5$ m^2 to remove as much as possible of CO_2 in the first stage at a vacuum pressure of 0.2 bar. This scenario results in a gentle growth in the power of the vacuum system while the feed pressure remains at the minimum value. The same optimization strategy is seen at the higher CO_2 capture (70-90%) where the feed pressure is increased to ~2.6 bar to avoid a dramatic increase of membrane area in the first stage. For a CO_2 capture of 95%, the required membrane area reaches $6.67x10^5$ m^2 while the feed pressure is still kept at 2.6 bar. These maximum values of two decision variables in the optimization model might be further improved, by enhancing the CO_2 permeance of the Polaris™ membrane. A fictitious membrane with a CO_2 permeance of 2000 GPU would result in a significant reduction in membrane area [143]. It could contribute to a lower transmembrane pressure for 90% rate of CO_2 capture and hence electricity saving would be observed (beyond the scope of this study). Overall, our optimization model allows finding the optimal values of the required feed and vacuum pressures (<3 bar), as well as the membrane separation area ($1.5x10^6$ m^2) for the 90% CO_2 capture.

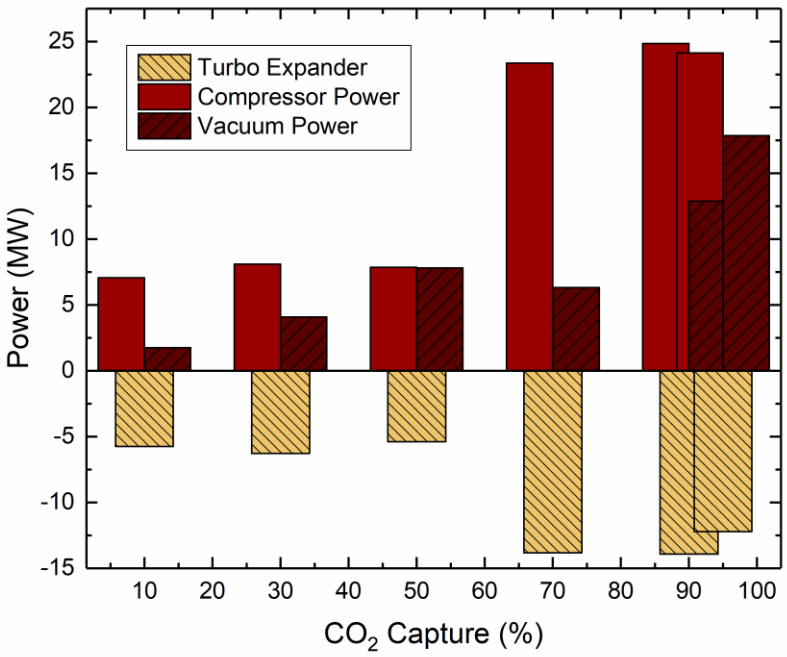

Figure 3.6 Effects of CO_2 capture on the energy consumption of equipment in the membrane process.

It is also possible to install a turbo expander after the retentate storage point to recover part of the consumed energy. Under this scenario, more than half of the electricity loss for all the optimization cases could be recovered. Hence, this must be regarded as an indispensable strategy for the integration of membrane technology to power plants. However, direct and indirect costs of equipment in the Energy Recovery Unit (ERU) would add up to the FCC. For instance, 13.9 MW is recovered in the ERU which is almost 36% of the total electricity required for the 90% CO_2 capture. Referring to Table 3.2, when bulk removal of CO_2 is the target of separation project, the total electricity loss for CO_2 capture in the range of 10, 30, and 50% rises smoothly and reach 32, 48, and 62 MW, respectively. Using an expander also allows to reduce them further by 12, 23, and 41 MW respectively, whereas an extra cost of 20 M$ on average is added to the FCC for each case. As shown, the energy recovery scheme seems be even more beneficial for the higher CO_2 capture demand (>50%) through which reasonable reduction in electricity loss (36%) is also observed.

Overall, 90% CO_2 capture with a CO_2 permeate purity of 98% using a two-stage membrane process is feasible at the expense of losing 150 MW and with aim of ERU 95 MW. As such, the capture cost is also estimated at 47 $/ton CO_2 which is competitive with other separation methods such as an amine absorption process. Table 3.3 shows a summary of the comparison of techno-economic analysis between this case study and other works taken from literature. In terms of energy consumption, the optimized process is competitive to the two-stage countercurrent air sweep membrane process in which 91 MW is consumed to reach the 90% CO_2 capture. Moreover, it outperforms the other multi-stage membrane processes since only 15% of the electricity generated in the 600 MW_e power plant is lost in the CO_2 capture unit.

Table 3.3 Comparison of separation performance of the optimized process with different membrane processes.

Membrane design	**TMA (MMm^2)**	**Electricity loss**	**Fraction of**	**Capture cost**		**TAC (M$/y)**	**CO_2 purity in**	**CO_2 capture**	**Reference**
				Reference	Estimation[2]				
Two-stage	3.0	145	24	2010	29	278	+95	90	[42]
Two-stage	1.3	91	15.1	2010	23	n/a	+95	90	[42]
Three-	1.8	255	42.5	n/a	n/a	n/a	98	85	[18]
Three-	6.1	175	29.1	n/a	n/a	n/a	98	85	[18]
Two-stage	1.4	130	21	n/a	n/a	n/a	98	95	[18]
Four-stage	2	176	29	2011	40	123.5	98	95	[91]
Two-stage	1.45	130	21	2011/2013	33	90	98	95	[92]
Two-stage	1.5	95	15.8	2010	47	191	98	90	This

1. Exclusive of CO_2 product compression.
2. Different cost models are used for CAPEX and OPEX calculations.

3.7.3 Optimized enzymatic-absorption process

This method is also recently proposed for CO_2 capture from flue-gas of power plants in several projects and somehow might be regarded as a more mature process compared to the membrane technology, owing to its simple separation mechanism. The flue-gas depleted of sulfur is initially compressed through a series of blowers to compensate for pressure drop in the absorption column. Then, the feed gas which enters from the bottom of the column flows upward and contacts counter-currently with the solvent sprayed from the top of the column. The details about the design and operating parameters of absorption and desorption processes are given in Table 3.4. As stated in the previous sections, the enzyme acts as a catalyst to accelerate the reactions of CO_2 hydration and dehydration (R1) in the absorption and desorption processes, respectively. In order to reach 90% CO_2 capture, carbonate to bicarbonate (CTB) index, defined as the ratio between contents of absorbed CO_2 and K_2CO_3 in the PC solvent, is to be confined to a range of 0.1-0.4 at different temperatures (20-40ºC) [189]. Hence, the CTB index changes and its effect on the required energy of CO_2 regeneration needs to be considered while the equivalent weight fraction (EWF) of K_2CO_3 of the PC solvent is kept constant at 20% in this study. Literature experimental work shows that increasing EWF of K_2CO_3 in a PC solvent above the specified range results in severe technical issues such as a corrosion tendency of the solution and precipitation of $KHCO_3$ during operations [190].

Table 3.4 Input data used for optimization of the enzymatic-absorption process.

Parameters	**Values**	
Equipment properties	Absorption	Desorption
Height of packing (*m*)	15	19
Diameter of packed bed (*m*)	8.5	8.5
Packing type	Mellapak 350X	Mellapak 350X
Feed characteristics		
Temp of flue-gas entering absorber (*˚C*)	47	
Temp of solvent entering absorber (*˚C*)	40	
Lean CO_2 loading (*mol CO_2/mol K_2CO_3*)	0.1~0.4	
Pressure at the top of stripper (*atm*)	0.3~0.6	
Utility price		
Water (*$/kGal*)	1.023	
PC (*$/ton*)	500	
PC corrosion inhibitor (*% of PC*)	20	
CA enzyme (*$/kg*)	480	

3.7.3.1 Optimal value of the lean CTB index

Figure 3.7a shows the effects of solvent flowrate ratio at the absorption inlet (L/G ratio) on extent of CO_2 capture and rich solvent CTB index, for different values of lean CTB index. In the case of 90% CO_2 capture, the lowest L/G ratio is found to be 5.5 for a lean CTB index of 10% while the rich CTB reaches 0.647. Similarly, the highest L/G ratio at 90% CO_2 capture is estimated to be 10.8 for a lean CTB of 40%. In that case, the rich CTB index has a value of 0.68. As such, changes in the lean CTB from 10% to 20% and 30% result in approximately 20 and 55% increases in the PC solvent flowrate, respectively. In all cases, the rich CTB reduces at increasing solvent flowrate and the lowest change of CTB conversion is estimated at 70% for 40% lean CTB. Hence, optimal values of L/G ratio and lean CTB must be determined while considering their overall effects on the energy penalty incurred in the desorption process. Figure 3.7b shows the relation between the lean CTB index of the solvent, and heat of CO_2 regeneration for 90% CO_2 capture at different vacuum pressures in the desorption column. A minimum of regeneration heat is found to be 3.35 MJ/kg CO_2 for 23.5% lean CTB index at a vacuum pressure of 0.3 bar. Moreover, the local minimum is observed when varying the lean CTB at constant vacuum pressure. In this case, the optimal lean CTB index is estimated to be in the range of 23.5 to 24.5% when the desorption pressure increases from 0.3 to 0.6 bar. As shown in Figure 3.7b, the selection of a lean CTB of 10% is not justifiable as the energy demand would dramatically increase (6.5-7.5 MJ/kg CO_2). However, the leaner the CTB, the lower the flowrate of the PC solvent is required resulting in a reduction of pump size.

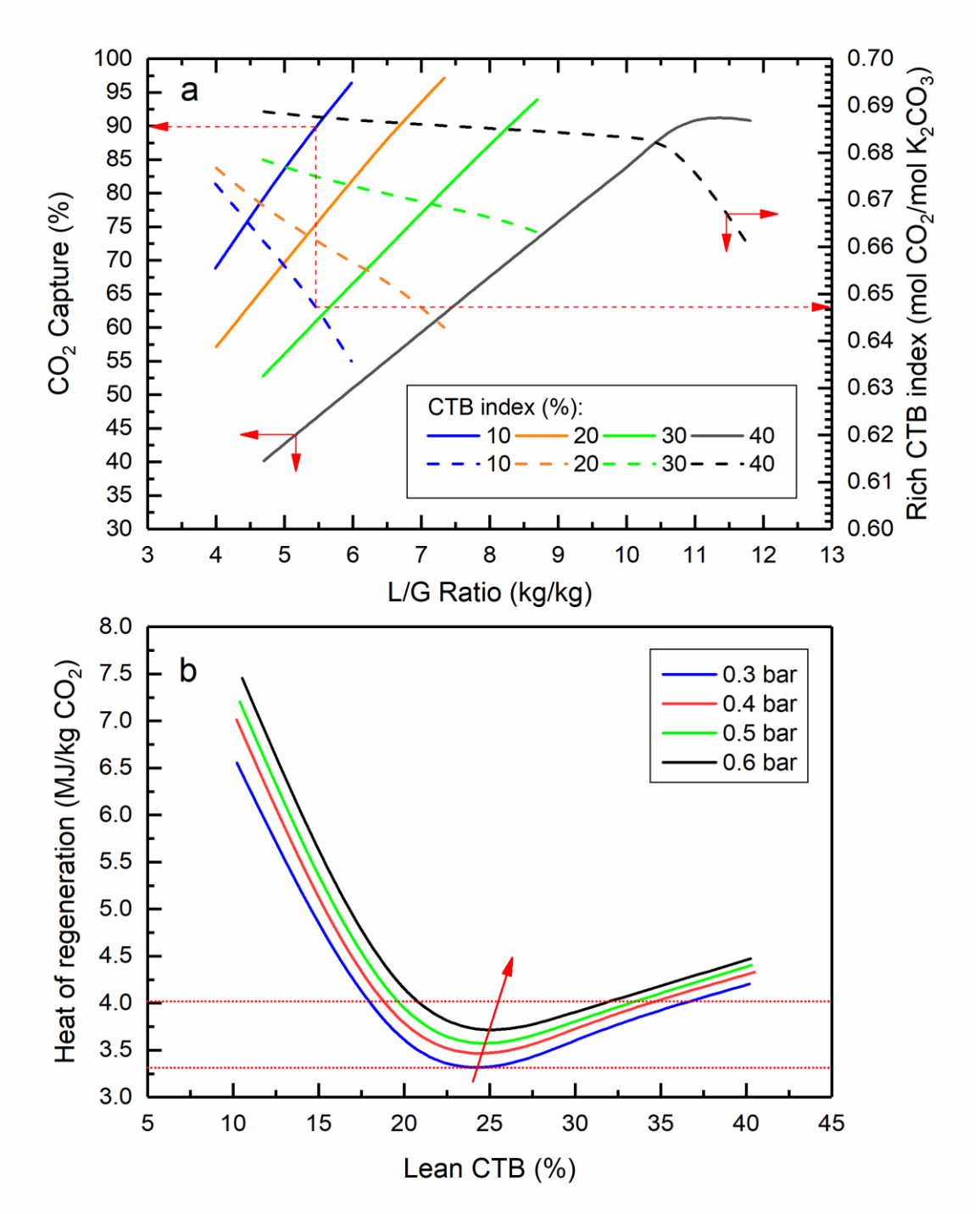

Figure 3.7 a) Effects of solvent flowrate on the CO_2 capture in the enzymatic-absorption process (example of a 600 MW_e power plant), b) Effects of the lean CTB index on the heat of CO_2 regeneration (90% CO_2 capture).

Figure 3.8 also shows the repartition of heat consumption in the CO_2 desorption process at different values of the lean CTB index. The stripping temperature has no significant influence on the heat of

CO_2 desorption and as observed in this figure, this heat remains unchanged independently of the lean CTB. The sensible heat is dependent on the average flowrate of lean and rich solvents, as well as boiling temperature in the reboiler. It also increases linearly while the lean CTB index varies from 10 to 40%. As shown, the largest heat power is required for the generation of the stripping vapor when the CTB index is as low as 10%. According to the heat analysis, the vaporization heat has the dominant effect on the required heat in the enzymatic-absorption process. It is therefore expected that the heat of CO_2 regeneration is minimized at the lean CTB index range of 20 to 25% when the vaporization thermal power is decreased to 6000 kW. Overall, the separation performance using those values of CTB is competitive with the reference amine absorption process in which the energies of CO_2 regeneration are estimated at 3.3 and 3.0 MJ/kg CO_2 using 30 and 40 wt.% MEA solutions, respectively [121].

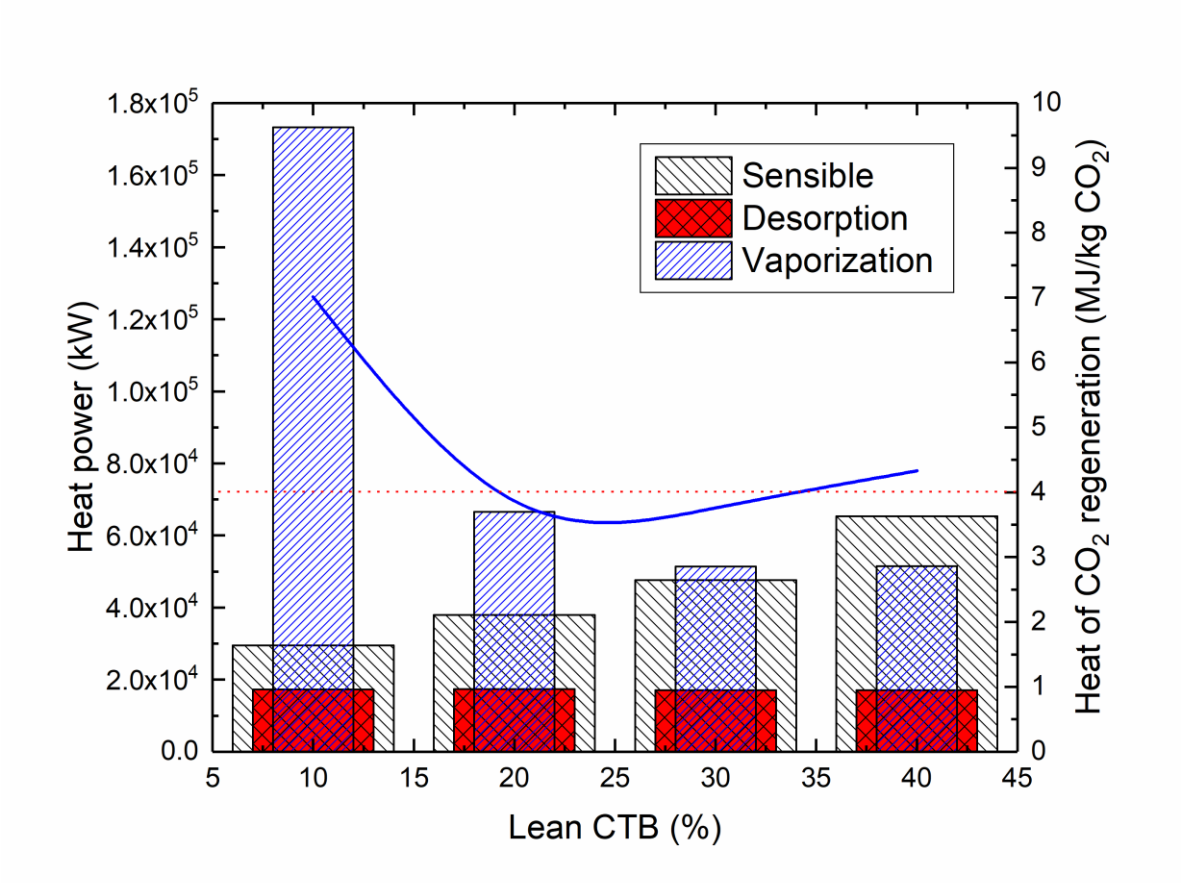

Figure 3.8 Heat analysis of the desorption process at different lean CTB level (90% CO_2 capture).

3.7.3.2 Effects of vacuum pressure on electricity loss

The operation at vacuum pressure favors the desorption process with a high reduction in the stripping temperature, probably allowing to use steam at a very low pressure (VLP) vapor available in power plants [191]. Moreover, it contributes to maintain catalytic stability of the enzyme in PC solvent which is sensitive to high stripping temperature (>85 ºC). Figure 3.9 shows the effects of desorption pressure on the stripping vapor flowrate and required energy for the vacuum system at 90% CO_2 recovery. Generally, a high CTB conversion demands higher energy to strip off CO_2 from the rich solvent. The simulation results show that the CO_2 removal occurs partially at the top of the desorption column due to flash evaporation and a larger part of CO_2 is then released inside the column due to reaction of CO_2 desorption. Under these conditions, the boiling temperature of lean solvent in the reboiler varies from 67 to 84^{o}C when increasing the vacuum pressure from 0.3 to 0.6 bar. Then, a temperature difference of 10^{o}C is assumed between the rich and lean solvent over the length of stripper. As stated in the previous section, the use of a lean CTB of 10% requires the lowest circulation flowrate, where the CTB conversion reaches the highest level. In this case, the boil-up ratio in the reboiler is set to the maximum value to generate adequate stripping vapor flowrate along the desorption column. The higher amount of CO_2 absorbed in the rich solvent is then transferred to the gas phase until the solvent reaches the lean CTB of 10%. The higher the gas flowrate, the higher the size of the desorption column required to avoid technical issues such as flooding. The required flowrate of the stripping gas reduces by 50% for the CTB of 20% and then levels off in the range of 30 and 40%. As for electricity loss, the vacuum system energy consumption is highly dependent on the required pressure ratio. As shown, the lowest penalty obtained at a pressure of 0.6 bar is estimated at 14 MW which is 55% lower than that estimated at 0.3 bar. Thus, another trade-off is observed between the vacuum pressure and amount of the stripping vapor and directly affects both OPEX and CAPEX. In the optimization problem, optimal value of the vacuum pressure is determined when the total electricity loss due to CO_2 regeneration and vacuum operation is minimum.

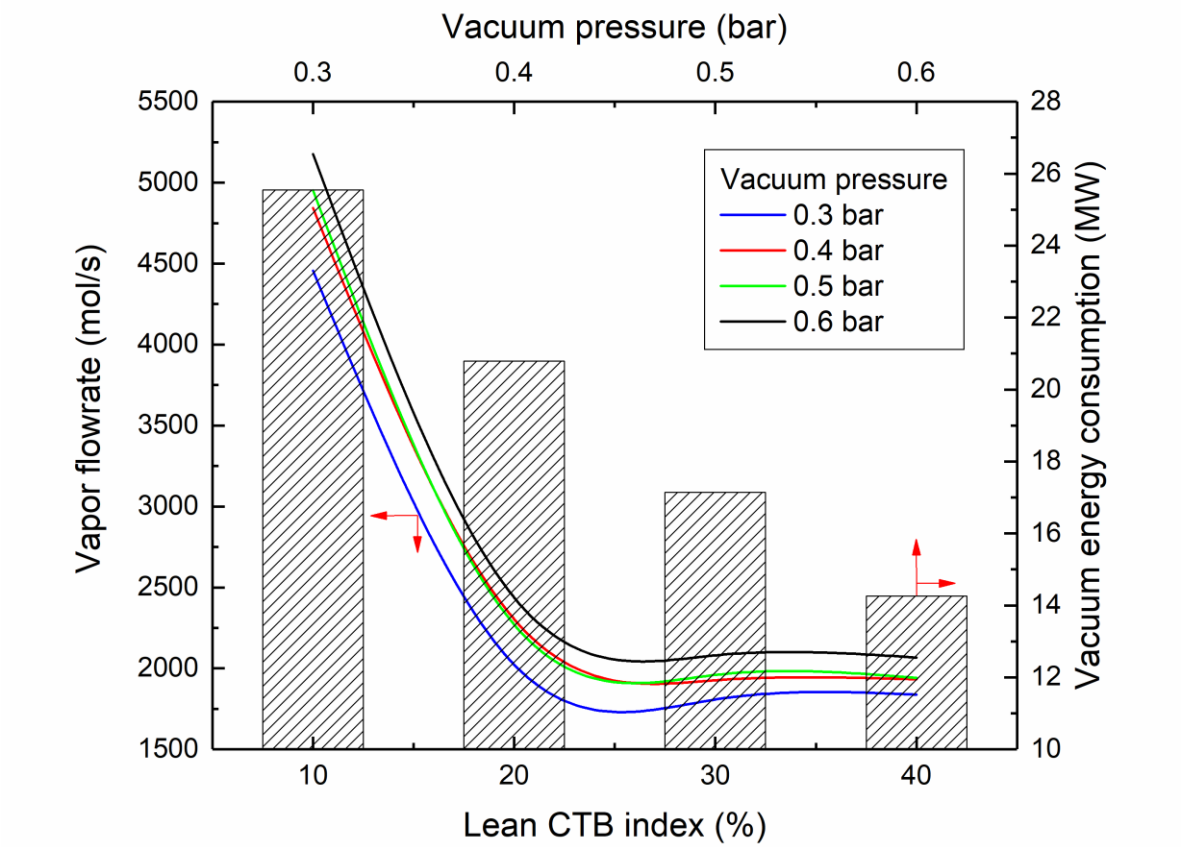

Figure 3.9 Relation between the lean CTB and performance of vacuum system.

Figure 3.10 shows the trends of energy consumption in the desorption and vacuum units when different values of the lean CTB index and stripper pressure are selected. An optimum region is observed with minimal heat of CO_2 regeneration when the CTB index ranges between 21 and 26% at different vacuum pressures. In this case, 44 and 70 MW is consumed for regeneration and 25 and 14 MW is also needed for the vacuum systems. In the case of moderate vacuum pressure (0.4 bar), the total electricity loss is estimated at 89.13 MW at CTB 23.7% which is 15% of the total power plant energy generated (600 MW_e).

These simulation results clearly show that the total required energy for CO_2 capture using the catalyzed PC solvent is competitive to the membrane separation processes, including the optimum two-stage (95 MW) discussed in this paper and a two-stage air sweep (91 MW) [143] for 90% CO_2 capture. Furthermore, the total electricity loss of the enzymatic-absorption process is 32 and 29 lower compared to MEA absorption processes (case 1 and 2) [155]. This reduction is due to the use of low-

quality steam to strip off CO_2 from the PC solution at lower temperature instead of extracting the steam from high-pressure (HP) and intermediate-pressure (IP) turbines in the MEA absorption process. It is expected that the required steam for the CO_2 regeneration in the stripper is supplied from low-quality steam as the boiling temperature of the PC solvent reduces to 74°C at 0.4 bar. Table 3.5 also presents a summary of techno-economic analysis of CO_2 absorption using the catalyzed PC solvent.

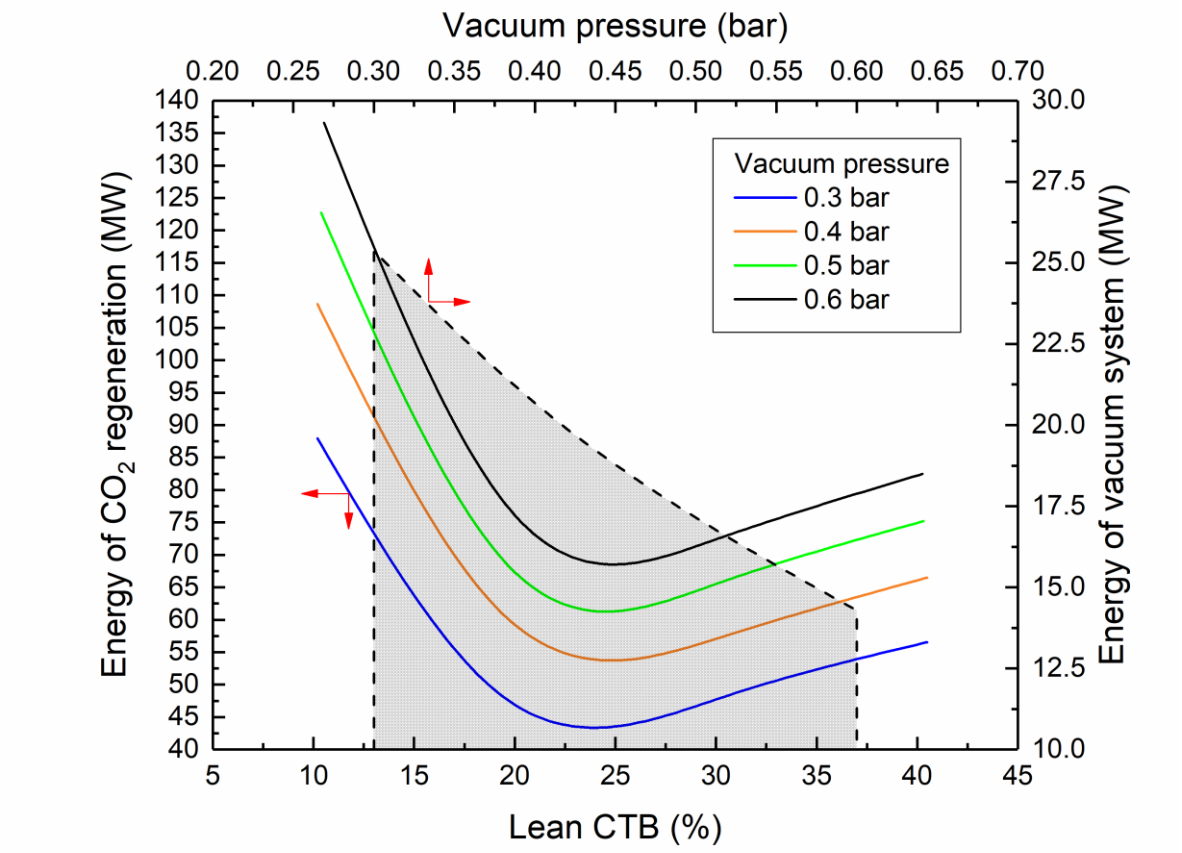

Figure 3.10 Effects of the lean CTB level on the electricity loss of plant.

Table 3.5 Summary of techno-economic analysis of CO_2 capture using the enzymatic-absorption process.

Parameters	Value	Unit
Flue gas blower	14.51	*M$*
Absorber vessel	17.70	*M$*
Absorber packing	46.77	*M$*
Stripper vessel	22.71	*M$*
Stripper packing	59.11	*M$*
Lean solvent tank	0.98	*M$*
Lean circulation pump	4.68	*M$*
Rich circulation pump	5.80	*M$*
Cross heat exchangers	4.25	*M$*
Lean solvent cooler	2.05	*M$*
Reboiler	6.55	*M$*
Stripper condenser	2.16	*M$*
Condenser pump	14.25	*M$*
Multistage compression	22.42	*M$*
Multistage intercooler	5.68	*M$*
Vacuum blower	29.44	*M$*
Vacuum blower intercooler	1.98	*M$*
Total capital cost	261.05	*M$*
CAPEX		
total annual capital cost	40.41	*M$*
Raw material and utility cost	53.74	*M$*
Cooling water	0.008	*M$*
PC solvent	3.83	*M$*
Enzyme	4.86	*M$*
Inhibitor	0.38	*M$*
electricity	44.65	*M$*
OPEX		
Total annual operating cost	65.82	*M$*
TAC		
Total annual cost	106.23	*M$*
ENERGY CONSUMPTION		
Flue-gas blower	8.15	*MW*
Circulation pump	4.23	*MW*
Steam extraction	53.21	*MW*
Water condenser pump	2.79	*MW*
Vacuum systems	20.76	*MW*
Total electricity loss	89.13	*MW*
Fraction of energy used	14.85	*%*
Multistage CO_2 compression	43.61	*MW*
CO_2 capture cost	27.85	*$/ton CO_2*

3.8 Conclusion

The CO_2 emission from fossil-fuel power plants is recognized to be the main contributor to greenhouse gases. Herein, we assessed and compared the separation performances of two alternative methods including membrane technology and enzymatic-absorption process to capture CO_2 from a 600 MW_e power plant. Our results revealed that the use of a two-stage membrane process was economically and technically competitive to the currently-used separation methods. As such, the optimal values of the required membrane area and feed pressure were set to $1.5x10^6$ m^2 and 2.7 bar, respectively. This optimized process allowed us to reduce the electricity loss to 95 MW for a CO_2 capture of 90%, which still accounted for 15% of total power plant output. The optimization results showed that more than 60% of the total energy was consumed for compression and vacuum systems. In this case, the optimal CAPEX and OPEX were estimated at 102 and 88 M$, respectively. It was also found that the use of turbo expander allowed to recover more than 36% of energy lost in the process. The related separation costs and electricity loss were highly dependent on the extent of CO_2 capture. The membrane process was more suitable to remove CO_2 bulk up to 50% where total annual cost and energy consumption were cut down by half of those for a CO_2 capture of 90%.

For the enzymatic-absorption process, the optimization results showed that an optimum region can be found while the desorption process occurred at different ranges of vacuum pressure (0.3-0.6 bar). The leaner CTB index resulted in a higher energy penalty in the stripper whereas the circulation rate of the PC solvent between absorption and desorption units was minimized. The optimization results revealed that the lowest heat of CO_2 regeneration at 0.4 bar was found to be 3.35 MJ/kg CO_2 as the lean CTB 23.5% was chosen. In this case, the electricity loss for desorption and vacuum systems reached 53.2 and 20.7 MW, respectively. The CAPEX and OPEX were also estimated at 40 and 65 M$ to remove 90% of CO_2 in the flue-gas. In comparison, the enzymatic-absorption process was superior to the membrane technology as both the TAC and electricity loss were found lower by 44 and 6.5%, respectively. According to this study, the membrane technology could become more efficient provided that the membrane purchase cost is decreased and CO_2 permeance at low-pressure (<1.5 bar) enhanced. As for the enzymatic-absorption process, a lower enzyme cost would also have beneficial effects on CO_2 capture cost.

Nomenclature

AMP	2-Amino-2-Methyl-Propanol
ASC	advanced supercritical
BCU	bulk capture unit
CAPEX	capital expenditure

CA	carbonic anhydrase
CCS	carbon capture and storage
COE	cost of electricity
CPU	CO_2 purifier unit
CSI	CO_2 solutions Inc.
CTB	carbonate to bicarbonate conversion
DRS	data regression system
DEA	diethanolamine
EDA	2-ethanediamine
ENRTL	electrolyte non-random two-liquid model
ERU	energy recovery unit
EWF	equivalent weight fraction
ERU	expander recovery unit
FCC	fixed capital cost
G	molar flowrate of gas (*mol/s*)
GHG	greenhouse gas
HP	high pressure
IP	intermediate pressure
k	reaction rate constant (*1/s*)
k_{OH}	rate constant of reaction ($m^3/mols$)
K_C	turnover number of enzyme (s^{-1})
K_{eq}	equilibrium constant
K_M	Michaelis constant (mol/m^3)
L	molar flowrate of liquid (*mol/s*)
MTR	membrane technology and research
MDEA	methyldiethanolamine
MINLP	mixed integer nonlinear programming
MEA	monoethanolamine
OPEX	operational expenditure
ORC	organic Rankine cycles
P	pressure (*Pa*)
PA	Paris agreement
PC	potassium carbonate
PCC	post-combustion carbon capture
PSA	pressure Swing Adsorption
PZ	piperazine
TAC	total annual cost
r	rate of reaction (*1/s*)
T	temperature (*K*)
TEA	triethanolamine
TSA	temperature Swing Adsorption
TMA	total membrane area (m^2)
DOE	department of energy
VSA	vacuum swing adsorption
VLP	very low pressure

Chapitre 4

Techno-Economic Analysis of a Hybrid System for Flue-Gas Separation: Combining Membrane and Enzymatic-Absorption Processes

4.1 Résumé

Les centrales électriques à combustibles fossiles fournissent une grande partie de l'énergie mondiale pour les applications domestiques et industrielles au détriment du rejet d'un volume élevé de dioxyde de carbone (CO_2) dans l'atmosphère. Ce scénario doit être modifié en équipant les centrales électriques d'unités de capture du CO_2 afin de prévenir le changement climatique. Le marché de la séparation des gaz est actuellement dominé par la technologie d'absorption à base d'amines, qui est coûteuse, gourmande en énergie et moins respectueuse de l'environnement. Dans ce contexte, un système hybride comprenant des procédés de séparation par membrane et d'absorption enzymatique est proposé pour éliminer le CO_2 des gaz de combustion émis par une centrale électrique de 600 MWe. Comme les procédés autonomes susmentionnés souffrent d'un coût d'investissement et d'une consommation d'énergie élevés, le procédé hybride serait plus performant en partageant le captage partiel du CO_2 entre deux unités de séparation. Les résultats de l'optimisation révèlent que le procédé à membrane devient économiquement plus efficace en éliminant 75 % du CO_2 des gaz de combustion. Le captage complet du CO_2 par l'unité d'absorption enzymatique permet alors de réduire remarquablement le taux de circulation du solvant entre les unités d'absorption et de désorption, ainsi que l'énergie de régénération du CO_2. Globalement, le procédé hybride contribue à réduire la perte totale d'électricité de 124 MW et le coût annuel total de 139 M$, soit respectivement 10 et 37% de moins que ceux du procédé autonome à membrane. Enfin, l'analyse technico-économique montre le fort potentiel de compétitivité du système hybride proposé pour le traitement des gaz de combustion, tout en estimant le coût du captage à 36 $/tonne de CO_2.

4.2 Abstract

Fossil-fuel power plants supply a large part of global energy for domestic and industrial applications at the expense of releasing a high volume of carbon dioxide (CO_2) in the atmosphere. This scenario must be changed by retrofitting the power plants with CO_2 capture units so as to prevent climate change. The gas separation market is currently dominated by amine-based absorption technology, which is costly, energy-intensive, and less eco-friendly. Herein, a hybrid system including membrane

and enzymatic-absorption processes is proposed to remove CO_2 in flue-gas emitted from a 600 MW_e power plant. As the above-mentioned standalone processes suffer from high investment cost and energy consumption, the hybrid process would exhibit better performance through sharing partial CO_2 capture between the two separation units. The optimization results reveal that the membrane process becomes economically more efficient through removing CO_2 in bulk by 75% from the flue-gas. The complete CO_2 capture through the enzymatic-absorption unit then allows to remarkably reduce solvent circulation rate between absorption and desorption units, as well as the energy of CO_2 regeneration. Overall, the hybrid process contributes to decrease the total electricity loss by 124 MW and the total annual cost by 139 M$, which are 10 and 37% lower than those in the standalone membrane process, respectively. Finally, the techno-economic analysis shows high competitiveness potential of the suggested hybrid system for flue-gas treatment while estimating the capture cost at 36$/ton CO_2.

4.3 Introduction

The fossil fuels (coal, oil, and gas) are the primary global energy source since the industrial revolution and currently provide more than 70% of our total energy demands [192]. A consequence of this is the production of a high volume of CO_2 via burning the fossil fuels in chemical industries, cement manufactures, and power plants and inconsiderately releasing most of it in the atmosphere. Under this scenario, the emission of CO_2, as a major contributor to the greenhouse gases (GHGs), increases on the one hand deforestation and industrial agriculture and, on the other hand, soil erosion, all together impacting the Earth's carbon cycle and thus causing climate changes. In 2019, the global average CO_2 level reached 412 ppm which is 45% more than before the pre-industrial revolution. It is even expected that the CO_2 level will exceed 550 ppm by 2050 if the current pathway of global CO_2 emission known as the "business as usual" scenario is sustained [193]. Fortunately, the United Nations Framework Convention on Climate Change (UNFCCC) has attempted to unify nations to seriously deal with the climate change. In the framework of the Conferences of Parties (COP), ambitious objectives have been set to stabilize the concentration of GHGs in the atmosphere at a level at which anthropogenic (human) activities pose no threat to the climate system [194]. Later in the Paris Agreement (PA), the parties reached an agreement to combat climate change by reducing GHGs emissions, in order to keep a global temperature rise in this century well below 2ºC above pre-industrial levels [195]. To do so, it is a must to reduce cumulative emission by at least 470 Gt_{CO_2} by 2050 compared to current and planned policies to meet that goal [196].

In this situation, a controversial question raises: how to meet global energy demand while fossil energy is still a fundamental driver of not only economic but also multi-aspects of life progress?

Electricity production from fossil-fuel-based power plants might truly represents our long-lasting dependency on this energy source. In this case, approximately 30% of global CO_2 emission is generated by combustion of fossil fuels in power plants [5] and this number is also projected to increase with the global economic growth. Focusing on the 2°C target, the carbon capture and storage (CCS) method has and will continue to play an important role to deal with CO_2 emissions until developments of more efficient technologies [197]. However, CCS technologies still need to be improved in order to reduce the cost and energy of CO_2 capture, and to solve the operational issues. The CCS method may involve three main technologies: i) post-conversion processes which remove CO_2 generated in a chemical plant; ii) pre-conversion processes which transform fossil fuels into a clean-burning gas and then removes the remaining CO_2; and iii) oxy-fuel combustion processes which collect pure CO_2 and steam gases by burning fossil fuels in an atmosphere of pure oxygen instead of air [1, 2]. Among them, the post-conversion process is the most mature and it is also found to be more easily retrofitted to the existing industrial sectors such as oil refineries, biogas sweetening units, and specifically cement and power plants [3]. Furthermore, the post-conversion processes are classified into different separation methods: absorption, adsorption, cryogenic, and membrane technologies. The method selection then becomes a challenge as each process has a separation mechanism and, more importantly, is only effective under specific conditions. It is therefore essential to precisely consider process parameters such as feed characteristics (pressure, temperature, flowrate, and composition), product specifications (CO_2 purity and recovery), and economic aspects (capital and operation costs) prior to implementing a process. Despite this, there are still some critical constraints which highly affect the incorporation of these processes into cement and power plants. Thus, the separation market is now dominated by a solvent-based absorption process which came into commercial use more than 60 years ago. However, this separation method is not fully attractive on technical, environmental, and economic aspects. Hence, a brief summary of the current outlooks of the post-conversion CO_2 capture (PCC) methods is needed to objectively reveal pros and cons and also underline their potentials to be merged as a hybrid system.

4.3.1 Performance, limits, and potentials of conventional separation methods

Thus far, much attention has been drawn to the PCC methods in order to simultaneously improve removal performance and operational issues. Assuming that all processes are technically viable for integration into power plants, CO_2 capture cost would still play a major role in assessing a process in terms of applicability and profitability. It is therefore essential to identify the existing bottlenecks of all processes which impose serious limitations on further developments and impede the full

commercialization. To do so, more details about the PCC processes are provided in the following sections.

4.3.1.1 Absorption

Absorption is a matured technology which was successfully used for removing acid gases from various gas mixtures such as natural gas, biogas, and flue-gas for many decades [125, 145]. In a typical process, flue-gas contacts counter-currently a lean-solvent at low pressure and moderate temperature in a packed or tray column. The CO_2 in the flue-gas is initially dissolved at a gas-liquid interface and then diffuses through the liquid phase. The efficiency of the CO_2 removal can also be enhanced by a chemical reaction which occurs mostly in the liquid film. The CO_2 rich-solvent is then regenerated in a stripper column operated at higher temperature to recover the solvent through breaking CO_2-solvent bonds [198]. For the solvent regeneration, a high amount of energy must be taken for example from the power plant in order to supply adequate heat duty for the reboiler. In addition, other properties including CO_2 removal capacity, stability towards degradation by SO_x and NO_x and oxidation, CO_2 reactivity should be taken into account in the solvent selection. Generally, a large number of solvents, including single amine solvents [199] such as diethanolamine (DEA), monoethanolamine (MEA), and methyldiethanolamine (MDEA), ammonia-based solvents [200], amino acid salt-based solvents [201], and carbonate salt-based solvents [13], have received high interest for flue-gas separation. In comparison, MEA is still a preferable solvent for most absorption cases. The energy requirement for MEA regeneration, which varies between 3.0 to 4.5 MJ/kg CO_2, is still high and accounts for more than 80% of the total energy consumption [152]. Overall, an absorption process is suitable for capturing low concentration CO_2 (3-15%) from flue-gas. As a high CO_2 recovery is obtained for a capture cost in a range of 40-100$/ton CO_2 [4], this process is still more economical compared to most separation methods. However, this process has some major drawbacks as: low separation efficiency for low CO_2 concentration in the feed, high energy consumption for solvent regeneration, non-eco-friendly process, scaling-up issues, solvent degradation (SO_x and NO_x) and oxidation, and high corrosiveness to equipment. In this case, the absorption technology, as part of a hybrid system, would be a viable option in order to reduce not only energy penalty for solvent regeneration but also replacement cost of degraded solvent [5].

4.3.1.2 Adsorption

Adsorption is also regarded as a promising alternative technique for removing CO_2 from flue-gas of power plants. The separation mechanism relies on gas abilities to be adsorbed on a solid surface and to be desorbed from *via* a sequential process. In this case, gas components temporarily bind with

adsorbents according to their molecular characteristics and/or affinities to adsorbent materials and then, are released through splitting the gas-solid bonds. In fact, an adsorption process is a heterogenous dissolution of undesired gas in a solid phase instead of a liquid phase compared to an absorption process. A wide range of materials such as molecular sieves, carbonaceous materials, zeolites, metal organic frameworks (MOFs), and amine-based porous structures might be used as adsorbent [23, 123]. But some critical factors such as absorption capacity for CO_2, adsorption/desorption kinetics, CO_2 selectivity, regeneration conditions, durability, stability to humidity and impurities such as O_2, CO, NO_x, and SO_x, synthesis cost all together should be considered for development of a commercial adsorbent [124]. Pressure Swing Adsorption (PSA), Vacuum Swing Adsorption (VSA), and Temperature Swing Adsorption (TSA) are commercial processes which might be implemented for flue-gas separation. High investment and operation costs, and complex process control are the main disadvantages of the PSA process [23, 85]. The main drawbacks of the TSA process are: high energy consumption, large cycle times between absorption and desorption, thermal aging of adsorbents, and high requirement of adsorbent inventories [202]. The VSA process is limited to be used for small-scale flue-gas separation (50 MW power plant) due to shortcoming in commercial large vacuum trains providing approximately 100,000 m^3/h at 50 kPa vacuum [128]. In comparison, the lowest energy requirement for adsorbent regeneration is estimated at 3.3 MJ/kg CO_2 as the VSA is used [203]. Overall, none of the above-mentioned processes is competitive with the MEA absorption process, not only due to low performance of the existing adsorbents but also to integration technical barriers into power plants.

4.3.1.3 Cryogenic process

The separation principle relies on difference between thermodynamic properties of the gas components in a mixture. Then, all cryogenic processes involve phase transitions to make a binary/tertiary system for removing undesired components from a gas mixture [198]. As the triple point for CO_2 is 216.31 K at 5.18 bar, an appropriate thermodynamic condition allows CO_2 to either condense or sublime whereas other components remain in the gas phase. As to flue-gas separation, it seems to be unrealistic to compress such a high-volume gas and to reduce the temperature until CO_2 turns to liquid or solid phase. Thus, the cryogenic method might be more suitable, provided availability of cold energy such as Liquified Natural Gas (LNG) compensates for penalty cost of the gas compression. Under this scenario, different cryogenic technologies might be proposed for flue-gas separation. In cryogenic distillation [5], flue-gas which is chilled in a pre-cooling unit enters a high-pressure plate column. A gas-liquid mixture is formed in the column due to differences in boiling temperature of the gas components. This allows N_2 getting enriched upwards and escaping from the

top of the column whereas CO_2 is liquified and then, accumulates at the bottom of the column. Operating problems due to solid formation, and blockage at top section of the columns are as a result of operating at a high pressure and extremely low temperature [204]. This cryogenic process is cost-effective, provided the cold energy is available at low cost. In this case, the CO_2 avoided cost is estimated at 52.8$/ton CO_2 that is competitive with 54.5$/ton CO_2 for the amine-based absorption process. Overall, the great advantage of the cryogenic method is to achieve higher CO_2 purity (99.9%) and recovery (99.9%) than other separation technologies. This technology also offers some advantages over other existing amine-based absorption and adsorption processes.

4.3.1.4 Membrane technology

Membrane technology is not mature compared to the above-mentioned separation methods, but it is attractive due to its simple separation mechanism in flue-gas separation. The separation principle is based on permeation abilities of the gas components of a mixture passing through a thin membrane layer [198]. Polymeric membranes, which have better advantages than other membrane types, are commonly chosen for industrial gas separations. These membranes consist of a dense selective layer on a porous support layer. The permeation through the top layer depends upon gas diffusivity and solubility whereas the beneath porous layer aims only at improving mechanical stability. Most of membrane plants need to be operated at high pressure as this ensures adequate driving force to meet product specification. Upon initial review, the treatment of flue-gas using membranes might be impossible due to high energy penalty incurred by compression. This scenario appears to be the same as observed for adsorption and cryogenic methods which are therefore less competitive than amine-based absorption processes. The separation efficiency highly depends on membrane characteristics (permeability and selectivity) and desired level of purity. A well-known trade-off between selectivity and permeability described by Robeson plots [7], imposes limitations on the development of commercial membranes

Moreover, a multi-stage membrane separation process is required for removing CO_2 from the flue-gas of power plants to obtain a high CO_2 purity (above 95%) and recovery (90%). It is then essential to precisely consider integration of the membrane technology so that an increase in the cost of electricity of less than 20% is obtained according to targets of the U.S. Department of Energy (DOE) [205]. But few commercial membranes can be chosen for a realistic project of the flue-gas separation. One of such membranes is Polaris^{TM} which has a CO_2 permeance of 1000 GPU and a CO_2/N_2 selectivity of 50 at 30^{o}C. Polaris^{TM} mounted into spiral wound membrane modules was used for a CO_2 capture plant integrated into a 600 MW coal-fired power plant and then, satisfied the DOE criteria [4]. In this case, 90% CO_2 capture at a cost of 23$/ton CO_2 was achieved at expense of only

16% of the total power plant equating to 97 MW. This process was slightly modified through merging with a membrane-based air separation unit in order to enrich O_2 in the sweep gas going to the coal burner [206]. Despite complexity of these processes, the CO_2 capture cost is still competitive with other separation technologies. As discussed above, membrane technology might be however more effective when used in a hybrid process for bulk removal of CO_2.

4.3.2 Hybrid systems for flue-gas separation

Numerous studies have been devoted to enhancing process efficiency and reducing CO_2 capture cost at the same time for the PCC separation technologies. In turn, the existing separation methods are less economically attractive and thus, amine-based absorption is still the preferred process for flue-gas separation due to its high maturity and cost-effectiveness. Another approach is to initiate a hybrid system through combining multiple separation technologies. A compelling consequence is that the hybrid system would benefit from advantages of the incorporated processes. This aims to not only reduce CO_2 capture cost but also solve operational issues induced by implementing an individual process. Few works have been published to explain the merits of hybrid systems for flue-gas separation. Thus, separation performance and economical aspects of such hybrid systems are briefly discussed below.

Membrane Technology & Research, Inc. (MTR) and the University of Texas at Austin (UT Austin) introduced a hybrid membrane-absorption system to capture CO_2 from a coal-fired power plant [207]. This system merged a crossflow, air-swept Polaris™ membrane process with a UT Austin's 5 m piperazine advanced flash stripper in series and parallel configurations. In both cases, the flue-gas leaving the coal burner contained 25% CO_2 and the air-sweep system was used to generate driving force in the membrane unit. In the series arrangement, the flue-gas was fed to the absorption system in order to capture 50% of CO_2, followed by removing the reminder through the membrane system to achieve 90% CO_2 capture. The main advantage was that the absorber operated at a higher lean-loading state and thus, resulted in reducing the regeneration energy and solvent emissions. In the parallel arrangement, the flue-gas was split into two streams and equally fed to the absorber and membrane units. The main advantage was to reduce the absorber size to half of the original size in the series arrangement and hence, capital cost would reduce. Kundu et al. [12] also simulated a hybrid process (membrane-absorption) to capture 85% of CO_2 with a purity of 98% from a flue gas stream. A two-stage membrane process exploiting Polaris™ membrane captured a fraction of CO_2 in the flue gas, followed by an absorption process using monoethanolamine (MEA) to eliminate the residual CO_2. This study showed that a higher reduction of the energy penalty in the absorption process was obtained at a higher rate of CO_2 capture in the membrane unit. In the case of Polaris™ performance,

the required separation area in the hybrid process was also varied by only 4% of the initial value (640 m^2) when changing the CO_2 recovery from 0.1 to 0.6. In turn, the energy demand of the hybrid system was found to be 1.83-3.70 GJ/ton CO_2 which was less than that in the standalone absorption process (3.5 GJ/ton CO_2). Kusuma et al. [208] also proposed a new hybrid process to achieve 90% CO_2 removal from flue-gas. Contrary to the previous processes, a single-stage membrane unit was placed after the gas pressurized stripping (GPS) unit in order to reduce energy penalty of solvent regeneration. Instead of a reboiler for solvent regeneration, two inter-heaters in parallel with the GPS column supplied required energy for CO_2 desorption. Then, nitrogen as a stripping gas was also injected from the bottom of the GPS column which was provided from either a treated flue-gas or a permeate product of the membrane unit. The hybrid process outperformed both a conventional MEA absorption process and a MDEA/PZ absorption with steam stripping as 49 and 22% reductions in the total energy consumption were achieved, respectively. In comparison, the least equivalent work was found to be 0.189 and 0.194 kWh/kg CO_2 for Polaris^{TM} and commercial membranes respectively, which was still much lower than 0.37 kWh/kg CO_2 estimated for the baseline standalone MEA absorption process.

Belaissaoui et al. [209] simulated a hybrid membrane-cryogenic process for removing CO_2 from flue-gas of a coal-fired power plant. Flue-gas was initially fed to a single-stage membrane unit to produce a CO_2 concentrated gas stream on the permeate side, followed by a cryogenic unit to capture 90% of CO_2 in the carrier gas. Two Polaris™ membranes with CO_2/N_2 selectivities of 50 and 100 were used to evaluate CO_2 capture in the membrane process. The required energy was then estimated at 1.4-3.7 GJ per ton of CO_2 recovered, while CO_2 mole fraction in the permeate product varied from 0.38 to 0.85. For all simulation cases, the CO_2/N_2 selectivity changes from 50 to 100 without significant impact on the membrane process energy requirement. In the cryogenic process, the required energy decreased from 1.8 to 1.07 GJ/ton CO_2 only for the range of CO_2 content reported for the membrane process. For a CO_2 mole fraction less than 0.35, the cryogenic process was ineffective resulting in a dramatic rise in the energy requirement (2.4-8.5 GJ/ton CO_2). Overall, this hybrid process seems to be competitive with a baseline MEA absorption process, provided purity and capture of CO_2 were set to 89% and 85%, respectively. Under these conditions, the energy demand was then found to be 3.5 GJ/ton CO_2. Anantharaman et al. [210] also proposed a “membrane-low temperature” hybrid process for the post-combustion CO_2 capture from coal-fired power plants. For the single-stage membrane process, a membrane with a CO_2/N_2 selectivity of 80 and a permeance of 5 Nm^3/m^2.bar.h (~1800 GPU) was chosen to remove 90% of CO_2 in the flue gas. They reported that the energy penalty of the hybrid process was strongly dependent on CO_2 concentration in the permeate stream. To achieve 85%

CO_2 capture, the optimum CO_2 concentration was to be set at 65-67%. In turn, the CO_2 avoided cost decreased to 48 $€_{2008}$/ton CO_2 which was then 9% more cost-efficient than a baseline MEA absorption process. In addition to Polaris™ membrane tested at 30-40ºC, Liu et al. [211] showed that the characteristics of commercially available polyimide membranes (Matrimid® 5218) noticeably improved at sub-ambient temperature. By reducing temperature from 0 to -50ºC, the CO_2/N_2 selectivity increased to 157 which was 58 times higher than the initial measurement at 35ºC. Later, Song et al. [212] introduced a novel low temperature membrane-cryogenic hybrid process to capture CO_2 from coal-fired power plants. A three-stage membrane process operated at low temperature (-16ºC) and moderate pressure (4 bar) was arranged between a pre-cooling unit supplied in cold energy by a liquefied natural gas (LNG) and a cryogenic unit. They used Matrimid® 5218 [211] with CO_2/N_2 selectivities of 27 and 80 and permeance of 292 and 143 GPU respectively, measured at 35 and -20ºC to evaluate separation performance of the standalone membrane and hybrid processes. The energy consumption of this hybrid system was then estimated at 1.7 MJ/kg CO_2 which was competitive with the standalone membrane process (2.8 MJ/kg CO_2) [4] and the conventional membrane-cryogenic hybrid system (3.5 MJ/kg CO_2) [209]. Furthermore, the capital cost of the hybrid process decreased by 55% and 37% compared to the membrane and the hybrid processes, respectively. In addition, the operational cost was also reduced by 39.3 and 43.3%, respectively. Fong et al. [213] considered a hybrid system consisting of cryogenic, VSA, TSA, and membrane unit to retrofit a 300 MW coal-fired power plant. The flue-gas stream was initially fed to a VSA unit to produce a N_2-rich product stream. The CO_2-rich stream (64.5 mol.%) of the VSA unit saturated with water was compressed to 17.8 bar and thereafter fed to a TSA adsorption unit to enhance CO_2 recovery. The final CO_2 enrichment process is then carried out using the low-temperature and Polaris™ membrane units. Under an optimum condition to achieve 88.9% CO_2 capture with a CO_2 purity of 98.2, the specific shaft work was found to be 1.4_e GJ per ton CO_2 captured. In this case, the specific shaft work was almost identical to a standalone MEA absorption process (1.3_e GJ/ton CO_2 captured). Overall, the main drawbacks would be high capital and maintenance costs, and complexity of process control due to the incorporation of four different technologies. Under this scenario, the comparable energy penalty might be altered and thus, making this process less effective than other post-conversion CO_2 capture technologies.

4.3.3 Membrane-Absorption (MA) hybrid system

As discussed, all hybrid systems take special advantage of the membrane technology so as to remove the bulk of CO_2 from flue-gas. Either permeate or retentate product is then further treated *via* one of the conventional separation methods to meet product specification. More specifically, this approach

aims at effectively combining membrane technology with another separation method while their operational issues and economic shortcomings would be attenuated in the hybrid process. A hybrid system should require less energy expended to each of the individual processes working as a standalone operation. Therefore, the footprint should also be lower. Undoubtedly, these changes would lead to substantial reductions in both operation and capital costs.

Currently, Polaris^{TM}, an advanced membrane, offers separation performance superior to the commercial ones and hence, might be considered an appropriate choice for removing CO_2 from flue-gas of power plants. Nonetheless, when both CO_2 purity and recovery are set to 90%, the Polaris^{TM} membrane process with very high CO_2/N_2 selectivity (α>100) is still energy-intensive and not competitive with MEA absorption process [209]. In the absorption process, much attention has been drawn to the new solvent formulation in order to reduce energy cost and improve environmental signature. The Econamine FG Plus^{SM} (EFG+), which is a Fluor proprietary amine-based technology, proves better performance than the traditional MEA-based absorption process. To capture 90% of CO_2, the energy consumption is 3.24 kJ/ton CO_2 which is almost 20% lower than that of the MEA counterparts [214]. Nevertheless, the EFG+ process also suffers from some critical limitations in the case of amine emission from absorber and ammonia formation due to solvent oxidation. Another scenario needs to be considered to implement non-amine solvents to not only overcome these issues but also remain cost effective. Carbonate solutions such as Potassium Carbonate (PC) might be adopted to remove CO_2 from flue-gas due to its high stability, low regeneration energy, limited toxicity, and low cost [13]. In comparison to amine-based solvents, the intrinsic PC rate of reaction is slower and hence this translates to a lower mass transfer of CO_2 into the liquid phase. Moreover, this results in a higher capital investment as a larger absorber is required to offset the inferior reaction efficiency. Hopefully, the rate of CO_2 absorption can be accelerated through adding active components such as organic, inorganic, enzymatic, and ion liquid promoters. Hu et al. [171] made a comprehensive review about the efficient methods for improving the absorption kinetics and discussed their impacts on realistic processes. In most cases, a mediated solvent fails to come into commercial applications due to toxicity and carcinogenic effects, deterioration of CO_2 driving force, reduction of CO_2 solubility, increase of energy requirement for solvent regeneration, and solvent corrosivity and degradation. By contrast, the enzymatic promoters exhibit high potentials for extensively being adopted in the absorption process. The enzymatic Carbonic Anhydrase (CA) which is found in human body to catalyze CO_2 hydration and dehydration can allow effective CO_2 capture from flue-gas. Thee et al. [215] reported that addition of CA (0.4, 0.8, and 1.4 µM) supplied by Novozymes to the PC solution (30 wt.%) at 40ºC improved the pseudo-first-order rate coefficient and

thus, the overall absorption process of CO_2 by 14, 20, and 34%, respectively. Similarly, Ye and Lu [175] observed the improvement of CO_2 absorption by two to six times by addition of 300 mg/L of CA to the PC solution (20 wt.%) at 40-60^oC. Fradette [216] patented the process of biocatalytic gas treatment using a spray absorber bioreactor in which a solvent catalyzed by CA contacted counter-currently the CO_2-containing gas phase. This test, which was conducted in a lab-scale apparatus, proved the enhancement in the CO_2 absorption rate compared to packed-bed reactors filled with immobilized CA enzyme. Later, CO_2 Solutions Inc. (CSI) was to be the pioneer of commercialization of the CA catalyzed solvent for absorption processes [217]. In 2015, the proprietary low-cost solvent was deployed to demonstrate the removal performance in a large-scale CO_2 absorption process (10 tons CO_2/day). The reboiler heat duty was found to be 3.6 GJ/ton CO_2 when 80% CO_2 capture was realized. Furthermore, the total CO_2 capture cost was estimated at 28$/ton which was lower than that reported for the amine-based absorption process (40-100$/ton CO_2) [4]. In addition, the enzyme catalyst performance was stable, and no solvent degradation was observed after total operation of more than 2,500 hours. From the review of the published literature, the catalyzed PC solvent proves to be highly competitive with costly and non-eco-friendly amine-based counterparts. Undoubtedly, the removal performance of this industrial case can be further improved through a sensitivity study to find optimal values of the process parameters.

4.3.4 Objectives of the present study

Herein, a hybrid process is proposed for CO_2 capture from the flue-gas of a 600 MW_e fossil-fuel power plant through combining membrane gas separation and enzymatic-absorption technologies. In turn, the hybrid process benefits from most of the technical and economic aspects of the above-mentioned separation methods. Such integration would offer a better scenario for flue-gas treatment as CO_2 removal is shared between two distinctive processes. Hopefully, this plan would reduce energy penalty related to the CO_2 capture unit compared to those in the standalone membrane and enzymatic-absorption processes. To do so, it is imperative to specify the extent of CO_2 capture in each separation unit prior to exceeding a threshold at which the cost of CO_2 capture and energy consumption tend to rise dramatically. In such a case, the hybrid process needs to be accurately optimized to reduce the energy penalty as much as possible through minimizing the equivalent work of gas compression and permeation evacuation systems in membrane modules and required reboiler heat duty for stripping off CO_2 from a rich solvent in stripper columns. Hence, a techno-economic analysis is made to investigate the separation performance for the standalone technologies and the hybrid system under different operating conditions. In turn, this approach allows to determine optimal process parameters and thus, representing their impacts on the cost of CO_2 capture and electricity loss. Later, the results

of the economic analysis associated with the hybrid process are individually compared to those in the standalone processes while the CO_2 capture is set to 90% as the reference of comparison. Process cost models taken from ref. [182] and [218] are also used to precisely determine the CO_2 capture cost and to explicitly underline the contribution of both operation cost (OPEX) and capital cost (CAPEX) in the hybrid process. This study finally provides important insights into the integration of the membrane technology for the enzymatic-absorption process and also aims at facilitating the transition of hybrid system to the flue-gas separation market.

4.4 Modeling and optimization of hybrid system

4.4.1 Membrane permeation model

Herein, a gas permeation model developed by Gilassi et al. [90] is used due to its good performance for simulation of a flue-gas separation process under different operating conditions. This model is also used for the optimization of a multi-stage membrane process in that optimum operating parameters and efficient process layout are determined while annual separation cost is minimized [182]. For brevity, more details about the optimization results and techno-economic analysis associated with a standalone membrane process for flue-gas treatment is given in Ref. [218].

4.4.2 Enzymatic-absorption model

When CO_2 is absorbed into an unpromoted PC solvent, it proceeds according to the following overall reaction [178]:

$$CO_{2(g)} + K_2CO_{3(aq)} + H_2O_{(l)} \rightleftharpoons 2KHCO_{3(aq)} \quad (4.R1)$$

As potassium carbonate (K_2CO_3) and bicarbonate ($KHCO_3$) are strong electrolytes, they are fully dissociated in water. Thus, the reaction (4.R1) is preferably represented in the form of ionic speciation as:

$$CO_2 + CO_3^{2-} + H_2O \rightleftharpoons 2HCO_3^- \quad (4.R2)$$

The above reaction consists of several elementary steps depending on the pH value of the solution. More details are also available in ref [218].

Herein, the simulation of CO_2 capture in a packed-bed column using the catalyzed PC solvent is carried out using Aspen Plus® (version 10.1). A non-equilibrium rate-based model is developed using

a built-in RadFrac model that is suitable to simulate the CO_2 diffusion from a gas phase to a liquid phase according to the double film theory. The RadFrac model is also chosen to simulate the CO_2 stripping process from the rich solvent in a packed-bed column. The Aspen database provides the property parameters of gas and liquid mixtures, kinetic and equilibrium constants relevant to the system (H_2O-K_2CO_3-CO_2) in the liquid phase, as well as the Henry's constants for CO_2 in water and PC solution. Moreover, the Redlich-Kwong (RK) equation of state to estimate gas fugacity, and Electrolyte Non-Random Two-Liquid (ENRTL) thermodynamic model to calculate liquid components activity are chosen due to non-idealities in the gas and liquid phases. The vapor-liquid equilibrium (VLE) data is also taken from the results of experimental works reported by Tosh et al. [219]. The gas- and liquid-side mass transfer coefficients and effective interfacial area are calculated using the Rocha et al. [220] correlations according to different types of structured packings. The kinetic reaction rates of CO_2 absorption into catalyzed PC solution are taken from the data reported in Ref. [185]. More details about the performance of this simulation model can also be found in our previous study [218]. In general, the primary objective, in optimization of chemical absorption process, is to minimize the energy for solvent regeneration in the stripper which accounts for more than 70% of the total energy consumption. Therefore, a techno-economic analysis is made to find optimal values of the process variables while the reboiler heat duty is minimized. More specifically, this approach in which the optimization of OPEX corresponds to the optimization of CAPEX aims at identifying the optimum enzymatic-absorption process as the final objective.

4.4.3 Optimization method

The optimization approach used for a hybrid system consists in finding optimum decision variables for each separation process through which the cost of CO_2 capture is minimized. In this case, a techno-economic optimization is initially carried out for the standalone membrane based and enzymatic-absorption processes. This allows to precisely define a correlation between separation efficiency and economical aspects at different extents of CO_2 capture. Figure 4.1 illustrates a process flow diagram of the hybrid system used for flue-gas treatment. As shown, the flue-gas is initially sent to a pre-treatment unit to subsequently remove humidity and trace of impurities such as SO_x and NO_x, and reduce the temperature to 40^{o}C. The cooled gas is then fed to the membrane unit wherein bulk removal of CO_2 is expected. At this stage, optimization target is to minimize the total annual separation cost at different extents of CO_2 capture varying from 10 to 90%. The treated gas depleted of CO_2 (retentate stream) is then sent to the enzymatic-absorption unit where the reminder of CO_2 is removed in the absorber using the catalyzed PC solvent. To optimize this unit, the reboiler heat duty is needed to decrease as much as possible during solvent regeneration in the stripper so as to reach a CO_2 capture

of 90% with a CO_2 purity of ~95%. The effluent of CO_2 released from the top of the stripper column is then sent to a mixing point to be merged with the permeate stream of the membrane unit already enriched to CO_2. The CO_2 final product is then compressed to 150 bar using a multi-stage compression unit for transportation. Above all, different optimization problems need to be conceptualized for different extents of CO_2 capture from 10 to 90%. This approach allows finding the optimal costs of CO_2 capture for each separation process and hence, resulting in the optimum point of hybrid process integration. Moreover, a parametric study is carried out to underline the effect of partial CO_2 capture on OPEX and CAPEX estimations.

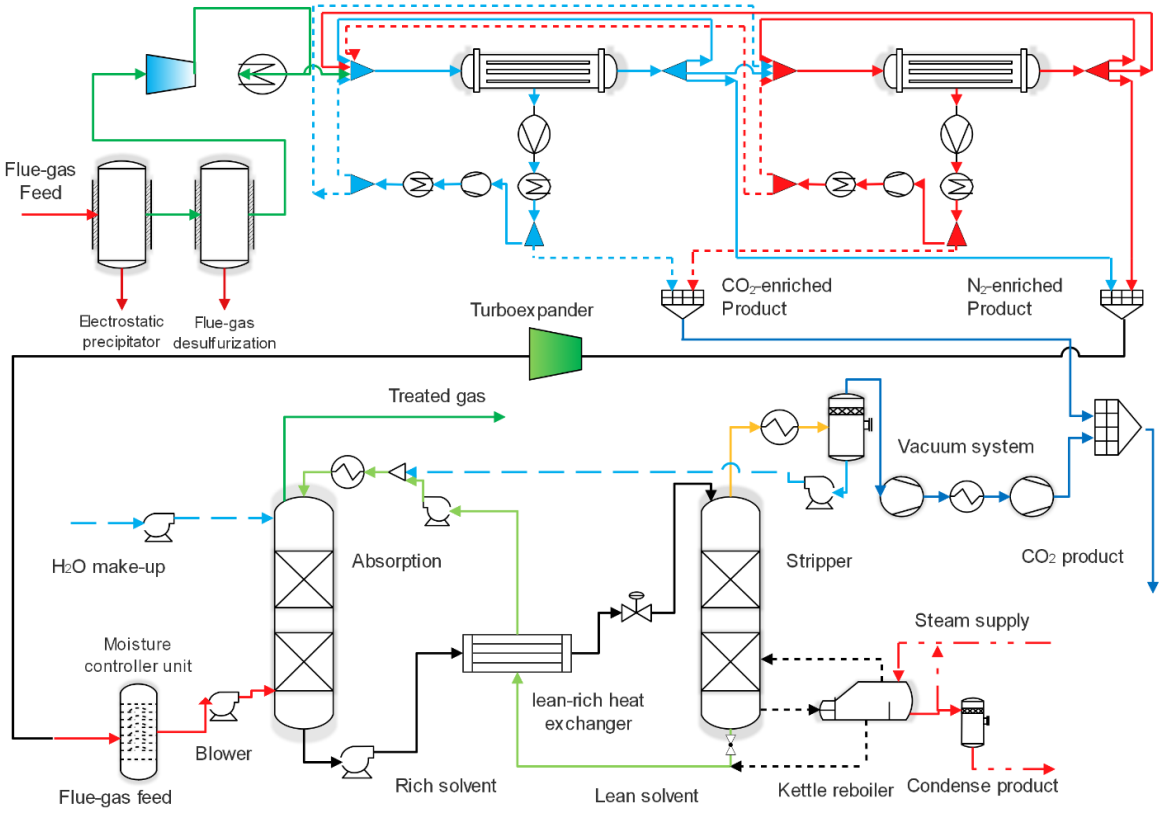

Figure 4.1 Process flow diagram of a hybrid process including pre-treatment, membrane, and enzymatic-absorption units.

4.5 Results and discussion

4.5.1 Process description

As the use of standalone membrane technology to capture 90% of the CO_2 in flue-gas would result in high penalty of energy consumption and also high demand in membrane separation area, this process might be used as a main CO_2 removal unit in a hybrid process. According to the results of our previous

work, the range of CO_2 capture demanded in the membrane process has a very sensitive effect on the annual separation cost [218]. Thus, a hybrid layout embodying consecutively a membrane unit and another separation process would allow sharing the burden of CO_2 capture. Table 4.1 presents the flue-gas properties and characteristics used for this study. As shown in Figure 4.1, the first two units including electrostatic precipitator (EP) and flue-gas desulfurization (FGD) are used to remove unwanted substances. The moisture content which is then 11-13 vol.% in the flue-gas needs to be trapped through a drying unit. Otherwise, not only higher membrane area would be required due to the superior permeance of H_2O, but also the whole process would demand more resistant to corrosion equipment and hence increased capital cost. Then, the dried gas is compressed and thereafter fed to a two-stage membrane process in which the target is to remove a sizable fraction of the CO_2. In this case, the CO_2 capture in the range of 30 to 70% has the lowest impact on both CAPEX and OPEX spending [218]. Part of the energy consumed by compressors and vacuum systems in the membrane process could be regained through turboexpanders in the energy recovery unit (ERU). The discharge pressure is then adjusted to offset the pressure drop in equipment and pipeline. The flue-gas needs to be re-humidified before feeding to the absorption column. This step is necessary to avoid absorbing moisture by the gas in counter-current contact with the solvent. The leftover CO_2 is finally captured in the enzymatic-absorption unit. The CO_2-rich gaseous product released from the desorption column is mixed with the CO_2 collected in the permeate stream and then sent to a multi-stage compression unit for final transportation.

Table 4.1 Flue-gas properties used for the optimization problem.

Parameters	**Value**
Mass flow (*kg/s*)	616.0
Pressure (*kPa*)	101.6
Temperature (˚*C*)	47
Composition	Wet gas (*vol.%*)
N_2 + Ar	71.62
CO_2	13.30
H_2O	11.25
O_2	3.81
SO_2	0.005
NO_x	0.0097

4.5.2 Required solvent for CO_2 capture in the hybrid process

The ratio between inlet mass flowrates of solvent and gas in the absorption column (L/G ratio), is regarded as a reference parameter for the required solvent in a typical absorption process. In the

benchmark amine absorption process, the optima of required solvent per ton CO_2 capture are estimated at 27.8 and 22 m^3/ton CO_2 when 30 and 40 wt.% MEA solutions are exploited [121]. Then, the solvent regeneration heat is found to be 3.29 and 3.01 MJ/kg CO_2, respectively. In comparison, the L/G ratio of the enzymatic-absorption process is almost 50% higher than that of the MEA process. This would raise concern about the tremendous amount of water which would be required in a 600 MW_e power plant with a standalone absorption CO_2 capture unit. Undoubtedly, the enzymatic-absorption process would not be in preference to be installed in regions lacking water resources. Figure 4.2 shows the relation between the L/G ratio and total CO_2 capture rate for different CO_2 contents in the gas fed to the absorber (retentate). The leaner the CTB level, the lower the solvent flow needed to reach 90% CO_2 capture. Regardless of the CO_2 content removed in the membrane process, the level of the lean CTB might be varied from 10 to 40% in order to reach the total 90% CO_2 capture. This is attributed to the variation in CO_2 equilibrium pressure in a PC solvent with temperature (in this study the solvent temperature was set at 40^{o}C). Under these conditions, CO_2 is assumed to remain at solubility equilibrium even at the top of the absorption column. As shown in Figure 4.2, when 30, 50, and 70% of the CO_2 in the flue-gas feed are initially captured in the membrane unit, the L/G ratio reaches the minimum values of 1.8, 3.1, and 4.1 (*kg solvent/kg gas*) at 10% lean CTB, respectively. However, this lean CTB value of 10% results in maximizing the energy of CO_2 regeneration in the desorption unit. The L/G ratio in the optimized standalone enzymatic-absorption process was estimated at 7.1 at a lean CTB level of 23.5% [218]. In the hybrid process, the L/G ratio drops significantly to 2.5, 4, and 5.2 for those values of the CO_2 capture while using the same level (23.5%) of lean CTB (not shown in Figure 4.2). The reduction of the L/G ratio aims at decreasing the volume of enzyme in the PC solvent by reducing the PC solvent flowrate. Thus, the results displayed in Figure 4.2 allow estimating the trade-off conditions for a low L/G ratio (low cost of enzyme) and the energy expense in the desorption process.

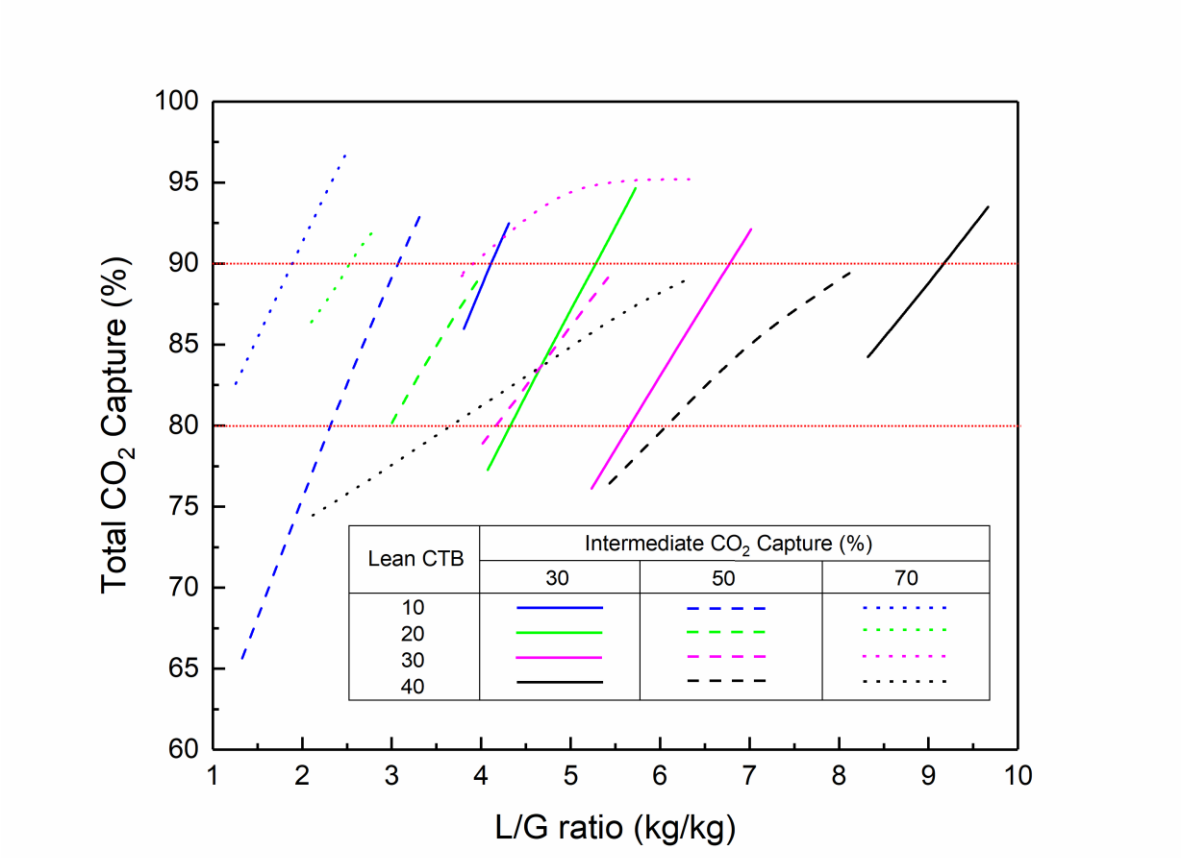

Figure 4.2 Relation between the L/G ratio in the absorber and total CO_2 capture rate in the hybrid process.

Figure 4.3 also shows the variations in total CO_2 capture as a function of L/G ratio at 30% intermediate CO_2 capture and a comparison of the hybrid process with the standalone enzymatic-absorption process. The latter results are established in ref. [218]. The lower the lean CTB, the higher the shift in CTB level is observed. Undoubtedly, using a solvent with a leaner CTB is more expedient as a lower circulation rate of the solvent is required to reach the same level of CO_2 capture. In addition, Figure 4.3 also represents the variations in rich CTB with L/G ratio for two values of the lean CTB index, 10 and 40% in both the hybrid and standalone absorption processes. An example of the comparison between these two processes is shown for 10% lean CTB. The standalone process requires L/G ratio = 5.5 resulting a rich CTB value of 0.65. At the same lean CTB value, the hybrid process with 30% intermediate CO_2 capture then requires L/G = 4.0 while the rich CTB is reduced to 0.60. The lower change between the lean and rich CTBs would result in reducing the required energy

of CO_2 desorption. The lowest rich CTB is also found to be 52% for the lean CTB 10% when 70% of the CO_2 is removed in the membrane unit.

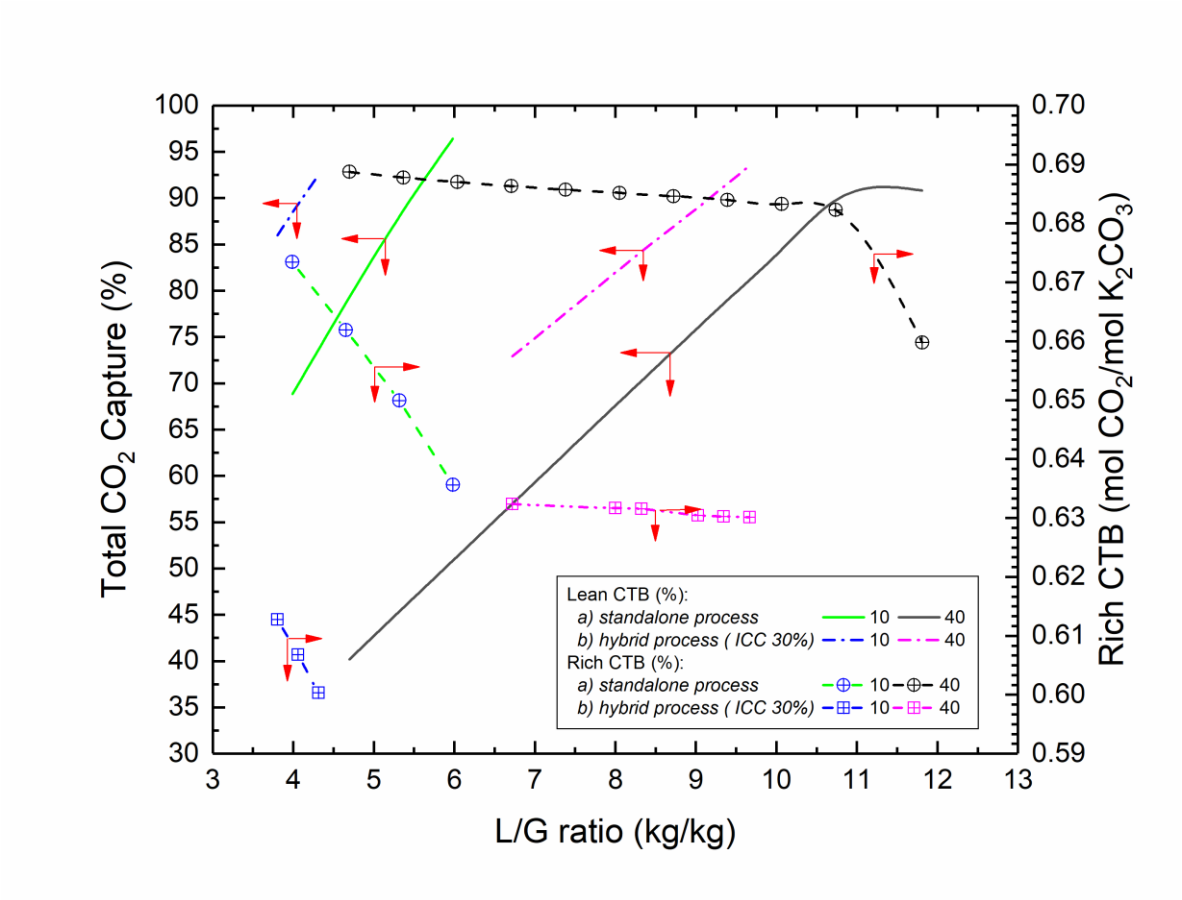

Figure 4.3 Variation of the lean and rich CTB indexes at different L/G ratio in the single and hybrid enzymatic-absorption processes.

4.5.3 Hybrid process energy analysis

Figure 4.4 illustrates to what extent the lean CTB index and intermediate CO_2 capture (ICC) in the hybrid process affect the heat of CO_2 recovery in the stripper column. The total heat requirement shows a steady decline as a higher fraction of CO_2 is removed by the membrane separation unit. In all cases, the heat of vaporization is maximum at the lower value of the lean CTB (10%) which corresponds to the maximum variation between lean and rich CTB. The same downward trend is observed with the other two heat consumptions. At constant intermediate CO_2 capture, the sensible heat varies in opposite trend compared to the heat of vaporization. In comparison, the heat of desorption depends only on ICC and not on lean CTB value. As a result, the optimal heat consumption

is observed at 20 to 30% lean CTB at all ICC values. The main advantage of using PC solvent instead of amine solutions is the lower heat required for the CO_2 desorption process. In comparison to amine-based solvents, the split of energy for the desorption process reveals that the CO_2 desorption and sensible heats consume around 46 and 15% of the total required energy, respectively [170]. In the case of the PC solvent, the heat of CO_2 recovery which is almost equally divided between the vaporization and sensible heats is found to be optimum for the CTB values between 20 and 30% regardless of intermediate CO_2 capture rate in the hybrid process.

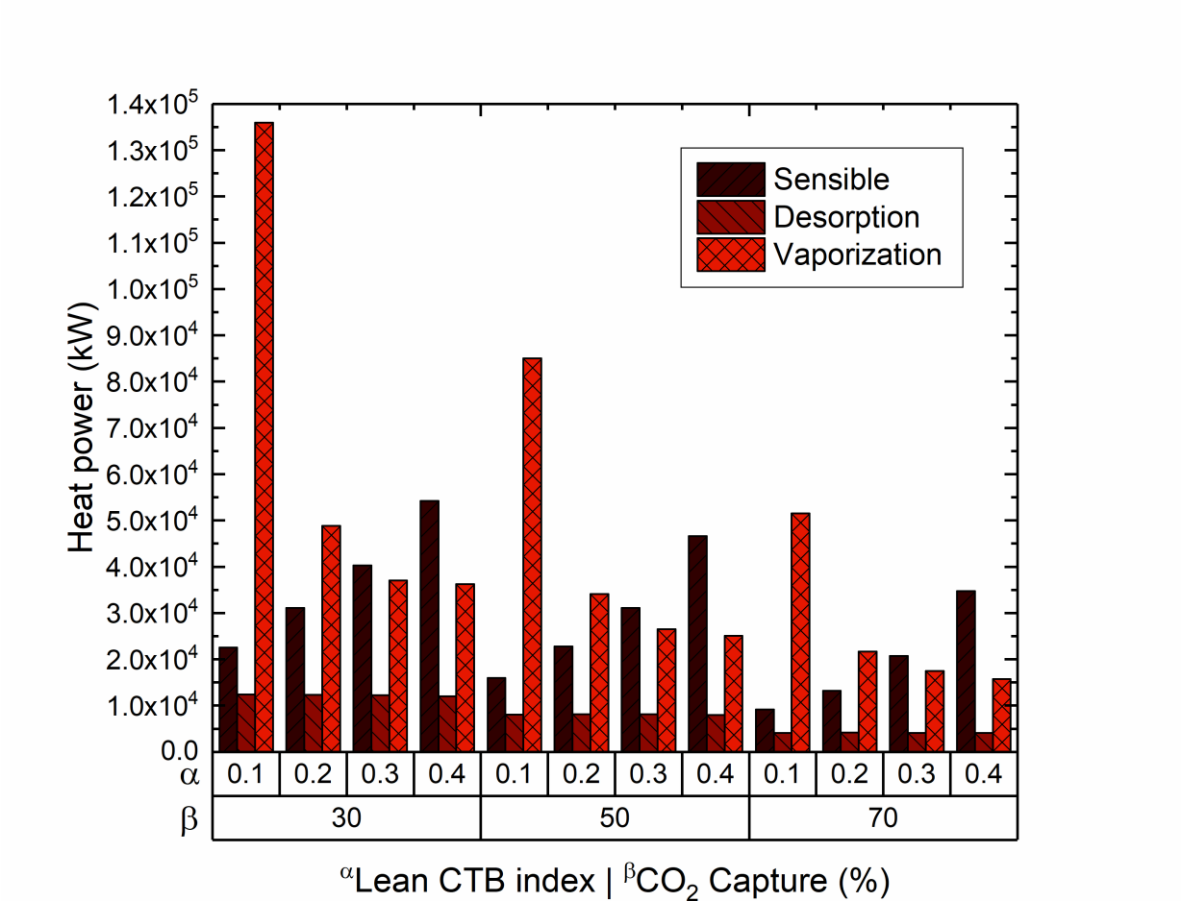

Figure 4.4 Effects of lean CTB index and ICC in the hybrid process on the heat of CO_2 recovery in the stripper column.

The majority of enzymes are very sensitive to temperature and their stability would decay at high temperature. It is therefore essential to adjust the stripper temperature by varying the vacuum pressure. In this case, the boil-up temperature in the reboiler can be diminished from 85 to 64°C through varying the pressure from 0.6 to 0.3 bar. On one hand, this temperature change contributes to decrease the energy penalty for the CO_2 desorption in the stripper by exploiting low quality steam. In comparison, in the MEA absorption process, the stripper temperature is set to about 120°C at a

pressure of 1.5 bar which is deemed to be less efficient due to steam extraction from high pressure (HP) turbines.

Figure 4.5 presents the effects of vacuum pressure on the electricity loss in the CO_2 desorption process. The lower the vacuum pressure, the lower the electricity loss is required to strip off CO_2 in the desorption column. As shown, the lowest energy penalty is found to be approximately 15 MW over the lean CTB range from 20 to 27% for an intermediate CO_2 capture of 70%. Under the same conditions, the energy penalty rises by 34% when half of the CO_2 in the flue-gas is removed by the membrane separation unit. The optimization results also show that the rate of CO_2 capture below 50% might not be appealing in the hybrid process as barely 16 MW can be saved with respect to the required energy in the optimum standalone enzymatic-absorption process [218]. It should be noted that the use of vacuum systems also incurs extra penalty to the whole energy requirement for the CO_2 desorption.

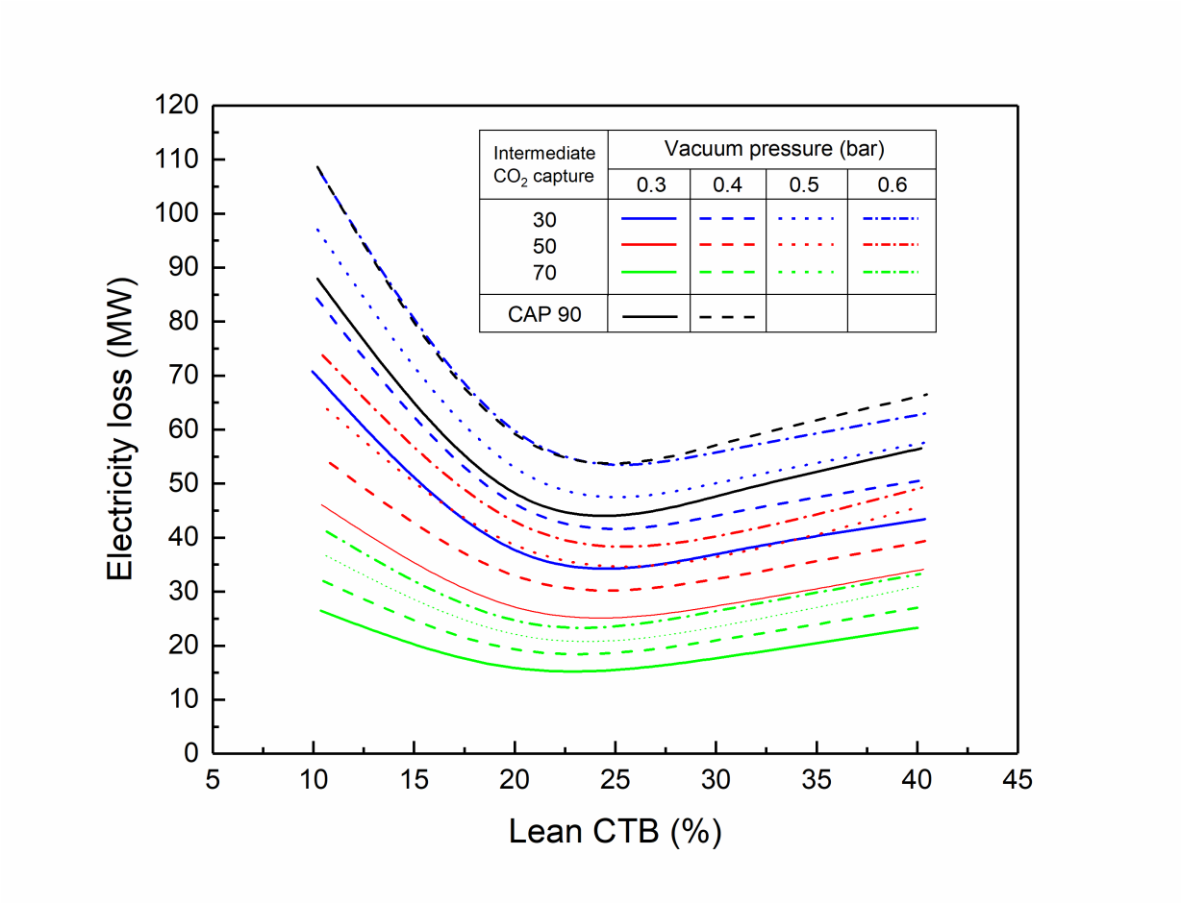

Figure 4.5 Effects of vacuum pressure in the stripper and ICC in the hybrid process on electricity loss for a 600 MW_e power plant.

Figure 4.6 shows the electricity lost by the vacuum systems at different pressure setpoints of the stripper in the hybrid process. The power requirement of the vacuum pumps is mainly dependent on the ratio between charge and discharge pressures as well as the flow of inlet vapor. Thus, there is a decreasing trend in the power consumption regardless of the extent of intermediate CO_2 capture. In the case of a 50% CO_2 capture, the power required for the vacuum pumps changes from 12.3 and 7.5 MW in the hybrid process which is equivalent to half of the electricity loss in the optimum standalone enzymatic-absorption process. A higher flowrate of stripping vapor is required in the desorption column at the same lean CTB. Referring to our previous study about the optimization of the standalone membrane process [218], its integration to the enzymatic-absorption process, on the one hand, results in energy consumption of 23, 41, and 63 MW when the rate of intermediate CO_2 capture is varied from 30, 50 to 70%, respectively. On the other hand, this change would result in the reduction of the operation cost of vacuum systems as well as their size and capital costs. Moreover, it has a substantial effect on the circulation rate of solvent between absorption and desorption columns (Figure 4.7). This allows decreasing the energy requirement for the lean and rich solvent pumps.

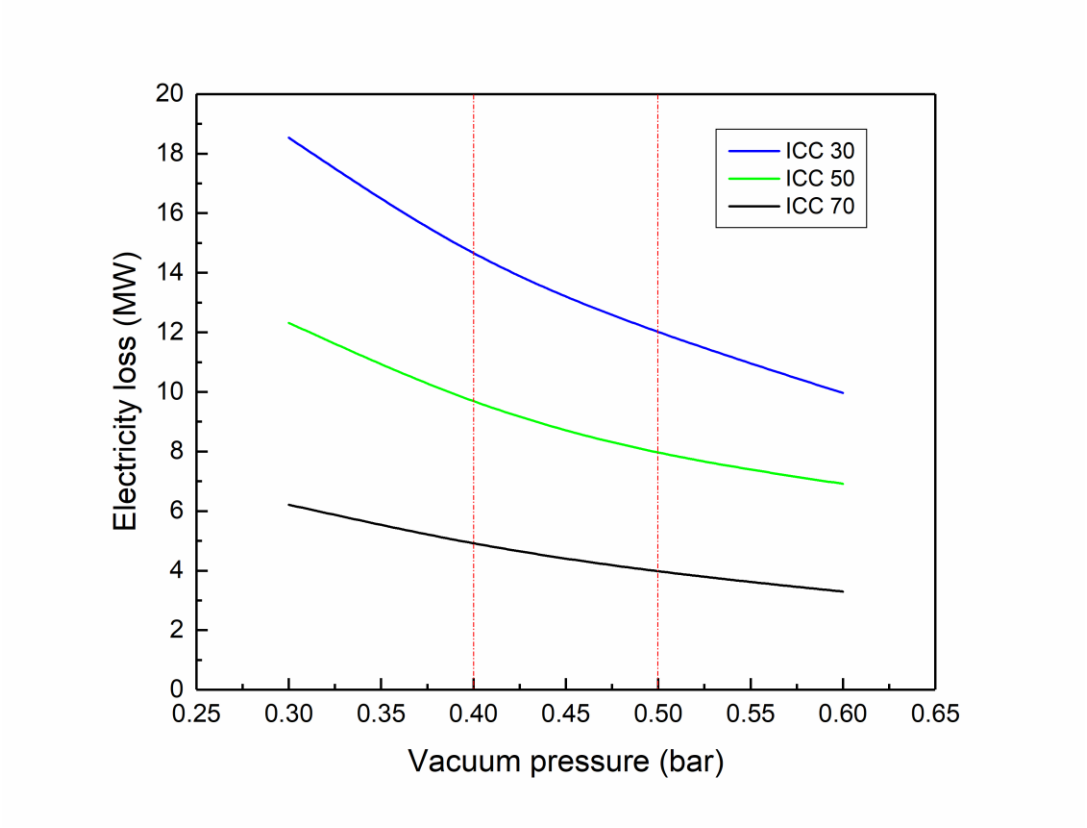

Figure 4.6 Electricity loss by the vacuum systems at different pressure setpoints in the enzymatic-absorption process.

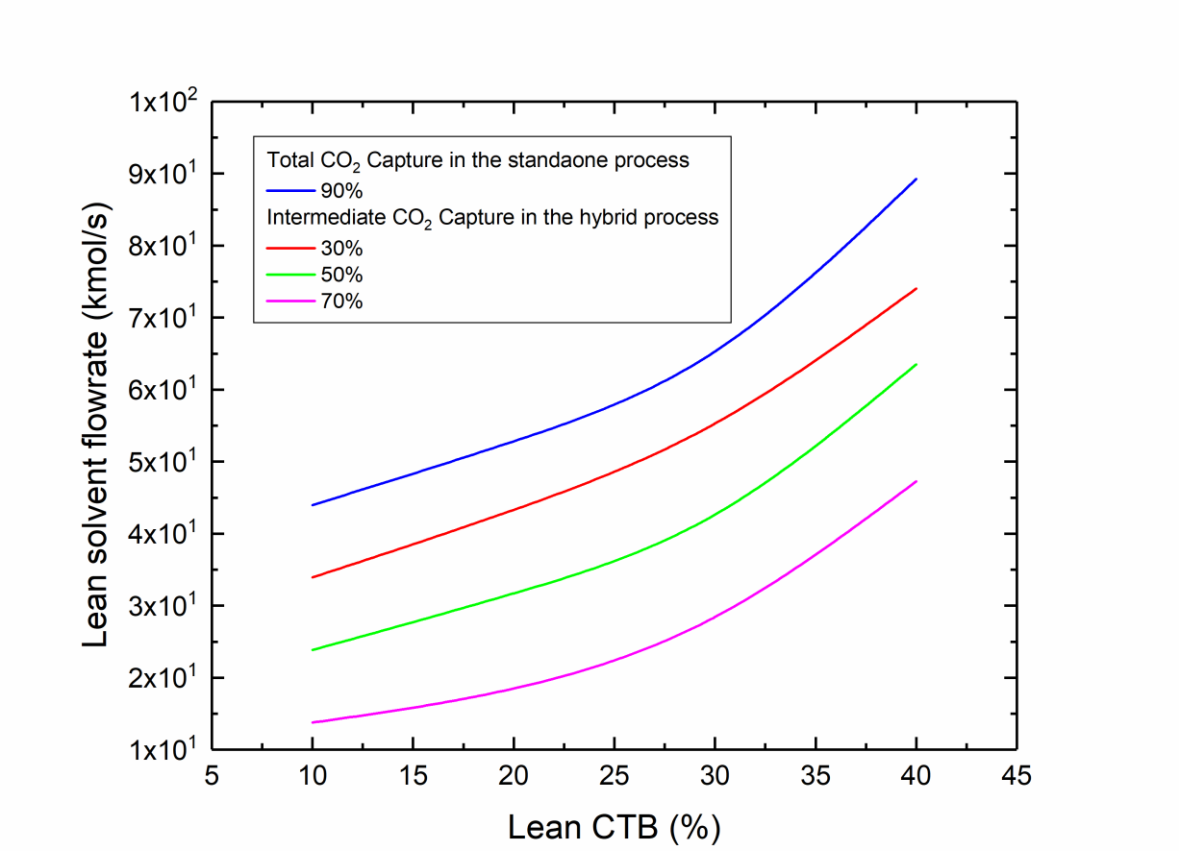

Figure 4.7 Comparison between the circulation rate of solvent between absorption and desorption in the standalone enzymatic-absorption and hybrid processes.

4.5.4 Separation efficiency of the hybrid process

The hybrid process might offer different promising solutions to alleviate technical and economic issues consistently limiting both membrane-based and enzymatic-absorption processes. Referring to our previous study [218], a two-stage membrane process is proposed to treat the flue-gas emitted from a 600 MW_e power plant. Despite the fact that the development of commercial membranes is still challenging, another model based on realistic process data is then required to more accurately predict membrane lifetime for a typical gas separation process. The simulation results reveal that at least 1.5 Mm^2 of Polaris membrane is necessary to reach 90% CO_2 capture using simultaneously compression and evacuation systems. As the ideal span of membrane life is usually deemed to be 5 years, the operation and maintenance costs (usually calculated over 25 years) would dramatically increase at the current high rate of 50$/$m^2$ membrane. It is also imperative to note that any deterioration in membrane permselectivity over operation time directly impacts on product specifications. The moisture content of flue-gas also affects operational and economic aspects of the gas treatment

process. Water has a higher permeance than CO_2 in the feed gas and hence higher separation area is demanded for the same degree of separation. Thus, most of the equipment needs to be resistant to such content of moisture resulting in higher capital cost. Under this scenario, the outlook for the commercialization of membrane technology for flue-gas separation seems to be far away from other counterparts. Similarly, absorption technology using catalyzed PC solvent has shown promising potential to be exploited in flue-gas processing. Undoubtedly, the main drawback of this separation method is the high circulation rate of PC solvent to remove 90% of CO_2 from the flue-gas compared to amine-based absorption processes. In addition, the enzyme stability under realistic operating conditions is extremely important as enzyme make-up at a rate of 480$/kg looks costly. The process of CO_2 desorption at a vacuum pressure of 0.6 bar could be realized at 84°C at which the enzyme is more prone to decay. Hence, the further improvement of the standalone enzymatic-absorption technology is highly contingent on the production of more stable enzymes at reasonable price. Comparatively, it is also needed to decrease the PC solvent flowrate for a given fraction of CO_2 removal.

Figure 4.8 shows the relation between the extent of CO_2 capture and electricity loss for a standalone two-stage membrane unit integrated into a 600 MW_e power plant. The trend is divided in two different sections. Initially, the electricity loss steadily increases to 72 MW when the CO_2 capture varies from 10 to 75% in the presence of a turboexpander. A steeper rising trend is then depicted over the higher capture rate so that the energy loss peaks at 162 MW for a CO_2 capture of 95%. This analysis clearly reveals that the membrane technology becomes very expensive in energy loss as the higher values of CO_2 capture are reached, even in the presence of a turboexpander. As shown in Figure 4.8, about half of the energy used for the flue-gas separation could be recovered when the extent of CO_2 capture ranges from 10 to 70% while using a turboexpander. Above all, the exploitation of an Energy Recovery Unit (ERU) including turboexpanders might contribute to more efficiently integrate a membrane process with other CO_2 separation technologies.

In a typical CO_2 absorption process, a Low Compression Unit (LCU) including parallel blowers is used to conduct flue-gas emitted in a power plant and then inject it into an absorption column. According to the simulation results of our previous work [218], the LCU power consumption is estimated to be around 8 to 10 MW depending on pressure drop in absorption columns, which is approximately 8% of the total energy loss of a CO_2 capture unit integrated into a 600 MW_e power plant. In a hybrid process, it is then feasible to replace the LCU with an ERU in order to simultaneously reduce electricity loss and capital cost of equipment (including blowers and piping systems). Thus, merging the two separation methods technically might be more attractive at an

intermediate CO_2 capture rate below 70%. Under this scenario, the electricity loss associated to the partial CO_2 capture might vary from 10 to 50 MW in the hybrid process.

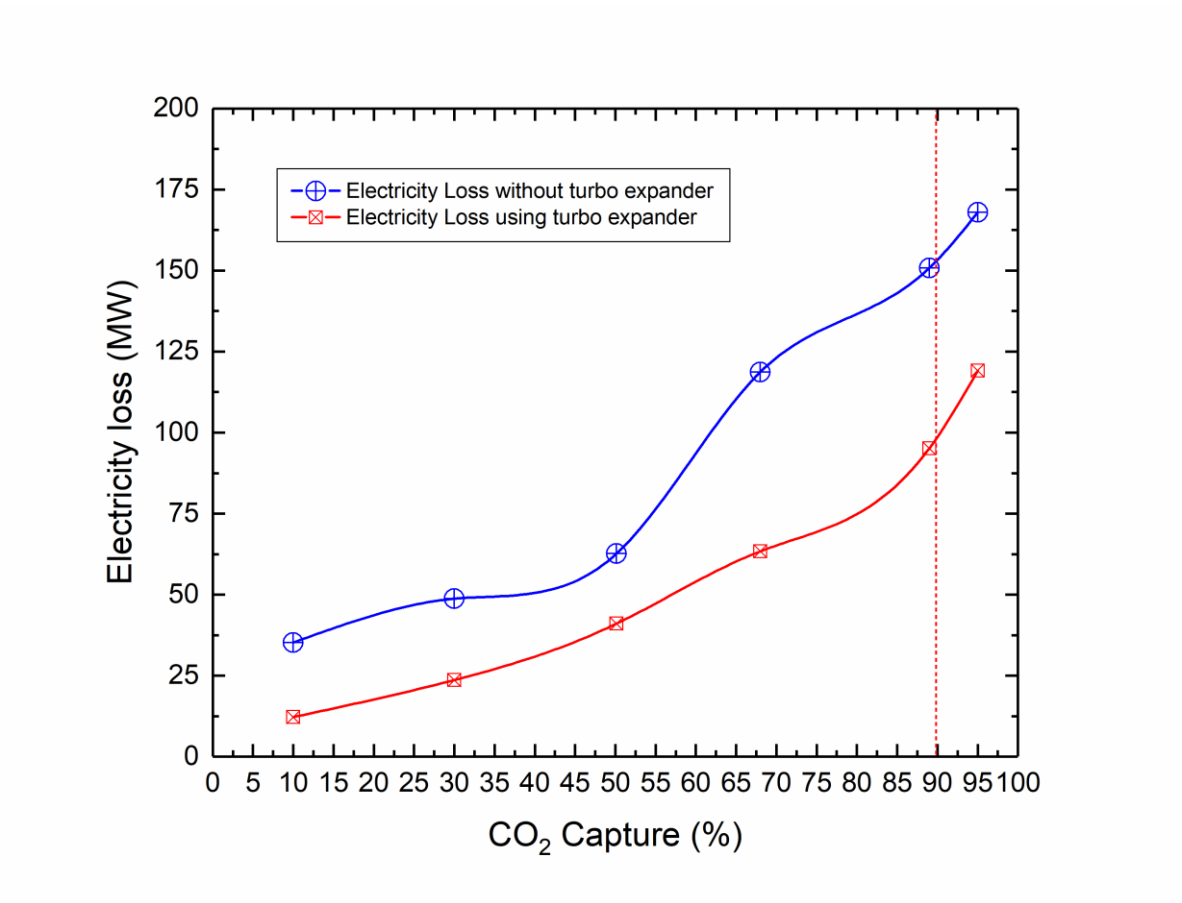

Figure 4.8 Relation between the extent of CO_2 capture and electricity loss for a standalone two-stage membrane unit integrated into a 600 MW_e power plant (Calculated from results in [218]).

Figure 4.9 presents the overall electricity loss of the hybrid process including CO_2 compression and storage (CCS) energy consumption under different operating and design conditions. An optimum value for the lean CTB index might be varied from 20 to 30% to hit a low point of electricity loss for a target of intermediate CO_2 capture ranging from 30 to 70%. As discussed in the previous sections, the electricity loss for the CO_2 regeneration generally tends to be decreased when the stripping pressure is reduced from 0.6 to 0.3 bar. At a pressure of 0.3 bar (Figure 4.9a), the electricity loss of the standalone process for a total CO_2 capture of 90% is found to be 126.44 MW at the lean CTB index range of 22.5 to 25.5%. It is then ascertained that the energy loss in the proposed hybrid process exploiting the ERU might be competitive with the standalone enzymatic-absorption process. As such,

the total electricity loss is reduced to 124.82 MW at 0.3 bar when 30% of CO_2 in the flue-gas (ICC 30%) is removed by the membrane unit. Similarly, the optimum value of the energy loss is found to be 125.45 MW for 50% ICC at 0.3 bar when the CTB index ranges from 20 to 25%. As shown, both curves associated with the hybrid cases having 30 and 50% ICC overlap each other at the same optimum ranges of the CTB index. The reason is that the energy saved through the membrane unit offsets the energy consumed by the enzymatic-absorption unit in the hybrid process including CO_2 recovery, vacuum systems, solvent circulation pumps, and condenser pumps. More interestingly, the curve of the energy loss for all cases of the hybrid process is below that those of the standalone enzymatic-absorption process when a leaner solvent (CTB index<20%) is circulated between the absorption and desorption columns. As shown in Figure 4.9a, this lean CTB zone of the diagram represents an optimum region in which the hybrid process would be recommended. As shown, the total energy loss is estimated at below 145 MW (24% of total electricity generated in the power plant) for 50 and 70% ICCs when the leanest CTB (10%) is chosen. However, this results in an increase in the total energy loss by 15 and 10%, respectively, compared to the optimum value of the energy loss in the standalone enzymatic-absorption process (126.44 MW). Despite the energy saving for the CO_2 recovery, another advantage of the hybrid configuration is to significantly reduce the solvent flowrate by 44, and 68% for the ICCs of 50, and 70% respectively, compared to that in the standalone reference process (shown in Figure 4.7). On the contrary, there is no significant advantage in the energy saving for the intermediate CO_2 capture of 30% when the CTB index is below 20%. This indicates that such reduction of the CO_2 mole fraction in the intermediate feed which is around 11%, would still require a high amount of lean solvent (CTB of 10 to 20%) and hence a high heat of CO_2 recovery at a constant stripper pressure of 0.3 bar. In comparison, the CO_2 mole fraction in the intermediate feed reduces to 8 and 5.3% for 50 and 70% ICCs, respectively. This also reveals that such a standalone enzymatic process might be more effective when a feed gas contains CO_2 mole fraction below 8% or a lower CO_2 capture is demanded above this CO_2 concentration. Furthermore, in comparison to the other cases, at the higher vacuum pressure shown in Figure 4.9, 70% CO_2 removal through the membrane unit appears appealing, providing a solvent with a lean CTB index below 20% is chosen for the enzymatic-absorption process in the hybrid system.

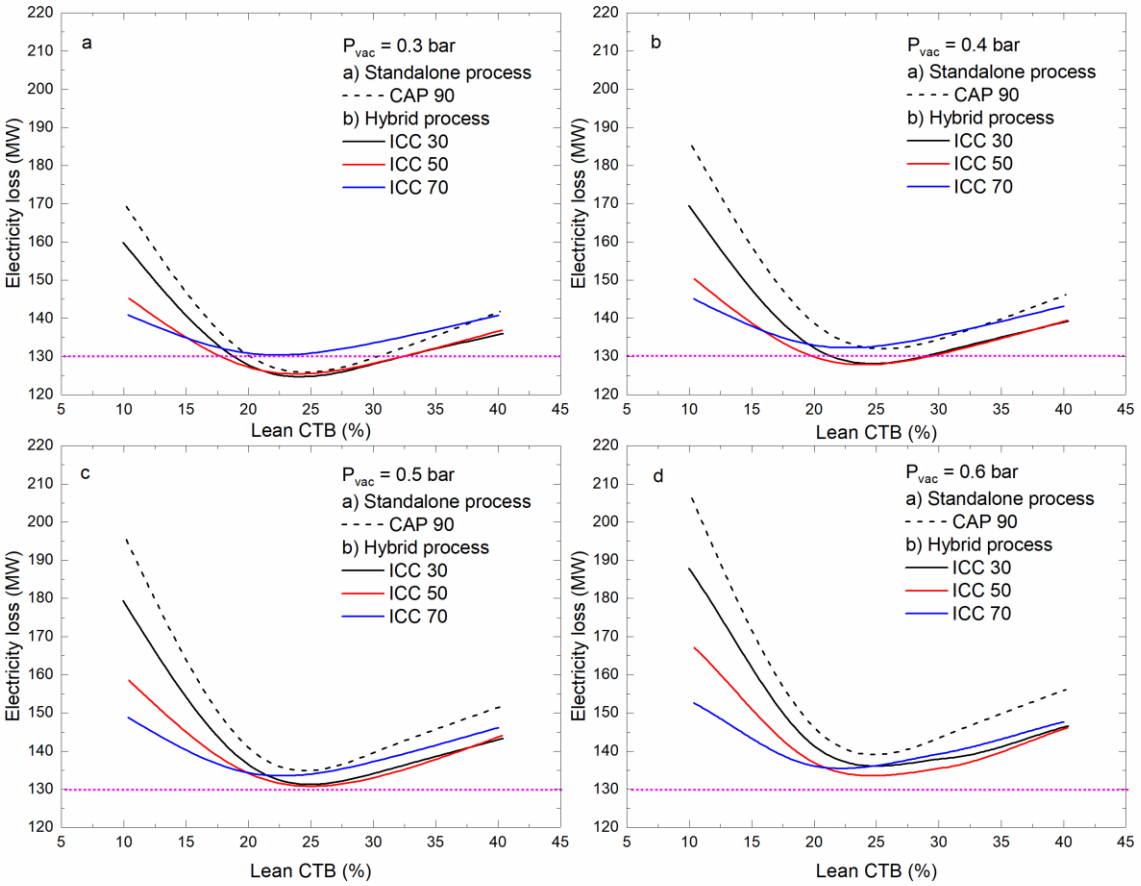

Figure 4.9 Overall electricity loss of the hybrid process at different operating and design conditions.

As shown in Figure 4.9, a rising trend in the electricity loss can be observed by increasing the vacuum pressure from 0.3 to 0.6 bar for the hybrid and standalone reference processes. In this case, the optimal values of the electricity loss are estimated at 128, 132, and 135 MW for the vacuum pressures of 0.4, 0.5, and 0.6 bar, respectively. As shown, the use of the hybrid process seems to be more effective when the lean CTB index is set to below 20%. However, this process also outperforms the standalone reference process in most cases, so that the energy loss is also lower by more than 10% on average at high CTB index values (>20%).

4.5.5 Cost analysis of CO_2 capture

As an example of the detailed cost calculations, a summary of techno-economic analysis of the hybrid process in the case of an intermediate CO_2 capture of 30% at 0.3 bar is given in Table 4.2. The cost of CO_2 capture varies depending on the separation technology chosen for retrofitting a power plant. The TAC which is the sum of CAPEX and OPEX could be regarded as a techno-economic factor (TEF) for the technology adoption. Undoubtedly, addition of a CO_2 capture unit to a power plant is not technically and economically attractive as not only it incurs extra expenditure to investment cost but also consumes a part of the electricity generated. This raises the question about choosing a criterion for selection of an optimum CO_2 capture process. It is therefore needed to find the impact of both CAPEX and OPEX on CO_2 capture cost while comparing different flue-gas separation technologies.

Table 4.2 Summary of techno-economic analysis of CO_2 capture using the hybrid process (ICC 30%, 0.3 bar).

Parameters	Cost	Unit
Absorber vessel	10.79	*M$*
Absorber packing	18.73	*M$*
Stripper vessel	15.03	*M$*
Stripper packing	27.93	*M$*
Lean solvent tank	0.83	*M$*
Lean circulation pump	3.62	*M$*
Rich circulation pump	4.35	*M$*
Cross heat exchangers	1.56	*M$*
Lean solvent cooler	1.84	*M$*
Reboiler	5.94	*M$*
Stripper condenser	1.99	*M$*
Water pump	5.82	*M$*
Multistage compression	17.26	*M$*
Multistage intercooler	4.48	*M$*
Vacuum blower	29.44	*M$*
Vacuum blower intercooler	1.83	*M$*
Total capital cost	151.46	*M$*
CAPEX		
Absorption process	23.44	*M$*
Membrane process	39.56	*M$*
Raw material and utility cost	44.41	*M$*
Cooling water	0.003	*M$*
PC solvent	1.53	*M$*
Enzyme	3.87	*M$*
Inhibitor	0.15	*M$*
Electricity	38.86	*M$*
OPEX		
Absorption process	52.19	*M$*
Membrane process	21.12	*M$*
TAC		
Total annual cost	139.31	*M$*
ENERGY CONSUMPTION		
Solvent circulation pump	2.96	*MW*
Steam extraction	34.80	*MW*
Cooling water pump	1.14	*MW*
Multistage CO_2 compression	43.61	*MW*
Vacuum systems	18.67	*MW*
Membrane unit	23.64	*MW*

Table 4.3 presents a summary of techno-economic analysis of standalone membrane and enzymatic-absorption processes, and hybrid systems to capture 90% of CO_2 in flue-gas of a 600 MW_e power plant. The highest TAC (191 M$) belongs to the membrane process, which is approximately 82 and 38% higher than those in enzymatic-absorption and hybrid processes, respectively. Moreover, for the membrane process the cost repartition shows that 53% of the TAC is spent on the CAPEX which is on average 50% higher compared to the other processes. In comparison, the OPEX is also the highest and the overall CO_2 capture cost is estimated at 47.34$/ton CO_2. The results reveal that comparatively the standalone absorption is economically attractive as resulting in the lowest capture cost around 27-28$/ton CO_2. The results show that the energy penalty under two different stripping pressures at 0.3 and 0.4 bar are only 9.5 and 4%, respectively, lower than that in the standalone membrane process. As reported, the hybrid process is reducing the TAC by 37% including approximately 38 and 14% reduction in CAPEX and OPEX compared to the standalone membrane process. Furthermore, the required solvent in the hybrid process is decreased to 13-19 m^3/tons CO_2 that is 50% lower than that in to the standalone enzymatic-absorption process. Overall, the best performance of the hybrid process is observed when the intermediate CO_2 capture is set to 30% and the stripper pressure is set to 0.3 bar. In this case, the capture cost is found to be 36.52$/ton CO_2 at the expense of an electricity loss of 124.82 MW.

Table 4.3 Techno-economic results of hybrid, standalone membrane and enzymatic-absorption processes (CAP 90%).

Parameters	**Membrane**	**Absorption Process**		**Hybrid Process**	
Intermediate CO_2 capture (*%*)	-	-	-	30	50
Stripper pressure (*bar*)	-	0.3	0.4	0.3	0.4
Stripper temperature ($^{\circ}C$)	-	67	74	67	74
CAPEX (*M$*)	102.2	40.08	40.41	63.00	61.51
OPEX (*M$*)	88.8	63.51	65.82	76.31	76.31
Total annual cost (*M$*)	191.0	103.60	106.23	139.31	137.82
CO_2 capture cost (*$/ton CO_2*)	47.34	27.16	27.85	36.52	36.13
Electricity loss (*MW*)	95.14	82.83	89.13	81.22	85.16
Electricity loss including CO_2	138.14	126.44	132.74	124.82	128.76
Required Solvent (*m^3/ton CO_2*)	-	33.4	33.6	19	13

4.6 Conclusion

Fossil-fuels are still dominating the world energy markets. Our dependency on oil and gas is increasing while no alternative energy source properly meets the global demands. Climate change is ubiquitous and consensually attributed to the high content of GHGs in the atmosphere. One of the main CO_2 producers is the fossil-fuel power plants which presently supply a large portion of the

global energy. To combat the climate change, different CO_2 capture technologies might be retrofitted to power plants to remove CO_2 from flue-gas, and then transport it to storage tanks or using it for other applications. Compared to other separation methods, an amine-based absorption process is currently the most mature and accepted technology for flue-gas treatment. This method is however costly, energy-intensive, and less eco-friendly. It is of high interest to introduce other technologies which are technically and environmentally more attractive than the amine-absorption process. The membrane-based gas separation process has a higher investment cost, and research on fabrication of commercial membrane products is still in progress. An enzymatic-absorption process appears to be more feasible for flue-gas separation. However, the energy penalty as the result of retrofitting of a CO_2 capture unit is still high. Herein, a hybrid system, including membrane and enzymatic-absorption processes, is investigated for removing CO_2 from flue-gas of a 600 MW_e power plant.

The simulation results revealed that the hybrid process might be more efficient as bulk CO_2 removal by 70% from flue-gas is carried out in the membrane unit. Thus, the hybrid process is initialized for different intermediate CO_2 capture including 30, 50, and 70% between membrane and enzymatic-absorption processes. At these ICC values, this scenario initially allowed recovering about half of the energy used for CO_2 capture in the membrane unit using a turboexpander. Then, the flue-gas more depleted in CO_2 could directly be injected to the absorption unit without being compressed through parallel blowers. This minor modification in the process layout aimed at reducing up to 10% of total energy loss and also around 14 M$ required for flue-gas compression compared to the reference standalone enzymatic-absorption process. The lower the CO_2 content in the feed gas, the lower the flowrate of solvent is required to circulate between the absorption and desorption units depending on the values of the lean CTB index. In comparison to the reference standalone process, the L/G ratio is decreased by 26, 43, and 65% at extents of intermediate CO_2 capture of 30, 50, and 70% respectively, for a lean CTB index of 23.5% in the hybrid process. In all cases, the heat of CO_2 recovery decreased as a lower stripping vapor flowrate is required in the desorption column to strip off the remainder CO_2. Thus, the heat of vaporization dropped by 50% using a solvent with a lean CTB index of 10%. Overall, the optimal value of the lean CTB index is found to be in a range of 20 to 30% at which the energy penalty is minimized. It is also revealed that the hybrid process is solely efficient for the range of the partial CO_2 capture of 50 and 70% thereby the electricity loss of CO_2 desorption is reduced by 15 and 27 MW, respectively. As shown in Figure 4.6, this also allowed reducing the required energy for the vacuum systems to 4.9 and 9.7 MW at stripper pressure of 0.4 bar which are 75.5 and 51.5% lower than in the reference standalone process. Above all, the lowest electricity loss for the hybrid process is estimated at 124.82 MW at an intermediate CO_2 capture of 30% and a stripper vacuum

pressure of 0.3 bar. In comparison, the hybrid process consumed a lower fraction of energy output of the power plant while the lean CTB value is set to below 20%. The lowest energy loss was then found to be 128, 132, and 135 MW when the stripping pressure is fixed at 0.4, 0.5, and 0.6, respectively (Figure 4.9).

The results of techno-economic analysis revealed that the CAPEX of the hybrid system is approximately 64% lower, and 35% higher than those in the standalone membrane and enzymatic-absorption processes, respectively. Then, the OPEX is also estimated at around 76 M$ that is 15% higher than in the standalone enzymatic-absorption process. In comparison, the highest CAPEX and OPEX were those of the standalone membrane process, hence resulting in a costly CO_2 capture process (47.34$/ton CO_2). More interestingly, the hybrid system allowed reducing the total electricity loss to 124.82 MW which is 1.2 and 6% lower compared to those in the standalone enzymatic-absorption processes operating at vacuum pressures of 0.3 and 0.4 bar, respectively. In this case, the capture cost is estimated at 36$/ton CO_2 which is around 23% higher than in the standalone enzymatic-absorption process (27-28$/ton CO_2). In summary, the suggested hybrid process exhibited a positive contribution in both technical and economic aspects. The main approach was to share CO_2 capture between two different processes in series, resulting in more effective saving of electricity for flue-gas treatment. This study also revealed the pros and cons of the hybrid process in which the membrane unit is used for a significant CO_2 removal and the enzymatic-absorption unit pushes CO_2 capture rate to a desired level. Overall, purchased cost reduction of membrane and enzyme, improvement of membrane permselectivity at a retentate pressure below 1.5 bar, and enhancement of catalyzed PC-solution reaction rate might result in further reducing the CO_2 capture cost.

Nomenclature

CA	carbonic anhydrase
CAPEX	capital expenditure
CAP	capture rate (%)
CCC	cryogenic carbon capture
CCS	CO_2 compression and storage
COP	conferences of the parties
CSI	CO_2 Solutions Inc
CTB	carbonate to bicarbonate conversion
DEA	diethanolamine
DOE	department of energy
ENRTL	electrolyte non-random two-liquid
ERU	energy recovery unit
FGD	flue-gas desulfurization

GHG	greenhouse gas
GPS	gas pressurized stripping
HP	high pressure
ICC	intermediate CO_2 capture
k	reaction rate constant (*1/s*)
L	molar flowrate of liquid (*mol/s*)
LCU	low compression unit
LNG	liquified natural gas
MA	membrane-absorption
MDEA	methyldiethanolamine
MEA	monoethanolamine
MMMs	mixed matrix membranes
MOFs	metal organic frameworks
MTR	Membrane Technology & Research
OPEX	operation expenditure
P	pressure (*Pa*)
PA	Paris Agreement
PC	potassium carbonate
PCC	post-conversion CO_2 capture
PSA	pressure swing adsorption
r	rate of reaction (*1/s*)
RK	Redlich-Kwong
T	temperature (*K*)
TAC	total annual cost
TEF	techno-economic factor
TMA	total membrane area (m^2)
TSA	temperature swing adsorption
VLE	vapor-liquid equilibrium
VSA	vacuum swing adsorption

Conclusion

The fossil fuels are currently dominating global energy markets. Unfortunately, this dependency has increased the content of greenhouse gases (GHGs), especially CO_2 in the atmosphere resulting in critical environmental issues. To deal with such emissions, this PhD thesis initially aimed at evaluating two promising gas separation methods including membrane and enzymatic-absorption technologies to thoroughly demonstrate their potentials and limitations while used as CO_2 capture units in different chemical and industrial projects. This research study then introduced a novel hybrid system to benefit from the potentials of the individual above-mentioned separation methods. The CO_2 capture is somehow shared between two processes to result in the lowest overall energy and cost penalties. A summary of the main findings through this research study can be presented as follows:

1. A new optimization approach was proposed for CO_2 removal from different industrial emitters using a membrane-based separation process. The optimization technique which embeds all possible configurations of hollow fiber membrane modules in a superstructure network allowed finding an optimized layout process at minimum annual gas separation cost. Then, a two-stage process was found to be the most profitable layout to upgrade biogas for different CO_2 contents ranging from 10 to 40% in feed when a membrane with a CO_2/CH_4 selectivity of 33.2 and a CO_2 permeance of 86.3 GPU was used. A techno-economic analysis revealed that the CO_2 capture cost was highly dependent on the rate of CH_4 recovery. The membrane area had a determinant role in the optimization model when a low CH_4 recovery of 90% was required. Conversely, the feed pressure was maximized to supply sufficient driving force to reach a CH_4 recovery higher than 95%.

2. The optimization model was later employed to set the required module number in the separation process. It was revealed that the use of smaller modules was more realistic as the packing fraction was highly decreased by increasing the module length (<50%) whereas the use of current modules with high packing fraction (>90%) led to drastically increased weight and footprint of a separation package. This versatile model was then used to show the effect of a typical membrane characteristics on the CO_2 capture cost. The result showed that membrane modification technique should be performed in a way that CO_2 permeance was increased at constant CH_4 permeance resulting in a 15% reduction of the gas separation cost.

It was finally revealed that a reduction of the membrane purchase cost from 50 to 25 $\$/m^2$ resulted in decreasing the optimized feed pressure regardless of CO_2/CH_4 selectivity. The lower membrane purchase cost had a moderate impact on the gas separation cost, but the optimized feed pressure significantly decreased with membrane cost.

3. A techno-economic analysis was made to evaluate the separation performance of membrane and enzymatic-absorption technologies using the CO_2 capture unit in a 600 MW_e power plant. Two optimization approaches were suggested to determine the most efficient process under the same operating conditions. Initially, a two-stage membrane process was introduced as the optimized layout in which the required membrane area and feed pressure were set to $1.5x10^6$ m^2 and 2.7 bar, respectively. Overall, this process was to be economically and technically competitive to the currently-used separation methods as the electricity loss was decreased to 95 MW for a CO_2 capture of 90% (15% of total power plant output). Above all, it was revealed that the membrane process was more suitable for bulk removal of CO_2 up to 50% as the total annual cost and energy consumption were cut down by half of those for a CO_2 capture of 90%.

4. In the case of the enzymatic-absorption process, the optimization results showed that an optimum region was observed while the desorption process was performed over a range of vacuum pressure (0.3-0.6 bar). As a general rule, the leaner the CTB index, the higher the overall energy penalty and the lower the circulation of the PC solvent were expected. Under this scenario, the lowest heat of CO_2 regeneration at 0.4 bar was estimated to be 3.35 MJ/kg CO_2 as the lean CTB was set to 23.5%. In this case, the electricity loss for the desorption and vacuum systems reached 53.2 and 20.7 MW, respectively. The main limitation of this process was the high consumption of water compared to traditional MEA absorption process resulting in larger equipment size and more energy loss through solvent pumping. In comparison, the enzymatic-absorption process outperformed the membrane technology as both the TAC and electricity loss were found lower by 44 and 6.5%, respectively.

5. A hybrid system, including membrane and enzymatic-absorption processes, was introduced to remove CO_2 from flue-gas of a 600 MW_e power plant. At intermediate CO_2 capture

between 30 to 70%, the scenario of CO_2 partial capture in the hybrid process aimed at recovering about half of the energy lost for CO_2 capture in the membrane unit using a turboexpander. In this case, the flue-gas depleted in CO_2 was routed to the absorption unit without being compressed through parallel blowers. This modification in the hybrid process layout allowed decreasing by up to 10% the total energy loss and around 14 M$ pertaining to the flue-gas compression compared to the standalone enzymatic-absorption process. In comparison to the reference process, the L/G ratio was decreased by 26, 43, and 65% at extents of intermediate CO_2 capture of 30, 50, and 70% respectively, for a lean CTB index of 23.5% in the hybrid process. Moreover, the heat of CO_2 recovery also decreased since a lower stripping vapor flowrate was then required in the desorption column to strip off the remaining CO_2. Consequently, the optimal value of the lean CTB index was estimated to be in a range of 20 to 30% resulting in minimizing the energy penalty of the CO_2 capture unit. The simulation results showed that the hybrid process remained efficient over the range of the partial CO_2 capture of 50 and 70% at which the electricity loss of CO_2 desorption was reduced by 15 and 27 MW, respectively. Moreover, the required energy for the vacuum systems was reduced to 4.9 and 9.7 MW respectively, at the stripper pressure of 0.4 bar which were 75.5 and 51.5% lower than in the standalone enzymatic-absorption process. Above all, the lowest electricity loss for the hybrid process was estimated at 124.8 MW at an intermediate CO_2 capture of 30% and a stripper vacuum pressure of 0.3 bar. In comparison, the hybrid process consumed a lower fraction of energy output of the power plant while the lean CTB value was set below 20%. The lowest energy loss was also found to be 128, 132, and 135 MW when the stripping pressure was set at 0.4, 0.5, and 0.6 bar, respectively.

6. The techno-economic analysis showed that in the hybrid system, the CAPEX was approximately 64% lower, and 35% higher than those in the standalone membrane and enzymatic-absorption processes, respectively. The OPEX was also estimated at around 76 M$ that was 15% higher than in the standalone enzymatic-absorption process. In comparison, the highest CAPEX and OPEX were associated to the standalone membrane process resulting in a costly CO_2 capture process (47.34$/ton CO_2). In the case of energy analysis, the proposed hybrid system allowed reducing the total electricity loss to 124.8 MW which was 1.2 and 6% lower compared to those in the standalone enzymatic-absorption processes operating at vacuum pressures of 0.3 and 0.4 bar, respectively. In this case, the

capture cost was estimated at 36$/ton CO_2 which was around 23% higher than in the standalone enzymatic-absorption process (27-28$/ton CO_2). Herein, the feasibility of the hybrid system was measured by retrofitting it in a 600 MW_e power plant to capture CO_2 from the generated flue gas. All things considered, this process exhibited positive contributions in both technical and economic aspects. The techno-economic analysis highlighted the pros and cons of this hybrid process in which a membrane unit was used for a significant CO_2 removal and an enzymatic-absorption unit set CO_2 capture rate to a desired level.

Recommendations

This thesis clearly demonstrated the feasibility of the combination of two different gas separation technologies including membrane and enzymatic-absorption processes to form a hybrid system to capture CO_2 from a typical 600 MW_e power plant. One of the main outcomes was to present how two distinct optimization approaches have to be implemented in order to find the local optimum with respect to an objective function for each above-mentioned process, and ultimately resulting in minimizing the overall hybrid gas separation cost and energy penalty of the power plant. To complete this work, some recommendations are proposed to enhance the separation performance of the hybrid process as well as to effectively shed light on its integration in the market of gas separation technology.

In the membrane process, a sensitivity analysis could also be performed to reveal the effects of the membrane CO_2 permeance and CO_2/N_2 selectivity on not only overall gas separation cost but also process layout configuration. Under this scenario, one of the main criteria is to set the feed pressure below 1.5 bar while altering the above-mentioned characteristics of a typical membrane. It is of high interest that a robust model be initialized to predict a membrane lifetime during a typical separation process under different operating conditions and feed composition. Despite highlighting membrane separation performance in a realistic CO_2 capture project, this approach will conduct the current research on membrane modules utilization to an industrial-scale gas separation pathway through which a rapid commercialization of this technology will be more achievable. Similarly, in the enzymatic-absorption process, a sensitivity analysis could also be carried out to present the effects of enzyme type and concentration in the PC solvent on the CO_2 removal performance as well as OPEX and CAPEX in a realistic CO_2 separation project. As the purchase cost of enzyme constitutes a large part of the CAPEX, more research could be performed to enhance the reaction rate of the existing catalyzed PC-solution and hence resulting in more economical CO_2 capture.

Referring to the results of this study, a new hybrid process could be introduced by combining the above-mentioned processes to examine the separation performance of membrane technology. Instead of a multi-stage membrane process, only a single-stage membrane unit might be required to reach the desired CO_2 purity in the product stream, resulting in a reduction in both OPEX and CAPEX. Furthermore, a new comprehensive optimization model may be developed which encompasses a large network of process layouts including membrane and enzymatic-absorption processes. This approach considers not only the effects of all decision variables on gas separation cost and energy loss due to using a CO_2 capture unit, but also determines the optimal process layout for the hybrid system.

Annexe A Chapter 1 supplementary materials

A.1 Cross-flow configuration

In the cross-flow pattern, the gas mixture is introduced in the shell and then flows radially perpendicular to the fiber membrane. The retentate stream leaves the fiber bundle at the center of module whereas the permeate stream leaves the fiber axially. Figure A.1 illustrates a schematic diagram of a cross-flow membrane separation module. The individual volume and surface area of the elements, forming a ring shape with a length *dr* and thickness *dz*, can be calculated as:

$$\Delta v = 2\pi r_m(\Delta r)(\Delta z) \tag{A.1}$$

$$\Delta A_f = \frac{8\pi r_m(\Delta r)(\Delta z)(1-\varepsilon)}{d_o} \tag{A.2}$$

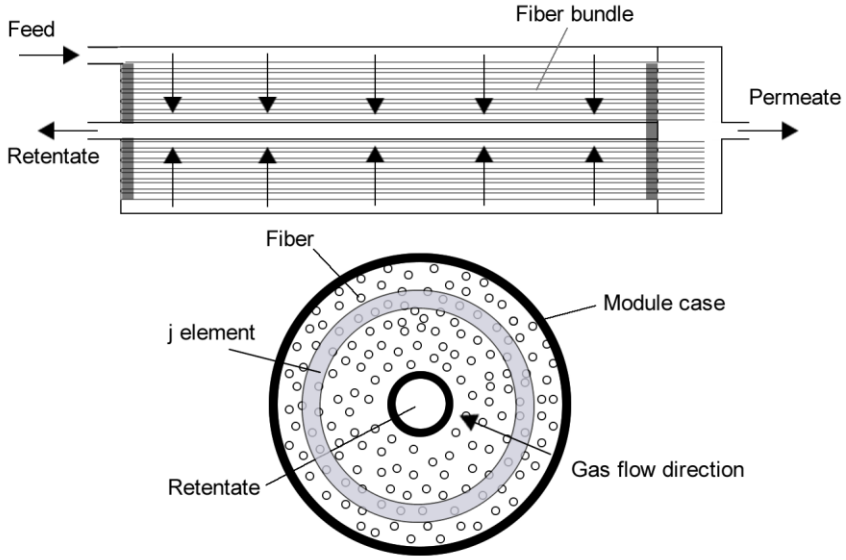

Figure A.1 Schematic diagram of a cross-flow membrane separation module.

Figure A.2 presents a schematic diagram of the first element in contact with the feed gas. The mass balance equations are given as:

$$\Delta V_t(i,1) = \sum_{c=1}^{m} \Delta V_c(i,1) \tag{A.3}$$

$$\Delta V_c(i,1) = \Delta A_f Q_c[P_s x_{s,c}(i-1,1) - P_t y_{p,c}(i,1)] \tag{A.4}$$

$$V_s(i,1) = V_s(i-1,1) - \Delta V_t(i,1) \tag{A.5}$$

$$V_p(i,1) = \Delta V_t(i,1) \tag{A.6}$$

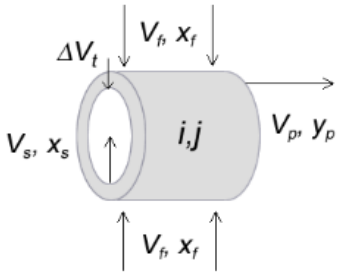

Figure A.2 Schematic diagram of the first element in contact with the feed gas for the cross-flow configuration.

Figure A.3 shows a schematic diagram of two successive elements in the cross-flow configuration. The permeate composition and flow rate with respect to the composition and flow rate of the previous element are given by:

$$\Delta V_t(i,j) = \sum_{c=1}^{m} V_c(i,j) \tag{A.7}$$

$$\Delta V_c(i,j) = \Delta A_f Q_c[P_s x_{s,c}(i-1,j) - P_t y_{p,c}(i,j)] \tag{A.8}$$

$$V_s(i,j) = V_s(i-1,j) - \Delta V_t(i,j) \tag{A.9}$$

$$V_p(i,j) = V_p(i,j-1) + \Delta V_t(i,j) \tag{A.10}$$

The retentate composition is given by:

$$x_{x,c}(i,j) = \frac{x_{x,c}(i-1,j)V_s(i-1,j) - \Delta V_c(i,j)}{V_s(i,j)} \tag{A.11}$$

For the first element, an initial value of pressure is guessed and used in a numerical iteration method such as the Secant method to calculate the outlet pressure.

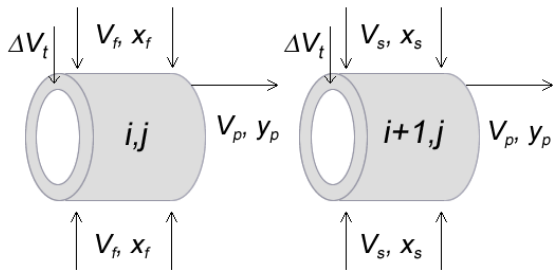

Figure A.3 Schematic diagram of two successive elements in the cross-flow configuration.

A.2 Counter-current flow configuration

In a counter-current flow pattern, the separation efficiency is expected to be better than the other configurations as the permeate pressure build-up inside the fiber is at its lowest value [89]. The solution method previously used for the co-current flow cannot be implemented as the permeate composition and flow rate of the first element are unknown. So, a new numerical algorithm is required to solve complex counter-current systems. Figure A.4 shows a schematic diagram of the counter-current element.

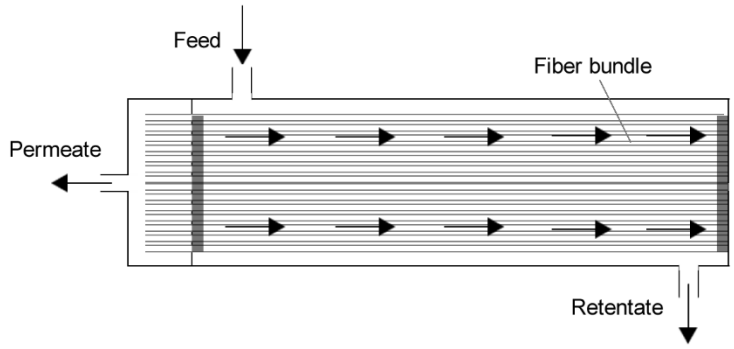

Figure A.4 Schematic diagram of a counter-current flow membrane separation module.

Figure A.5 also shows a schematic diagram of the last element (nth element) in the module. The main equations for this element are defined as follows:

$$\Delta V_t(n) = \sum_{c=1}^{m} \Delta V_c(n) \tag{A.12}$$

$$\Delta V_c(n) = \Delta A_f Q_c [P_s x_{s,c}(n) - P_t y_{p,c}(n)] \tag{A.13}$$

$$V_s(n) = V_s(n-1) - \Delta V_t(n) \tag{A.14}$$

$$V_p(n) = \Delta V_t(n) \tag{A.15}$$

where $V_s(n\text{-}1)$ represents the molar flow rate of the previous element. Figure A.6 shows a schematic diagram of two successive elements in the counter-current system.

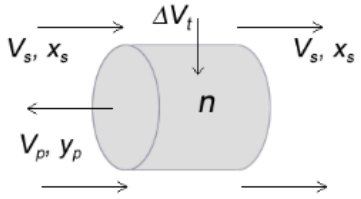

Figure A.5 Schematic diagram of the last element in the counter-current flow configuration.

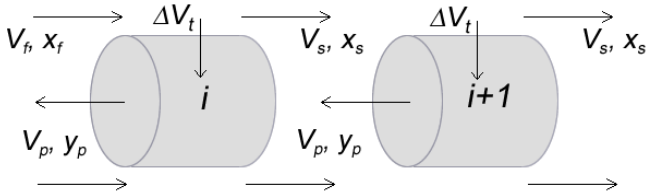

Figure A.6 Schematic diagram of two successive elements in the counter-current flow configuration.

The new numerical technique is introduced in which the unknown variables including permeate composition and flow rate are the results obtained for a cross-flow configuration, as initial values for the counter-current configuration. They represent the minimum values for the flow rate and mole composition by which the first loop of numerical iteration can be initialized [46]. Moreover, the mass balance equations can be redefined for the new counter-current system. In this way, the local composition and flow rate of the retentate stream of each element is calculated by solving simultaneously Eq. (A.16) and (A.17):

$$x_{s,c}(i) = \frac{x_{s,c}(i-1)V_s(i-1) + Q_c \Delta A_f P_t y_{p,c-cross}(i)}{V_s(i) + Q_c \Delta A_f P_s(i)} \tag{A.16}$$

The sum of all the retentate compositions must satisfy the following condition:

$$\sum_{c=1}^{m} x_{x,c}(i) = 1 \tag{A.17}$$

Thus, a new series of retentate and permeate flow rates is updated by using Eq. (12)-(15). The new permeate mol fractions are given by:

$$y_{p,c}(i) = \frac{y_{p,c-cross}(i+1)V_p(i+1) + Q_c \Delta A_f P_s x_{s,c}(i)}{V_p(i) + Q_c \Delta A_f P_t(i)} \tag{A.18}$$

$$y_{p,c}(n) = \frac{Q_c \Delta A_f P_s x_{s,c}(n)}{V_p(n) + Q_c \Delta A_f P_t(n)} \tag{A.19}$$

$$\sum_{c=1}^{m} y_{p,c}(i) = 1, \sum_{c=1}^{m} y_{p,c}(n) = 1 \tag{A.20}$$

The numerical algorithm consists of an iteration loop in which the new values for the permeate composition are replaced by the previous values until a convergence criterion ($\varepsilon = 10^{-6}$) is satisfied:

$$\left| y_{p,i,new}(1) - y_{p,i,old}(1) \right| \leq \varepsilon \tag{A.21}$$

$$\left| x_{s,i,new}(n) - x_{s,i,old}(n) \right| \leq \varepsilon \tag{A.22}$$

A.3 Heat Transfer Analysis

Experimental data in the literature show that gas permeabilities change with temperature which directly affects the permeate flow rate and stage cut [61]. In this case, temperature drop estimation in the shell and fiber must be performed to avoid gas condensation during a separation process. When penetrant gases pass through a very thin membrane, the sharp pressure change between the shell and fiber results in a temperature change of both residue and permeate streams. This phenomenon is also seen in valves when the pressure difference between the up and down streams is high. In this case, the process is isenthalpic; i.e. the enthalpy is the same at the inlet and outlet of the valve. The Joule-Thomson factor (μ_{JT}) can be introduced to calculate the temperature change in the shell and fiber sides and its value for different gas components changes with pressure and temperature as:

$$\mu_{JT} = \frac{\vartheta_m - T_s \left(\frac{\partial \vartheta_m}{\partial T_s} \right)_{P_s}}{C_P} \tag{A.23}$$

where ϑ_m, T_s, P_s, and C_p represent the molar volume, temperature, pressure, and heat capacity at constant pressure, respectively. An equation of state can be chosen to determine the molar volume and its derivation over the residue temperature at constant pressure. The change in pressure and temperature at both sides can be linked to the JT factor as [221]:

$$T_s - T_t = \mu_{JT}(P_s - P_t) \tag{A.24}$$

Similar to an isothermal system, an algorithm involving 'succession of states' method is used to analyze the heat transfer along the module. A schematic diagram of the heat transfer model is shown in Figure A.7. Referring to the Coker's model [47], the temperature of the permeate and retentate sides are calculated using the heat balance equation over each element using:

$$\rho\gamma.\nabla H = -\nabla.q + \gamma.\nabla P + \overline{\nabla \nu} : \bar{\tau} \tag{A.25}$$

$$F(i)H(i) - F_{pe}H(i) - F(i+1)H(i+1) = q_{cond} \tag{A.26}$$

where F and q_{cond} denote the molar flow rate and heat flux transferred by conduction defined as:

$$q_{cond} = U\Delta A_f (T_t - T_s) \tag{A.27}$$

$$U = \left[\frac{1}{h_t} \frac{r_{outer}}{r_{inner}} + \frac{r_{outer}}{k_m} \ln(\frac{r_{outer}}{r_{inner}}) + \frac{1}{h_s} \right]^{-1} \tag{A.28}$$

where U, h_t, and h_s are the overall, fiber, and shell side heat transfer coefficients, respectively. The thermal conductivity of the membrane (k_m), which depends on the thermal conductivity of the permeated gas and porous support, is given as:

$$k_m = \chi_{po} k_{po} + (1 - \chi_{po}) k_g \tag{A.29}$$

where χ_{po} is the volume fraction of polymer in the porous support. An Arrhenius-type equation is also used to estimate the gas permeability (p) along the module, while temperature changes in the elements are given by:

$$p(T) = p(T_{ref}) \exp\left[-\frac{E}{R_g} \left(\frac{1}{T} - \frac{1}{T_{ref}} \right) \right] \tag{A.30}$$

where E and R_g are the activation energy of permeability and ideal gas constant, respectively.

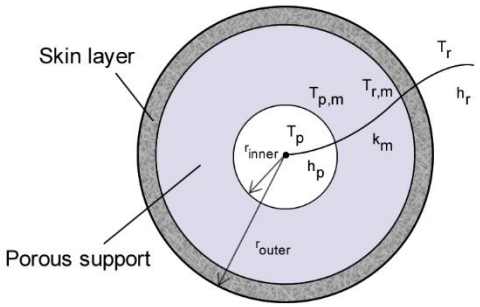

Figure A.7 Schematic diagram of heat transfer in a fiber [47].

Nomenclature

ΔA_f	membrane separation area
C_p	specific heat capacity at constant pressure
d	diameter
E	activation energy
F	molar flow rate
H	enthalpy
h	heat transfer coefficient
k	gas thermal conductivity
P	pressure
p	permeability
Q	permeance
q	heat
r	module inner radius
R_g	universal gas constant
T	temperature
U	overall heat transfer coefficient
$\Delta\upsilon$	element volume
V	molar flow rate
ΔV_t	permeate flow rate
x	shell side mole fraction
y	fiber side mole fraction
z	element thickness

Greek symbols

γ	gas velocity
ε	void fraction
μ	Joule-Thomson coefficient
ρ	density

ϑ	molar volume
τ	stress tensor
χ	volume fraction

Subscripts

c	gas component index
cond	conduction
f	feed side
i	element number
JT	Joule-Thomson
m	membrane
o	outer
p	permeate
po	polymer
ref	reference
s	shell side
t	fiber side

Annexe B Biogas Upgrading and Optimization

B.1 Abstract

Biogas is a valuable renewable energy source produced by the anaerobic digestion (AD) of biodegradable organic materials. Its main components are methane (CH_4) and carbon dioxide (CO_2), with traces of contaminants such as ammonia (NH_3), water vapor (H_2O), hydrogen sulfide (H_2S), methyl siloxanes, nitrogen (N_2), oxygen (O_2), carbon monoxide (CO) and hydrocarbons. Because biogas production is very versatile, it is of high interest to optimize methane purification. Upgrading is thus the process of improving the quality of CH_4 by removing CO_2 and other contaminants before it can be used. Depending on the biogas initial composition, operating conditions, and operating costs, different separation methods such as absorption, adsorption, cryogenic distillation, and membrane technology were developed. But over the years, operating costs and energy consumption were two important challenges limiting the biogas market. In this chapter, the advantages and disadvantages of the current biogas upgrading methods are presented and discussed. But recently, because of simplicity, membrane processes are showing promising separation results since membrane technology has high potential to displace conventional separation methods for CO_2 and H_2S removal from the biogas. Nevertheless, like any industrial process, membrane separation systems require an optimization step to determine the system configuration and operating parameters to reduce costs. Furthermore, hybrid systems are now being proposed to minimize both capital and operation costs compared to single type separation units, even under multi-stage operation. Here, a multi-stage biogas upgrading process using current commercial polymer hollow fibers is proposed to improve the separation efficiency and CH_4 purity while reducing operating costs. A techno-economic analysis is also presented to determine the most efficient membrane separation process for biogas upgrading.

B.2 Introduction

Today, one important problem to face is to manage energy resources due to the growth of global population, world modernization, and depletion of fossil fuel resources. The latter is of high importance as limited resources are available and it estimated that the equivalent of over 11 billion tons of oil in fossil fuels are consumed annually [222]. In this case, crude oil reserves, as an strategic energy resource, disappear at the rate of 4 billion tons per year. It is expected that all the oil reserves will run out by 2052 even if the rate of growing population is constant. But gas production can partially be used as a secondary energy source to reduce oil consumption. Nevertheless, this strategy only helps to slightly extend the consumption deadline by 2060 [57]. The life style of the modern world even brings up standards to minimize the energy consumption but the fossil fuels still run out. Coal is also seen as a fossil fuel and it is estimated that 869 billion tons of reserves are available based on the current production rate. So coal utilization can step up to fill the gap left through the depletion of the oil and gas reserves for the next 110 years [223]. Despite the depletion forecast, burning fossil fuels release a high volume of CO_2 in the atmosphere and intensify the global warming effect. Thus, the availability of the fossil fuels will be limited to meet the global energy demand which is continuously rising.

Currently, numerous communities, particularly in developing countries, do not even have access to basic energy supplies. The fossil fuel price is also driven by global market balance which is significantly dependent on events happening in the producing countries as well as world political decisions. This leads to unstable economic situation for all dependent and non-dependent countries. Statistical data predicts a growth of 30% for the global energy demand by 2035. Although fossil fuels is expected to remain the dominant source of global energy (~70%), renewable energies combined

with alternative sources such as nuclear, solar and hydroelectric power will compensate for the difference [60]. This situation attracted the public attention leading to research and development being done on alternative and renewable energy sources, especially when the production is clean, versatile and economical. More recently, biological processes were proposed to produce biogas from biomass (organic materials). This biogas is now seen as a clean energy source to complement others such as wind and solar energies. These sources will supply an increasing amount of the global needs and reduce the present dependency on fossil fuels.

Biogas production is considered to be more environment friendly and even contributes to the reduction of greenhouse gases (GHG) emissions in the atmosphere. Following biological processes, the crude biogas, for which the main product to enrich is CH_4, requires a purification plan to meet the standards. In this case, refined biogas is extracted from a series of treatment processes in which acid gases (CO_2 and H_2S) and undesired components (N_2, H_2O, and other contaminations) are captured to avoid operational problems (corrosion, erosion and fouling) and the reduction of its heating value. Thus, biogas as a fuel can emit lower carbon monoxide (CO), nitrogen oxide (NO_x) and hydrocarbons than fossil fuels. It was even reported that engines running with purified biogas are quieter than diesel engines [85]. The biogas can be used for other applications such as heat, steam and electricity generation, household fuel for cooking, and fuel cell. Highly purified biogas is also appropriate as feed (raw material) in industrial and chemical plants (syngas and hydrogen production). Hence, biogas can be a versatile energy source.

Biogas use dates back over hundred years in India and China. The use of biogas in Europe started around 1985 and there is now over 17,240 biogas and 367 biomethane plants in EU (2015) supplying energy services [224]. These plants can generate a total power of 8293 MW_{el} per year. In industrialized countries, the main purpose of biogas production is power generation [225]. Germany is the pioneer of biogas use in Europe with its 8928 upgrading plants providing electricity for more than 9.3 million households [226]. Further analysis also shows that 250 billion standard cubic meters (Nm^3) of biomethane can be produced from digested feedstock by 2050 which would provide 50% of the required natural gas for the 28 EU members [227]. There are also 242 anaerobic digesters operating on livestock farms in the United States which contribute to reduce GHG emissions. These plants also generate electrical power for over 13 million MWh per year which is the equivalent of 1670 MW of fossil fuel fired generation [64]. In Canada, the biogas production from all major sources supplies 2420 million cubic meters (m^3) per year of renewable natural gas. This represents only 3% of the Canadian natural gas demand that is required to generate 810 MW of electricity or 1.3% of Canada's electricity demand [228].

Biogas production plan can also be fully compatible with the targets highlighted in the Kyoto protocol (1992) and Paris agreement (2016) as part of the United Nations Framework Convention on Climate Change (UNFCCC) to mitigate and control GHG emissions. Refined biogas has the potential to become an imperative energy source and even make a sizable contribution to the global energy supply of the future. More interestingly, the combustion of the refined biogas emits less GHG than biodiesel and bioethanol [229, 230]. In addition, the use of biogas as a clean energy source can reduce the deforestation in developing countries which is one of the main source of anthropogenic GHG emissions [231]. This objective is surely attainable but requires global cooperation to displace fossil energies. The modern biogas upgrading approach is not available in some countries such as China and India and the inhabitants directly use crude biogas for local purposes. In this case, the acid gases (CO_2 and H_2S) and the combustion products (CO, SO_2, NO_x) are released in the atmosphere with bad environment impact [232]. This should get more attention from all governments to fundamentally invest in the modernization of biogas production plants, especially for domestic uses. Currently, the biogas upgrading market and technologies are rapidly evolving to keep up with other bioenergy sources. In this review, the biogas production by anaerobic digestion (AD) technology and its use are

presented. The mature and semi-mature upgrading techniques for acid gases removal are also discussed to highlight their advantages and disadvantages for biogas separation. In this context, these techniques often suffer from operation instability and most of them have high costs and are chemically intensive. Moreover, various biogas purification processes using membrane technology are presented to make a techno-economic analysis and compare its performance with conventional methods.

B.3 Biogas production and uses

Biogas as a renewable energy source is produced by anaerobic digestion (AD) and mainly contains CH_4 (40-75 vol.%) and CO_2 (15-60 vol.%). Crude biogas also contains other compounds (contaminants) such as traces of ammonia (NH_3), water vapor (H_2O), hydrogen sulfide (H_2S), methyl siloxanes, nitrogen (N_2), oxygen (O_2), carbon monoxide (CO) and hydrocarbons [73, 233]. A variety of biological waste such as animal waste, landfills, diary waste, and water treatment plants through fermentation technology can be converted to biogas in line with the petroleum-based products [23]. These bioprocesses also manage to recycle residual organic wastes and reduce GHG concentration in the atmosphere. It is of high importance to avoid CH_4 emission as its effect on the environment is 23 times greater than CO_2 [234]. Table B.1 shows typical biogas composition before upgrading. Nevertheless, the carbon oxidation-reduction state of the organic matter in waste materials and type of AD process determine the biogas composition [84]. The use of biogas as an energy source dates back around 10 BC to heat up water but limited amount of information is available about later years. In 1859, a purification plant for wastewater was built in India to provide biogas for a hospital. Similarly, the first biogas production plant was used in the 1900s in southern China [73]. Currently, in rural areas of developing countries, the local farm-based manure facilities are the most usual use of AD-technology. Millions of low-technology digesters (fixed dome digester and floating drum digester) are still used in China and India to provide biogas for domestic uses including cooking and lighting [235, 236].

From a biology point of view, AD involves a series of processes breaking down biodegradable materials in the absence of oxygen. For instance, the methane conversion is arbitrarily found in nature while air is excluded from the organic materials submerged in water [237]. In the case of biogas, AD is a biological process in which methane is produced from organic matter through three major phases: hydrolysis, acetogenesis, and methanogenesis [77]. Figure B.1 shows a schematic diagram of the conversion of organic matter to CH_4, CO_2 and other biogas components. In AD, the conversion is highly dependent on the structure of the microbial community present in the digester [238]. In the hydrolysis phase, extracellular enzymes depolymerize organic macromolecules (carbohydrates, proteins and fats) to produce sugar intermediates. This phase is mainly conducted by enzymes such as *Clostridia* and *Bacilli* [239]. Then, the degrading reaction results in the production of acetic acid, long chain fatty acids and CO_2 [240]. In the acetogenesis phase, different bacteria, generically called "acetogens", are ready to degrade the long chain fatty acids to produce acetic acid, molecular hydrogen and CO_2. In the methanogenesis phase, another type of bacteria (acetotrophic and hydrogenotrophic), also called "methanogens", degrade acetic acid to produce methane. The acetotrophic methanogens use acetate as a substrate in the acetotrophic methanogenesis process while the hydrogenotrophic methanogens decline CO_2 concentration by using H_2 as an electron donor in the hydrogenotrophic methanogenesis process [236]. The fatty, acetic acids and O_2 concentration in the system need to be controlled as these bacteria are inactive in such an environment [241]. The AD process normally occurs at thermophilic (53-58 °C) or mesophilic (30-40 °C) temperatures, during 12-25 days [242]. Table B.2 presents other environmental requirements for an AD system. Despite increasing attention on the use of AD technology, this process is complex and less information is available on the behavior of methanogens in the digester. For instance, the biogas production efficiency in winter (December around 24 ^{o}C) is lower than summer (April around 36 ^{o}C) due to lower ambient temperature and the associated shift in the microbial community [243]. Overall, the gaseous

product of AD is used for industrial or domestic applications, while the liquid and solid substances are collected to be used as fertilizers and value-added products, respectively.

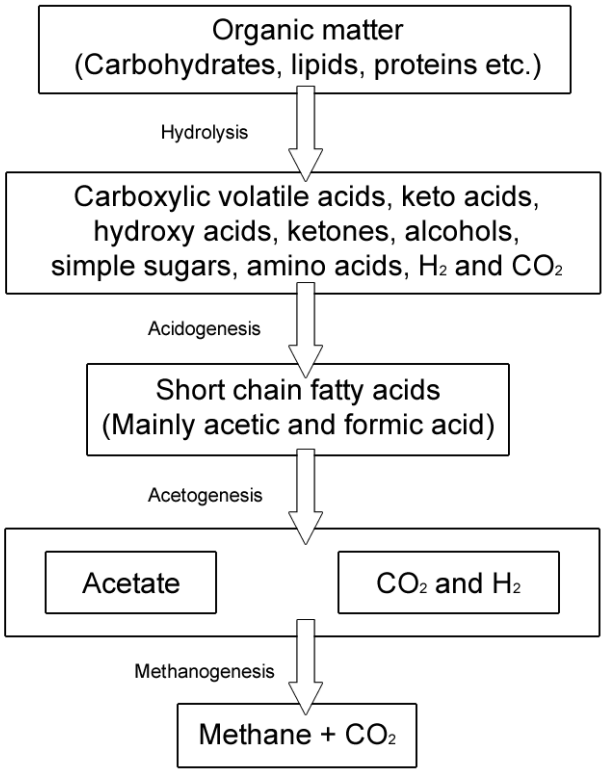

Figure B.1 Schematic diagram of the conversion of organic matter to CH_4, CO_2 and other biogas components.

Table B.1 Typical biogas composition [23].

Component	Agricultural waste	Landfills	Industrial waste
Methane	50-80	50-80	50-70
Carbon dioxide	30-50	20-50	30-50
Hydrogen sulphide	0.75	0.10	0.80
Hydrogen	0-2	0-5	0-2
Nitrogen	0-1	0-3	0-1
Oxygen	0-1	0-1	0-1
Carbon monoxide	0-1	0-1	0-1
Ammonia	Traces	Traces	Traces
Siloxanes	Traces	Traces	Traces
Water	Saturation	Saturation	Saturation

Table B.2 Environmental requirements for AD systems [73].

Parameter	Hydrolysis/acidogenesis	Methane formation
pH value	5.2-6.3	6.7-7.5
C:N ratio	10-45	20-30
DM content (%)	<40	<30
Redox potential (mV)	+400 to -300	<-250
Required C:N:P:S ratio	500:15:5:3	600:15:5:3
Trace elements	No special requirements	Essential: Ni, Co, Mo, Se

Further analysis is needed to estimate the final biogas cost including production and upgrading processes before sharing in the market compared to the other energy sources. With respect to modern biogas production plan, different separation methods are used to convert over crude biogas (high CO_2 content) to refined biogas (low CO_2 content). Otherwise, the high contaminants content like CO_2 and N_2 results in a low biogas specific heating value (15-30 MJ/Nm^3) and Wobbe index [20, 86]. Biogas can also be used as fuel for combustion reboiler without upgrading. For instance, the crude biogas with CO_2 content higher than 50% can be used for internal combustion engines but produces lower power output [23]. Other components such as H_2S and O_2 are corrosive in the presence of H_2O and maybe explosive, respectively. Pre-treatment methods such as air/oxygen dosing of digester biogas, iron chloride dosing of digester slurry, biological removal on a filter bed and iron oxide pellets are used to reduce the high concentration of sulphur compounds in biogas. But these methods are less effective when low sulphur level is required [81]. Moreover, condensation and adsorption by silica gel, activated carbon and aluminum oxide, as well as absorption in glycol or hygroscopic salts are commonly used to remove H_2O [75]. Similarly, NH_3 and halogenated hydrocarbons compounds also corrode equipment and pipeline network [75, 234]. Moreover, silicone oxide generated by methyl siloxanes combustion can remain in biogas combustion equipment and noticeably reduce their performance due to abrasion and overheating [244]. Hence, all these components must be removed using a series of pre-treatment processes to avoid equipment deteriorating and low efficiency of biogas products.

Biogas production in high quantity to inject into the natural gas network is of interest. After the purification process, the refined biogas will have the same characteristics as natural gas and can therefore be used for various applications. Table B.3 reports on the properties of other fuel gases compared to biogas. Biogas as the alternative is appropriate for domestic stoves, though its heating value is lower than natural gas at a pressure of 20 mbar (gauge) [78]. In this case, biogas distribution through the pipeline networks also needs to meet with the natural gas standards on safety and utilization to avoid issues such as corrosion. Conventional methods such as chemical and physical absorption, adsorption, cryogenic distillation, and membrane technology can be used to convert crude biogas to natural gas. Currently, some countries are more committed to supply a part of their energy sources from biogas products. They proposed requirements for the refined biogas with different restrictions for grid injection (see Table B.4). In Denmark, up to 25% of biogas with a methane content of 90% is injected into the natural gas network and a lower amount (<60%) is used after mixing with natural gas [73]. Biogas is also suitable for vehicle fuel while this application is less problematic compared to injection into the natural gas network. It can be compressed, transported by mobile containers or pipeline to the stations and then offered as a clean and lower cost fuel. The calorific value of the biogas-air mixture is about 15% lower than a gasoline-air mixture for vehicles resulting in a 15% power reduction at the same engine compression ratio [73]. However, this lower power leads to a 60-80% reduction in GHG emissions compared to fossil fuels. Vehicles designed for natural gas are also compatible with biogas and similarly, different countries, especially the EU, have a plan to cut their dependency on fossil fuels by using biogas products. For instance, Sweden

introduced its own fuel vehicle standards in which the CH_4 content in the biogas needs to be higher than 95% with limits for dew point, sulphur content, and some other minor components. Moreover, free parking, lower tax on biogas vehicles and fuel, toll exemption, and financial support for investment in biogas vehicles are some initiatives made by the Swedish government to further develop the biogas vehicle sector [245]. One of the challenges for biogas use as vehicle fuel is the production cost. It is estimated to be about 0.22-0.88 USD/m^3 of methane for 500 m^3/h plants using residues and waste as feedstock, while it is 1.00-1.55 USD/m^3 of methane for 100 m^3/h plants. As the natural gas price was around 0.13 USD/m^3 in 2016, the cost analysis shows that further development in the biogas preparation and upgrading is required [246]. Even in Germany, which has the most upgraded biogas, only 1.4% of biomethane is used as vehicle fuel [246]. Biogas with a low CH_4 content (~20 mol%) is also useful and can be injected into an internal combustion chamber to generate electricity. Currently, almost half of the biogas produced in the USA and 90% in EU are used to generate electrical power. The global biogas use as vehicle fuel also reaches only 1%. This shows that using raw biogas in turbines is simpler and more economical than other applications which mostly require complex purification processes to meet the standard requirements. Biogas can also be used in fuel cells. A fuel cell is an electrochemical device converting the chemical energy of a fuel/oxidizer mixture into electricity [78]. In a molten carbonate fuel cells (MCFC), biogas with a CH_4 content above 65% is suitable to supply H_2 for the chemical reaction. No further purification is needed as CO_2 is necessary to maintain the carbonate content in the electrolyte. H_2S is however removed from the fuel gas stream to avoid poisoning the Ni catalyst in the anode.

In brief, several applications and their performance highly depend on the biogas composition. Finding low-cost biogas production and upgrading methods results in a thriving growth of the global energy market. The versatility of biogas use shows its potential for the partial or complete displacement of fossil energy sources. The sustainability of biogas is also unique and resulting in a secure energy resource that does not fluctuate with external conditions.

Table B.3 Characteristics of different fuel gases [235].

Parameter	Unit	Natural Gas	Town Gas	Biogas
Heating value	MJ/m^3	36.14	16.1	21.48
Density	kg/m^3	0.82	0.51	1.21
Wobbe index	MJ/m^3	39.9	22.5	19.5
Max. ignition velocity	m/s	0.39	0.70	0.25
Theoretical air requirement	m^3 air/m^3 gas	9.53	3.83	5.71
Max. CO_2 content in stack gas	vol.%	11.9	13.1	17.8
Dew point	°C	59	60	60-160

Table B.4 Pipeline specifications when supplying upgraded biogas to the natural gas grid [23].

Compound	Unit	France	Germany	Austria	USA
Wobbe index	kW h m^{-3}	13-15.7	12.8-15.7	13.3-15.7	-
Heating value	kW h m^{-3}	-	8.4-13.1	10.7-12.8	9.8-11.4
CO_2	mol%	<2	<6	<2	<2
H_2S	mol%	<Dew point	<Dew point	<Dew point	<120 ppm
H_2O	mol%	<0.00052	<0.0003	<0.0004	<0.00037
H_2	mol%	<6	<5	<4	-
O_2 dehydrated gas network	mol%	-	<3	<4	<0.2-1
O_2 not dehydrated gas network	mol%	-	<0.5	<0.5	<0.2-1

B.4 Biogas upgrading methods

The raw biogas must undergo necessary removal operations before its use as a fuel or in other applications. Biogas cleaning is a primary process to remove impurities such as NH_3, water, siloxane and other low-concentration contaminates. The product, still containing CO_2 and H_2S, is then purified through an upgrading process. The final properties such as methane concentration, acid gases content, and specific heat value must correspond to natural gas and bio-methane before it can be distributed to the natural gas network or used in direct applications like fuel cells. The current biogas upgrading methods are: absorption, adsorption, cryogenic distillation, and membrane technology. Each method is described next for comparison purposes in terms of advantages and limitations.

B.4.1 Absorption

Absorption is a mature technology producing high methane gas content (above 90%). The undesirable gas components are transferred to a liquid phase provided they are soluble. Hence, the separation efficiency greatly depends on the affinity between the acid gas and the absorbent. Based on absorbent properties, absorption can be categorized into two major groups. In physical absorption, moderate absorbents are chosen to form a weak intermolecular bond with the acid gases. The separation process is more efficient to operate at low temperature and high pressure to enhance the solubility of acid gases in the liquid phase. On the other hand, in chemical absorption strong absorbents are chosen to form a covalent bond with acid gases and the separation performance is usually independent of operating conditions. The absorption process can even be operated at ambient temperature and pressure. Nevertheless, the process selection is highly dependent on the raw biogas composition and product use, as well as investment, operational and maintenance cost. In this way, high-pressure water scrubbing (HPWS) and organic physical scrubbing (OPS) are physical absorption, while amine scrubbing (AS) and inorganic solvents scrubbing (ISS) are chemical absorption [23].

B.4.1.1 Amine scrubbing

Amine scrubbing is an absorption process removing acid gases such as CO_2 and H_2S by using amine-based solutions. The strong covalent bond formed with amine solutions can capture a high amount of the acid gases in the separation process. In the case of CO_2, the absorption process involves an exothermic reaction between the absorbent and CO_2 while the system temperature is kept low. Figure B.2 shows a process flow diagram of acid gas removal using amine scrubbing. As a rule, the absorption process is recommended when the CO_2 concentration in the feed gas is low [247]. In the first column (absorber unit), the downflowing amine solution absorbs the acid gases from the upflowing raw biogas and produces a sweetened gas leaving from the top of the column. The product

can be directly used in other applications such as enhance oil recovery (EOR). More interestingly, the absorbent is selectively reacted with CO_2 and no CH_4 is lost during the separation. The bottom product, H_2S and/or CO_2-rich stream, is send to the regeneration unit (stripper with a reboiler) to recover the laden absorbent at high temperature (100-120 ^oC) or low pressure. The recovered absorbent is then recirculated to reuse in the absorber unit. In the case of process design, the absorbent selection is the essential step as the acid gases content in the product streams depends on the absorbent characteristics such as loading capacity. The absorption column can be fitted with packing and trays based on the separation target and costs [248]. Amine solutions such as diethanolamine (DEA), monoethanolamine (MEA), and methyldiethanolamine (MDEA), diglycolamine (DGA), triethanolamine (TEA), piperazine (PZ) and hot potassium carbonate solution are typically used [73, 199, 248]. In the case of CO_2 removal, MEA is a common absorbent and its use results in a significant reduction of energy consumption in the absorption process [82, 249]. Moreover, numerous studies were carried out with respect to single and mixed-absorbent selection, and their removal performance [250-252]. As a rule, the selection procedure reconciles the CO_2 removal performance and absorbent recuperation in the regeneration unit. It is also essential to take into consideration the corrosion degree and degradation properties [253]. low operational cost and high CH_4 recovery are two main advantages resulting from this process as the most common CO_2 and H_2S removal method [254]. Nevertheless, absorption is seen as an energy-intensive method. Using a reboiler in the regeneration unit as a heat supplier leads to extra processing costs. In this way, the regeneration unit requires a high amount of energy to purify the CO_2-rich absorbent and to produce pure CO_2. The main disadvantages are high investment costs, high energy consumption, absorbent corrosion, absorbent degradation by O_2 or other compounds, precipitation of salts, and foaming. Inorganic solvent scrubbing (ISS) is similar to amine separation mechanism while removing the acid gases using potassium, sodium carbonates or aqueous ammonia solutions [23].

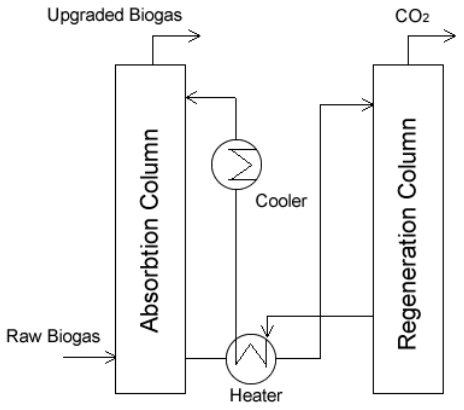

Figure B.2 The process flow diagram of acid gas removal using amine scrubbing.

B.4.1.2 Water scrubbing

The separation principle is based on the solubility of gas components in a liquid phase. Unlimited supply and economical aspects are the reasons to use water as a solvent with the aim of introducing a less complex operation and more environmentally friendly process compared to chemical absorption. Water scrubbing is seen as the simplest and cheapest process amongst all the separation methods [232]. This method also requires fewer infrastructure and can operate at low flow rate which is appropriate for biogas production plants [255]. The differences in solubility of acid gases (CO_2 and H_2S) and CH_4 in water leads to two distinctive process configurations to upgrade biogas into biomethane. High-pressure water scrubbing (HPWS) and near atmospheric pressure water scrubbing (NAPWS) are currently used. Similar to chemical absorption, the separation can be carried out in

columns with or without packed bed. For column selection, it is required to analyze design parameters such as feed pressure, temperature, flow rate and acid gas composition, as well as water flow rate and purity. Using a scrubbing column without packed bed results in lower CO_2 separation efficiency (~40 vol.%) compared to the same system with a packed bed column which provides a higher contact area for gas-liquid mass transfer [256]. The poor CO_2 solubility in water leads to increased water flow rate and to modify the column size and packing density. However, CO_2 solubility is about 30 times higher than CH_4 in water. In this case, the operating pressure can be controlled between 0.8 and 1.2 MPa to increase the CO_2 partial pressure resulting in better solubility in water [257]. Similarly, H_2S is removed in the first column through contact with the downflowing water stream as its solubility in water is much higher than CO_2. However, this simultaneous removal procedure in the first column causes some operational issues as gaseous H_2S is poisonous and its dissolution in water is corrosive as well. Thus, a pre-treatment unit is required to eliminate H_2S, condensed moisture and particles before feeding the raw biogas to the scrubber unit [78]. CH_4 recovery can be as high as 95% and the separation process is counter-current [258]. The raw biogas is fed into the column particularly at low temperature (<40 ^oC) from the bottom while the pressurized water as the absorbent is sprayed from the top [259]. Figure B.3 shows a flow diagram of a water scrubbing process using scrubber and regeneration units. In this case, the acid gases (CO_2 and H_2S) are dissolved in water and gradually removed from the upflowing sweetened gas stream. The laden stream can also be sent to the regeneration unit to regenerate through contact with air injected into the bottom of the stripping column at atmospheric pressure. Then, the purified water stream is recirculated to the first scrubbing column. Moreover, the recovery process requires lower water demand and is more stable compared to the single-stage scrubber system [259]. The energy consumption of the CO_2 recovery process is lower compared to the chemical absorption process in which the CO_2-absorbent bound is relatively strong and broken only at high temperature. This process generally performs well when high CO_2 purity (80-90%) is required. Despite the impact of elevated operating pressure on the separation performance, CH_4 solubility in water also increases. Thus, CH_4 dissolved in the CO_2-rich water stream also increases by 5%. It is essential to send the off-gas stream to another treatment unit prior to feeding into the second column. In this way, a flash tank is needed to separate CH_4 at 2-4 bars and to recycle it to the bottom of the scrubber column [256, 257]. This separation configuration results in high CH_4 recovery (80-99%) [256]. Water scrubbing process is also highly sensitive to the presence of N_2 and O_2 in the raw biogas. These gases cannot be removed in the scrubber column and will be collected in the CH_4-rich stream. Thus, the bio-methane product including N_2 and O_2 will have lower heating value limiting its application. In the case of process design, operating at higher pressure results in lower water flow rate but the energy requirement for pumping and recompression also increases [84].

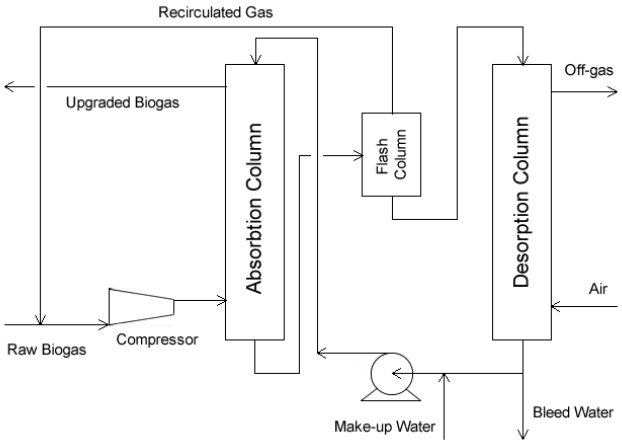

Figure B.3 The flow diagram of a water scrubbing process using scrubber and regeneration units.

B.4.1.3 Organic solvent scrubbing

The basic principle of this technology is similar to water scrubbing. In the physical absorption process, a nonreactive absorbent is used to physically absorb the acid gases inside the biogas. Organic solvents such as methanol (Rectisol) and dimethyl ethers of polyethylene glycol (Selexol) are commonly used since they have higher affinity for the acid gases than water. As the gas solubility in the absorbent depends on both partial pressure and temperature, the separation mechanism is to absorb the undesired gas components at high pressure and low temperature and to desorb them at low pressure and high temperature [260]. Figure B.4 shows a flow diagram of an organic solvent scrubbing process. Similarly to water scrubbing, the physical absorption process is performed in the scrubber column. The raw gas is first compressed up to 6-8 bars and thereafter cooled before injection at the bottom of the column. In this counter-current process, the absorbent is also cooled and thereafter fed into the scrubber column in which the temperature is kept to 20 ^{o}C [260]. The laden absorbent is then sent to the regeneration unit to regenerate at high temperature (50-80 ^{o}C) and/or low pressure (1 bar). Air as stripping agent provided by blowers is injected into the bottom of the packed desorption column to remove the dissolved CO_2 from the absorbent. The vented air is normally released to the atmosphere after passing through a series of bio-filters [237]. The CH_4 concentration in the product is around 93-99% [224]. At higher operating pressure, higher CH_4 loss in the off-gas stream is detected and consequently, it needs to be recovered in a flash tank at atmospheric pressure before injecting into the desorption column. Otherwise, an extra treatment unit is required to clean the exhaust gas. Similarly, a pretreatment unit is also required to remove O_2 and N_2 gases prior to the scrubber unit to avoid reducing the product quality. The common absorbent in this technology is Selexol in that the CO_2 solubility is about five times higher than water [85, 261]. This superior property results in reduced absorbent volume, recycling rate and plant size, as well as investment and operating costs. The anti-corrosion nature of the organic solvent also favors using of equipment constructed by non-stainless steel materials [262]. In the case of Selexol (Genosorb) separation performance, this absorbent is able to simultaneously remove H_2S, water, O_2, N_2 and CO_2 [234]. Compared to reactive absorbents, Selexol has a lower vapor pressure so that absorbent loss in the regeneration process is minimized [86]. To desorb H_2S, stripping of the laden stream is carried out with steam or inert gas rather than with air [85]. A pre-treatment unit using activated carbon filters is often used to completely remove H_2S in the raw biogas prior to feeding into the scrubber column [84, 237]. A point of concern about the Selexol process is the high amount of dissolved CH_4 in the pressurized off-gas stream leading to low selectivity and increased operational cost due to the gas treatment unit. Organic solvent scrubbing can be operated at a temperature of less than -20 ^{o}C due to the low freezing point of the absorbent. But it is required to use stainless steel equipment and pipeline to avoid corrosion problems [254]. Other commercial physical absorption methods are Rectisol and Purisol which can also be chosen based on biogas composition and cost analysis. The Rectisol process, which operates at a temperature of 213-263 K and a pressure of 30-80 atm, is more complex compared to other physical absorption methods [263-265]. Overall, the advantages of physical absorption are lower operating pressure and less corrosive absorbents compared to chemical absorption. The disadvantages are: high investment and operational costs, complex operation and high energy consumption.

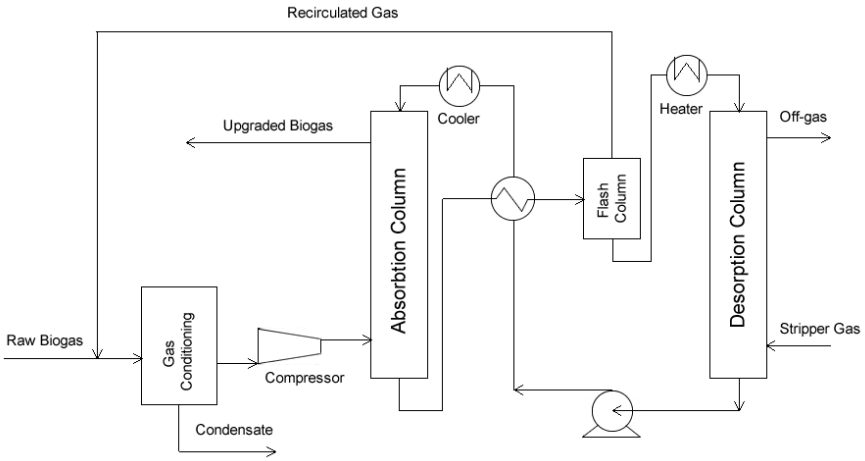

Figure B.4 The flow diagram of an organic solvent scrubbing process.

B.4.2 Adsorption

The main separation principle of this technology is the transfer of solute in the biogas stream to the surface of solid materials. Adsorption processes are classified into pressure swing adsorption (PSA), vacuum swing adsorption (VSA), temperature swing adsorption (TSA) and electrical swing (ESA). PSA is superior to TSA due to its higher product throughput combined with lower capital and energy costs [266]. In PSA and VSA, an adsorption column is filled with granular porous solids having a large surface area per unit volume to differentially adsorb the undesired gas components [267]. Typical solid materials are activated carbon, titanosilicates, silica gels, alumina and zeolites. The selection is based on the gas molecular properties [23, 86, 268]. The adsorption mechanism of these materials is also categorized by their equilibrium and kinetic types depending on the gas residence time in the column. The separation here is based on acid gases adsorbing in higher volume or faster rather than CH_4 [259]. Figure B.5 shows a process flow diagram of a pressure swing adsorption unit for biogas upgrading. The separation performance of PSA is dependent on the ability of the adsorbent materials to retain the acid gases under different operating pressures. Due to the different molecular size of CH_4 (3.8 Å) and CO_2 (3.4 Å), an adsorbent with a pore size of 3.7 Å can be chosen to selectively capture CO_2 molecules and let CH_4 molecules through [269]. In this case, the CO_2 molecules enter the matrix structure of the porous materials to be retained while the CH_4 molecules are passing over the active surfaces [270]. A desorption process, which is the reverse operation of adsorption, is performed to release the molecules trapped on the adsorbent back to the gas phase. The capacity of adsorbent materials (maximum amount of material adsorbed) depends on the temperature, pressure and biogas composition. Adsorption usually takes place at high pressure and low temperature, while desorption is performed at low pressure and high temperature.

Three or four vessels (adsorption, depressurization, desorption and pressurization) are usually used in a PSA unit. These vessels operate sequentially so the energy consumption for gas compression decreases and the upgraded gas pressure is used by other vessels [267]. This process also consists of four phases. The biogas is first compressed to 4-10 bars and thereafter fed to the desulfurization unit. H_2S removal is highly essential before injecting into the adsorption unit as H_2S is irreversibly adsorbed resulting in adsorbent deterioration. The desulfurized biogas is then sent to a dehydrator unit to remove water and other condensable impurities [86]. As the dry biogas is fed to the first vessel, CO_2 is adsorbed at the adsorbent surface, while CH_4 is released from the top of the adsorption vessel with a very small pressure drop. In this case, CH_4 content in the upgraded biogas reaches 95% or more with a vapor pressure of less than 10 ppm H_2O [267]. When the adsorption bed is saturated with CO_2, the inlet of the first vessel is closed and the raw biogas is injected into the subsequent vessel.

The CO_2/CH_4 gas mixture containing high CH_4 content is then recirculated to the inlet of the PSA unit or even the digester for lower CH_4 loss [267]. Later, desorption is initialized by decreasing the column pressure to ambient or vacuum so the trapped CO_2 starts releasing from the adsorbent surface. The CO_2-rich gas stream is then evacuated from the bottom of the vessel. Moreover, a low trace of CH_4 (2%) is lost in the off-gas stream and therefore has to be treated by using catalytic oxidation, regenerative thermal oxidation, and flameless oxidation operations [224]. Finally, a purge gas using either CO_2 upgraded gas or raw biogas is blown through the vessel at low pressure to clean all CO_2 desorbed from the adsorbent surface [86, 259, 271]. The PSA process mainly benefits from the pressure-equilibrium principle. The outlet gas of a vessel during purging can be used to pressurize the gases inside the other vessels and consequently the total energy consumption of the process decreases [259]. In PSA, one vessel always remains in the adsorption phase while the others still operate in the regeneration phase and therefore the cyclic procedure characterizes a continuous operation. The advantages of PSA are high CH_4 recovery, high pressure product, and low power consumption. The PSA process unit also operates independently of cold and hot sources (heat exchangers and refrigerators) so a biogas adsorption plant can be adapted in any part of the world [271]. The disadvantages of PSA are high investment costs, high operation costs and complex process control [23, 85]. Moreover, H_2S removal and tail-gas treatment units before and after the main adsorption unit are necessary limiting PSA compared to other biogas upgrading methods.

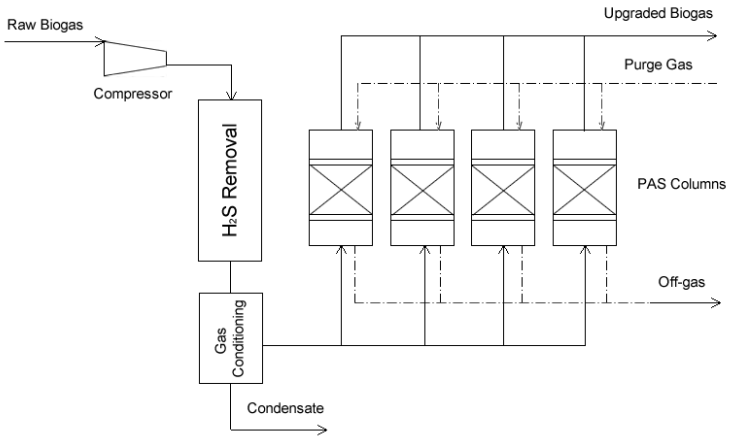

Figure B.5 The process flow diagram of a pressure swing adsorption unit for biogas upgrading.

The VSA process is similar to PSA, but the adsorption and desorption units operate at atmospheric pressure and under vacuum condition, respectively [272]. The PVSA process is another type of PSA in which the pressure in the adsorption and desorption units are above atmospheric and under vacuum, respectively. The separation principle of TSA process is based on the periodic variation of the temperature of an adsorbent bed [273]. The adsorption and regeneration processes occur at low and high temperatures, respectively. Thus, proper insulation is required to eliminate heat losses to the surrounding, particularly during the regeneration step. This method is suitable for the treatment of low adsorbate concentration feed such as impurity and volatile organic compound (VOC) removals of the air stream. In the regeneration unit, a hot gas or steam is injected into the packed column resulting in increased adsorbent bed temperature releasing the trapped undesired components. This method is normally recommended when compression or vacuum to a large volume of a low-pressure gas stream is difficult [274]. The TSA cycle time also varies from some minutes to several days. For an efficient process, it is necessary to apply high rapid adsorbents as to operate more cycles. TSA main drawbacks are: high energy consumption, thermal aging of the adsorbent and the need for large adsorbent inventories [202]. In ESA, a voltage is applied to heat the adsorbent and release the adsorbed gases. This technique is not very common in the industry [23].

B.4.3 Cryogenic distillation

The separation principle is based on the difference in boiling points of constituents in the gas mixture. This gas purification method involves sequential condensation and distillation at extremely low temperature. In the case of biogas upgrading, impurities (mainly CO_2) can be captured from the gas stream through condensation as CH_4 has a lower boiling point (-161.5°C) than CO_2 (-78.2°C) at atmospheric pressure. Figure B.6 shows a flow diagram of a cryogenic distillation process used for biogas upgrading. The raw biogas is cooled and thereafter compressed to 10-20 bars using a series of heat exchangers and compressors. The compressed gas is then dried to avoid pipeline blockage and equipment clogging due to traces of condensed water in the feed gas. Later, the dried gas is sent to another cooling unit to decrease its temperature to -25 °C at which the impurities such as water, H_2S, siloxanes and halogens are removed. Further purification is also carried out using a coalescence filter and a SOXISA® catalyst to remove the remaining contaminants [259]. In the next step, the gas is further cooled to -45 °C to lose the condensed CO_2 (30-40%) through a separator. The gas is finally cooled down to -55 °C and then expanded through nozzles while being injected into the column. The CO_2 removal process mainly takes place in the column through a phase transition mechanism [275, 276]. In this case, gaseous CO_2 starts to sublime inside the column operated at 40-80 bars and -110 °C [84, 277]. The separation system also tends to reach an equilibrium state at which most of the CO_2 solidifies, while CH_4 remains in the gas phase. The solid CO_2 accumulated at the bottom of the column is heated up to liquefy before transportation, while the gas mixture containing high CH_4 content is routed to the primary cooling unit to use as a cooling medium [237, 278]. CH_4 loss is low (<2%) and purity is high (>97%) regardless of the initial CO_2 content in the raw biogas and feed flow rate [23, 279].

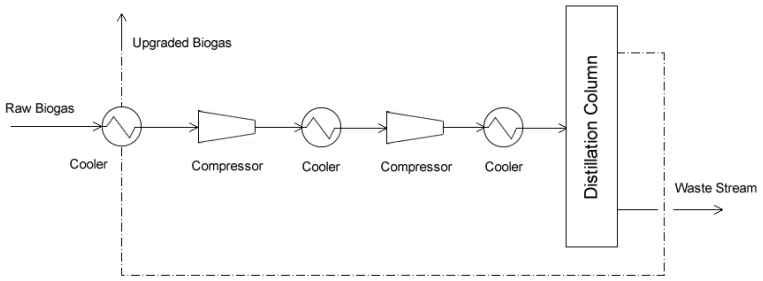

Figure B.6 The flow diagram of a cryogenic distillation process used for biogas upgrading.

This technology is also more suitable for upgrading landfill gas in which the N_2 content is relatively high. In this case, N_2 is separated from the gas mixture by using an extra column operated at lower CH_4 condensation temperature. Thus, CH_4 is liquefied at the bottom and gaseous N_2 leaves from the top [280]. In the case of specific calorific value, liquid biomethane (LBM) is also equivalent to liquid natural gas (LNG) and can easily be fed to the fuel grid [86]. In the case of process thermodynamics, the formation of binary or tertiary phases depends on the gas composition and operating parameters. Thus, the raw biogas properties are highly modified by the CH_4 content so that higher pressure and/or lower temperature are required for CO_2 condensation and sublimation [259]. Commercial simulation packages are able to simulate basic cryogenic processes using a suitable thermodynamic model for different gas mixtures. The main step to control the separation process and improve the removal efficiency is the selection of an equation of state (EOS). Thus, simulation companies normally suggest their own thermodynamic models for these non-ideal systems. The cryogenic method is still in development and requires reliable EOS to precisely estimate the equilibrium data for biogas upgrading. Currently, Scandinavian GTS, Aerion technologies/Terracasatus technology, and Prometheus energy are the commercial suppliers for biogas upgrading using cryogenic distillation [281]. The main advantage of the cryogenic method is that the separation product, CH_4, is highly pure

and in the liquid phase which can simply be used for other applications. The use of a large number of equipment, such as compressors, turbines, heat exchangers and distillation columns, requires higher capital and operating costs than other separation methods [235]. Hence, this technique is extremely energy intensive. In addition, a techno-economic analysis shows that a cryogenic process is more economical than a water scrubbing process at medium size plants as it requires lower investment and operational costs [237]. This technique is still not matured enough to be commercialized at large scale so that its global market share is only 4%. Nevertheless, this purification process is synergic and leads to liquid products [84, 279]. The technical data of cryogenic distillation is also strictly classified and few reliable investment and operational information are available for further analysis.

B.4.4 Membrane technology

In membrane technologies, the separation principle is based on the different permeations of gas components through a thin selective layer (membrane). The main parameter is permeation which is the product between chemical solubility and diffusivity of the target component in the membrane [85]. Membrane technology is widely used in various industries such as food, biotechnology and pharmaceutical. Recent attention has been also focused on the use of this technology for gas phase separations. This method has even potential to displace conventional methods for acid gas removal from biogas due to low energy consumption, simple design and scale-up, ease of installation and operation, and low capital and maintenance costs. However, there are some limitations of using membranes for CO_2 removal processes. In the case of process design, this technology is categorized into high and low-pressure processes. The primary group is a gas-gas based process operated at 8-20 bars while the permeation depends on the membrane characteristics, gas composition and operating parameters. The latter is an absorbent-gas based process operated at atmospheric pressure and the permeation depends on the solvent affinity for the acid gases as well [269]. In the field of gas separation, material selection and membrane fabrication are the essential steps to establish a separation process. Membranes are also classified into organic or polymeric and inorganic or ceramic membranes. Thus, membranes present a wide range of physical and chemical properties to choose from and can be fabricated based on these processing needs. For instance, polysulfone, polyimide or polydimethylsiloxane are commonly used for biogas upgrading. Moreover, polyimide, cellulose acetate, perfluoro polymers, silicon rubbers and polysulfone are chosen to remove acid gases from natural gas. Mixed matrix membranes (MMM) is another group of membrane benefiting from the incorporation of an inorganic filler in a polymer film. Studies on the performance of current membranes have shown that the trade-off between selectivity and permeability, which is a common feature of rubbery and glassy polymer membranes, can be advantageously improved by using MMM. Hence, numerous ongoing research projects aiming at fabricating membranes with higher permselectivity and lower costs are commercially attractive. Generally, several procedures such as thermal treatment, polymer blending, reactively formed interpenetrating networks, cross-linking, thermal rearrangement, and particle addition are selected to improve the performance of polymer membranes in gas separation [282]. Polymer membranes have several advantages for commercial scale gas phase separations. These include their low cost (cheaper than inorganic membrane), good mechanical stability at high pressure and temperature, and easy formability to both flat sheets and hollow fibers. They are however limited in membrane performance as they suffer from the trade-off between selectivity and permeability. This is described by the well-known Robeson upper bond plots [7]. Plasticization is another problem for the commercialization of membrane technology and occurs while the CO_2 concentration in the feed gas is high. Plasticization refers to a phenomenon in which the CO_2 permeability increases while selectivity decreases due to a shift of the glass transition temperature of the membrane due to the dissolved gas molecules. In this case, the permeated CO_2 is acting as a plasticizer and causes the membrane to swell and even change the polymer structure. In addition, in the presence of CO_2 and heavy hydrocarbons, polymer chain motion increases. During plasticization, gas molecules penetrate through the loosely packed chain and reduce the separation

efficiency. Some methods such as thermal treatment, cross-linking, and polymer blending can be used to prevent membrane plasticization.

Membrane gas separation processes require a large surface area for high gas capacity. Currently, three types of membrane contactors including hollow fiber, spiral wound and envelop are used for gas separation [283]. Hollow fiber and spiral wound modules provide larger surface area than envelop module. In contrast to the spiral wound module, the use of hollow fiber module is more economical because of its higher effective surface area per unit volume of membrane module. In terms of industrial applications, a typical gas separation process normally requires hundreds to thousands of square meters of fibers. It is therefore essential to minimize membrane fabrication cost and to increase the membrane life time without deteriorating membrane permselectivity. With respect to biogas composition and operating conditions, the gas can be fed to the shell side (shell-side feed) at pressures up to 1000 psig and to the tube side (bore-side feed) for pressures as high as 150 psig. The transmembrane pressure is also seen as a main driving force needed to be set accurately. A higher feed pressure leads to a better separation performance but increases energy consumption. The cost of gas pressurization also constitutes about 60% of the total separation cost. Ultimately, membrane technology has high potential to displace conventional separation methods due to the promising results of pilot upgrading. This can probably be achieved if improvements in membrane properties and reduction in production costs are performed.

In a typical membrane separation system, the number of modules and their configuration, as well as transmembrane pressure, highly affect both the separation efficiency and hydrocarbon loss. Depending on the product composition and application, using a single module for biogas upgrading may be possible. But this configuration is economically less attractive as CH_4 loss is often about 10-15%. Normally, a single-stage membrane operates at a low feed flow rate (1-2 MMSCFD) due to low capital and operation costs [87]. Using a permeate recycle stream aims at reducing CH_4 loss and increase CH_4 recovery (up to 95%). For process design, different compression strategies including feed compression, vacuum pumping and feed compression with an energy recovery system (ERS), might be chosen to improve the separation efficiency. Figure B.7 shows a schematic flow diagram of various single stage membrane units. Increasing the feed pressure improves the separation driving force resulting in better separation performances and a reduction in required membrane area. The use of a vacuum pump on the downstream of a membrane module leads to an efficient transmembrane pressure, but may not always be possible in industrial cases [284]. In addition, the use of steam or inert gas as sweep gas on the permeate side is an another way to increase the driving force [284, 285]. However, a large amount of energy is required for steam production [286]. When N_2 as an inert agent is fed to the permeate side, its separation from the permeated compounds is also an issue [287]. Hence, the selection of compression strategy needs to consider the feed gas composition, membrane characteristics and operation parameters to optimize the upgrading costs and production.

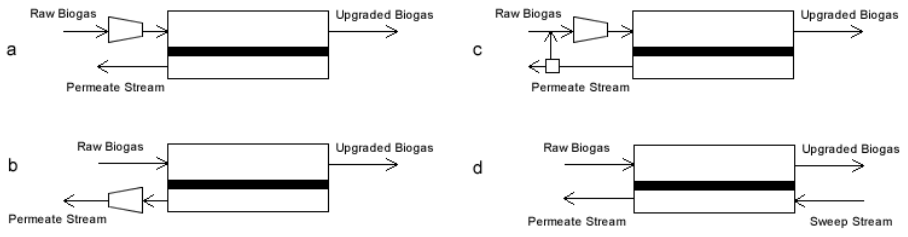

Figure B.7 The schematic flow diagram of various single stage membrane units.

No specific configuration is available to select for a typical gas separation process as some design and economical parameters such as feed composition, membrane characteristics and operation

parameters determine the number of modules. For biogas upgrading, at least two membrane modules are required to achieve an acceptable CH_4 content in the retentate stream and to recover the maximum amount of CH_4 (minimize the lost in the permeate stream). In contrast to single stage membrane units, using two membrane modules can highly improve both CH_4 recovery and purity of the separation process. Figure B.8 shows different configurations of two membrane modules. It can be seen that the retentate or permeate stream from the first and second modules can be recycled and mixed with the fresh feed with or without using a compressor. Three stage membrane modules can also be used for biogas upgrading while the unpressurized feed is mixed with the permeate stream of the third module and the permeate stream of the second module is sent to the first module as fresh feed [288]. This configuration resembles the two-stage module and both systems do not require extra compressor for the recycle stream. Figure B.9 shows a schematic diagram of three stage membrane systems for biogas upgrading.

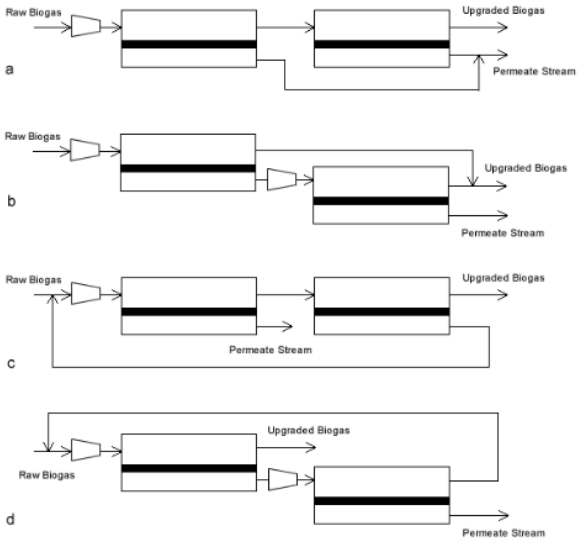

Figure B.8 Two stage membrane configuration.

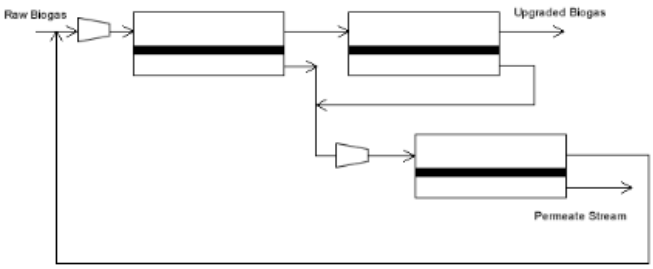

Figure B.9 Three stage membrane configuration.

B.4.5 Hybrid systems

In hybrid systems, membrane technology and conventional methods (absorption, adsorption and cryogenic distillation) are combined to improve the overall separation performance while reducing operation cost. Currently, amine absorption process still has a high portion of the acid gases capture market as the separation performance of membrane processes is very low to compete with

conventional methods. The number of commercial membranes used for gas separation is also limited although numerous research studies are currently in progress to find a solution for the trade-off in membrane permselectivity. In comparison, the simplicity of membrane separation is unique allowing to economically purify a gas mixture by minimizing environmental impacts. Since conventional methods mainly suffer from high energy-consumption, high capital and maintenance costs, and require a high amount of space (important for off-shore applications), a hybrid system probably constitutes a better separation configuration to benefit from the advantages of each process while limiting their respective drawbacks. In this case, various separation designs can be made based on the feed properties. For instance, in a hybrid membrane/absorption process, the membrane unit is used to remove the bulk of acid gases from the raw biogas before feeding to the absorber unit. This allows to reduce the total amount of required absorbent for absorption and avoid environmental issues. The integration with a cryogenic process can also result in a reduction of capital and operation cost by decreasing equipment and plant size.

The first hybrid system including membrane and chemical absorption units was introduced by Bhide et al. [289] to remove acid gases and purify CH_4. Figure B.10 shows a schematic flow diagram of the separation process. An asymmetric cellulose acetate (CA) membrane with a CO_2/CH_4 selectivity of 21 and H_2S/CH_4 selectivity of 19 was used to simultaneously remove the acid gases. The membrane separation system consists of three membrane units to minimize both the CH_4 loss and separating cost. The feed gas flow rate was 35 MMSCFD and the retentate/permeate pressures were set to 800/20 psia. The retentate stream largely depleted in the acid gases is then sent to the absorber unit for further purification using a diethanolamine (DEA) solution while the permeate stream, enriched in CO_2 and H_2S, is used for other applications. The separation results of the hybrid system was then compared with the ones of using a single membrane and absorption units. The techno-economic analysis showed that the total separation cost highly depended on the H_2S concentration in the feed gas. The hybrid system and membrane unit had the lowest total separation cost for the feed with and without H_2S, respectively. The result also showed that the total separation cost of the hybrid system was lower than that of the gas absorption process alone. In the hybrid system, a large amount of CO_2 (~78%) was captured using the membrane unit resulting in a lower absorbent circulation rate and plant size. The total separation cost of the single membrane unit changed with the feed gas composition as higher acid gas concentration needed higher membrane area and power to obtain higher CH_4 purity and recovery.

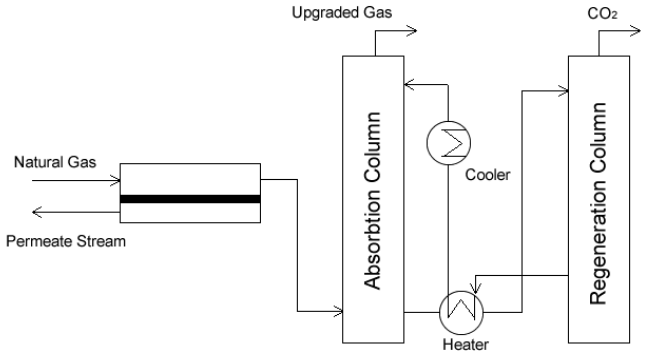

Figure B.10 The schematic flow diagram of a hybrid process including membrane and chemical absorption units.

Few studies have been published on the separation performance of hybrid processes for biogas upgrading. For instance, Scholz et al. [287] analyzed seven different membrane hybrid processes including pressurized water scrubbing, amine absorption, and cryogenic distillation to compare their separation performance and upgrading cost with conventional methods. Figure B.11 shows a

schematic flow diagram of the hybrid processes studied. In all cases, the separation objective was to deliver the refined biogas to the natural gas grid. Thus, the crude biogas was initially compressed up to 9 and 16 bars. It was also assumed that the biogas had low O_2 and N_2 contents due to the fermentation of agricultural waste. In the hybrid membrane/PWS process, a membrane system was used for two distinct separation scenarios. In the first configuration, the membrane system removed as much CO_2 as possible from the feed gas, while the retentate stream was enriched by CH_4 up to 98% at 9 bars. The permeate stream was then directed to the PWS unit for further purification. Thus, CH_4 lost in the permeate stream was upgraded and mixed with the CH_4-rich gas stream. The liquid stream enriched in CO_2 at first was injected into a flash vessel to recover CH_4 at 3 bars and then sent to a regeneration unit to separate water and CO_2 using air at 1 bar. In the second configuration, the membrane system was used to enriched CO_2 in the permeate stream. The retentate gas enriched to 70% CH_4, was then fed to the PWS unit for further upgrading. In all cases, the gas leaving the hybrid system contained low saturated water and a trace of H_2S. It is therefore essential to treat the gas using desulfurization and drying units prior to grid injection. In the hybrid membrane/absorption, a membrane system was similarly used for the bulk and partial removal of CO_2 before feeding to the absorption unit. In this case, H_2S in the permeate and retentate gas was removed in the desulfurization unit. In the first configuration, the free-sulfured gas was fed to the absorber column from the bottom while DEA solution was sprayed from the top. The gas leaving the absorber column contained CH_4 and saturated water. The polished gas was then injected into the natural gas grid after a drying treatment process. The laden absorbent was also purified through the regeneration step using three flash vessels. Both the absorbent and lost CH_4 were recovered at 9-10 bars and then recycled to the absorber column. In the second configuration, the permeate stream was similarly upgraded using the same absorption unit. The CH_4-rich stream was compressed to 16 bars and then mixed with the retentate stream of the membrane system. In the hybrid membrane/cryogenic process, the crude biogas was initially dried and desulfurized before feeding the membrane unit. The permeate gas was then compressed to 20 bars and cooled to -25°C. The gas is finally injected into a low-temperature cryogenic distillation column for further upgrading. In this case, the CH_4 recovery was higher than 99%.

A techno-economic analysis provides a better cost estimation for the different upgrading processes. The investment cost was highly dependent on the gas flow rate. For a gas flow rate higher than 1500 m^3 (STP)/h, the investment cost was the lowest for PW1. The cryogenic process had also the lowest investment cost when the gas flow rate was lower than 1500 m^3 (STP)/h. On the contrary, the highest investment cost was for AP1 and rapidly increased with increasing gas flow rate. This resulted in a direct cost increase for supplying equipment such as vessels, heat exchanger, pumps and columns for the higher capacity plant.

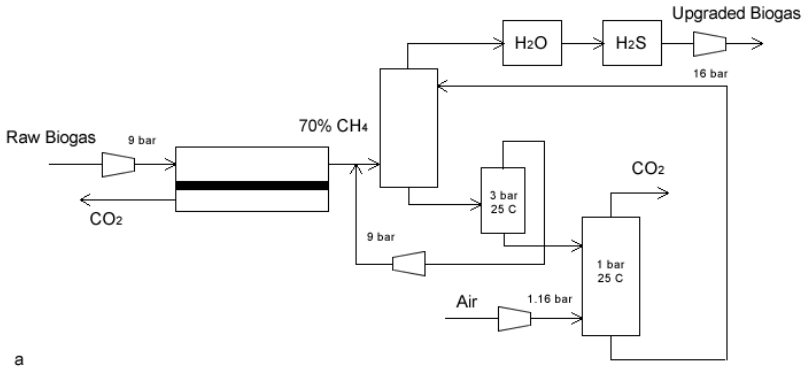

a

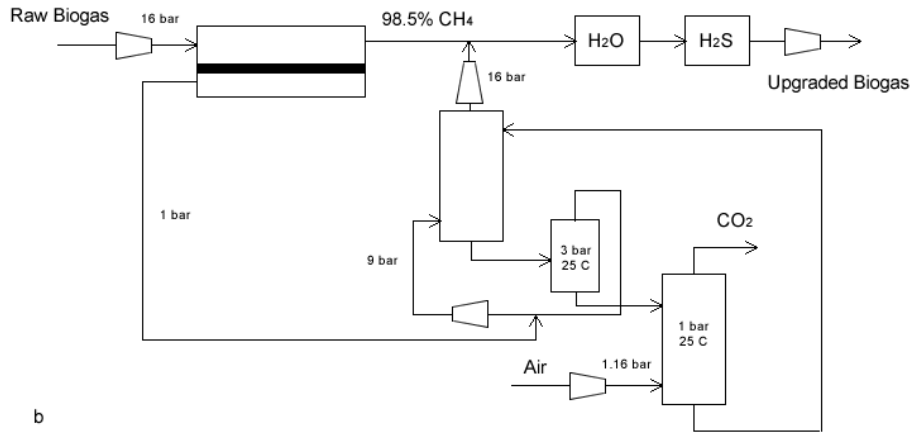

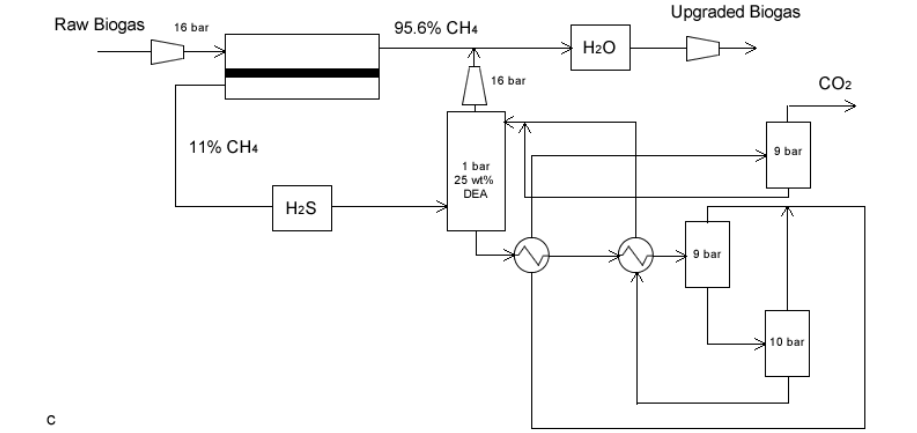

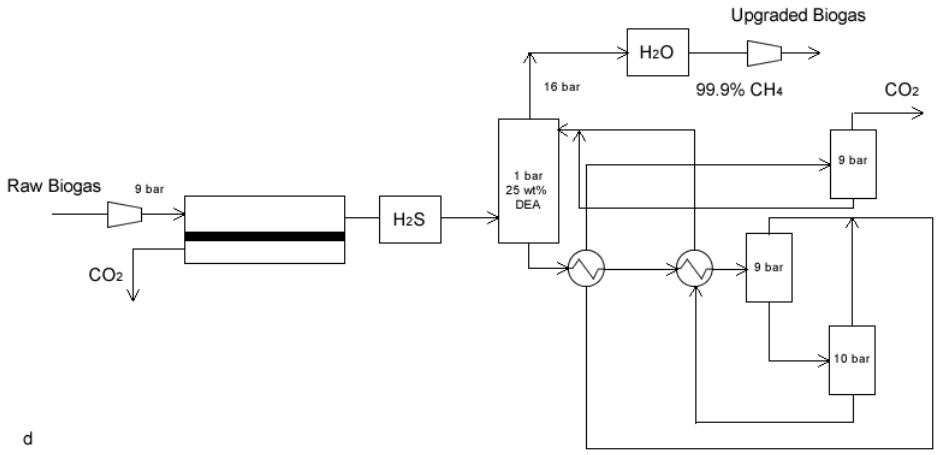

Figure B.11 The schematic flow diagram of hybrid systems including membrane and a, b) pressurized water scrubbing processes, c, d) amine absorption processes, e) cryogenic distillation

The investment cost reached the mean value for the three-stage membrane process. In the case of operating cost, the cryogenic process had the highest value whereas water scrubbing processes had the lowest values amongst all the processes. Figure B.12 shows the annual cost of biogas upgrading processes for a gas flow rate of 1000 m^3 (STP)/h. The lowest value is for water scrubbing and membrane processes. Both the investment and operating costs for amine scrubbing and cryogenic processes are equal. In the case of CH_4 recovery, PW1 and AP1 have the lowest values as high volume of CH_4 is lost on the permeate side of the membrane unit. This indicates some deficiency in the bulk removal of CO_2 for the membrane unit. However, increasing the transmembrane pressure leads to a decrease in the total CH_4 loss for PW1 and AW1. Overall, the three-stage membrane process was more interesting due to its lowest CH_4 loss and annual cost.

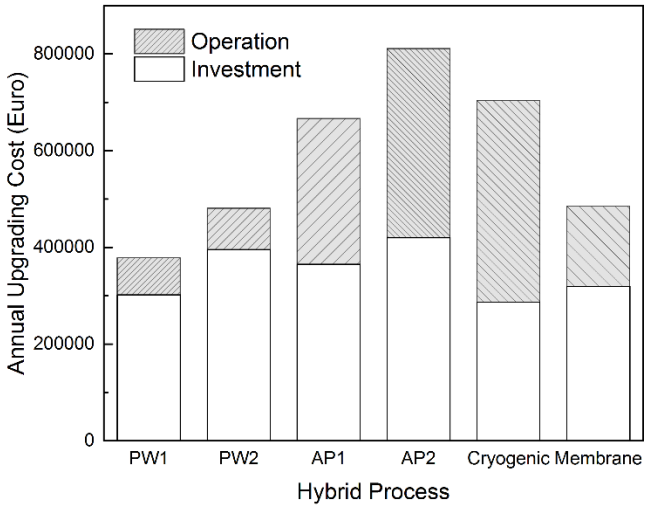

Figure B.12 Annual cost of biogas upgrading processes for a gas flow rate of 1000 m3 (STP)/h.

Figure B.13 shows a flow diagram of another hybrid process including TSA and membrane units for the separation of CO_2 from biogas [80]. The CO_2 concentration in the biogas is 40 vol.% and the feed flow rate is set to 200 Nm^3h^{-1}. In the first stage, a gas blower with a pressure of 1.4 bar is set to overcome the transport resistance across the adsorption beds in series. In the first step, H_2O, H_2S, VOCs and siloxanes are removed in the water separator and desulfurization units, which benefits from a high-efficiency iron-oxide adsorbent. The free-sulphur gas is then sent to the TSA towers in which all the other gaseous impurities are removed through the packed adsorbents [290]. In the second stage, a three-stage membrane system is proposed to purify the TSA product. A polymer membrane (polyetherimide-biomaleimide) with a CO_2 permeability of 25 GPU and a CO_2/CH_4 selectivity of 55 is also chosen to remove CO_2. The retentate and permeate pressures are set to 30 and 3 bars, respectively. The TSA product is initially compressed to be fed to the first membrane unit (A1) and generate a CH_4-rich retentate and a CO_2-rich permeate stream. The retentate gas leaving A1 is further upgraded to 97 vol.% in the second membrane unit (A2). The permeate gas is then recompressed and recirculated to A1 to minimize the CH_4 loss (0.67 vol.%). Similarly, the third membrane unit (A3) is used to upgrade the CO_2 up to 99 vol.%. For transportation, the CO_2-rich product can be later compressed and sent to a sequestration point.

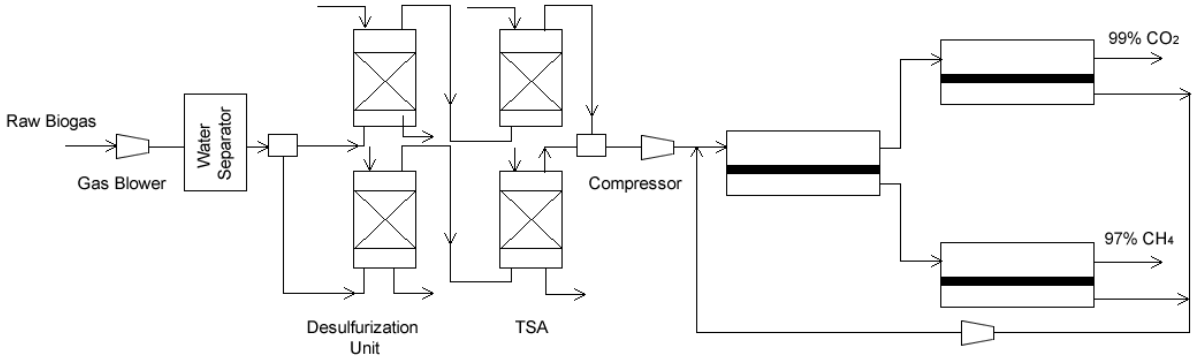

Figure B.13 The flow diagram of another hybrid process including TSA and membrane units for the separation of CO_2 from biogas.

Another hybrid membrane system was proposed by Makaruk et al. [291] to desulfurize and upgrade biogas using rubbery and glassy membranes [291]. Figure B.14 shows a schematic flow diagram of the hybrid separation process. In the case of high H_2S content, their utilization results in a rise in the total separation costs due to the higher required membrane area and compression energy for CH_4 recovery. Thus, rubbery membranes can be used for H_2S removal because they have higher H_2S/CH_4 than CO_2/CH_4 selectivities. In the case of biogas processing, the raw biogas is initially compressed and thereafter fed to the rubbery membrane unit. PDMS [poly(dimethyl siloxane)] and Pebax® [poly(amide-6-b-ethylene oxide)]) with H_2S/CH_4 selectivities of 10.5 and 54 are chosen for the first separation stage. The retentate stream depleted of H_2S is then sent to the glassy membrane unit to remove CO_2. After a bulk removal of CO_2, the CH_4-rich retentate stream can be used for other applications. The permeate streams of the first unit are desulfurized and then mixed with the permeate stream of the second unit. The gas mixture holding a high CH_4 content is then used as fuel for combustion engines to produce heat and electricity. This proposed hybrid system is suitable for biogas upgrading only if a high H_2S/CH_4 selective rubbery membrane is chosen for the first separation unit.

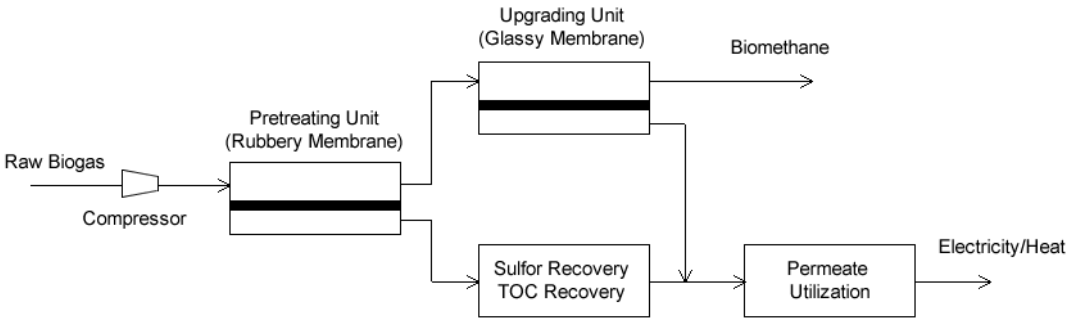

Figure B.14 The schematic flow diagram of the hybrid separation process.

The above-mentioned methods can be used for biogas upgrading. As mentioned, absorption and adsorption processes mainly suffer from operational problems and even have adverse impacts on the environment. Cryogenic distillation is highly energy-intensive, while membrane technology is also immature to fabricate a commercial product with high selectivity and permeability. Finally, hybrid systems are complex systems and require more analysis on costs and manufacturing technology. Nevertheless, membrane separation units are eco-friendly and even more compatible with a biogas in a production line. Therefore, improvement of membrane properties is the subject of the current investigations. Hopefully, this can increase the number of commercial membranes operating at lower

transmembrane pressure with improved lifetime. In this case, it is expected that CH_4 recovery reaches 99% while the CO_2 capture costs decrease compared to the current separation methods.

B.5 Case study: biogas membrane separation

As discussed above, biogas separation using membrane technology is simpler and more environmentally friendly compared to the other methods. The separation performance depends on biogas flow rate, membrane characteristics, separation area, as well as operating parameters such as pressure and temperature. Using a numerical model to determine the gas quality in both permeate and retentate streams under different operating conditions aims to properly assess the performance of membrane processes. Here, a numerical model based on Fick's law is used to design single and two stage separation units to predict the required separation area and operating pressure for a typical biogas treatment process. The model assumptions are: 1) steady state process under isothermal condition, 2) permeability is independent of pressure and gas composition, 3) membrane fibers do not deform at high pressure, 4) polarization at the membrane surface is negligible, 5) pressure drop inside the fibers is calculated using the Hagen-Poiseuille equation, and 6) the gas flow is laminar and ideal gas behavior is considered. The differential mass balance of the retentate and permeate streams are given as:

$$\frac{dUx}{dz} = N\pi d_o Q_1 (P_h x - P_l y) \tag{B. 1}$$

$$\frac{dU(1-x)}{dz} = N\pi d_o Q_2 (P_h (1-x) - P_l (1-y)) \tag{B. 2}$$

$$\frac{dU}{dz} = N\pi d_o Q_1 \left[(P_h x - P_l y) + (P_h (1-x) - P_l (1-y))/\alpha \right] \tag{B. 3}$$

where U, x, and y represent the volumetric flow rate, retentate and permeate mole fractions, respectively. N, d_o, and Q are the fibers number, fiber outer diameter, and gas permeability, respectively. α also stands for the CO_2/CH_4 selectivity.

Hollow fiber membrane modules (HFMM) can be operated under three different flow configurations including counter-current, co-current, and cross flow. In a counter-current flow pattern, the separation efficiency is expected to be better than the other configurations as the permeate pressure build-up inside the fiber is at the lowest value [89]. Hence, the process simulation of the biogas purification is here carried out based on the counter-current flow pattern to maximize the CH_4 recovery. It is worth noting that in a realistic membrane separation process, raw biogas undergoes a series of treatment processes to lose compounds such as water, H_2S, and other trace of contaminates. Later, the gas mixture containing CH_4 and CO_2 is fed to single or multi-stage membrane units. As discussed above, membrane technology has high potential to displace conventional separation methods. This target strongly ties not only to the membrane characteristics, but also to the process configuration. In this study, three different process configurations are chosen to simulate the biogas separation process with respect to the fixed costs (membrane and compressor). This also aims to find the optimal values of required membrane area and operating pressure for the desired production. In this way, the numerical model is used to predict CH_4 mole fraction in both retentate and permeate streams, and to determine a range of CH_4 loss in three different cases. In a realistic industrial case, the final product enriched in

CH_4 (>97%) can be injected into the natural gas grid. Table B.5 shows the membrane characteristics, feed gas properties, and cost analysis parameters for a typical biogas separation process.

Table B.5 Membrane characteristics, feed properties, and cost analysis parameters.

Item	Parameter	Value
Membrane characteristics	Permeance of CO_2 (GPU)	28.70
	Permeance of CH_4 (GPU)	0.65
Feed gas characteristics	CO_2 mole fraction	0.25
	CH_4 mole fraction	0.75
	Flow rate (m^3/h)	350
	Pressure (Pa)	$3\sim1.6x10^6$
Product characteristics	CH_4 mole fraction	>0.95
	Pressure (Pa)	$1x10^6$
Module characteristics	Outer diameter (μm)	160
	Inner diameter (μm)	90
Cost parameters	Membrane cost ($\$/m^2$)	50
	Compressor cost ($)	$8650\ (U/\eta)^{0.82}$

Figure B.7a shows a schematic flow diagram of a single stage membrane unit for biogas upgrading. As shown, the biogas (CH_4/CO_2 mixture) is initially compressed up to three different pressures (8, 12 and 16 bars). The pressurized gas is then fed to a single membrane unit consisting of parallel hollow fiber membrane modules. The permeate pressure is also kept at ambient pressure to provide separation driving force for the polymer membrane. Figure B.15 presents the relations between the CH_4 mole fraction, the membrane separation area and the total cost at different pressures. CH_4 mole fraction in the product stream is below the desired value (>97%) while the feed gas pressure is 8 bars. It is obvious that increasing membrane area has no significant effect on the product enhancement. When the feed gas pressure increases up to 12 bars, CH_4 mole fraction sharply increases with increasing membrane area. The desired CH_4 mole fraction in the retentate stream (>97%) is achieved for membrane area higher than 1600 m^2. As shown, increasing the feed gas pressure up to 16 bars gives rise to sharp increases of the CH_4 mole fraction and a reduction in the total cost. In this case, higher CH_4 mole fraction (>97%) is also achieves if the membrane area increases up to 1800 m^2. However, this option increases the total cost separation. The modeling results shows that the variation of the feed gas pressure and membrane area are two alternatives resulting in higher CH_4 mole fraction in the retentate stream. Figure B.16 presents the relations between the CH_4 mole fraction, the membrane separation area and the CH_4 loss at different pressures. For the desired CH_4 mole fraction of 97%, the CH_4 loss decreases from 12 to 9% when the feed gas pressure increases from 12 to 16 bars. It is therefore seen that a single membrane unit needs only a membrane area of 1100 m^2 at 16 bars and has the lowest CH_4 loss of 9%. In a realistic industrial case, it is highly recommended to recover the CH_4 lost in the permeate stream. Otherwise, a flare is used to burn this CH_4 before releasing in the atmosphere as CH_4 has more effect on the environment than CO_2.

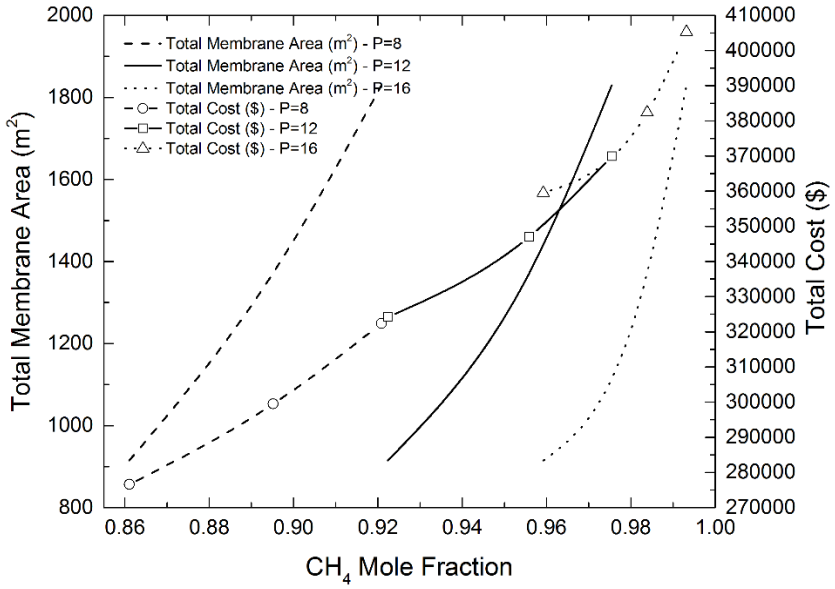

Figure B.15 Relations between the CH_4 mole fraction, membrane separation area and total cost at different pressures.

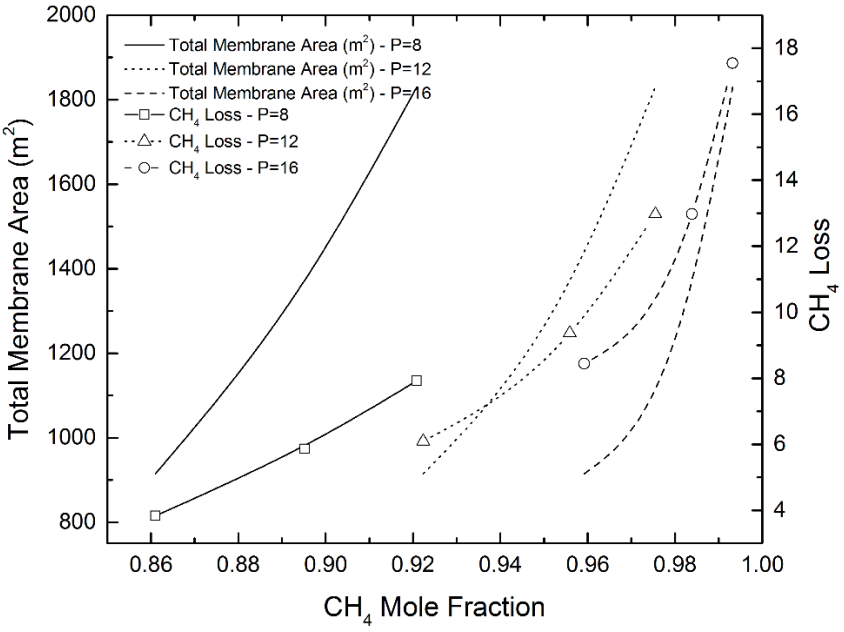

Figure B.16 Relations between the CH_4 mole fraction, membrane separation area and CH_4 loss at different pressures.

Figure B.8b shows a schematic flow diagram of a two stage membrane units for biogas upgrading. A second membrane unit is designed to recover the CH_4 lost in the permeate stream of the first membrane unit. The CH_4 mole fraction reaches up to 97% using the first membrane unit operated at 16 bars. Similarly, the pressure and membrane area are alternatives which can be optimized for the

CH_4 mole fraction and CH_4 loss in the second membrane unit. Figure B.17 presents the relations between CH_4 mole fraction, total membrane area and total cost for three different pressures (3, 4.5 and 6 bars). The simulation result shows that the desired CH_4 mole fraction in the product stream is more easily obtained using two membrane units. In the first case, the membrane area needs to dramatically increase to compensate for the low feed gas pressure in the second membrane stage. In the other case, the CH_4 mole fraction achieves the desired values for the lower membrane area compared to the first case. Moreover, a slight increase in the membrane area results in a sharp increase in the total cost. Figure B.18 presents the relations between the CH_4 mole fraction and CH_4 loss for two membrane units. The total CH_4 loss for the two-stage membrane system decreases to 4%. Similarly, the design including higher pressure and lower membrane area is superior to the other cases so that both CH_4 loss and total cost are minimized. In this configuration, the first unit is used to maximize the CH_4 quality in the retentate without considering CH_4 losses. Even for low CO_2/CH_4 selectivity, both pressure and membrane area can be modified to reach the desired production. Using the second membrane unit can also be used while the retentate stream of the first membrane unit is returned to the second membrane unit. Figure B.8a shows another schematic flow diagram of a two stage membrane system for biogas upgrading. This configuration is not suitable for biogas upgrading using a membrane with a CO_2/CH_4 selectivity of 44 as the CH_4 loss exceeds 10% even with increasing the membrane area. But the advantage is that no extra compressor is required to compress the retentate stream of the first membrane unit compared to the previous module configuration. One solution is to use a higher CO_2/CH_4 selective membrane that may result in decreasing the CH_4 loss in the first and second membrane units. The other solution is to use an additional membrane unit to recover the CH_4 lost in the permeate stream of the first and second membrane units. Despite increasing the membrane cost, this option also requires to install an extra compressor resulting in higher total cost.

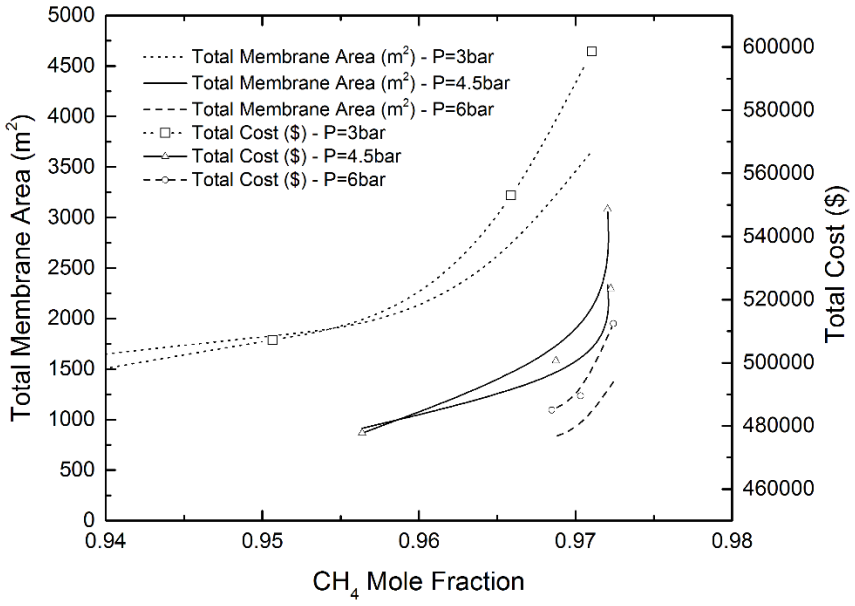

Figure B.17 Relations between CH_4 mole fraction, total membrane area and total cost for three different pressures (3, 4.5 and 6 bars).

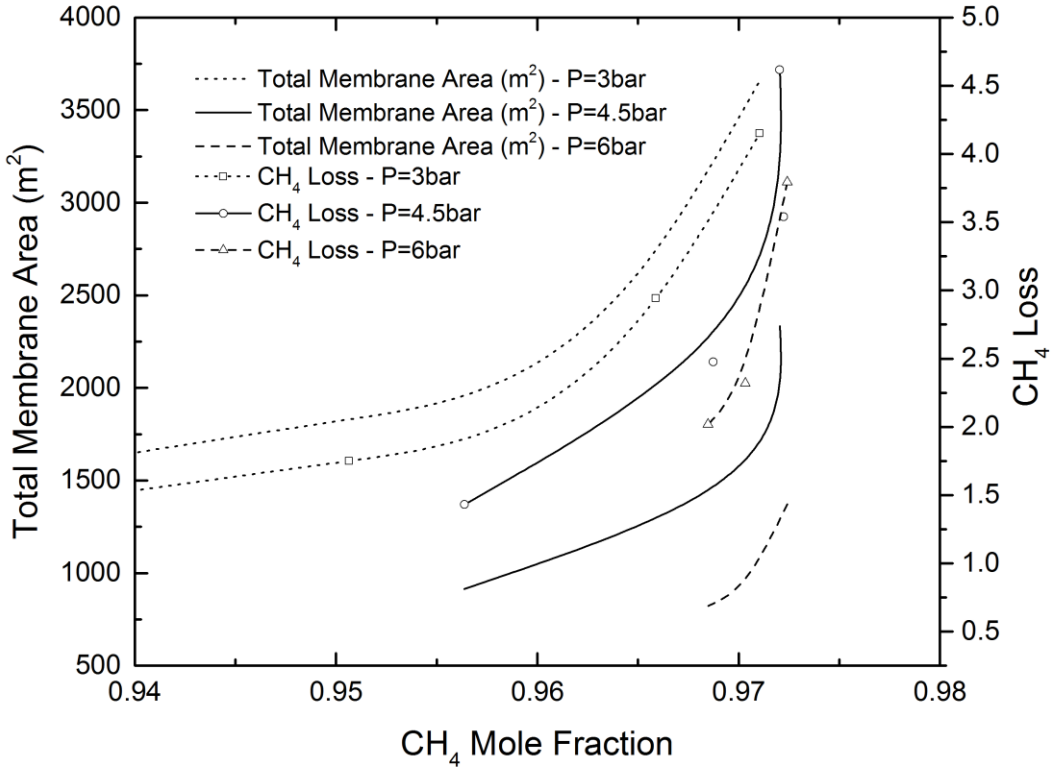

Figure B.18 Relations between the CH_4 mole fraction and CH_4 loss for two membrane units.

B.6 Conclusions and perspectives

Biogas as a renewable energy source is highly attractive to use for vehicle fuel, for injection in natural gas grid, as well as energy source for heat and electricity productions. Its production involves the anaerobic digestion (AD) of biodegradable organic materials and is completely independent of other energy sources. This production mechanism also abides by the eco-friendly rules compared to the fossil fuels. The presence of high amount of acid gases is avoidable due to the production mechanism and is therefore considered as one of the current points of concern for the commercialisation at larger scale. The biogas treatment is a necessary step prior to the final use. In this way, absorption, adsorption, cryogenic distillation and membrane technology are the common purification methods proposed for biogas upgrading. But these methods suffer from operational problems and have adverse effects on the environment. They are also energy-intensive and require to operate at high pressure and/or temperature. Membrane technology is currently more attractive due to simplicity, ease of installation, and low operation cost. However, this technology is less competitive than other methods as a limited number of commercial membranes are available. Hence, numerous investigations are being conducted to improve the membrane performance for biogas upgrading. The use of a hybrid system is another alternative having the advantages of both membrane technology and other conventional methods. However, this method also needs further analysis on both process design, investment and operating costs to increase their share of the biogas purification market. All these purification methods still require more initiatives and practical solutions to minimize negative environmental impacts. Hopefully, both production and purification units can form a more efficient

environmentally friendly cycle so that many countries will be ready to invest in their development for different biogas projects. Without any doubts, the depletion of fossil fuels, high energy demand, and harmful effects of greenhouse gas on the environment are very important reasons to produce an energy revolution in the world. Biogas, along with other renewable energy sources, can play a significant role to partially supply the global energy demand in the near future. The availability of primary materials and short production time also aim to limit the fluctuation of energy cost. Furthermore, increasing the number of biogas production plants, especially in strategic regions, can play a role in political decisions taken on energy and eventually stabilize the global energy market. Finally, concerns about global climate changes and current uncertainties about the loyalty of nations towards the environmental protection via protocols, can be good advocates for biogas use not only as a clean energy source, but also as a wise choice to save our planet and bring back some peace to the world. Nevertheless, more work, experimental and theoretical, needs to be done to improve on biogas upgrading costs and performances.

Nomenclature

d	fiber diameter (cm)
N	fibers number
P	pressure (Pa)
Q	permeance ($cm^3/cm^2.s.Pa$)
U	flow rate (cm^3/s)
x	mole fraction
y	mole fraction
Subscripts	
h	high
l	low
o	outer
Greek letters	
α	permeance selectivity
η	compressor efficiency

Bibliography

1. Cuéllar-Franca, R.M. and Azapagic, A. *Carbon capture, storage and utilisation technologies: A critical analysis and comparison of their life cycle environmental impacts.* Journal of CO_2 Utilization, 2015. **9**: p. 82-102.
2. Leung, D.Y., Caramanna, G., and Maroto-Valer, M.M. *An overview of current status of carbon dioxide capture and storage technologies.* Renewable and Sustainable Energy Reviews, 2014. **39**: p. 426-443.
3. Koytsoumpa, E.I., Bergins, C., and Kakaras, E. *The CO_2 economy: Review of CO_2 capture and reuse technologies.* The Journal of Supercritical Fluids, 2018. **132**: p. 3-16.
4. Merkel, T.C., Lin, H., Wei, X., and Baker, R. *Power plant post-combustion carbon dioxide capture: an opportunity for membranes.* Journal of Membrane Science, 2010. **359**(1-2): p. 126-139.
5. Aaron, D. and Tsouris, C. *Separation of CO_2 from Flue Gas: A Review.* Separation Science and Technology, 2005. **40**(1-3): p. 321-348.
6. Gilassi, S., Taghavi, S.M., Kaliaguine, S., and Rodrigue, D., *Biogas Upgrading and Optimization*, in *Biogas: Production, Applications and Global Developments*, A. Vico , et al., Editors. 2017, Nova Science: USA.
7. Robeson, L.M. *The upper bound revisited.* Journal of Membrane Science, 2008. **320**(1): p. 390-400.
8. Bhide, B. and Stern, S. *Membrane processes for the removal of acid gases from natural gas. I. Process configurations and optimization of operating conditions.* Journal of Membrane Science, 1993. **81**(3): p. 209-237.
9. Ahmad, F., Lau, K., Shariff, A., and Murshid, G. *Process simulation and optimal design of membrane separation system for CO 2 capture from natural gas.* Computers & Chemical Engineering, 2012. **36**: p. 119-128.
10. Deng, L. and Hägg, M.-B. *Techno-economic evaluation of biogas upgrading process using CO_2 facilitated transport membrane.* International Journal of Greenhouse Gas Control, 2010. **4**(4): p. 638-646.
11. Belaissaoui, B., Moullec, Y., Willson, D., and Favre, E. *Hybrid membrane cryogenic process for post-combustion CO_2 capture.* Journal of Membrane Science, 2012. **415**: p. 424-434.
12. Kundu, P.K., Chakma, A., and Feng, X. *Effectiveness of membranes and hybrid membrane processes in comparison with absorption using amines for post-combustion CO_2 capture.* International Journal of Greenhouse Gas Control, 2014. **28**: p. 248-256.
13. Borhani, T., Azarpour, A., Akbari, V., Alwi, S., and Manan, Z. *CO_2 capture with potassium carbonate solutions: A state-of-the-art.* International Journal of Greenhouse Gas Control, 2015. **41**: p. 142-162.
14. Fradette, L., Lefebvre, S., and Carley, J. *Demonstration results of enzyme-accelerated CO_2 capture.* Energy Procedia, 2017. **114**: p. 1100-1109.
15. *Total energy consumption* 2016 [cited 2017 1 June]; Available from: https://yearbook.enerdata.net/.
16. Balzani, V. and Armaroli, N., *Energy for a sustainable world: from the oil age to a sun-powered future*. 2010: John Wiley & Sons.
17. *Canada's Second Biennial Report on Climate Change*. 2016 [cited 2017 1 June]; Available from: https://www.ec.gc.ca/GES-GHG/default.asp?lang=En&n=02D095CB-1.

18. Pires, J., Martins, F., Alvim-Ferraz, M., and Simões, M. *Recent developments on carbon capture and storage: An overview.* Chemical Engineering Research and Design, 2011. **89**(9): p. 1446-1460.
19. Rubin, E.S., Mantripragada, H., Marks, A., Versteeg, P., and Kitchin, J. *The outlook for improved carbon capture technology.* Progress in Energy and Combustion Science, 2012. **38**(5): p. 630-671.
20. Harasimowicz, M., Orluk, P., Zakrzewska-Trznadel, G., and Chmielewski, A. *Application of polyimide membranes for biogas purification and enrichment.* Journal of Hazardous Materials, 2007. **144**(3): p. 698-702.
21. Markoš, J., *Mass Transfer in Chemical Engineering Processes*. 2011, Croatia: InTech.
22. Mansourizadeh, A. and Ismail, A.F. *Hollow fiber gas–liquid membrane contactors for acid gas capture: a review.* Journal of Hazardous Materials, 2009. **171**(1): p. 38-53.
23. Chen, X.Y., Vinh-Thang, H., Ramirez, A.A., Rodrigue, D., and Kaliaguine, S. *Membrane gas separation technologies for biogas upgrading.* RSC Advances, 2015. **5**(31): p. 24399-24448.
24. Zhang, Y., Sunarso, J., Liu, S., and Wang, R. *Current status and development of membranes for CO_2/CH_4 separation: a review.* International Journal of Greenhouse Gas Control, 2013. **12**: p. 84-107.
25. Cui, Z. and Muralidhara, H., *Membrane technology: a practical guide to membrane technology and applications in food and bioprocessing*. 2010, Burlington, USA: Elsevier.
26. Blaisdell, C.T. and Kammermeyer, K. *Counter-current and co-current gas separation.* Chemical Engineering Science, 1973. **28**(6): p. 1249-1255.
27. Oishi, J., Matsura, Y., Higashi, K., and Ike, C. *An analysis of gaseous diffusion separating unit.* Nippon Genshiryoku Gakkai-Shi, 1961. **3**(12): p. 923.
28. Naylor, R.W. and Backer, P.O. *Enrichment calculations in gaseous diffusion: Large separation factor.* AIChE Journal, 1955. **1**(1): p. 95-99.
29. Weller, S. and Steiner, W.A. *Separation of gases by fractional permeation through membranes.* Journal of Applied Physics, 1950. **21**(4): p. 279-283.
30. Brubaker, D.W. and Kammermeyer, K. *Separation of gases by plastic membranes-permeation rates and extent of separation.* Industrial & Engineering Chemistry, 1954. **46**(4): p. 733-739.
31. Pan, C.Y. and Habgood, H. *Gas separation by permeation part I. Calculation methods and parametric analysis.* The Canadian journal of Chemical Engineering, 1978. **56**(2): p. 197-209.
32. Bansal, R., Jain, V., and Gupta, S.K. *Analysis of separation of multicomponent mixtures across membranes in a single permeation unit.* Separation Science and Technology, 1995. **30**(14): p. 2891-2916.
33. Walawender, W. and Stern, S. *Analysis of Membrane Separation Parameters. II. Counter-current and Cocurrent Flow in a Single Permeation Stage.* Separation Science, 1972. **7**(5): p. 553-584.
34. Stern, S. and Walawender Jr, W. *Analysis of membrane separation parameters.* Separation Science and Technology, 1969. **4**(2): p. 129-159.
35. Shindo, Y., Hakuta, T., Yoshitome, H., and Inoue, H. *Calculation methods for multicomponent gas separation by permeation.* Separation Science and Technology, 1985. **20**(5-6): p. 445-459.
36. Pan, C. *Gas separation by high-flux, asymmetric hollow-fiber membrane.* AIChE journal, 1986. **32**(12): p. 2020-2027.
37. Lim, S., Tan, X., and Li, K. *Gas/vapour separation using membranes:: Effect of pressure drop in lumen of hollow fibres.* Chemical Engineering Science, 2000. **55**(14): p. 2641-2652.

38. Murad Chowdhury, M.H., Feng, X., Douglas, P., and Croiset, E. *A new numerical approach for a detailed multicomponent gas separation membrane model and AspenPlus simulation.* Chemical Engineering & Technology, 2005. **28**(7): p. 773-782.
39. Khalilpour, R., Abbas, A., Lai, Z., and Pinnau, I. *Analysis of hollow fibre membrane systems for multicomponent gas separation.* Chemical Engineering Research and Design, 2013. **91**(2): p. 332-347.
40. Khalilpour, R., Abbas, A., Lai, Z., and Pinnau, I. *Modeling and parametric analysis of hollow fiber membrane system for carbon capture from multicomponent flue gas.* AIChE Journal, 2012. **58**(5): p. 1550-1561.
41. Kundu, P.K., Chakma, A., and Feng, X. *Simulation of binary gas separation with asymmetric hollow fibre membranes and case studies of air separation.* The Canadian Journal of Chemical Engineering, 2012. **90**(5): p. 1253-1268.
42. Thundyil, M.J. and Koros, W.J. *Mathematical modeling of gas separation permeators—for radial crossflow, countercurrent, and cocurrent hollow fiber membrane modules.* Journal of Membrane Science, 1997. **125**(2): p. 275-291.
43. Ahmad, F., Lau, K., Shariff, A., and Yeong, Y.F. *Temperature and pressure dependence of membrane permeance and its effect on process economics of hollow fiber gas separation system.* Journal of Membrane Science, 2013. **430**: p. 44-55.
44. Marić, I. *The Joule–Thomson effect in natural gas flow-rate measurements.* Flow Measurement and Instrumentation, 2005. **16**(6): p. 387-395.
45. Marić, I. *A procedure for the calculation of the natural gas molar heat capacity, the isentropic exponent, and the Joule–Thomson coefficient.* Flow Measurement and Instrumentation, 2007. **18**(1): p. 18-26.
46. Coker, D., Freeman, B., and Fleming, G. *Modeling multicomponent gas separation using hollow-fiber membrane contactors.* AIChE journal, 1998. **44**(6): p. 1289-1302.
47. Coker, D., Allen, T., Freeman, B., and Fleming, G. *Nonisothermal model for gas separation hollow-fiber membranes.* AIChE journal, 1999. **45**(7): p. 1451-1468.
48. Lock, S., Lau, K., and Shariff, A. *Effect of recycle ratio on the cost of natural gas processing in countercurrent hollow fiber membrane system.* Journal of Industrial and Engineering Chemistry, 2015. **21**: p. 542-551.
49. Scholz, M., Harlacher, T., Melin, T., and Wessling, M. *Modeling gas permeation by linking nonideal effects.* Industrial & Engineering Chemistry Research, 2012. **52**(3): p. 1079-1088.
50. Hosseini, S.S., Roodashti, S.M., Kundu, P.K., and Tan, N.R. *Transport properties of asymmetric hollow fiber membrane permeators for practical applications: Mathematical modelling for binary gas mixtures.* The Canadian Journal of Chemical Engineering, 2015. **93**(7): p. 1275-1287.
51. Faiz, R. and Al-Marzouqi, M. *Mathematical modeling for the simultaneous absorption of CO_2 and H_2S using MEA in hollow fiber membrane contactors.* Journal of Membrane Science, 2009. **342**(1): p. 269-278.
52. Ghasem, N., Al-Marzouqi, M., and Rahim, N.A. *Modeling of CO_2 absorption in a membrane contactor considering solvent evaporation.* Separation and Purification Technology, 2013. **110**: p. 1-10.
53. Luis, P., Garea, A., and Irabien, A. *Modelling of a hollow fibre ceramic contactor for SO_2 absorption.* Separation and Purification Technology, 2010. **72**(2): p. 174-179.
54. Wang, R., Li, D., and Liang, D. *Modeling of CO_2 capture by three typical amine solutions in hollow fiber membrane contactors.* Chemical Engineering and Processing: Process Intensification, 2004. **43**(7): p. 849-856.

55. Rezakazemi, M., Niazi, Z., Mirfendereski, M., Shirazian, S., Mohammadi, T., and Pak, A. *CFD simulation of natural gas sweetening in a gas–liquid hollow-fiber membrane contactor.* Chemical Engineering Journal, 2011. **168**(3): p. 1217-1226.
56. Sohrabi, M.R., Marjani, A., Moradi, S., Davallo, M., and Shirazian, S. *Mathematical modeling and numerical simulation of CO_2 transport through hollow-fiber membranes.* Applied Mathematical Modelling, 2011. **35**(1): p. 174-188.
57. Eslami, S., Mousavi, S.M., Danesh, S., and Banazadeh, H. *Modeling and simulation of CO_2 removal from power plant flue gas by PG solution in a hollow fiber membrane contactor.* Advances in Engineering Software, 2011. **42**(8): p. 612-620.
58. Gilassi, S. and Rahmanian, N. *CFD modelling of a hollow Fibre membrane for CO_2 removal by aqueous amine solutions of MEA, DEA and MDEA.* International Journal of Chemical Reactor Engineering, 2016. **14**(1): p. 53-61.
59. Wang, R., Zhang, H., Feron, P., and Liang, D. *Influence of membrane wetting on CO_2 capture in microporous hollow fiber membrane contactors.* Separation and Purification Technology, 2005. **46**(1): p. 33-40.
60. Zhang, H.-Y., Wang, R., Liang, D.T., and Tay, J.H. *Theoretical and experimental studies of membrane wetting in the membrane gas–liquid contacting process for CO_2 absorption.* Journal of Membrane Science, 2008. **308**(1): p. 162-170.
61. Tranchino, L., Santarossa, R., Carta, F., Fabiani, C., and Bimbi, L. *Gas separation in a membrane unit: experimental results and theoretical predictions.* Separation Science and Technology, 1989. **24**(14): p. 1207-1226.
62. Sidhoum, M., Sengupta, A., and Sirkar, K. *Asymmetric cellulose acetate hollow fibers: studies in gas permeation.* AIChE journal, 1988. **34**(3): p. 417-425.
63. Feng, X., Ivory, J., and Rajan, V.S. *Air separation by integrally asymmetric hollow-fiber membranes.* AIChE journal, 1999. **45**(10): p. 2142-2152.
64. Rautenbach, R., Knauf, R., Struck, A., and Vier, J. *Simulation and design of membrane plants with AspenPlus.* Chemical Engineering & Technology, 1996. **19**(5): p. 391-397.
65. Sada, E., Kumazawa, H., Wang, J.S., and Koizumi, M. *Separation of carbon dioxide by asymmetric hollow fiber membrane of cellulose triacetate.* Journal of Applied Polymer Science, 1992. **45**(12): p. 2181-2186.
66. Sircar, S. and Golden, T. *Purification of hydrogen by pressure swing adsorption.* Separation Science and Technology, 2000. **35**(5): p. 667-687.
67. Prasad, R., Shaner, R., and Doshi, K. *Comparison of membranes with other gas separation technologies.* Polymeric Gas Separation Membranes, 1994: p. 531-614.
68. Gottschlich, D.E. and Roberts, D.L., *Energy minimization of separation processes using conventional/membrane hybrid systems*. 1990, EG and G Idaho, Inc., Idaho Falls, ID (USA).
69. Smith, A. and Klosek, J. *A review of air separation technologies and their integration with energy conversion processes.* Fuel Processing Technology, 2001. **70**(2): p. 115-134.
70. Baker, R.W. *Future directions of membrane gas separation technology.* Industrial & engineering chemistry research, 2002. **41**(6): p. 1393-1411.
71. Chen, X.Y., Kaliaguine, S., and Rodrigue, D. *A Comparison between Several Commercial Polymer Hollow Fiber Membranes for Gas Separation.* Journal of Membrane and Separation Technology, 2017. **6**(1): p. 1-15.
72. Tien-Binh, N., Vinh-Thang, H., Chen, X.Y., Rodrigue, D., and Kaliaguine, S. *Crosslinked MOF-polymer to enhance gas separation of mixed matrix membranes.* Journal of Membrane Science, 2016. **520**: p. 941-950.
73. Deublein, D. and Steinhauser, A., *Biogas from waste and renewable resources: an introduction*. 2011, Mörlenbach: Wiley-VCH.

74. Shen, Y., Linville, J.L., Urgun-Demirtas, M., Mintz, M.M., and Snyder, S.W. *An overview of biogas production and utilization at full-scale wastewater treatment plants (WWTPs) in the United States: challenges and opportunities towards energy-neutral WWTPs.* Renewable and Sustainable Energy Reviews, 2015. **50**: p. 346-362.
75. Persson, M., Jönsson, O., and Wellinger, A. *Biogas upgrading to vehicle fuel standards and grid injection*. in *IEA Bioenergy task*. 2006.
76. Petersson, A. and Wellinger, A. *Biogas upgrading technologies–developments and innovations.* IEA bioenergy, 2009. **20**: p. 1-19.
77. Andriani, D., Wresta, A., Atmaja, T.D., and Saepudin, A. *A review on optimization production and upgrading biogas through CO_2 removal using various techniques.* Applied Biochemistry and Biotechnology, 2014. **172**(4): p. 1909-1928.
78. Sun, Q., Li, H., Yan, J., Liu, L., Yu, Z., and Yu, X. *Selection of appropriate biogas upgrading technology-a review of biogas cleaning, upgrading and utilisation.* Renewable and Sustainable Energy Reviews, 2015. **51**: p. 521-532.
79. Bauer, F., Hulteberg, C., Persson, T., and Tamm, D., *Biogas upgrading-Review of commercial technologies*, in *SGC Rapport*. 2013, Svenskt gastekniskt center.
80. Shao, P., Dal-Cin, M., Kumar, A., Li, H., and Singh, D.P. *Design and economics of a hybrid membrane–temperature swing adsorption process for upgrading biogas.* Journal of Membrane Science, 2012. **413**: p. 17-28.
81. Rasi, S., Läntelä, J., and Rintala, J. *Trace compounds affecting biogas energy utilisation–A review.* Energy Conversion and Management, 2011. **52**(12): p. 3369-3375.
82. Wang, M., Lawal, A., Stephenson, P., Sidders, J., and Ramshaw, C. *Post-combustion CO_2 capture with chemical absorption: a state-of-the-art review.* Chemical Engineering Research and Design, 2011. **89**(9): p. 1609-1624.
83. Gilassi, S., Taghavi, S.M., Kaliaguine, S., and Rodrigue, D., *Biogas: Biogas Upgrading and Optimization*. Production, Applications and Global Developments, ed. A. Vico , et al. 2017, USA: Nova Science.
84. Muñoz, R., Meier, L., Diaz, I., and Jeison, D. *A review on the state-of-the-art of physical/chemical and biological technologies for biogas upgrading.* Reviews in Environmental Science and Bio/Technology, 2015. **14**(4): p. 727-759.
85. Zhao, Q., Leonhardt, E., MacConnell, C., Frear, C., and Chen, S. *Purification technologies for biogas generated by anaerobic digestion.* Compressed Biomethane, CSANR, Ed, 2010.
86. Ryckebosch, E., Drouillon, M., and Vervaeren, H. *Techniques for transformation of biogas to biomethane.* Biomass and Bioenergy, 2011. **35**(5): p. 1633-1645.
87. Baker, R.W. and Lokhandwala, K. *Natural gas processing with membranes: an overview.* Industrial & Engineering Chemistry Research, 2008. **47**(7): p. 2109-2121.
88. Callison, A. and Davidson, G. *Offshore processing plant uses membranes for CO_2 removal.* Oil & Gas Journal, 2007. **105**(20): p. 56-56.
89. Pan, C. *Gas separation by permeators with high-flux asymmetric membranes.* AIChE Journal, 1983. **29**(4): p. 545-552.
90. Gilassi, S., Taghavi, S.M., Rodrigue, D., and Kaliaguine, S. *Simulation of gas separation using partial element stage cut modeling of hollow fiber membrane modules.* AIChE Journal, 2018. **64**(5): p. 1766-1777.
91. Li, K., Acharya, D., and Hughes, R. *Mathematical modelling of multicomponent membrane permeators.* Journal of Membrane Science, 1990. **52**(2): p. 205-219.
92. Lock, S., Lau, K., Ahmad, F., and Shariff, A. *Modeling, simulation and economic analysis of CO_2 capture from natural gas using cocurrent, countercurrent and radial crossflow hollow fiber membrane.* International Journal of Greenhouse Gas Control, 2015. **36**: p. 114-134.

93. Dehkordi, J.A., Hosseini, S.S., Kundu, P.K., and Tan, N.R. *Mathematical modeling of natural gas separation using hollow fiber membrane modules by application of finite element method through statistical analysis.* Chemical Product and Process Modeling, 2016. **11**(1): p. 11-15.
94. Qi, R. and Henson, M.A. *Membrane system design for multicomponent gas mixtures via mixed-integer nonlinear programming.* Computers & Chemical Engineering, 2000. **24**(12): p. 2719-2737.
95. Scholz, M., Alders, M., Lohaus, T., and Wessling, M. *Structural optimization of membrane-based biogas upgrading processes.* Journal of Membrane Science, 2015. **474**: p. 1-10.
96. Uppaluri, R.V., Linke, P., and Kokossis, A.C. *Synthesis and optimization of gas permeation membrane networks.* Industrial & Engineering Chemistry Research, 2004. **43**(15): p. 4305-4322.
97. Bhide, B. and Stern, S. *A new evaluation of membrane processes for the oxygen-enrichment of air. I. Identification of optimum operating conditions and process configuration.* Journal of Membrane Science, 1991. **62**(1): p. 13-35.
98. Arias, A.M., Mussati, M.C., Mores, P.L., Scenna, N.J., Caballero, J.A., and Mussati, S.F. *Optimization of multi-stage membrane systems for CO_2 capture from flue gas.* International Journal of Greenhouse Gas Control, 2016. **53**: p. 371-390.
99. Purnomo, I. and Alpay, E. *Membrane column optimisation for the bulk separation of air.* Chemical Engineering Science, 2000. **55**(18): p. 3599-3610.
100. Chang, H. and Hou, W.-C. *Optimization of membrane gas separation systems using genetic algorithm.* Chemical Engineering Science, 2006. **61**(16): p. 5355-5368.
101. Datta, A.K. and Sen, P.K. *Optimization of membrane unit for removing carbon dioxide from natural gas.* Journal of Membrane Science, 2006. **283**(1-2): p. 291-300.
102. Kookos, I.K. *A targeting approach to the synthesis of membrane networks for gas separations.* Journal of Membrane Science, 2002. **208**(1-2): p. 193-202.
103. Peters, M.S., Timmerhaus, K.D., West, R.E., Timmerhaus, K., and West, R., *Plant design and economics for chemical engineers*. Vol. 4. 1968, New York: McGraw-Hill.
104. Turton, R., Bailie, R.C., Whiting, W.B., and Shaeiwitz, J.A., *Analysis, synthesis and design of chemical processes*. 2008, Boston: Pearson Education.
105. Bergman, T.L., Incropera, F.P., DeWitt, D.P., and Lavine, A.S., *Fundamentals of heat and mass transfer*. 2011, New York: John Wiley & Sons.
106. Zhang, C. and Koros, W.J. *Ultraselective carbon molecular sieve membranes with tailored synergistic sorption selective properties.* Advanced Materials, 2017. **29**(33): p. 1701631.
107. Tien-Binh, N., Rodrigue, D., and Kaliaguine, S. *In-situ cross interface linking of PIM-1 polymer and UiO-66-NH2 for outstanding gas separation and physical aging control.* Journal of Membrane Science, 2018. **548**: p. 429-438.
108. Haider, S., Lindbråthen, A., and Hägg, M.-B. *Techno-economical evaluation of membrane based biogas upgrading system: A comparison between polymeric membrane and carbon membrane technology.* Green Energy & Environment, 2016. **1**(3): p. 222-234.
109. Aliaga-Vicente, A., Caballero, J.A., and Fernández-Torres, M.J. *Synthesis and optimization of membrane cascade for gas separation via mixed-integer nonlinear programming.* AIChE Journal, 2017. **63**(6): p. 1989-2006.
110. *The Global Status of CCS*. 2019 [cited 2019 1 December]; Available from: https://indd.adobe.com/view/2dab1be7-edd0-447d-b020-06242ea2cf3b.
111. Cebrucean, D., Cebrucean, V., and Ionel, I. *CO_2 Capture and Storage from Fossil Fuel Power Plants.* Energy Procedia, 2014. **63**: p. 18-26.

112. *Greenhouse gas sources and sinks: executive summary 2018*. 2018 [cited 2019 18 January]; Available from: https://www.canada.ca/en/environment-climate-change/services/climate-change/greenhouse-gas-emissions/sources-sinks-executive-summary-2018.html.
113. Andrew, R.M. *Global CO_2 emissions from cement production.* Earth Syst. Sci. Data, 2018. **10**(1): p. 195-217.
114. Amrollahi, Z., Ystad, P., Ertesvåg, I.S., and Bolland, O. *Optimized process configurations of post-combustion CO_2 capture for natural-gas-fired power plant – Power plant efficiency analysis.* International Journal of Greenhouse Gas Control, 2012. **8**: p. 1-11.
115. Liang, Z., Rongwong, W., Liu, H., Fu, K., Gao, H., Cao, F., Zhang, R., Sema, T., Henni, A., Sumon, K., Nath, D., Gelowitz, D., Srisang, W., Saiwan, C., Benamor, A., Al-Marri, M., Shi, H., Supap, T., Chan, C., Zhou, Q., Abu-Zahra, M., Wilson, M., Olson, W., Idem, R., and Tontiwachwuthikul, P. *Recent progress and new developments in post-combustion carbon-capture technology with amine based solvents.* International Journal of Greenhouse Gas Control, 2015. **40**: p. 26-54.
116. Singh, A., Sharma, Y., Wupardrasta, Y., and Desai, K. *Selection of amine combination for CO_2 capture in a packed bed scrubber.* Resource-Efficient Technologies, 2016. **2**: p. S165-S170.
117. Li, X., Wang, S., and Chen, C. *Experimental Study of Energy Requirement of CO_2 Desorption from Rich Solvent.* Energy Procedia, 2013. **37**: p. 1836-1843.
118. Chang, H. and Shih, C.M. *Simulation and optimization for power plant flue gas CO_2 absorption-stripping systems.* Separation Science and Technology, 2005. **40**(4): p. 877-909.
119. Alie, C., Backham, L., Croiset, E., and Douglas, P.L. *Simulation of CO_2 capture using MEA scrubbing: a flowsheet decomposition method.* Energy Conversion and Management, 2005. **46**(3): p. 475-487.
120. Singh, D., Croiset, E., Douglas, P.L., and Douglas, M.A. *Techno-economic study of CO_2 capture from an existing coal-fired power plant: MEA scrubbing vs. O_2/CO_2 recycle combustion.* Energy Conversion and Management, 2003. **44**(19): p. 3073-3091.
121. Abu-Zahra, M.R.M., Schneiders, L.H.J., Niederer, J.P.M., Feron, P.H.M., and Versteeg, G.F. *CO_2 capture from power plants: Part I. A parametric study of the technical performance based on monoethanolamine.* International Journal of Greenhouse gas control, 2007. **1**: p. 37-46.
122. Wang, Y., Zhao, L., Otto, A., Robinius, M., and Stolten, D. *A Review of Post-combustion CO_2 Capture Technologies from Coal-fired Power Plants.* Energy Procedia, 2017. **114**: p. 650-665.
123. Hinkov, I., Lamari, F.D., Langlois, P., Dicko, M., Chilev, C., and Pentchev, I. *Carbon dioxide capture by adsorption.* Journal of Chemical Technology & Metallurgy, 2016. **51**(6).
124. Sayari, A., Belmabkhout, Y., and Serna-Guerrero, R. *Flue gas treatment via CO_2 adsorption.* Chemical Engineering Journal, 2011. **171**(3): p. 760-774.
125. Dutcher, B., Fan, M., and Russell, A.G. *Amine-based CO_2 capture technology development from the beginning of 2013-A Review.* ACS Applied Materials & Interfaces, 2015. **7**(4): p. 2137-2148.
126. Ntiamoah, A., Ling, J., Xiao, P., Webley, P.A., and Zhai, Y. *CO_2 Capture by Temperature Swing Adsorption: Use of Hot CO_2-Rich Gas for Regeneration.* Industrial & Engineering Chemistry Research, 2016. **55**(3): p. 703-713.
127. Riboldi, L., Bolland, O., Ngoy, J.M., and Wagner, N. *Full-plant Analysis of a PSA CO_2 Capture Unit Integrated In Coal-fired Power Plants: Post-and Pre-combustion Scenarios.* Energy Procedia, 2014. **63**: p. 2289-2304.
128. Webley, P.A. *Adsorption technology for CO_2 separation and capture: a perspective.* Adsorption, 2014. **20**(2-3): p. 225-231.

129. Chaffee, A.L., Knowles, G.P., Liang, Z., Zhang, J., Xiao, P., and Webley, P.A. *CO_2 capture by adsorption: Materials and process development.* International Journal of Greenhouse Gas Control, 2007. **1**(1): p. 11-18.
130. Wolsky, A.M., Daniels, E.J., and Jody, B.J. *CO_2 capture from the flue gas of conventional fossil-fuel-fired power plants.* Environmental Progress, 1994. **13**(3): p. 214-219.
131. Tuinier, M.J., Hamers, H.P., and van Annaland, S.M. *Techno-economic evaluation of cryogenic CO_2 capture—A comparison with absorption and membrane technology.* International Journal of Greenhouse Gas Control, 2011. **5**(6): p. 1559-1565.
132. Clodic, D. and Younes, M. *A new Method for CO_2 Capture: Frosting CO_2 at Atmospheric Pressure*. in *Greenhouse Gas Control Technologies-6th International Conference*. 2003. Elsevier.
133. Hart, A. and Gnanendran, N. *Cryogenic CO_2 capture in natural gas.* Energy Procedia, 2009. **1**(1): p. 697-706.
134. Song, C.-F., Kitamura, Y., Li, S.-H., and Ogasawara, K. *Design of a cryogenic CO_2 capture system based on Stirling coolers.* International Journal of Greenhouse Gas Control, 2012. **7**: p. 107-114.
135. Song, C., Liu, Q., Deng, S., Li, H., and Kitamura, Y. *Cryogenic-based CO_2 capture technologies: State-of-the-art developments and current challenges.* Renewable and Sustainable Energy Reviews, 2019. **101**: p. 265-278.
136. Tuinier, M.J., van Annaland, S.M., and Kuipers, J.A.M. *A novel process for cryogenic CO_2 capture using dynamically operated packed beds—An experimental and numerical study.* International Journal of Greenhouse Gas Control, 2011. **5**(4): p. 694-701.
137. Bernardo, P. and Clarizia, G. *30 years of membrane technology for gas separation.* Chemical Engineering, 2013. **32**: p. 1999-2004.
138. Schlumberger. *CYNARA Acid Gas Removal Membrane Systems*. 2019 [cited 2019 23 January]; Available from: https://www.slb.com/services/processing-separation/gas-treatment/acid-gas-treatment-removal/cynara-acid-gas-removal-membrane.aspx.
139. Merkel, T., Amo, K., Baker, R., Daniels, R., Friat, B., He, Z., Lin, H., and Serbanescu, A., *Membrane process to sequester CO_2 from power plant flue gas*. 2009, Membrane Technology & Research Incorporated.
140. Ramasubramanian, K., Verweij, H., and Ho, W.S. *Membrane processes for carbon capture from coal-fired power plant flue gas: A modeling and cost study.* Journal of Membrane Science, 2012. **421**: p. 299-310.
141. Chen, X., Kaliaguine, S., and Rodrigue, D. *Correlation between Performances of Hollow Fibers and Flat Membranes for Gas Separation.* Separation & Purification Reviews, 2017: p. 1-22.
142. Fong, J., Anderson, C.J., Xiao, G., Webley, P.A., and Hoadley, A.F.A. *Multi-objective optimisation of a hybrid vacuum swing adsorption and low-temperature post-combustion CO_2 capture.* Journal of Cleaner Production, 2016. **111**: p. 193-203.
143. Merkel, T.C., Lin, H., Wei, X., and Baker, R. *Power plant post-combustion carbon dioxide capture: an opportunity for membranes.* Journal of membrane science, 2010. **359.1**(2): p. 126-139.
144. Ling, H., Liu, S., Gao, H., and Liang, Z. *Effect of heat-stable salts on absorption/desorption performance of aqueous monoethanolamine (MEA) solution during carbon dioxide capture process.* Separation and Purification Technology, 2018. **212**: p. 822-833.
145. Pellegrini, L.A., Moioli, S., and Gamba, S. *Energy saving in a CO_2 capture plant by MEA scrubbing.* Chemical Engineering Research and Design, 2011. **89**(9): p. 1676-1683.

146. Oyenekan, B.A. and Rochelle, G.T. *Energy Performance of Stripper Configurations for CO_2 Capture by Aqueous Amines.* Industrial & Engineering Chemistry Research, 2006. **45**(8): p. 2457-2464.
147. Oyenekan, B.A. and Rochelle, G.T. *Alternative stripper configurations for CO_2 capture by aqueous amines.* AIChE Journal, 2007. **53**(12): p. 3144-3154.
148. Moullec, L.Y. and Kanniche, M. *Screening of flowsheet modifications for an efficient monoethanolamine (MEA) based post-combustion CO_2 capture.* International Journal of Greenhouse Gas Control, 2011. **5**(4): p. 727-740.
149. Chen, S., Lu, Y., and Rostam-Abadi, M., *Integrated vacuum absorption steam cycle gas separation*. 2011, Google Patents.
150. Moullec, Y., Neveux, T., Azki, A., Chikukwa, A., and Hoff, K. *Process modifications for solvent-based post-combustion CO_2 capture.* International Journal of Greenhouse Gas Control, 2014. **31**: p. 96-112.
151. Cousins, A., Wardhaugh, L.T., and Feron, M. *A survey of process flow sheet modifications for energy efficient CO_2 capture from flue gases using chemical absorption.* International Journal of Greenhouse Gas Control, 2011. **5**: p. 605-619.
152. Oh, S.-Y., Binns, M., Cho, H., and Kim, J.-K. *Energy minimization of MEA-based CO_2 capture process.* Applied Energy, 2016. **169**: p. 353-362.
153. Li, K., Leigh, W., Feron, P., Yu, H., and Tade, M. *Systematic study of aqueous monoethanolamine (MEA)-based CO_2 capture process: techno-economic assessment of the MEA process and its improvements.* Applied Energy, 2016. **165**: p. 648-659.
154. Alie, C., Douglas, P., and Croiset, E. *Simulation and optimization of a coal-fired power plant with integrated CO_2 capture using MEA scrubbing*. in *Proceedings of the Eighth International Conference on Greenhouse Gas Control Technologies*. 2006.
155. Zhai, R., Yang, Y., Oakey, J.E., and Susini, G.A. *Integration and evaluation of a power plant with a monoethanolamine-based CO_2-capture process.* Carbon Management, 2014. **3**(6): p. 541-551.
156. Sanpasertparnich, T., Idem, R., Bolea, I., and Tontiwachwuthikul, P. *Integration of post-combustion capture and storage into a pulverized coal-fired power plant.* International Journal of Greenhouse Gas Control, 2010. **4**: p. 499-510.
157. Zhang, G., Yang, Y., Xu, G., Zhang, K., and Zhang, D. *CO_2 capture by chemical absorption in coal-fired power plants: Energy-saving mechanism, proposed methods, and performance analysis.* International Journal of Greenhouse Gas Control, 2015. **39**: p. 449-462.
158. Goto, K., Yogo, K., and Higashii, T. *A review of efficiency penalty in a coal-fired power plant with post-combustion CO_2 capture.* Applied Energy, 2013. **111**: p. 710-720.
159. Duan, L., Zhao, M., and Yang, Y. *Integration and optimization study on the coal-fired power plant with CO_2 capture using MEA.* Energy, 2012. **45**(1): p. 107-116.
160. Farajollahi, H. and Hossainpour, S. *Application of organic Rankine cycle in integration of thermal power plant with post-combustion CO_2 capture and compression.* Energy, 2017. **118**: p. 927-936.
161. Mota-Martinez, M.T. and Hallett, J.P. *Solvent selection and design for CO_2 capture–how we might have been missing the point.* Sustainable Energy & Fuels, 2017. **1**(10): p. 2078-2090.
162. Nwaoha, C., Supap, T., Idem, R., Saiwan, C., Tontiwachwuthikul, P., Al-Marri, M.J., and Benamor, A. *Advancement and new perspectives of using formulated reactive amine blends for post-combustion carbon dioxide (CO_2) capture technologies.* Petroleum, 2017. **3**(1): p. 10-36.

163. Mumford, K.A., Wu, Y., Smith, K.H., and Stevens, G.W. *Review of solvent based carbon-dioxide capture technologies.* Frontiers of Chemical Science and Engineering, 2015. **9**(2): p. 125-141.
164. Fernandez, S.E., Goetheer, E.L.V., Manzolini, G., Macchi, E., Rezvani, S., and Vlugt, T.J.H. *Thermodynamic assessment of amine based CO_2 capture technologies in power plants based on European Benchmarking Task Force methodology.* Fuel, 2014. **129**: p. 318-329.
165. *CO_2 Enhanced Separation and Recovery*. 2011 [cited 2019 1 December]; Available from: https://cordis.europa.eu/project/rcn/88422/reporting/en.
166. Mangalapally, H., Notz, R., Asprion, N., Sieder, G., Garcia, H., and Hasse, H. *Pilot plant study of four new solvents for post combustion carbon dioxide capture by reactive absorption and comparison to MEA.* International Journal of Greenhouse Gas Control, 2012. **8**: p. 205-216.
167. von Harbou, I., Mangalapally, H., and Hasse, H. *Pilot plant experiments for two new amine solvents for post-combustion carbon dioxide capture.* International Journal of Greenhouse Gas Control, 2013. **18**: p. 305-314.
168. Davis, J.D., *Thermal degradation of aqueous amines used for carbon dioxide capture*, in *Chemical Engineering*. 2009, The University of Texas at Austin: USA.
169. Wang, T. and Jens, K.-J. *Oxidative degradation of aqueous PZ solution and AMP/PZ blends for post-combustion carbon dioxide capture.* International Journal of Greenhouse Gas Control, 2014. **24**: p. 98-105.
170. Dash, S.K., Samanta, A.N., and Bandyopadhyay, S.S. *Simulation and parametric study of post combustion CO_2 capture process using (AMP+ PZ) blended solvent.* International Journal of Greenhouse Gas Control, 2014. **21**: p. 130-139.
171. Hu, G., Nicholas, N.J., Smith, K.H., Mumford, K.A., Kentish, S.E., and Stevens, G.W. *Carbon dioxide absorption into promoted potassium carbonate solutions: A review.* International Journal of Greenhouse Gas Control, 2016. **53**: p. 28-40.
172. Mumford, K.A., Smith, K.H., Anderson, C.J., Shen, S., Tao, W., Suryaputradinata, Y.A., Qader, A., Hooper, B., Innocenzi, R.A., Kentish, S.E., and Stevens, G.W. *Post-combustion Capture of CO_2: Results from the Solvent Absorption Capture Plant at Hazelwood Power Station Using Potassium Carbonate Solvent.* Energy & Fuels, 2012. **26**(1): p. 138-146.
173. Thee, H., Suryaputradinata, Y.A., Mumford, K.A., Smith, K.H., da Silva, G., Kentish, S.E., and Stevens, G.W. *A kinetic and process modeling study of CO_2 capture with MEA-promoted potassium carbonate solutions.* Chemical engineering journal, 2012. **210**: p. 271-279.
174. Thee, H., Nicholas, N., Smith, K.H., da Silva, G., Kentish, S.E., and Stevens, G.W. *A kinetic study of CO_2 capture with potassium carbonate solutions promoted with various amino acids: glycine, sarcosine and proline.* International Journal of Greenhouse Gas Control, 2014. **20**: p. 212-222.
175. Ye, X. and Lu, Y. *CO_2 absorption into catalyzed potassium carbonate–bicarbonate solutions: Kinetics and stability of the enzyme carbonic anhydrase as a biocatalyst.* Chemical Engineering Science, 2014. **116**: p. 567-575.
176. Zhang, S. and Lu, Y. *Kinetic performance of CO_2 absorption into a potassium carbonate solution promoted with the enzyme carbonic anhydrase: Comparison with a monoethanolamine solution.* Chemical Engineering Journal, 2015. **279**: p. 335-343.
177. Astarita, G., Savage, D.W., and Longo, J.M. *Promotion of CO_2 mass transfer in carbonate solutions.* Chemical Engineering Science, 1981. **36**: p. 581-588.
178. Sanyal, D., Vasishtha, N., and Saraf, D.N. *Modeling of carbon dioxide absorber using hot carbonate process.* Industrial & Engineering Chemistry Research, 1988. **27**(11): p. 2149-2156.

179. Danckwerts, P.V. *The absorption of carbon dioxide into solutions of alkalis and amines (with some notes on hydrogen sulfide and carbonyl sulfide).* The Chemical Engineer, 1966: p. 244-280.
180. Lu, Y., Ye, X., Zhang, Z., Khodayari, A., and Djukadi, T. *Development of a carbonate absorption-based process for post-combustion CO_2 capture: the role of biocatalyst to promote CO_2 absorption rate.* Energy Procedia, 2011. **4**: p. 1286-1293.
181. Russo, M.E., Olivieri, G., Marzocchella, A., Salatino, P., Caramuscio, P., and Cavaleiro, C. *Post-combustion carbon capture mediated by carbonic anhydrase.* Separation and Purification Technology, 2013. **107**: p. 331-339.
182. Gilassi, S., Taghavi, S.M., Rodrigue, D., and Kaliaguine, S. *Optimizing membrane module for biogas separation.* International Journal of Greenhouse Gas Control, 2019. **83**: p. 195-207.
183. Marriott, J. and Sørensen, E. *The optimal design of membrane systems.* Chemical Engineering Science, 2003. **58**(22): p. 4991-5004.
184. Austgen, D.M., Rochelle, G.T., Peng, X., and Chen, C. *Model of vapor-liquid equilibria for aqueous acid gas-alkanolamine systems using the electrolyte-NRTL equation.* Industrial & Engineering Chemistry Research, 1989. **28**(7): p. 1060-1073.
185. Zaks, A. and Reardon, J., *Advanced Low Energy Enzyme Catalyzed Solvent for CO_2 Capture*. 2013, Akermin Inc., St. Louis, MO (United States).
186. Raynal, L., Bouillon, P.-A., Gomez, A., and Broutin, P. *From MEA to demixing solvents and future steps, a roadmap for lowering the cost of post-combustion carbon capture.* Chemical Engineering Journal, 2011. **171**: p. 742-752.
187. Ulrich, G.D. and Vasudevan, P.T., *Chemical engineering: process design and economics; a practical guide*. 2004: Process Publ.
188. Mores, P.L., Arias, A.M., Scenna, N.J., Mussati, M.C., and Mussati, S.F. *Cost-based comparison of multi-stage membrane configurations for carbon capture from flue gas of power plants.* International Journal of Greenhouse Gas Control, 2019. **86**: p. 177-190.
189. Qi, G., Liu, K., Frimpong, R.A., House, A., Salmon, S., and Liu, K. *Integrated bench-scale parametric study on CO_2 capture using a carbonic anhydrase promoted K_2CO_3 solvent with low temperature vacuum stripping.* Industrial & Engineering Chemistry Research, 2016. **55**(48): p. 12452-12459.
190. Lu, Y., Rostam-Abadi, M., Ye, X., Zhang, S., Ruhter, D., Khodayari, A., and Rood, M., *Development and Evaluation of a Novel Integrated Vacuum Carbonate Absorption Process*. 2012, University of Illinois.
191. Warudkar, S.S., Cox, K.R., Wong, M.S., and Hirasaki, G.J. *Influence of stripper operating parameters on the performance of amine absorption systems for post-combustion carbon capture: Part I. High pressure strippers.* International Journal of Greenhouse Gas Control, 2013. **16**: p. 342-350.
192. (IEA), I.E.A. *Global Energy & CO_2 Status Report 2017*. 2018 [cited 2019 1 December]; Available from: https://www.connaissancedesenergies.org/sites/default/files/pdf-actualites/geco2017.pdf.
193. Daisy, D. *Rising CO_2 levels could push 'hundreds of millions' into malnutrition by 2050*. 2018 [cited 2019 1 December]; Available from: https://www.carbonbrief.org/rising-co2-levels-could-push-hundreds-of-millions-into-malnutrition-by-2050.
194. UNFCCC, C. *United Nations framework convention on climate change*. 1992 [cited 2019 1 December]; Available from: https://unfccc.int/resource/docs/convkp/conveng.pdf.
195. UNFCCC. *Adoption of the Paris Agreement*. 2015 [cited 2019 1 December]; Available from: https://unfccc.int/resource/docs/2015/cop21/eng/l09.pdf.

196. Agency, I.R.E. *Global energy transformation; a road map to 2050*. 2018 [cited 2019 1 December]; Available from: https://www.irena.org/-/media/Files/IRENA/Agency/Publication/2018/Apr/IRENA_Report_GET_2018.pdf.
197. Bui, M., Adjiman, C.S., Bardow, A., Anthony, E.J., Boston, A., Brown, S., Fennell, P.S., Fuss, S., Galindo, A., and Hackett, L.A. *Carbon capture and storage (CCS): the way forward.* Energy & Environmental Science, 2018. **11**(5): p. 1062-1176.
198. Gilassi, S., Taghavi, S.M., Kaliaguine, S., and Rodrigue, D., *Biogas Upgrading and Optimization*, in *Biogas: Production, Applications and Global Developments:*, A. Vico , et al., Editors. 2017, Nova Science: USA.
199. Yang, H., Xu, Z., Fan, M., Gupta, R., Slimane, R.B., Bland, A.E., and Wright, I. *Progress in carbon dioxide separation and capture: A review.* Journal of Environmental Sciences, 2008. **20**(1): p. 14-27.
200. Yu, H., Qi, G., Xiang, Q., Wang, S., Fang, M., Yang, Q., Wardhaugh, L., and Feron, P. *Aqueous ammonia based post combustion capture: results from pilot plant operation, challenges and further opportunities.* Energy Procedia, 2013. **37**: p. 6256-6264.
201. Ciftja, A.F., Hartono, A., and Svendsen, H.F. *Selection of Amine Amino Acids Salt Systems for CO_2 Capture.* Energy Procedia, 2013. **37**: p. 1597-1604.
202. Clausse, M., Bonjour, J., and Meunier, F. *Adsorption of gas mixtures in TSA adsorbers under various heat removal conditions.* Chemical Engineering Science, 2004. **59**(17): p. 3657-3670.
203. Liu, Z., Wang, L., Kong, X., Li, P., Yu, J., and Rodrigues, A.E. *Onsite CO_2 Capture from Flue Gas by an Adsorption Process in a Coal-Fired Power Plant.* Industrial & Engineering Chemistry Research, 2012. **51**(21): p. 7355-7363.
204. Maqsood, K., Mullick, A., Ali, A., Kargupta, K., and Ganguly, S. *Cryogenic carbon dioxide separation from natural gas: a review based on conventional and novel emerging technologies.* Reviews in Chemical Engineering, 2014. **30**(5): p. 453-477.
205. Figueroa, J.D., Fout, T., Plasynski, S., McIlvried, H., and Srivastava, R.D. *Advances in CO_2 capture technology—The U.S. Department of Energy's Carbon Sequestration Program.* International Journal of Greenhouse Gas Control, 2008. **2**(1): p. 9-20.
206. Scholes, C.A., Ho, M.T., Wiley, D.E., Stevens, G.W., and Kentish, S.E. *Cost competitive membrane—cryogenic post-combustion carbon capture.* International Journal of Greenhouse Gas Control, 2013. **17**.
207. Freeman, B., Hao, P., Baker, R., Kniep, J., Chen, E., Ding, J., Zhang, Y., and Rochelle, G.T. *Hybrid membrane-absorption CO_2 capture process.* Energy Procedia, 2014. **63**: p. 605-613.
208. Kusuma, V.A., Li, Z., Hopkinson, D., Luebke, D.R., and Chen, S. *Evaluating the energy performance of a hybrid membrane-solvent process for flue gas carbon dioxide capture.* Industrial & Engineering Chemistry Research, 2016. **55**(43): p. 11329-11337.
209. Belaissaoui, B., Le Moullec, Y., Willson, D., and Favre, E. *Hybrid membrane cryogenic process for post-combustion CO_2 capture.* Journal of Membrane Science, 2012. **415**: p. 424-434.
210. Anantharaman, R., Berstad, D., and Roussanaly, S. *Techno-economic performance of a hybrid membrane–liquefaction process for post-combustion CO_2 capture.* Energy Procedia, 2014. **61**: p. 1244-1247.
211. Liu, L., Sanders, E.S., Kulkarni, S.S., Hasse, D.J., and Koros, W.J. *Sub-ambient temperature flue gas carbon dioxide capture via Matrimid® hollow fiber membranes.* Journal of Membrane Science, 2014. **465**: p. 49-55.
212. Song, C., Liu, Q., Ji, N., Deng, S., Zhao, J., Li, Y., and Kitamura, Y. *Reducing the energy consumption of membrane-cryogenic hybrid CO_2 capture by process optimization.* Energy, 2017. **124**: p. 29-39.

213. Fong, J.C.L.Y., Anderson, C.J., Xiao, G., Webley, P.A., and Hoadley, A.F. *Multi-objective optimisation of a hybrid vacuum swing adsorption and low-temperature post-combustion CO_2 capture.* Journal of Cleaner Production, 2016. **111**: p. 193-203.
214. Reddy, S., Scherffius, J., Freguia, S., and Roberts, C. *Fluor's Econamine FG Plus SM Technology: An Enhanced Amine-Based CO_2 Capture Process*. in *Proceedings of the second annual conference on carbon sequestration*. 2003. Alexandria, VA.
215. Thee, H., Smith, K.H., da Silva, G., Kentish, S.E., and Stevens, G.W. *Carbonic anhydrase promoted absorption of CO_2 into potassium carbonate solutions.* Greenhouse Gases: Science and Technology, 2015. **5**(1): p. 108-114.
216. Fradette, S., *Process and apparatus using a spray absorber bioreactor for the biocatalytic treatment of gases*, in *Patent number WO2004056455A1*. 2004.
217. Fradette, L., Lefebvre, S., and Procedia, C.J. *Demonstration results of enzyme-accelerated CO_2 capture.* Energy Procedia, 2017. **114**: p. 1100-1109.
218. Gilassi, S., Taghavi, S.M., Rodrigue, D., and Kaliaguine, S. *Techno-economic evaluation of membrane and enzymatic-absorption processes for CO_2 capture from flue-gas* Separation and Purification Technology, 2020: p. Accepted.
219. Tosh, J.S., Field, J., Benson, H., and Haynes, W., *Equilibrium study of the system potassium carbonate, potassium bicarbonate, carbon dioxide, and water*. 1959, Bureau of Mines Pittsburgh, USA.
220. Rocha, A.J., Bravo, J.L., and Fair, J.R. *Distillation Columns Containing Structured Packings: A Comprehensive Model for Their Performance. 2. Mass-Transfer Model.* Industrial & Engineering Chemistry Research, 1996. **35**(5): p. 1660-1667.
221. Schneider, W. *Vapor flow through a porous membrane—a throttling process with condensation and evaporation.* Acta Mechanica, 1983. **47**(1): p. 15-25.
222. *The End Of Fossil Fuels*. 2017 [cited 2017 1 July]; Available from: https://www.ecotricity.co.uk/our-green-energy/energy-independence/the-end-of-fossil-fuels.
223. *World Energy Resources: Coal* 2013 [cited 2017 1 July]; Available from: https://www.worldenergy.org/wp-content/uploads/2013/10/WER_2013_1_Coal.pdf.
224. Beil, M. and Hoffstede, U. *Guidelines for the implementation and operation of biogas upgrading systems.* Kassel: Fraunhofer IWES, 2010.
225. *World Energy Resources Bioenergy 2016*. 2016 [cited 2017 1 July]; Available from: https://www.worldenergy.org/wp-content/uploads/2017/03/WEResources_Bioenergy_2016.pdf.
226. Friedl, G. *Biogas production in Germany: Status quo and future trends*. Available from: http://www.handelskammer.dk/fileadmin/ahk_daenemark/Veranstaltungen/Bioenergi/4-20160301_EE_AHK-GR_Daenemark_PPP_Friedl_2016.pdf.
227. Thrän, D. and Kaltschmitt, M. *Competition–Supporting or preventing an increased use of bioenergy?* Biotechnology journal, 2007. **2**(12): p. 1514-1524.
228. *Biogas Potential*. 2017 [cited 2017 1 July]; Available from: http://biogasassociation.ca/about_biogas/biogas_potential.
229. Numjuncharoen, T., Papong, S., Malakul, P., and Mungcharoen, T. *Life-cycle GHG emissions of cassava-based bioethanol production.* Energy Procedia, 2015. **79**: p. 265-271.
230. Stefan, A., Mikko, H., Lucyna, L., and Markus, S. *Ethanol vs. Biogas used as car fuels*. Available from: http://213.229.136.11/bases/ainia_agrobiomet.nsf/0/AD1DA2009133A99BC1257846004E89EC/$FILE/EthanolvsBiogas.pdf.

231. Strassburg, B., Turner, R.K., Fisher, B., Schaeffer, R., and Lovett, A. *Reducing emissions from deforestation—The "combined incentives" mechanism and empirical simulations.* Global Environmental Change, 2009. **19**(2): p. 265-278.
232. Eze, J. and Agbo, K. *Maximizing the potentials of biogas through upgrading.* Am. J. Sci. Ind. Res, 2010. **1**(3): p. 604-609.
233. Jørgensen, P.J. *Biogas-green energy.* Faculty of Agricultural Sciences, Aarhus University, Tjele, Denmark, 2009.
234. Petersson, A. and WeLLInGer, A. *Biogas upgrading technologies–developments and innovations.* IEA Bioenergy, 2009. **20**.
235. Wellinger, A. and Lindberg, A. *Biogas upgrading and utilisation-IEA Bioenergy, Task 24-Energy from biological conversion of organic waste.* 2001.
236. Surendra, K., Takara, D., Hashimoto, A.G., and Khanal, S.K. *Biogas as a sustainable energy source for developing countries: Opportunities and challenges.* Renewable and Sustainable Energy Reviews, 2014. **31**: p. 846-859.
237. Hagen, M., Polman, E., Jensen, J., Myken, A., Jönsson, O., and Dahl, A. *Adding gas from biomass to the gas grid.* Contract No: XVII/4.1030, 2001(99-412).
238. Demirel, B. and Scherer, P. *The roles of acetotrophic and hydrogenotrophic methanogens during anaerobic conversion of biomass to methane: a review.* Reviews in Environmental Science and Biotechnology, 2008. **7**(2): p. 173-190.
239. Schlüter, A., Bekel, T., Diaz, N.N., Dondrup, M., Eichenlaub, R., Gartemann, K.-H., Krahn, I., Krause, L., Krömeke, H., and Kruse, O. *The metagenome of a biogas-producing microbial community of a production-scale biogas plant fermenter analysed by the 454-pyrosequencing technology.* Journal of biotechnology, 2008. **136**(1): p. 77-90.
240. Myint, M., Nirmalakhandan, N., and Speece, R. *Anaerobic fermentation of cattle manure: modeling of hydrolysis and acidogenesis.* Water Research, 2007. **41**(2): p. 323-332.
241. Lastella, G., Testa, C., Cornacchia, G., Notornicola, M., Voltasio, F., and Sharma, V.K. *Anaerobic digestion of semi-solid organic waste: biogas production and its purification.* Energy conversion and management, 2002. **43**(1): p. 63-75.
242. Holm-Nielsen, J.B., Al Seadi, T., and Oleskowicz-Popiel, P. *The future of anaerobic digestion and biogas utilization.* Bioresource technology, 2009. **100**(22): p. 5478-5484.
243. Rastogi, G., Ranade, D.R., Yeole, T.Y., Patole, M.S., and Shouche, Y.S. *Investigation of methanogen population structure in biogas reactor by molecular characterization of methyl-coenzyme M reductase A (mcrA) genes.* Bioresource technology, 2008. **99**(13): p. 5317-5326.
244. Abatzoglou, N. and Boivin, S. *A review of biogas purification processes.* Biofuels, Bioproducts and Biorefining, 2009. **3**(1): p. 42-71.
245. Jonsson, O. *Biogas upgrading and use as transport fuel.* Swedish gas center, 2004.
246. *Biogas for road vehicles technology brief*. 2017 [cited 2017 1 July]; Available from: http://www.irena.org/DocumentDownloads/Publications/IRENA_Biogas_for_Road_Vehicles_2017.pdf.
247. Feron, P., Jansen, A., and Klaassen, R. *Membrane technology in carbon dioxide removal.* Energy Conversion and Management, 1992. **33**: p. 5-8.
248. Higman, C. and Van der Burgt, M., *Gasification (Second Edition)*. 2008, Burlington: Gulf Professional Publishing.
249. Luis, P. *Use of monoethanolamine (MEA) for CO 2 capture in a global scenario: consequences and alternatives.* Desalination, 2016. **380**: p. 93-99.
250. Appl, M., Wagner, U., Henrici, H.J., Kuessner, K., Volkamer, K., and Fuerst, E. *Removal of CO2 and/or H2S and/or COS from gases containing these constituents.* US Patent, 1982. **4**.

251. Bishnoi, S. and Rochelle, G.T. *Absorption of carbon dioxide in aqueous piperazine/methyldiethanolamine.* AIChE Journal, 2002. **48**(12): p. 2788-2799.
252. Bishnoi, S., *Carbon Dioxide Absorption and Solution Equillibrium in Piperazine Activated Methyldiethanolanine*. 2001: University Microfilms.
253. Bell, D.A., Towler, B.F., and Fan, M., *Coal Gasification and its Application*. 2010: William Andrew.
254. Chaemchuen, S., Zhou, K., and Verpoort, F. *From Biogas to Biofuel: Materials Used for Biogas Cleaning to Biomethane.* ChemBioEng Reviews, 2016.
255. Kapdi, S., Vijay, V., Rajesh, S., and Prasad, R. *Biogas scrubbing, compression and storage: perspective and prospectus in Indian context.* Renewable energy, 2005. **30**(8): p. 1195-1202.
256. Tamm, D., Persson, T., Hulteberg, C., and Bauer, F. *Biogas upgrading-Review of commercial technologies.* SGC Rapport, 2013. **270**.
257. Wylock, C.E. and Budzianowski, W.M. *Performance evaluation of biogas upgrading by pressurized water scrubbing via modelling and simulation.* Chemical Engineering Science, 2017.
258. Babu, V., Thapliyal, A., and Patel, G.K., *Biofuels production*. 2013: John Wiley & Sons.
259. Bauer, F., Persson, T., Hulteberg, C., and Tamm, D. *Biogas upgrading–technology overview, comparison and perspectives for the future.* Biofuels, Bioproducts and Biorefining, 2013. **7**(5): p. 499-511.
260. Olajire, A.A. *CO_2 capture and separation technologies for end-of-pipe applications–a review.* Energy, 2010. **35**(6): p. 2610-2628.
261. Tock, L., Gassner, M., and Maréchal, F. *Thermochemical production of liquid fuels from biomass: Thermo-economic modeling, process design and process integration analysis.* Biomass and Bioenergy, 2010. **34**(12): p. 1838-1854.
262. Yu, C.-H., Huang, C.-H., and Tan, C.-S. *A review of CO_2 capture by absorption and adsorption.* Aerosol and Air Quality Research, 2012. **12**: p. 745-769.
263. Burr, B. and Lyddon, L. *A comparison of physical solvents for acid gas removal*. in *87th Annual Gas Processors Association Convention, Grapevine, TX, March*. 2008.
264. Niemczewska, J. *Characteristics of utilization of biogas technology.* Nafta-Gaz, 2012. **68**(5): p. 293-297.
265. Chen, W.-H., Chen, S.-M., and Hung, C.-I. *Carbon dioxide capture by single droplet using Selexol, Rectisol and water as absorbents: A theoretical approach.* Applied energy, 2013. **111**: p. 731-741.
266. Rege, S.U., Yang, R.T., Qian, K., and Buzanowski, M.A. *Air-prepurification by pressure swing adsorption using single/layered beds.* chemical engineering science, 2001. **56**(8): p. 2745-2759.
267. Krich, K., Augenstein, D., Batmale, J., Benemann, J., Rutledge, B., and Salour, D. *Biomethane from dairy waste.* A Sourcebook for the Production and Use of Renewable Natural Gas in California, 2005: p. 147-162.
268. Zhao, Z., Cui, X., Ma, J., and Li, R. *Adsorption of carbon dioxide on alkali-modified zeolite 13X adsorbents.* International Journal of Greenhouse Gas Control, 2007. **1**(3): p. 355-359.
269. Patterson, T., Esteves, S., Dinsdale, R., and Guwy, A. *An evaluation of the policy and techno-economic factors affecting the potential for biogas upgrading for transport fuel use in the UK.* Energy Policy, 2011. **39**(3): p. 1806-1816.
270. Gladstone, R. *High-BTU Projects Using Pressure Swing Adsorption (PSA) Technology.* Green Gas Energy LLC, 2007.
271. Grande, C.A., *Biogas upgrading by pressure swing adsorption*. 2011: INTECH Open Access Publisher.

272. Jee, J., Jung, J., Lee, J., Suh, S., and Lee, C. *Comparison of vacuum swing adsorption process for air separation using zeolite 10X and 13X.* Revue Roumaine de Chimie, 2006. **51**(11): p. 1095.
273. Bonjour, J., Chalfen, J.-B., and Meunier, F. *Temperature swing adsorption process with indirect cooling and heating.* Industrial & engineering chemistry research, 2002. **41**(23): p. 5802-5811.
274. Mason, J.A., Sumida, K., Herm, Z.R., Krishna, R., and Long, J.R. *Evaluating metal–organic frameworks for post-combustion carbon dioxide capture via temperature swing adsorption.* Energy & Environmental Science, 2011. **4**(8): p. 3030-3040.
275. Metz, B., Davidson, O., De Coninck, H., Loos, M., and Meyer, L. *Carbon dioxide capture and storage*. 2005 [cited 2016 20 December]; Available from: http://digital.library.unt.edu/ark:/67531/metadc12051/m1/16/.
276. Xu, G., Li, L., Yang, Y., Tian, L., Liu, T., and Zhang, K. *A novel CO_2 cryogenic liquefaction and separation system.* Energy, 2012. **42**(1): p. 522-529.
277. Hullu, J.d., Waassen, J., Van Meel, P., Shazad, S., and Vaessen, J. *Comparing different biogas upgrading techniques.* Eindhoven University of Technology, 2008: p. 56.
278. Biernat, K., Gis, W., and Samson-Bręk, I. *Review of technology for cleaning biogas to natural gas quality.* Silniki Spalinowe, 2012. **51**.
279. Thrän, D., Billig, E., Persson, T., Svensson, M., Daniel-Gromke, J., Ponitka, J., Seiffert, M., Baldwin, J., Kranzl, L., and Schipfer, F. *Biomethane–status and factors affecting market development and trade.* IEA Task, 2014. **40**.
280. Johansson, N. *Production of liquid biogas, LBG, with cryogenic and conventional upgrading technology-Description of systems and evaluations of energy balances.* 2008.
281. Kadam, R. and Panwar, N. *Recent advancement in biogas enrichment and its applications.* Renewable and Sustainable Energy Reviews, 2017. **73**: p. 892-903.
282. Adewole, J., Ahmad, A., Ismail, S., and Leo, C. *Current challenges in membrane separation of CO_2 from natural gas: a review.* International Journal of Greenhouse Gas Control, 2013. **17**: p. 46-65.
283. Scholz, M., Melin, T., and Wessling, M. *Transforming biogas into biomethane using membrane technology.* Renewable and Sustainable Energy Reviews, 2013. **17**: p. 199-212.
284. Merkel, T.C., Lin, H., Wei, X., and Baker, R. *Power plant post-combustion carbon dioxide capture: an opportunity for membranes.* Journal of membrane science, 2010. **359**(1): p. 126-139.
285. Pan, C.Y. and Habgood, H.W. *An analysis of the single-stage gaseous permeation process.* Industrial & Engineering Chemistry Fundamentals, 1974. **13**(4): p. 323-331.
286. Ramasubramanian, K., Verweij, H., and Ho, W.W. *Membrane processes for carbon capture from coal-fired power plant flue gas: A modeling and cost study.* Journal of membrane science, 2012. **421**: p. 299-310.
287. Scholz, M., Frank, B., Stockmeier, F., Falß, S., and Wessling, M. *Techno-economic analysis of hybrid processes for biogas upgrading.* Industrial & Engineering Chemistry Research, 2013. **52**(47): p. 16929-16938.
288. Makaruk, A. and Harasek, M. *Numerical algorithm for modelling multicomponent multipermeator systems.* Journal of Membrane Science, 2009. **344**(1): p. 258-265.
289. Bhide, B., Voskericyan, A., and Stern, S. *Hybrid processes for the removal of acid gases from natural gas.* Journal of Membrane Science, 1998. **140**(1): p. 27-49.
290. Rautenbach, R. and Welsch, K. *Treatment of landfill gas by gas permeation—pilot plant results and comparison to alternatives.* Journal of membrane science, 1994. **87**(1-2): p. 107-118.

291. Makaruk, A., Miltner, M., and Harasek, M. *Biogas desulfurization and biogas upgrading using a hybrid membrane system–modeling study.* Water Science and Technology, 2012. **67**(2): p. 326-332.